MICROALGAE BIOFUELS FOR DIESEL ENGINES IN AGRICULTURAL APPLICATIONS

A Dissertation submitted by

Saddam H. Al-lwayzy

B.Sc., M.Sc.

For the award of

Doctor of Philosophy

2014

Abstract

Diesel engines are the key components of several sectors in modern life. The dramatic growth of the world's population, economy and industry has increased the demand for petroleum diesel (PD) fuel. The increased use of depleting PD in recent years has highlighted the problems of high fuel prices and emissions. The emissions from combusting PD have been proven to affect human health and to contribute to the high carbon dioxide (CO_2) emissions that have led to global warming.

Alternative fuels have become essential for eliminating the PD problems. Biodiesel has attracted much attention as a renewable and environmentally friendly alternative fuel. The main drawback of using biodiesel as a fuel alternative to PD is the limited resources available, which cannot satisfy the demand for PD. Using vegetable oil for biodiesel purposes could create a food crisis. Potentially, microalgae are a promising alternative because of their high biomass and lipid productivity, and because they can contribute to reducing CO_2 pollution through the photosynthesis process. Microalgae have the ability to grow in a variety of difficult conditions such as in seawater, wastewater or deserts, thus avoiding influence on the agriculture sector.

In this work, fresh water microalgae *Chlorella vulgaris* (FWM-CV) was grown for biodiesel production and to study the effect of enhancing the lipid content using iron as stress treatment on the biodiesel properties. Different growing conditions were found to give different fatty acid methyl ester (FAME) components, which led to different biodiesel properties. However, this biodiesel was found to have acceptable properties for running diesel engines.

Single-cylinder diesel engine performance and exhaust gas emissions were evaluated using microalgae *Chlorella protothecoides* MCP-B100, MCP-B50, MCP-B20 and PD. The overall results indicated that MCP-B100 and its blends have fuel properties, engine performance and enhanced emissions comparable to those of PD. Statistical analyses showed that the effect of the fuel type on the studied parameters was statistically significant except for the fuel consumption (FC) rate, thermal efficiency and CO_2. MCP-B100 produced a reduction by 7%, 4.9%, 28% and 7.4% in the brake power, torque, CO and NO_x, respectively, and an increase by 10.2% and 15.8% in the brake specific fuel consumption (BSFC) and oxygen (O_2), respectively.

A second test was performed to study the effect of adding FWM-CV cells to enhance the energy content of emulsified water fuels on the performance and exhaust gas emissions of a single-cylinder diesel engine. The test was conducted using cottonseed biodiesel (CS-B100), emulsified water fuel in cottonseed biodiesel (CS-E20) and emulsified water fuel containing FWM-CV cells (CS-MB100). The general findings were that the CS-MB100 presented higher results of gross input power, brake power, torque, CO_2 and nitrogen oxide (NO_x) than CS-B100 and lower results than CS-B100. These findings indicate that the addition of FWM-CV cells to emulsified water fuel has a positive effect on fuel properties and engine performance.

An agricultural tractor power take-off (PTO) test was conducted using MCP-B20 to examine the performance and exhaust gas emissions under different operating conditions. The results indicated an insignificant difference in engine performance when MCP-B20 was used compared with PD. However, the analysis of variance (ANOVA) summary at rated PTO speed showed a significant reduction in the values of torque, power, carbon monoxide (CO), CO_2 and nitrogen monoxide (NO), and a significant increase in the O_2 lambda for MCP-B20 compared with those of PD.

Certification of Dissertation

I certify that the ideas, experimental work, results, analyses and conclusions reported in this dissertation are entirely my own effort, except where otherwise acknowledged. I also certify that the work is original and has not been previously submitted for any award, except where otherwise acknowledged.

……. / /2013

Signature of Candidature

Saddam Hussen Maree Al-lwayzy

ENDORSEMENT

……. / /2013

Signature of Principal Supervisor

……. / /2013

Signature of Supervisor/s

……. / /2013

Signature of Supervisor/s

Acknowledgments

This thesis would not have been possible without the many institutes and people who helped me complete my PhD project. First, thanks to God, the Iraqi government and the University of Southern Queensland for giving me this opportunity.

I would like to express my deepest appreciation to my principal supervisor, Associate Professor Talal Yusaf, for his guidance, remarks and engagement throughout the process of my learning in the field of internal combustion engines and biofuels. Thanks for their valuable, useful solutions to the great number of challenges during the period of study. I am highly grateful to my associate supervisor Dr Paul Baker for his great time and effort in setting up and running the engine and for his valuable comments and experience in engine and combustion theory. Thanks are also due to my associate supervisor Dr Troy Jensen, who helped me to perform the tractor test to fulfil the requirements of my sponsor, the Iraqi government, and provided constructive comments. Further, I would like to express my thanks to Dr Bernadette McCabe, Dr Vasanthadevi Aravinthan, Dr Pam Pittaway, Mr Peter Harris, Mrs Adele Jones and Mrs Morwenna Boddington for their assistance in the biological part of my thesis. The author would like to extend his thanks to professor; Frank Bullen for his continues support for this project. I also would like to convey many thanks to Mr Kim Larson for his valuable assistance and advice in the chemical analysis of the fuels. Thanks to Chris Galligan, Dean Beliveau and Brian Aston for their help in building the experimental apparatus. My colleagues Dr Belal Yousif, Ahmed Naji, Raed Ahmed and Ahmed Younis Al-Sabawy deserve thanks for their valuable guidance and assistance. Thanks to the Soley Institute for providing the project with microalgae oil and useful information and thanks to Queensland University of Technology (QUT) for providing us Cottonseed biodiesel. I wish to express my

special thanks to my beloved families back home, especially my mum and dad for all that they sacrificed for us and for their endless encouragement and support through the study time. Thanks also to my lovely brothers and sisters for their support along the way. Massive thanks to my wife and lovely sons for all their love and support and, to you, this thesis is dedicated.

List of Associated Publications

Journal papers

Al-lwayzy, S & Yusaf, T 2013, 'Chlorella protothecoides microalgae as an alternative fuel for tractor diesel engines', Energies, vol. 6, no. 2, pp. 766–83.

Al-lwayzy, Saddam H. and Yusaf, Talal and Jensen, Troy 2012 'Evaluating tractor performance and exhaust gas emissions using biodiesel from cotton seed oil', IOP Conference Series: Materials Science and Engineering, 36 (1). pp. 442-452. ISSN 1757-899.

Conferences

Allwayzy, S, Yusaf, T, McCabe, BK, Pittaway, P & Aravinthan, V 2010, 'Microalgae as alternative fuel for compression ignition (CI) Engines', paper presented at Southern Region Engineering Conference, Toowoomba, 11–12 November.

Contents

List of Figures

List of Tables

List of Abbreviations

A	area
ANOVA	Analysis of variance
ASTM	American standard for testing materials
ATDC	After top dead centre
B	Biodiesel
BMEP	Brake mean effective pressure
BP	Brake power, British Petroleum
BSFC	Brake specific fuel consumption
BTDC	Before top dead centre
C14:0	Myristic acid
C16:0	Palmitic acid
C16:1	Palmitoleic acid
C18:0	Stearic acid
C18:2	Linoleic acid
C18:3	α-Linolenic acid
CA	Crank angle
CI	Compression ignition
CMAR	Centre for Marine and Atmospheric Research
CO	Carbone monoxide
CO_2	Carbone dioxide
CP	*Chlorella protothecoides*

CS	Cottonseed
CSIRO	Commonwealth Scientific and Industrial Research Organisation
CV	*Chlorella vulgaris*
d	Characteristic dimension (cylinder bore diameter)
D	Diameter
DAQ	Data acquisition
Dw	dry weight
EDTA	Ethylenediaminetetraacetic acid
EG	Exhaust gas
FA	Fatty acid
FAME	Fatty acid methyl ester
FC	Fuel consumption
FWM-CV	Freshwater microalgae *Chlorella vulgaris*
GC-MS	Gas chromatography mass spectrometry
GIP	Gross input power
HC	Hydrocarbons
HO	Hydroxyl
HOT	Half open throttle
ICE	Internal combustion engine
ISC	Iron supplemented culture
L	Connecting rod length
LHV	Lower heating value
LSD	Least significant difference

MBL	Medium Woods Hole
Mdw	Microalgae dry weight
MCP	Microalgae *Chlorella protothecoides*
MW	Molecular weight
N	Engine speed
NaOH	Sodium hydroxide
NO	Nitrogen monoxide
NO_x	Oxides of nitrogen
O_2	Oxygen
OD	Optical density
P	Pressure
PBR	Photobioreactor
PCSO	Preheated crude sunflower oil
PD	Petroleum diesel
PLM	Professional lambda meter
PM	Particulate matter
PPM	Parts per million
PTO	Power take-off
QUT	Queensland University of Technology
rpm	Revolutions per minute
s	Second
sp.	Species
T	Temperature (also Torque)

TDC	Top dead centre
USQ	University of Southern Queensland
V	Volume
W	Weight
WOT	Wide open throttle
η_{th}	Brake thermal efficiency
θ	Crankshaft angular displacement from TDC
λ	Lambda
ρ	Density

CHAPTER ONE

Introduction

1.1 Introduction

The demand for diesel fuels is increasing due to the large number of diesel engines used in numerous systems. It is reported that over the last decades, the traffic use of fuel has increased by 16.42%, reaching the level of about 1,675,035 kT of oil (Tomić et al., 2013). The extensive use of petroleum diesel (PD) during the last decades has led to a rise in air pollution, health problems and fuel prices (Mohebbi et al., 2012). In addition, there is a large concern within academia and industry about the need for renewable, ecologically friendly and low-cost fuels because of the growth of the world's population and economy. Alternative and renewable fuels are one of the most substantial needs (Mata et al., 2010; Tomić et al., 2013). In light of this, biodiesel is becoming the most suitable alternative fuel for diesel engines, and it has been successfully used by several researchers (Dorado et al., 2003a; Nabi et al., 2009; Tomić et al., 2013).

Biodiesel can be used for diesel engines with less modification and using the same fuel system (Tomić et al., 2013). Further, biodiesel has a low effect on the environment compared with PD; that is, it produces less carbon dioxide (CO_2) than PD fuel. In addition, plants consume CO_2 during the life cycle of the biodiesel production.

With regard to using biodiesel in agriculture applications, it has good potential as an alternative to PD. Biodiesel can be produced by farmers on a small scale to run tractors, pumps and small engines for power generation (Crookes et al., 1997; Tomić et al., 2013).

Biodiesel can be produced from a wide range of feedstock, vegetables, plants, animals, fish oil and microorganisms. The first generation of biodiesel was produced from edible oil. However, production of the biodiesel form of edible oil presents a problem because it raises the price of edible oil for human usage. This has motivated researchers to focus on a second generation of biodiesel produced from non-edible oil. The main drawback of using non-edible plants as a source for fuel is that their cultivation requires a large amount of land and irrigation water, which also indirectly influences human food production. Further, the crops, waste cooking oil or animal fat, produce a limited amount of biodiesel and cannot satisfy the transportation demand for oil (Chisti, 2008). As a result, the new source of biofuel has to fulfil the main requirements of good productivity, low effect on human food and environmental friendliness. Therefore, researchers have been exploring the possibility of using microalgae as source of energy. Microalgae are one of the most promising sources of biomass feedstock for biodiesel because of their superior biomass productivity (Makareviciene et al., 2013). It has been reported that microalgae double their biomass in 24 hours (Ahmad et al., 2011).

Microalgae biomass feedstock can be a source of biofuel in different forms, including biodiesel (Pragya et al., 2013), direct biomass powder injection or biomass powder (cells) in emulsified water (slurry) in diesel or other biodiesel fuels (Scragg et al., 2003). As reported by Demirbas and Demirbas (2010), the oil productivity of microalgae per land unit is over 200 times that of the yield from vegetable oils.

Microalgae biodiesel has fuel characteristics very similar to PD, and it can be blended in any ratio with PD (Amin, 2009).

Recent research in the field of microalgae biofuels has reported that large-scale or commercial production of microalgae is still unavailable because of the infrastructure required for growing, harvesting, drying and oil extraction. This highlights the lack of data related to the use of microalgae biofuels in diesel engines (Chen et al., 2012; Demirbas & Demirbas, 2011; Haik et al., 2011; Pragya et al., 2013).

Haik et al. (2011) investigated the use of microalgae oil and biodiesel on engine performance from *Ankistrodesmus braunii* and *Nannochloropsis* species. In their study, exhaust gas emissions were not considered. Different microalgae species and growing conditions produce different amounts of biodiesel and different biodiesel quality (Demirbas & Demirbas, 2010). This motivated the investigation in the current study into the effect of using biofuels from microalgae *Chlorella protothecoides* (MCP) and freshwater microalgae *Chlorella vulgaris* (FWM-CV) on diesel engine performance and exhaust gas emissions.

The current study encompasses investigation into (1) the production of microalgae biomass and biodiesel (including growing, harvesting, drying and lipid extraction), (2) microalgae biofuel preparation and properties, and (3) the effect of biofuels from microalgae on diesel engine performance and exhaust gas emissions.

Due to infrastructure requirements, a major challenge in this research work was producing the required amount of biomass and biodiesel from microalgae. Adequate solutions were found to overcome this challenge, including obtaining the required amount of microalgae oil to run the engine test from our industrial partner.

The pulverised microalgae cells of *Chlorella* species are reported to be combustible in a diesel engine. However, the fuel system and the combustion parameters require major modifications. Scragg et al. (2003) reported using emulsified water fuel of pulverised microalgae cells in water and biodiesel to run an engine with minor modifications. The emulsified water fuel has less energy content associated with the water content in the emulsion that may affect the produced power. To overcome these issues, FWM-CV was added to the emulsified water fuel using advanced ultrasound technology to increase the combustion efficiency and reduce the nitrogen oxides (NO_x) emissions associated with biodiesel.

The literature review indicated that investigation into the use of microalgae biodiesel in tractor diesel engines and any power take-off (PTO) test was absent. Therefore, this study into the effect of using microalgae biodiesel on the engine performance and exhaust gas emissions of a tractor was conducted to fill this gap.

1.2 Objectives

The overall aim of this project was to study microalgae biofuels as an alternative, renewable and environmentally friendly fuel in laboratory diesel engines and for agricultural tractors. The objectives were:

1. to grow microalgae in a laboratory scale to produce microalgae biomass and oil to be converted to biodiesel (including growing, harvesting, drying and lipid extraction), and to study the influence of increasing the lipid content in the FWM-CV on the produced microalgae biodiesel properties
2. to study the chemical and physical properties of MCP-B100, MCP-B50 and MCP-B20, and to evaluate the performance and exhaust gas emissions of a

single-cylinder diesel engine under different operating conditions and compare the results with those of PD

3. to prepare emulsified water in cottonseed biodiesel (CS-B100) with and without adding FWM-CV cells, and to use ultrasound technology as an effective method to break down the FWM-CV colonies into individuals to overcome the problem of nozzle blockage and form homogenised emulsion
4. to study the effect of adding FWM-CV cells to the emulsified water on the performance and exhaust gas emissions of the single-cylinder diesel engine
5. to evaluate the tractor's performance and exhaust gas emissions using microalgae biodiesel based on the results obtained from the single-cylinder engine test.

1.3 Thesis Layout

The thesis consists of seven chapters as follows:

- **Chapter 1** includes an introduction and the objectives of the thesis and outlines the structure.
- **Chapter 2** presents a literature review on the alternative fuels for diesel engines with a focus on alternative fuels from microalgae as biodiesel and emulsified water fuel (with and without microalgae cells).
- **Chapter 3** covers the growth and production of FWM-CV biomass in a small-scale apparatus to be investigated as a source of biodiesel and to be used in emulsified water fuel. This chapter consists of:
    i. an introduction and detailed literature review of microalgae biodiesel production
    ii. the methods and the equipment used in the production process of growing, harvesting, lipid (fatty acid [FA]) extraction, transesterification

of the lipid to form fatty acid methyl esters (FAMEs) and the FAME analysis

iii. the results and discussion of the production process of the growing productivity, lipid production and FAME analysis under different growing conditions, as well as the calculated FWM-CV biodiesel physical properties

iv. the conclusion of the chapter.

- **Chapter4** focuses on the experimental work of MCP-B in a single-cylinder diesel engine using different blend ratios and different operating conditions. The structure of the chapter is as follows:

  i. a review of the literature on the effect of using biodiesels from various sources on diesel engine performance and exhaust gas emissions

  ii. the methods and the equipment used in converting the MCP oil into biodiesel, tests on some of the fuel properties and the engine test set-up.

  iii. the results and discussion of the comparison of the engine performance and exhaust gas emissions using MCP-B100, MCP-B50, MCP-B20 and PD under different engine operating conditions

  iv. the conclusion of the chapter.

- **Chapter 5** covers the use of FWM-CV powder in the form of emulsified water fuel (biodiesel 80% and water 20% [with and without FWM-CV cells]) in a single-cylinder diesel engine. The chapter's layout is as follows:

  i. introduction and review of other researchers' work on using emulsion fuels in diesel engines, including the advantages and the disadvantages; special focus is on the use of emulsified water fuel containing microalgae cells in diesel engine

ii. the methods and the equipment used to prepare the emulsified water fuels and test their physical properties

iii. the results and discussion of the effect of using the emulsified water fuel (with and without FWM-CV cells) on the single-cylinder diesel engine's performance and exhaust gas emissions

iv. conclusion of the chapter.

- **Chapter 6** presents the evaluation of the tractor engine performance and exhaust gas emissions when fuelled with MCP-B20. The evaluation was conducted using PTO. This chapter is structured as follows:

v. a review of the literature on the effect of using biodiesels from various sources using a tractor PTO test on the tractor engine's performance and exhaust gas emissions

vi. the methods and the equipment used to perform the PTO test

vii. the results and discussion of the comparison of the tractor engine's performance and exhaust gas emissions using MCP-B20 and PD under different load and speeds

viii. the conclusion of the chapter.

- **Chapter 7** presents the conclusion and suggestions for future work.

CHAPTER TWO

Literature Review

2.1 Introduction

This chapter contains a review of literature on diesel engines, diesel fuel and alternative fuels for diesel engines with a focus on biodiesel. A review of studies on microalgae as a source of biomass and biodiesel is also included. Studies on the production of microalgae biofuels in relation to producing microalgae biomass, harvesting and drying microalgae from the medium, microalgae oil extraction and biodiesel properties are reviewed. Studies on alternative fuels of biodiesel from various sources and emulsified water and emulsified slurry in diesel engines are considered in this chapter. Detailed literature reviews and specific results and findings are presented in each chapter as relevant.

2.2 Diesel Engines and Their Applications in the Agricultural Field

A diesel engine is a mechanical device that converts the chemical energy in fuel into mechanical energy through a combustion process. The diesel engine is an internal combustion engine (IC), which is known as a compression ignition (CI) engine because the combustion occurs as a result of the high temperature and pressure during the compression stroke (Pulkrabek, 2004). In about 1892, Rudolf Diesel created the diesel engine in a version that is similar to the current diesel engine

(Pulkrabek, 2004). Diesel engines are widely used in most sectors, including transportation, industry and agriculture, due to their low fuel consumption (FC) and adequate fuel to power conversion efficiency (Fahd *et al.* 2012). Diesel engines are preferred due to their high performance, lower fuel consumption FC and long life (Nadeem et al., 2006). Current diesel engines are designed to use PD, which is one of the products derived from the process of refining crude oil.

The main sectors that consume conventional liquid fuels are transport and agricultural (Sahoo et al., 2009). Mata et al. (2010) reported that transportation is the main cause of greenhouse gases in the European Union, and the agriculture sector is the third contributor by about 9%. Diesel engines are used in agricultural machinery in many ways to power the equipment. Tractors are the main power source on the farm. Every farmer has one or more tractors because it is crucial agricultural machinery equipment.

The increased demand for depleting liquid fossil fuels such as PD has resulted in many problems. PD prices have increased dramatically over the past decades (Campbell, 2008). Emissions from diesel fuel have been proven to contribute to the greenhouse gas emissions that have led to health problems and global warming (Hossain et al., 2008). Magara-Gomez et al. (2012) have reported that human epidemiological studies have revealed a relationship between diesel exhaust emissions and increased rates of lung cancer.

Governments, researchers and manufacturers are putting enormous efforts into reducing emissions from diesel engines (Campbell, 2008). However, the continuing increase in the number of diesel engines will have the same negative effect of emissions (Ozsezen et al., 2009). As a result of the long life of diesel engines, the

efforts to decrease diesel engine emissions using modern technology will be limited because older engines will still be in use and out of control (Nadeem et al., 2006).

Mariasiu and Varga (2010) have commented that using biodiesel in the agriculture sector is a key factor for enhancing the outcomes of the sector, and it is important to reduce the emissions from agricultural mechanisation for sustainable agriculture. To overcome the problems associated with fossil fuels, and especially PD, an alternative, lower emission fuel is needed for diesel engines.

2.3 Alternative Fuels for Diesel Engines

Developing alternative fuels for diesel engines has become essential to eliminate fossil fuel problems (Campbell, 2008; Chisti, 2007). Enhancing energy security by varying the sources of energy and reducing the demand for exported oil is another factor in the push towards alternative fuels. It is important for alternative fuels to be renewable and have less effect on the environment. Biofuels must be produced, supplied and distributed by being delivered to the engine using the current available technology in a safe way that has less effect on the engine's durability (Hansen et al., 2005).

Research into alcohol-based fuel such as ethanol as an alternative fuel for diesel engines started in the 1980s. The research revealed that using ethanol as a blend with PD was technically suitable for the current diesel engines; however, the production price of ethanol was relatively high and was thus not competitive with PD (Hansen et al., 2005). Campbell (2008) reported that many alternative fuels such as hydrogen and ethanol are still expensive compared with petroleum fuels. Hansen et al. (2005) reviewed the use of ethanol blends with PD in diesel engines and reported that the advantages of using an ethanol-diesel blend are that it is renewable and it has fewer

emissions than PD. Further, they reported a significant influence of ethanol-diesel blend properties on engine performance, durability, exhaust gas emission and fuel safety. Hansen et al. (2005) also reported that the ethanol blend has a flashpoint below 37.8 ºC, which means it is a Class I liquid, whereas PD is a Class II liquid. This makes the ethanol blend unsafe, and appropriate treatment in storage and handling is thus required.

Among the alternative fuels currently available for the diesel engine, fuels derived from vegetable oils and animal fat are receiving substantial attention. Crude vegetable oil can be used directly or in blends in diesel engines. Bettis et al. (1982) have evaluated biodiesel from different oils, including sunflower seed, safflower seed and rapeseed, in diesel engines for short and long terms. Their results showed that the energy content of the oil ranged from between 94% and 95% of the energy content of PD and the viscosity was about 11.1 to 17.6 times higher than that of PD. The results from their short-term test indicated comparable engine power and higher thermal efficacy by about 1.8% to 2.8% compared with PD. Long-term test results found significantly higher carbon deposits on the combustion chamber and exhaust port. Heavy gum accumulation was found on the injector and compression rings. They argued that treatment is essential for pure vegetable oils before it can be used long term as fuel for diesel engines.

The properties of vegetable oil are considered out of the limits of fuel recommended for diesel engines, which require some engine modification and/or oil treatment to prevent engine failure (Basha et al., 2009). Viscosity of crude oil is considerably higher than that of PD, which can be reduced in many ways, such as by blending the oil with diesel fuel, preheating the oil and transesterification to form biodiesel. Diya'uddeen et al. (2012) reported that using vegetable oil directly in diesel engines

can cause problems because of the poor atomisation, which requires a process such as pyrolysis, blending with PD, microemulsification and transesterification.

Canakci et al. (2009) tested the combustion and emission parameters of preheated crude sunflower oil (PCSO) in a diesel engine. Their study showed a statistically insignificant difference in the brake torque, thermal efficiency, carbon monoxide (CO), CO_2 level and smoke opacity between the PCSO and the PD. Converting crude oil to biodiesel is an effective method for enhancing fuel properties.

2.4 Transesterification of Oil to Form Biodiesel

Biodiesel can be produced using different techniques such as hydrodynamics, ultrasound and transesterification (Basha et al., 2009). Transesterification is the most common method used to form biodiesel. Transesterification is the process of converting vegetable oil or animal fat to biodiesel (Demirbas & Demirbas, 2011; Knothe et al., 2005; Wilson & Farag, 2012), and it has been widely used to enhance fuel properties and reduce viscosity (Knothe et al., 2005; Knothe & Steidley, 2007; Pereira et al., 2007). Biodiesel is the product of reacting triglyceride with an alcohol (usually methanol) in the presence of a base (usually sodium hydroxide [NaOH]) or an acid catalyst to form FA ester and glycerol (Atadashi et al., 2010). The most common alcohols used for transesterification are methanol and ethanol. The low cost of methanol makes it the most widespread alcohol used in this process. The transesterification reaction is presented in Figure 2.1

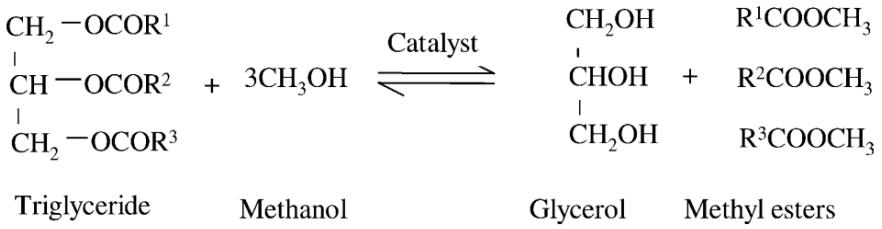

Figure 2.1 The transesterification formula of triglycerides (Meher et al., 2006)

The reaction shown in Figure 2.1 is an equilibrium reaction. Campbell (2008) reported that extra methanol was used to force the reaction to form biodiesel rather than triglyceride and the reaction could be sped up to be completed in about 90 minutes at 60 ºC.

2.5 Biodiesel Fuel

Biodiesel fuel is a promising area for research because of the increased demand for fuel, its high price and the associated environmental issues (Stalin & Prabhu, 2007). Biodiesel is one of the best options for diesel engines (Basha et al., 2009), and it is widely used in most sectors because of its low FC and adequate thermal efficiency (Dorado et al., 2003a; Nabi et al., 2009).

Biodiesel is renewable, environmentally friendly and non-toxic, can be produced from various feedstock resources and does not require significant modification to existing technology (Kass et al., 2009; Lin & Lin, 2006; Patil & Deng, 2009; Prasath et al., 2010; Stalin & Prabhu, 2007). Biodiesel can use the same infrastructure as that used for PD fuel distribution, handling and storage, and it is safer than PD because of its higher flashpoint (Campbell, 2008; Knothe et al., 2005). It has been reported that biodiesel fuel produces fewer emissions than PD in the whole range of air–fuel ratios (Basha et al., 2009). The use of biodiesel has been reported to be a possible solution for controlling CO_2 emission in the atmosphere. This is mainly because producing

vegetable oil through agriculture consumes CO_2 and closes the cycle of CO_2 (Desantes et al., 2009). Biodiesel is oxygenated, biodegradable, zero-sulphur and non-toxic (Knothe et al., 2005; Lin & Lin, 2006; Stalin & Prabhu, 2007), and it has been reported to have more complete combustion compared with that of PD (Bowman et al., 2006; Campbell, 2008).

However, biodiesel fuels from different feedstock have different fuel properties, it is commonly known with, higher cetane number, no sulphur and near-zero aromatic (Ozsezen et al., 2009) and higher lubricity compared with PD (Knothe et al., 2005; Lin & Lin, 2006; Stalin & Prabhu, 2007). Biodiesel has energy content comparable to that of PD and higher lubrication properties, which increase engine life (Campbell, 2008).

2.6 Biodiesel Feedstock

Biodiesel has been reported as the best alternative fuel for the future. It can be sourced from about 350 oil-bearing crops; however, only some of these sources are considered to have potential (Basha et al., 2009). Biodiesel can be obtained from a variety of sources, including forests, vegetables and animals.

Feedstock for biodiesel from the agricultural sector is limited (Campbell, 2008; Mata et al., 2010) and not sufficient to satisfy the world's demand for transportation fuel (Chisti, 2007). The commercial use of edible oils for biodiesel production may lead to another problem: food shortage. The second generation of biodiesel will use non-edible oil. Diya'uddeen et al. (2012) reported that non-edible agricultural resources for biodiesel such as rubber, jatropha, mahua, tobacco, castor and pongame seeds are practical alternatives that may reduce the use of edible oil. However, the cultivation of non-edible crops for biodiesel purposes will affect human food production by

using the available irrigation water and arable lands. Therefore, non-edible sources of biodiesel such as microalgae are promising alternative fuels for ICEs (Mustafa, 2011; Singh & Singh, 2010). Microalgae can be grown on a large scale on non-crop marginal lands and wastelands. For this reason, microalgae are considered a favourable feedstock for biodiesel that does not conflict with the agriculture sector and human food (Campbell, 2008; Chen et al., 2012; Mata et al., 2010).

2.7 Microalgae Fuels

Microalgae are unicellular photosynthetic organisms that use light energy and CO_2, with relatively higher photosynthetic efficiency compare to plants (Miao & Wu, 2006). Microalgae have the ability to convert CO_2 to oil through the photosynthetic process (Hossain et al., 2008; Mustafa, 2011; Singh & Singh, 2010).

Alternative fuels for current diesel engines have to meet certain chemical and physical property requirements. Biodiesel from microalgae has the potential to meet the world's fuel demand (Hossain et al., 2008; Mata et al., 2010; Widjaja et al., 2009). Microalgae biomass and biodiesel are promising sources of future fuels for diesel engines because of several factors:

- Microalgae are renewable and environmentally friendly and can contribute to reducing CO_2 levels in the atmosphere by consuming CO_2 and converting it to oil (Hossain et al., 2008).
- Chisti (2007) and Ayhan (2010) have reported that the demand for fuel for transportation can only be met by microalgae as a renewable source. Microalgae have higher biomass and lipid productivity per unit of area in comparison with crops (Amin, 2009; Demirbas, 2007; Demirbas M. F.,

2010). Microalgae oil production is seven to 31 times higher than that of palm oil (Hossain et al., 2008). The same amount of biodiesel from microalgae (for 30% weight per weight [w/w] oil content) as that from rapeseed or soybean crops requires less land around 49 to 132 times less (Balat & Balat, 2010). Further, microalgae grow under various conditions that have an insignificant influence on the human food supply chain (Mata et al., 2010; Widjaja et al., 2009). Chisti (2007) compared the amount of land required for different sources of biodiesel to satisfy 50% of the US transportation needs for fuel. As shown in Table 2.1, if corn and palm oil were planted, 24% and 846% of the US cropping area would be required, respectively, to meet 50% of the transportation fuel demand. In contrast, microalgae (with 30% oil content) would require only 2.5% of the existing area. Therefore, microalgae are the only source that has the ability to cover the transportation demand for fuel. Microalgae double their biomass in about one day (Chisti, 2007). The productivity of diatom algae is about 46,000 kg of oil per hectare per year (Demirbas, 2007).

Table 2.1 Comparison of oil yield from some sources of biodiesel (Chisti, 2007)

Crop type	Oil yield (L/ha)	Land area needed (M ha)[a]	Percentage of existing US cropping area[a]
Corn	172	1540	846
Soybean	446	594	326
Oil palm	5950	45	24
Microalgae [b]	58,700	4.5	2.5
[a] For meeting 50% of all transport fuel needs of the United States. [b] 30% oil (by wt) in biomass.			

- Microalgae can grow in a variety of conditions, including fresh water and marine water, and can be grown to treat waste water and remove CO_2 from industries and power plant (Campbell, 2008; Mata et al., 2010).

- Microalgae cells are combustible in powder form or as slurry in emulsified water in other fuels (Scragg et al., 2003).
- Some microalgae species have an oil content of about 80% of dry weight (Amin, 2009).
- Microalgae biodiesel characteristics are similar to those of biodiesel, according to the ASTM International (ASTM) standards, which means there is no need for diesel engines to undergo major changes (Campbell, 2008; Mata et al., 2010).
- Microalgae biofuel is non-toxic, contains no sulphur and is highly biodegradable. After extracting oil, the leftover material can be used as soil fertiliser or to produce ethanol (Demirbas & Demirbas, 2011).
- The cost of microalgae biodiesel can be lower than that of crop oil if produced on a large scale under suitable conditions and using appropriate technology (Hossain et al., 2008).

2.8 Microalgae Production

2.8.1 Microalgae Production

The Chinese were the first people to use microalgae in food industry, 2000 years ago. Development of microalgae biotechnology only started in the middle of the twentieth century (Harwood & Guschina, 2009). Generating renewable sources of energy using microalgae captured the interest during the energy crisis in the 1970s; currently, the applications of microalgae are very wide ranging (Spolaore et al., 2006). Studies were carried out from 1978 to 1996 in the United States to develop renewable transportation fuel from algae in particular, to produce biodiesel from high lipid content algae (Shen et al., 2009). This programme achieved great progress in

collecting species and investigating growing conditions. The low price of fuel in 1996 was one of the main factors to stop funding for this project. Interest in microalgae in the United States and worldwide for fuel and other applications has since risen again, especially after the increase in energy prices (Shen et al., 2009).

2.8.2 Microalgae Cultivation

The first step in growing microalgae is to select the most suitable species. The availability of the strain, the growing method and the reason for growing (such as for protein or biodiesel production) are the main factors to consider in selecting the species. The *Chlorella* species has great potential as a resource for biodiesel because of its fast growth and easy cultivation; however, its lipid content is relatively low (14% to 30%) (Illman et al., 2000). This lipid percentage is not sufficient for it to be a commercial alternative to PD (Liu et al., 2008). Growing microalgae requires light, water, nutrients, CO_2 and a temperature of 20ºC to 30 ºC. Any change in these factors can significantly affect the microalgae growth rate and lipid content. For effective and commercial microalgae growth, a higher concentration of CO_2 is required than that available naturally (Campbell, 2008).

Several studies have been conducted to enhance the productivity and the lipid content of some microalgae species by changing the growing conditions. For example, five species of *Chlorella* were grown by Illman et al. (2000) in a low-nitrogen medium in small, 2 L stirred tank bioreactors to determine the calorific value. The results showed that *Chlorella vulgaris* gave the highest growth rate. However, the highest calorific value, 29 kJ/g, was obtained with *Chlorella emersonii.* In another study, three species, *Botryococcus braunii*, *Chlorella vulgaris* and *Scenedesmus* species, were tested by Yoo et al. (2009) for biomass and biodiesel

production with different levels of CO_2; they also tested microalgae ability for CO_2 fixation, growth rate, total lipid content and FA profile. Liu et al. (2008) grew marine water *Chlorella vulgaris* in five levels of iron concentration in the medium. The results showed that the lipid content increased three to seven times to be up to 56.6% of biomass by dry weight in the medium supplemented with 1.2×10^{-5} mol/L $FeCl_3$.

Microalgae can be grown using many different methods, in large-scale or small-scale photobioreactors (PBRs). Although an enormous number of PBR designs have been proposed, technical and commercial factors prevent the adoption of all but a few of these for mass production of algae (Ugwu et al., 2008). Microalgae can be produced in open pond systems and closed system PBRs.

Open Pond Systems

The open system, which uses vessels such as raceway ponds and lakes, is the oldest system for growing algae, and it is still used for large-scale production, especially in the United States, China, India, Japan, Israel and Australia. Most of these productions are for food and β-carotene. Two types of open pond system are shown in Figure 2.2 (Shen et al., 2009).

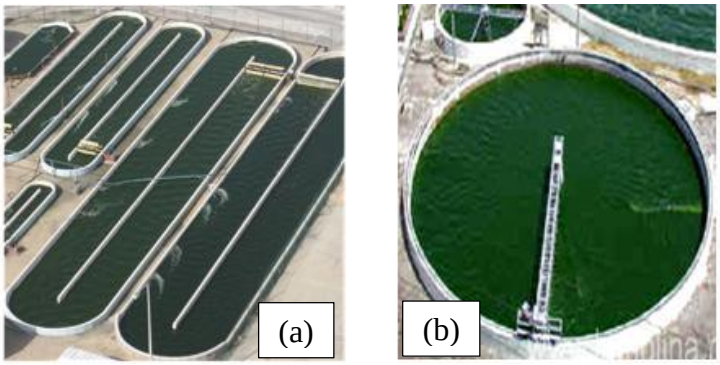

Figure 2.2 Open pond systems (a) raceway pond (b) circular pond

Photobioreactors (PBR)

PBRs are a closed system technology used to control the growing conditions of algae. Light, pH, CO_2 and nutrients are controlled. Many types of PBR have been reported, but the most popular types are the tubular and flat-plate PBRs, as shown in Figures 2.3 and 2.4 (Shen et al., 2009).

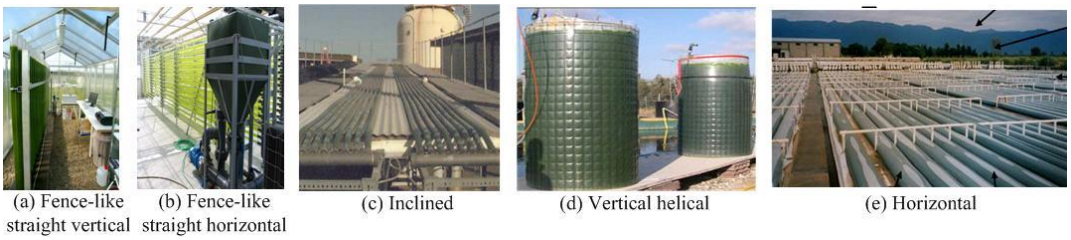

Figure 2.3 Different designs of tubular PBR (Shen et al., 2009)

Figure 2.4 Two different designs of flat-plate PBR (Shen et al., 2009)

2.8.3 Microalgae Harvesting and Oil Extracting

Harvesting microalgae has been described as one of the most challenging aspects of producing microalgae because of their low cell diameters, which range from 2 to 20 μm (Lardon et al., 2009). However, microscreen, centrifugation and flocculation are the most common harvesting methods currently used (Amin, 2009). Centrifugation is efficient and reliable, but expensive for producing microalgae as energy (Shen et al., 2009). The extraction of microalgae oil from the biomass can be conducted using physical or chemical methods. An oil press is used for physical extraction, while the

chemical extraction makes the extraction more effective. Microalgae lipid can be extracted using chemicals such as benzene, ether or hexane, which can be combined with a cold press to extract more than 95% of the total lipid present in the algae. Ultrasound can assist in lipid extraction: an ultrasonic reactor can be used to crack the cells' membranes by the action of cavitation bubbles that break the cell wall (Anderson & Sorek, 2009). The lipid from microalgae has also been extracted using chloroform and methanol (2/1, volume to volume [v/v]) in a study by Liu et al. (2008).

Hossain et al. (2008) determined the biomass productivity by weighing the microalgae biomass after filtration; the lipid was then extracted by drying the algae at 80 ^{o}C for 20 minutes. The dried microalgae were mixed with a mixture of 20 mL each of hexane and ether solution. After that, the mixture was left to settle for one day, and then the mixture was filtered to separate the biomass. The oil was evaporated using a rotary evaporator to release the hexane and ether solution.

2.8.4 Microalgae Oil and Biodiesel Properties

It is essential to choose a suitable microalgae species for biodiesel production because of the variation in chemical components (Huang et al., 2010). The main components of biodiesel are short-chain FAs (C14 to C18), which are components of FAs in *Chlorella* species. Long-chain FA and hydrocarbons are often found together in some specific microalgae species.

MCP biodiesel showed a high heating value of 41 MJ/kg and density of 0.864 kg/L in a study by Xu et al. (2006). This heating value is higher than the maximum calorific value of *Chlorella emersonii* and *Chlorella vulgaris* of 29 MJ/kg (Illman et al., 2000). The heating values of biodiesels from different sources of plants and/or

microalgae species vary. Biodiesel from microalgae has a higher heating value (41 MJ/kg) than the heating value (37 MJ/kg) of biodiesel from rapeseed or soybeans (Campbell, 2008; Xu et al., 2006).

A comparison between microalgae biodiesel, diesel fuel and the ASTM biodiesel standard is shown in Table 2.2. This table illustrates that the density of microalgae biodiesel is within the limits of the ASTM standard and higher than that of diesel. The viscosity of microalgae biodiesel is above the ASTM range as well as that of PD. The heating value of microalgae biodiesel is close to that of diesel. Further reviews are provided in Chapters 3 and 4.

Table 2.2 Comparison of properties of biodiesel from microalgal biodiesel, diesel fuel and the ASTM biodiesel standard (Miao & Wu, 2006)

Properties	Biodiesel from microalgae	Diesel fuel	ASTM biodiesel standard
Density (kg/L)	0.864	0.838	0.86–0.9
Viscosity (mm^2/s, cSt at 40 °C)	5.2	1.9–4.1	3.5–5.0
Flashpoint (°C)	115	75	Min 100
Solidifying point (°C)	−12	−50 to 10	–
Cold filter plugging point (°C)	−11	−3.0 (max −6.7)	Summer max 0; winter max < −15
Acid value (mg KOH/g)	0.374	Max 0.5	Max 0.5
Heating value (MJ/kg)	41	40–45	–
H/C ratio	1.81	1.81	

2.9 Diesel Engine Test Using Biodiesel Fuel

The FA components of biodiesel affect the fuel properties that lead to changes in engine characteristics such as injection timing and duration, combustion, performance and exhaust gas emissions (Ozsezen et al., 2009). Diesel engine combustion, performance and exhaust gas emissions using different sources of biodiesel have been widely studied. For instance, Al-Widyan et al. (2002) studied the use of ethyl ester from vegetable oil in a single-cylinder, direct injection diesel

engine. They performed a variable speed test using different blends with PD. The B100 fuel and the blend of B75 produced the best engine performance. Dorado et al. (2003a) tested biodiesel from waste olive cooking oil in a direct injection diesel engine. A satisfactory performance and statistically insignificant differences were achieved throughout the test using biodiesel and diesel fuel. However, up to a 26% increase in the brake specific fuel consumption (BSFC) and less than 8% of the power loss in comparison with those of PD were identified.

Biodiesel produced from unrefined rubber seed oil was experimentally investigated in CI engines by Ramadhas et al. (2005). They concluded that biodiesel from rubber seed oil is an acceptable alternative fuel that can run diesel engines successfully and no modifications are required. In another study, non-edible biodiesel from polanga (*Calophyllum inophyllum* L.) produced by a triple-stage transesterification process was tested by Sahoo et al. (2007) in a diesel engine. The test was conducted at different engine loads and speeds using polanga biodiesel in different blends with PD. B100 presented better results of thermal efficacy and exhaust gas emissions compared with those of PD. A study of the production of biodiesel from karanja oil was conducted by Stalin and Prabhu (2007). They concluded that B40 could run the engine with no modifications and at considerably lower cost. Four-cylinder diesel engine combustion, injection and performance were evaluated for used frying palm oil biodiesel and its blends with PD at full load conditions by Ozsezen et al. (2008). The main finding was that the brake power was lower than that from PD fuel for the biodiesel and its blends.

A constant engine speed test was performed by Ozsezen et al. (2009) using biodiesel from waste palm oil and canola oil. These biodiesels produced lower engine performance than diesel fuel. Although a reduction in CO, hydrocarbons (HC),

emissions and smoke opacity was recorded, the NO_x level was slightly increased by 22.13 % and 6.48 for waste palm oil and canola oil respectively. They concluded that these biodiesels could be used safely as fuel alternatives to PD based on the combustion results. In another study, waste cooking oil biodiesel was tested in a two-cylinder, four-stroke diesel engine in different blends with PD at different engine speeds. The blends of biodiesel from waste cooking oil enhanced the engine performance and gave better emission characteristics (Ghobadian et al., 2009).

An agricultural application diesel engine (3.5 kW) was used to investigate the optimum combination of different engine compression ratios and injection pressure using jatropha methyl ester for engine performance and emissions (Jindal et al., 2010). The results showed that brake thermal efficacy was increased and the BSFC and the emissions were reduced by increasing the compression ratio associated with increasing the injection pressure. In another study, Buyukkaya (2010) performed an experimental study using biodiesel from rapeseed oil and its blends of B5, B20, B70 B100 and PD in a diesel engine to evaluate the engine performance, combustion and exhaust gas emission characteristics. Combustion characteristics comparable to that of PD were found with biodiesel from rapeseed oil and its blends.

The combustion parameters and heat release from hazelnut biodiesel in a single-cylinder diesel engine were studied by Gumus (2010). The study was carried out for different blend ratios, loads, injection timing, injection pressure and compression ratios. It was concluded that although the hazelnut biodiesel blends ran the engine properly without modification, modifying the injection pressure, ignition timing, compression ratio and injection pressure significantly enhanced the engine combustion and heat release. Özener et al. (2012) tested different blend ratios of

biodiesel from soybean in a diesel engine as an alternative, environmentally friendly fuel to evaluate the combustion, engine performance and engine emissions.

The use of microalgae biodiesel in diesel engines has still not been fully addressed, and studies on its effect on engine performance, combustion and exhaust gas emissions are lacking. Haik et al. (2011) conducted study to understand the effect of using algae fuel on the combustion quality, in-cylinder pressure and heat release of in-cylinder pressure rise rate, maximum in-cylinder pressure and engine torque. They reported that the methyl ester properties of algae oil are similar to those of diesel, and thus they used algae fuel (both algae oil and algae oil methyl ester) successfully in a single-cylinder Ricardo engine. A detailed review is presented in Chapter 4.

2.10 Emulsified Water and Slurry Fuels

The higher NO_x emissions from biodiesel compared with those of PD are the main obstacle restricting the extended use of biodiesel fuel (Kass et al., 2009). Varatharajan and Cheralathan (2012) reported that the biodiesel market could be limited by the NO_x emissions. Emulsion fuel is formed from water in diesel or biodiesel fuel. Over the past 40 years, many studies have been conducted to decrease NO_x and parts per million (PPM) with no effect on fuel economy using emulsified water fuels (Kass et al., 2009). In addition, from the review of the causes of the high NO_x produced from biodiesel, researchers have concluded that the fuel's properties and characteristics influence the NO_x emission.

Nadeem et al. (2006) analysed the effect of emulsified water fuels prepared under different conditions on diesel engine performance and exhaust gas emissions. The variables affecting the preparation of emulsified water fuel were the blend ratio of water, diesel and surfactant, emulsification time and temperature, stirring intensity

and duration. They concluded that engine thermal efficiency insignificantly declined, but a significant reduction was achieved in the exhaust gas emissions. The emulsion of 15% water prepared using Gemini surfactant gave a high reduction in NO_x, particulate matter (PM), CO and sulphur oxide (SO_x).

The utilisation of single-cylinder diesel engines is preferred for fuel tests for several reasons, including their lower FC, ease of maintenance and sensors installation. A test close to the work of this thesis was performed by Davis et al. (2012). In their study, a single-cylinder Yanmar USA L70V engine was implemented to evaluate six types of fuel. The engine was connected to a Land and Sea water-brake dynamometer and gas analyser to evaluate the engine performance and NO_x emissions. The fuels were PD, B20, neat biodiesel (B100) and 10% (water by volume) emulsified water in PD (Em-PD), emulsified water in biodiesel B20 (Em-B20), and emulsified water in B100 (Em-B100). The study showed a significant reduction in NO_x emissions with Em-B20 and Em-B100 compared with PD and non-emulsified fuels. Power and thermal efficiencies were found to be significantly lower than those of B20 when the engine was fuelled with Em-B20.

The main drawback of emulsified water fuels is their high viscosity and lower heating value. Enhancing the heating value of emulsified water fuel is possible by adding high energy content additives. Emulsion fuels can be in the form of slurry. Slurry fuels are the fuels that contain suspension of finely ground particles (such as char) into bio-oil (Abdullah, 2010) or PD. Dealing with hydrocarbon particles (powder) such as char, coals and others partials as fuel is challenging in terms of injection, handselling, pumping and spray distribution. For diesel engine use, the particle size is another challenge that requires processing to pass through the injector. Forming a slurry of fine particles in liquid form is a proper solution for emulsified

water fuel and to overcome the challenges of using dry particles in diesel engines. Abdullah (2010) reported that slurry fuel technology was developed to improve fuel transportability and increase volumetric energy density. The rheological behaviour of emulsified water containing coal particles was investigated by Mishra et al. (2002), Boylu et al. (2004) and Abdullah et al. (2010). They reported that the viscosity varied based on the coal percentage, pH, temperature and particle size. Microalgae biomass has been proposed for use in diesel engines in the form of slurry of microalgae cells suspended in water that is emulsified in biodiesel. This technique was proposed by Scragg et al. (2003) to avoid the challenges of modifying a diesel engine to run with powder fuel. Further review and details are presented in Chapter 5.

2.11 Alternative Fuels for Agricultural Tractors

The agricultural sector has been seriously affected by the increased price of PD (Bettis et al., 1982). The vegetable oil production chain involves a series of agricultural and industrial processes in which diesel fuel is consumed. Using biodiesel fuel in the chain of vegetable oil production helps to reduce the demand on PD. Mariasiu and Varga (2010) commented that using biodiesel in the agriculture sector is a key factor to enhance the outcomes from the agricultural sector and stressed the importance of reducing emissions from agricultural mechanisation for sustainable agriculture. It has been reported that the production of biodiesel for use in agricultural tractors can be cost competitive with PD because of the useful by-product of biodiesel production that can be used as animal food or soil fertilisers (Tomić et al., 2013).

Tractors are the major power source in the agricultural field and one of the main fuel consumers in the biodiesel production chain. Tractor performance and exhaust gas

emissions using biodiesel fuels have been investigated in a few studies, such as those of Matthew et al. (2007), Neel et al. (2008), Mohebbi et al. (2012), Hunt et al. (2013) and Tomić et al. (2013). These studies found that biodiesel and diesel fuel had comparable results (details are presented in Chapter 6). It appears that microalgae biodiesel has not been studied as a fuel alternative for agricultural tractors.

2.12 Summary and the Research Gap

From the literature review, it can be summarised that diesel engines are an important power source for many sectors and significantly contribute to air pollution and high fuel prices. Alternative fuels for diesel engines are essential to overcome fossil fuel problems. One of the major arguments against the production of biodiesel from agricultural crops is that it will result in food shortages and raise food prices. However, the production of biodiesel from microalgae circumvents these arguments. Microalgae are preferred because of their higher biomass and biodiesel productivity and because they can convert CO_2 to useful oil. Different species of microalgae have different FAME profiles that affect the biodiesel properties. Biodiesel fuel has been successfully used in the current diesel engines with no modifications. Studies have found that, generally, biodiesel gives comparable to slightly lower power and lower exhaust gas emissions than PD.

The research gap

1. A large volume of published studies have discussed FAs and biodiesel from microalgae, but little attention has been paid to the effect of increasing the FWM-CV lipid content on the FA components and, therefore, on biodiesel properties.

2. Understanding of the influence of using MCP biodiesel (MCP-B) in any blend ratio on the diesel engine performance and exhaust gas emissions is still lacking.
3. Data related to the properties and the effect of emulsified water fuel with microalgae cells on diesel engine performance and emissions are still limited.
4. Agricultural tractor PTO testing with microalgae biodiesel (with any blend ratio) is lacking.

CHAPTER THREE

Biodiesel from Freshwater Microalgae *Chlorella Vulgaris* (FWM-CV)

3.1 Introduction

This chapter focuses on the growing of microalgae on a small scale only because large-scale production was not possible during the available time for this study. The research details the production of a small amount of microalgae, which provided a better understanding of biodiesel production from microalgae. The microalgae biomass production comprised microalgae growing, harvesting and lipid extraction. The lipid analysis under different growing conditions is presented in this chapter. The chapter consists of the following:

- background and literature review
- materials and methods
- results and discussion
- summary and conclusion of the chapter.

3.2 Background and Literature Review

3.2.1 *Chlorella Vulgaris* Biofuel

The *Chlorella* species grows fast and is easily cultivated, which makes it an ideal source of energy. The freshwater *Chlorella* species is considered an acceptable lipid

accumulation species (Cheirsilp & Torpee, 2012). However, it is not yet commercially viable because of its relatively low lipid content compared with that of other species (Liu et al., 2008). Therefore, increasing the lipid content in this species to increase lipid productivity is fundamental. Meeting the dual requirements of maximising biomass and lipid production is difficult to achieve. Widjaja et al. (2009) reported that various researchers have claimed that lipid storage in many microalgae can be enhanced under environmental stress. Increasing the lipid content under stress conditions would decrease the biomass productivity. The productivity of biomass and the productivity of the lipid content of *Chlorella vulgaris* can both be enhanced if specific culture conditions are applied, as reported by Lv et al. (2010). The lipid content was increased to up to 56.6% of the dry biomass weight by adding 1.2×10^{-5} mol/L $FeCl_3$ (Liu et al., 2008). The lipid content of *Chlorella vulgaris* is significantly affected by variation of the growing condition parameters. For example, Converti et al. (2009) stated that the lipid content of microalgae decreased from 14.71% to 5.90% when the growing temperature increased from 25 °C to 30 °C. A recent study by Lam and Lee (2012) confirmed that *Chlorella vulgaris* can grow when organic fertiliser is used as an alternative nutrient; however, it was noticed that it grew poorly in an open environment but survived when cultivated in reused water.

The FAMEs for biodiesel are important parameters because they vary with the biodiesel sources. Microalgae oil contains high values of palmitic acid, and the concentration of linoleic acid meets the requirement of the European legislation for biodiesel (Converti et al., 2009). The variation of the FAMEs can significantly affect the biodiesel properties. Woertz (2008) performed a study on the total lipid content in waste water for biodiesel production.

In most studies on biodiesel from microalgae, the focus has been on the lipid content; few studies have focused on the effect of the culture medium, such as waste water, nutrient type, growing time and other factors, on the properties (FAME profile) of biodiesel from algae.

3.2.2 FAMEs and Biodiesel Properties

Biodiesel chemical and physical properties are indicators of fuel quality. The differences between biodiesel properties result from the differences in the FA components in the biodiesels (Knothe, 2008). The properties of biodiesel fuel are the outcome of its individual fatty ester properties and structure, such as chain length, degree of unsaturation and branching of the chain. These parameters of the FA esters influence the cetane number, heat of combustion, cold flow viscosity and exhaust emissions (Knothe, 2005).

Precise measuring of biodiesel properties is relatively difficult and expensive. When small volumes of biodiesel are produced, calculating or estimating the biodiesel's physical properties based on their FAMEs is valuable. Ramírez-Verduzco et al. (2011) estimated the density, viscosity, cetane number and higher heating value for tallow and soybean biodiesel using a developed empirical equation. They found that the increase in the number of double bonds in the FAMEs caused a reduction in the values of cetane number, viscosity and higher heating value.

This chapter discusses the work of growing microalgae on a laboratory scale to achieve the following objectives:

- Culture FWM-CV in a complete nutrient medium (called MBL), and then compare the biomass productivity and the lipid productivity of FWM-CV with published results.
- Stimulate lipid production by adding iron to the microalgae culture to identify the FAMEs in the FWM-CV biodiesel and its physical properties.
- Study the effect of enhancing the lipid content on the FAMEs profile and the physical properties of the FWM-CV biodiesel.
- Produce FWM-CV biomass to be used as an additive with water to another biodiesel in a diesel engine.

3.3 Materials and Methods

3.3.1 Microalgae Strain

The *Chlorella* species is one of the most studied microalgae for biodiesel production. The species are fast growing and can grow in a variety of conditions. A culture of FWM-CV (CCAP 211/11) was obtained from the Centre for Marine and Atmospheric Research (CMAR) of the Commonwealth Scientific and Industrial Research Organisation (CSIRO) in Hobart, Tasmania. The microalgae samples were grown in MBL at room temperature by inoculating 1 mL of the stock culture into 40 mL of MBL medium for culture refreshment and to increase the amount of culture. The inoculation ratio for the experiments was then increased to 1:10.

3.3.2 Culture Medium

In this study, the MBL medium (Nicolas 1973) adapted for freshwater microalgae was used for the culture maintenance and experimental work. The stock solution was prepared from different chemicals, as detailed in Table 3.1, by dissolving the

chemical components in Milli-Q water. The stock solutions were stored in the refrigerator at of 4 ºC.

Table 3.1 Components of the MBL medium

Stock solutions		Concentration per litre of distilled water (g/L)	
1. $CaCl_2.2H_2O$		36.76	
2. $MgSO_4.7H_2O$		36.97	
3. $NaHCO_3$		12.60	
4. K_2HPO_4		8.71	
5. $NaNO_3$		85.01	
6. $Na_2SiO_3.9H_2O$		28.42	
7. Na_2EDTA		4.36	
8. $FeCl_3.6H_2O$		3.15	
9. Metal mix	$CuSO_4.5H_2O$	0.01	Each constituent was added separately to ~750 mL of dH_2O then completed to up to 1 L with dH_2O.
	$ZnSO_4.7H_2O$	0.022	
	$CoCl_2.6H_2O$	0.01	
	$MnCl_2.4H_2O$	0.18	
	$Na_2MoO_4.2H_2O$	0.006	
10. Vitamin stock	Cyanocobalamin (Vitamin B12)	0.0005	
	Thiamine HCl (Vitamin B1)	0.10	
	Biotin	0.0005	
11. Tris stock		250.0	

To prepare the MBL medium, 1 mL of each stock solution (1 to 11) was added to 1 L of Milli-Q water. The pH was adjusted to 7.2 using hydrochloric acid. The media was autoclaved at 121 °C (15 psi) for 15 minutes.

The stock solution of the iron stressor ($FeCl_3$ per EDTA) was prepared by dissolving 0.3244 g of EDTA and 0.1947 g of $FeCl_3$ in 200 mL of Milli-Q water, which was then autoclaved at 121 ºC for 15 minutes. One mL of this stock solution was added to each litre of media to reach the amount of 1.2×10^{-5} mol/L.

3.3.3 Culture Conditions

The FWM-CV was grown in the laboratories of the University of Southern Queensland (USQ) using a sterilised MBL medium. The lab temperature was

controlled and fixed at 22 ºC. Fluorescent light was used to supply constant light intensity for the culture, which was about 2500 lux or greater on a 16:8 light to dark cycle (Cheirsilp & Torpee, 2012). The cultures were grown in 5 L flasks. The cultures were supplied with air using an air pump to generate large, slow bubbles to mix the culture and to increase the contact of the microalgae with air. The air supply system was autoclaved and a 0.2 micron filter was used to prevent culture contamination.

3.3.4 Experimental Design

The small scale of microalgae growing was divided into two stages, as shown in Figure 3.1.

Stage 1 Culture growth: This stage aimed to refresh and increase the amount of culture and to understand the requirements for large-scale growing. It also aimed to evaluate the growth rate of the species to identify the growth rate of the late exponential phase, when the iron stressor would be added. The total lipid content was measured and analysed during this stage.

Stage 2 Culture enhancement: The aim of this stage was to study the effect of adding iron to the culture medium during the late exponential growth phase, as suggested by Liu et al. (2008), to increase the microalgae lipid content and the FAME components. To assess this addition, the culture was divided into two parts with three replicates being taking of each:

Part (a) The samples were kept as a control sample for 75½ days.

Part (b) A new medium was added to the culture in the ratio of 3:1 (v/v) on day 35, and after three days, 1.2×10^{-5} FeCl3/EDTA per litre was added to the

culture. The microalgae oil harvested was converted to biodiesel and analysed using gas chromatography mass spectrometry (GC-MS).

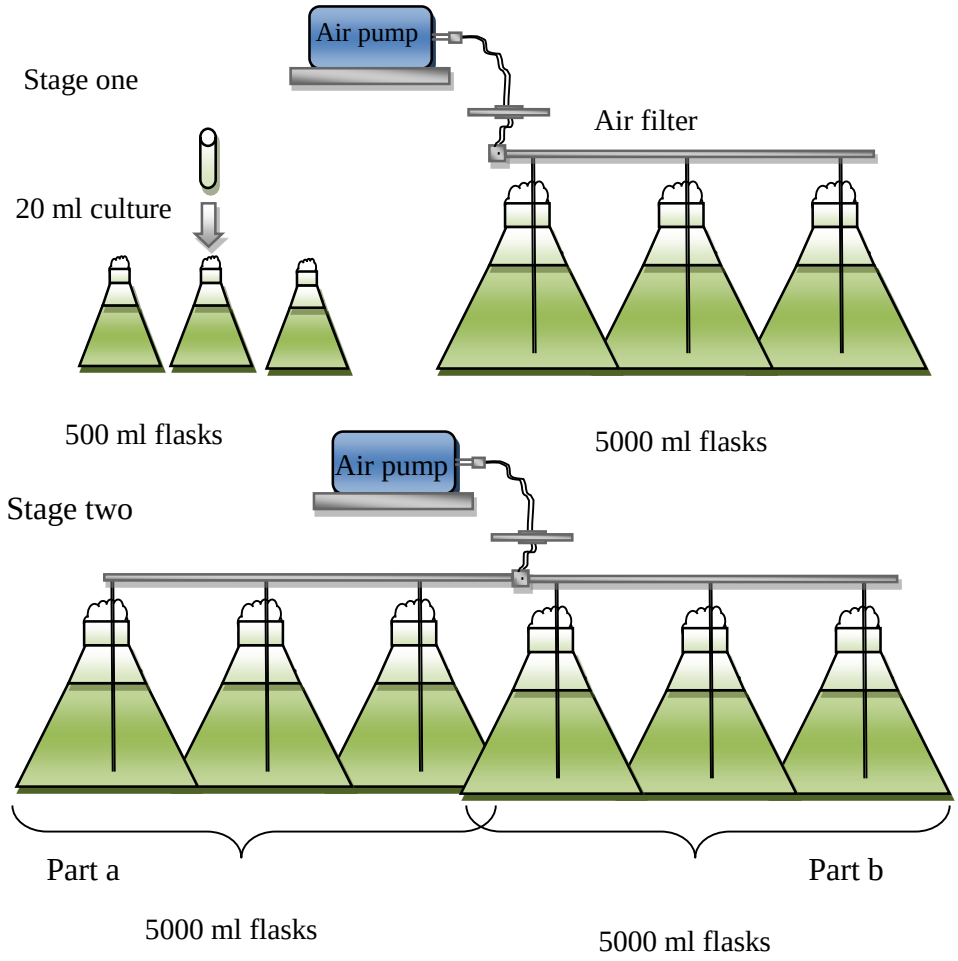

Figure 3.1 Schematic diagram for the experiment design

3.3.5 Growth Monitoring

The growth of the culture was measured using two different methods. The first method was to use a Neubauer haemocytometer and light microscope to measure the cell density for both chambers of the haemocytometer. The final cell number results from the mean of six counts of three measurements for both haemocytometer chambers were multiplied by the conversion factor of the Neubauer haemocytometer ($\times 10^4$). The second method was to monitor the growth curve by measuring the optical density (OD) of the culture at 515 nm. The OD is a simple and efficient

method for measuring the growth curve that enables a linear regression equation to be derived to describe the relationship between the OD and the cell density. The daily change in the culture growth was identified by monitoring the daily change in OD at 515 nm using a Jenway 6705 UV/visible spectrophotometer.

3.3.6 Microalgae Harvesting

The microalgae biomass was harvested using a Beckman Avanti J-251 high-speed centrifuge at 8000 rpm for 10 minutes. The samples were then transferred to pre-weighed Petri dishes. To determine the dry weight of the FWM-CV, the resulting biomasses were dried using a VirTis BenchTop K Manifold –55 °C freeze dryer for 24 hours and weighed (see Figure 3.2). Lyophilised cells were stored in desiccators until the time of oil extraction.

Another linear equation was derived to describe the relationship between the OD at 515 nm and the microalgae dry weight (Mdw). Three samples of 100 mL of microalgae culture at different growth phases and different microalgae concentrations were harvested using the centrifuge after measuring the OD. The samples were then freeze-dried and weighed to draw the relationship between the OD and the Mdw.

Figure 3.2 Freeze dryer

3.3.7 Lipid Extraction

The Folch (1957) for lipid extraction was used in this work. As recommended by Widjaja et al. (2009), each sample of dried microalgae was mixed with a solution of (2:1) chloroform (analytical grade, BDH chemicals) and methanol (analytical grade, Ajax Chemicals). The solution volume was 20 times greater than that of biomass. The mixture was then shaken for 20 minutes using a BioLine BL 4600 orbital shaker at 150 rpm. The solution, containing chloroform-methanol and lipid, was separated from the biomass by gravity filtration using MACHEREY-NAGEL MN 615 filter papers. This solution was collected in centrifuge tubes and then the lipid was rinsed in the test tube using chloroform to minimise lipid losses. These tubes were refilled by volume of Milli-Q water equal to 20% of the total volume of the sample. To separate the chloroform-methanol phase, the samples were centrifuged at 3000 rpm for 10 minutes. The upper layer was discarded by siphoning using a Pasteur pipette and the lower phase containing lipids was evaporated under vacuum in a rotary

evaporator. The samples were dried and left at room temperature for one day for further drying, then weighed to determine the lipid content.

3.3.8 Statistical Analysis

To evaluate the differences between various growing methods, Choix et al. (2012) used analysis of variance (ANOVA) and the Least Significant Difference (LSD) post hoc test to analyse the difference in the variables of volumetric productivity and growth rate of microalgae. The post hoc test is used if ANOVA (F-Test) showed a significant effect of the independent variable (consist of more than two levels) on the dependent variable to identify the significant differences between the means (Stevens, 1999). In this work, a one-way ANOVA test was performed using IBM SPSS Statistics 19 software to study the significance of the change in microalgae productivity parameters. The parameters investigated were microalgae dry weight g/L, biomass productivity mg/L.day, lipid content percentage and lipid productivity mg/L.day during the experiment in stage one, the control sample in stage two and the iron supplemented culture (ISC) sample test.

3.3.9 Transesterification

The oil extracted from the FWM-CV was converted to biodiesel using transesterification. The transesterification was conducted by heating the lipid to 48 ^{o}C; then 0.45 g of NaOH was added to 11 mL of methanol and shaken. Due to the low lipid weight, the amount of this mixture was increased to around 20 times greater than the lipid weight and then added to the lipid samples for 40 minutes with shaking. After 10 hours, the oil phase was separated to another flask and centrifuged to remove the glycerine.

3.3.10 FAME Analysis and Physical Properties

The FAMEs and their percentage in the FWM-CV biodiesel for both the control and the ISC samples were identified using the Shimadzu GC-2010 gas chromatograph mass spectrometer. The density, cetane number, kinematic viscosity and heating value of the biodiesels from the control and ISC samples were calculated from their FAMEs and their percentage.

3.4 Results and Discussion

3.4.1 Biomass Productivity

Monitoring microalgae growth rate using microscopy and a haemocytometer is a slow and time-consuming method, particularly when a large number of samples are to be tested. In contrast, OD using a spectrophotometer is an easy and quick method that gives a good indication of cell density, once a linear regression equation has been derived for FWM-CV, as presented in Equation 3.1 and Figure 3.3.

$f_{CD} = 1 \times 10^7 (f_{OD}) - 422466$ Equation 3.1
$R^2 = 0.98$,

Where f_{CD} is cell density in cell/mL, f_{OD} is the OD at 515 nm.

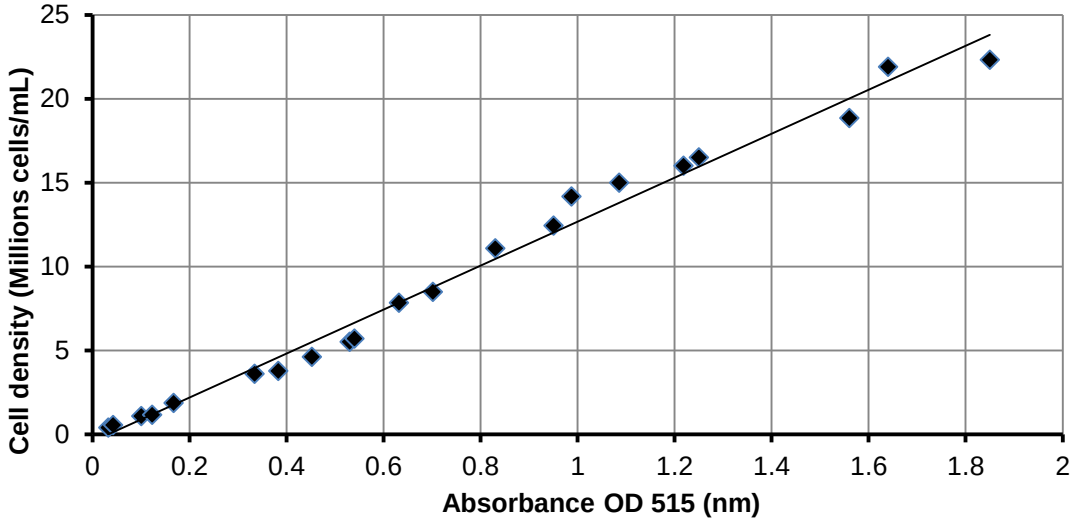

Figure 3.3 Correlation between optical density (OD) and cell density for FWM-CV in MBL medium

Cell density per volume of media could be an unsuitable indicator for biomass and biodiesel production. Thus, another linear correlation was found for FWM-CV in MBL between the OD and the dry weight of microalgae, as shown in Figure 3.4, where f_{Mdw} is the dry weight of microalgae in milligrams (Mdw).

$f_{Mdw} = 0.3497\ (f_{OD}) - 0.0022$ Equation 3.2
$R^2 = 0.978$.

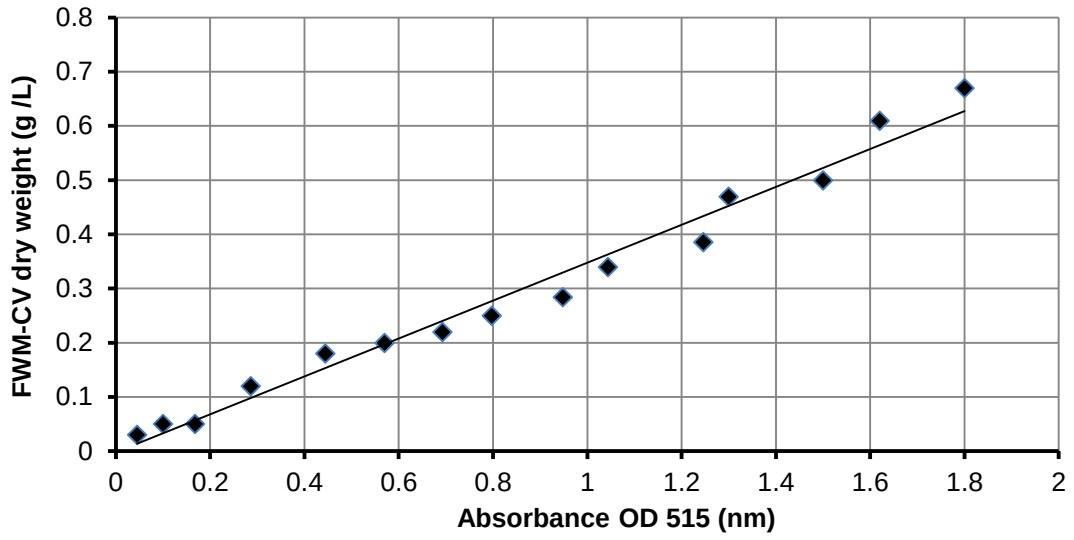

Figure 3.4 Correlation between optical density and microalgae dry weight (g/L) for FWM-CV in MBL medium

Figure 3.5 shows the growth curve of FWM-CV in MBL for 32 days. This figure shows that the growth rate in the first week was relatively slow because of the low inoculation ratio (small number of cells added to the new media). In the subsequent three weeks, the growth rate turned exponential. In the period of 28 to 32 days, the growth started to slow and the late exponential growth rate was identified to shift to the second stage.

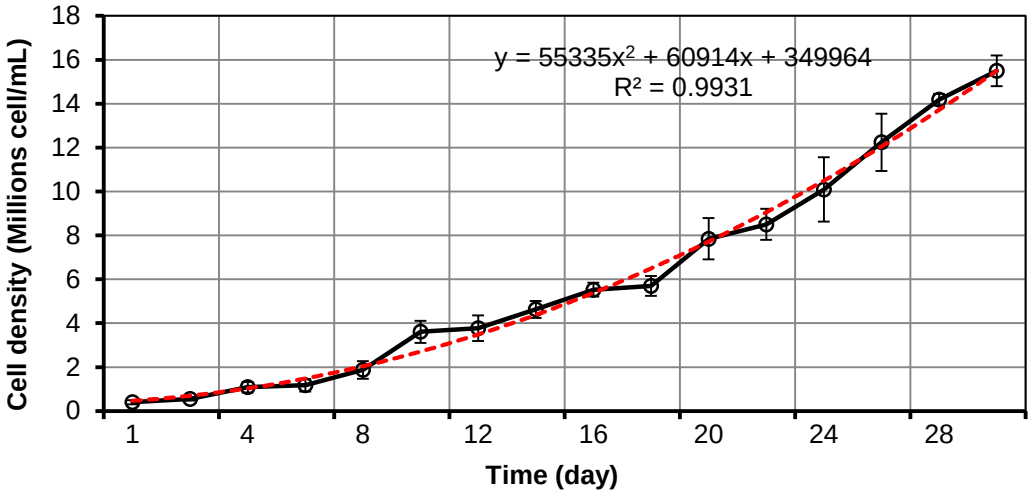

Figure 3.5 FWM-CV growth curve in MBL medium

In the first stage, the FWM-CV was grown in MBL for 40 days to increase the amount of cultures and to divide and transfer it to stage two of the experiment. Table 3.2 shows the summary of ANOVA and descriptive statistic of FWM-CV dry weight (g/L), biomass productivity (mg/L.day), lipid content (%) and lipid productivity (mg/L.day) for stage one and stage two (samples of control and ISC), and compares the results with the results of Lee et al. (2010) and Mata et al. (2010). Table 3.2 indicates that the dry weight of FWM-CV differed significantly in the samples in stage one, the control in stage two and the ISC differ significantly.

The post hoc LSD test presented in Table 3.2 indicates the differences between dry weights in each stage by different letters. The post hoc LSD shows that the maximum significant value of dry weight (0.89 g/L) was significantly higher than that of the control samples in stage two and stage one. It was also found that the control sample in stage two had a higher dry weight than stage one. These differences can be justified by the time of growing, also presented in Table 3.2. The longer the time of growing was, the higher the dry weight was. From Table 3.2, it can clearly be seen that the dry weight of microalgae in stage one of 0.49 g/L was lower than the results of Lee et al. (2010), although the growing time was longer. This can be attributed to the lower concentration of FWM-CV in the medium, which took a longer time to reach the concentration equal to that reported by Lee et al. (2010) in one week. The results in stage two of the control and ISC samples were 0.64 g/L and 0.89 g/L, respectively, which are both greater than Lee et al. (2010) results because of the significant difference in culturing time. The ISC sample surpassed the control sample in producing biomass dry weight because of the new medium added, and the extra period of three days. The biomass productivity (mg/L.day) in the ISC increased by 39.3% compared with the control sample.

Table 3.2 Microalgae *Chlorella vulgaris* productivities

Properties	Stage one		Stage two				F	CV **(Lee et al., 2010)**	CV **(Mata et al., 2010)**
			Control sample		ISC sample[+]				
	Means	SD	Means	SD	Means	SD			
Growing time (days)	40		75.5		78.5			7	–
Dry weight (g/L)	0.49c	0.04	0.64b	0.06	0.89a	0.08	41.64***	0.5	–
Biomass productivity (mg/L.day)	12.16b	1.11	10.6b	0.97	14.76a	1.33	13.39***	74.2	20–200
Lipid content %	10.06b	0.90	8.94b	0.82	19.27a	1.70	88.16***	14.96–5.58	5.0–58
Lipid productivity (mg/L.day)	1.23b	0.11	0.74 c	0.07	2.19a	0.19	121.76***	11.10–6.91++	11.2–40.0

[+] Iron supplemented culture in which new media and $FeCl_3$ were added after 38 days.
[++] Calculated from lipid content, dry weight, lipid productivity, biomass productivity and time.
*** $p \leq 0.001$.
[a,b,c] Means in the same row that do not share a letter are significantly ($p \leq 0.05$) different by the LSD post hoc.

To eliminate the differences in culturing time, the biomass productivity was measured by mg/L.day (dividing the biomass dry weight by the sample volume and the growing time), which provided a better indicator of productivity. The ANOVA test results shown in Table 3.2 presented very high significant differences between the biomass productivities in the studied test. The post hoc LSD test indicated that the ISC sample significantly surpassed the control sample in stage two and stage one by producing 14.755 mg/L.day. Meanwhile, the post hoc LSD test indicated that the 1.56 mg/L.day difference between the stage one sample and the control sample in stage two was insignificant. The difference in biomass productivities between stage one and the control sample in stage two was due only to the difference in the growing duration (all other conditions are the same). Increasing the time of growing from 40 days to 75.5 days resulted in a reduction in the nutrients in the medium, which affected the biomass productivity in the control sample in stage two. The significantly higher biomass productivity in the ISC samples (14.755 mg/L.day) compared with stage one and the control samples was caused by the new medium

added on day 38 that offered more nutrients. Table 3.2 also shows that the biomass productivity of FWM-CV in MBL given in stage one and stage two are lower than the results of Lee et al. (2010) and Mata et al. (2010). The reason for this difference was the low concentration of FWM-CV culture at the start of growing, which required a longer time to reach the same concentration as detailed in Lee et al. (2010) and Mata et al. (2010).

3.4.2 Lipid Content and Lipid Productivity

Table 3.2 presents a comparison of the biomass and lipid productivities of FWM-CV in the different stages. Table 3.2 shows that the lipid content and the lipid productivity significantly changed during the experiment. The results of the ISC sample indicate that the lipid content and the lipid productivity significantly increased from 8.9% to 19.3% and from 0.74 mg/L.day to 2.19 mg/L.day, respectively, as shown in Table 3.2. This increment is significantly lower than the results obtained by Liu et al. (2008). The stage one and the control sample results reveal a lower lipid content compared with the results obtained by Lee et al. (2010) and in the lower range of those of Mata et al. (2010). Possible reasons for the low results are the amount of time, low amount of nutrients for lipid production in the growing media and the low percentage of carbon sources in the autotrophic growing conditions present. The efficiency of the lipid extraction was also low and there was potential for loss of lipid in the glassware when transferring the product.

3.4.3 FAME Components

The differences in the FAME components in FWM-CV biodiesel for the control sample and ISC samples, which have been compared with the components reported by Harwood (2004), are illustrated in Table 3.3. The results demonstrate that adding

$FeCl_3$ to the medium in the ISC sample made a significant difference in the FAMEs of FWM-CV. The percentage of some FAMEs increased and others decreased in comparison with the control sample and the components reported by Harwood (2004). For instance, in the ISC sample, there was a significant reduction in the percentage of palmitic acid methyl ester ($C_{17}H_{34}O_2$) (4.5%) and α-linoleic acid methyl ester ($C_{19}H_{32}O_2$) (2.5%) compared with the results of the control sample and as reported by Harwood (2004). In contrast, there was a significant increase in the percentage of palmatoleic acid methyl ester ($C_{17}H_{32}O_2$), stearic acid methyl ester ($C_{19}H_{38}O_2$) and linoleic acid ($C_{19}H_{34}O_2$): 29.5%, 31.5% and 29.6%, respectively. Such changes affect the properties of biodiesel in terms of density, cetane number, kinematic viscosity and heat of combustion.

Table 3.3 FAMEs in microalgae *Chlorella vulgaris*

Fatty acids (FAs)	FA formulas	FAs of M-CV *(%)	FAME names	FAME formulas	FAMEs of FWM-CV (%)	
					Control	ISC
Acid (C14:0)	$C_{14}H_{28}O_2$	–	Myristic acid methyl ester (Methyl myristate)	$C_{15}H_{30}O_2$	–	2.33
Palmitic acid (C16:0)	$C_{16}H_{32}O_2$	26	Palmitic acid methyl ester (Methyl palmitate)	$C_{17}H_{34}O_2$	23.74	4.52
Palmatoleic acid (C16:1)	$C_{16}H_{30}O_2$	8	Palmatoleic acid methyl ester (Methyl palmitoleate)	$C_{17}H_{32}O_2$	16.48	29.54
Hexadecadienoic acid (C16:2)	–	7	-	-	-	-
Linolenic acid (C16:3)	–	2	-	-	-	-
Stearic acid (C18:0)	$C_{18}H_{36}O_2$	-	Stearic acid methyl ester (Methyl stearate)	$C_{19}H_{38}O_2$	21.84	31.50
Oleic acid (C18:1)	$C_{18}H_{34}O_2$	2	Oleic acid methyl ester (Methyl oleate)	$C_{19}H_{36}O_2$	-	-
Linoleic acid (C18:2)	$C_{18}H_{32}O_2$	24	Linoleic acid methyl ester (Methyl linoleate)	$C_{19}H_{34}O_2$	24.64	29.59
α-Linoleic acid (C18-3)	$C_{18}H_{30}O_2$	20	α-Linoleic acid methyl ester (Methyl gamma linolenate)	$C_{19}H_{32}O_2$	13.29	2.52

* Fatty acids (FAs) in microalgae *Chlorella vulgaris* (M-CV) (Harwood, 2004)

3.4.4 Physical Properties

Table 3.4 illustrates the physical properties of the common FAMEs as reported in the literature. These properties were used to calculate the physical properties for the FAMEs in the FWM-CV. Table 3.4 shows that the highest density value was 0.901 g/cm^3 for α-linoleic acid methyl ester ($C_{19}H_{32}O_2$), and the lowest density was for stearic acid methyl ester ($C_{19}H_{38}O_2$) at 0.864 g/cm^3. These values show agreement with the findings of Ramírez-Verduzco, Rodriguez-Rodriguez and Jaramillo-Jacob (2011) that for the same carbon number, increasing the number of double bonds increases the density.

Viscosity is one of the most important physical fuel parameters. Biodiesel normally has a higher viscosity than diesel (Knothe & Steidley, 2005). Table 3.4 shows that the saturated FAMEs, stearic acid methyl ester ($C_{19}H_{38}O_2$) and palmitic acid methyl ester ($C_{17}H_{34}O_2$), had a higher kinematic viscosity (5.85 mm^2/s and 4.38 mm^2/s, respectively) compared with the unsaturated FAMEs. Similarly, the saturated FAMEs presented a higher cetane number than that of the unsaturated FAMEs. The highest cetane numbers were 86.9 and 74.5 for stearic acid methyl ester ($C_{19}H_{38}O_2$) and palmitic acid methyl ester ($C_{17}H_{34}O_2$), respectively.

The heat of combustion is another important fuel property: it is an indicator of the energy in the fuel. Mehta and Anand (2009) found a high degree of correlation between the number of double bonds and the lower heating value of the FAMEs; for example, with C_{18} compounds, the lower heating value decreases with an increase in the number of double bonds. This is shown in Table 3.4, which presents the highest heat of combustion in the saturated FAME stearic acid methyl ester ($C_{19}H_{38}O_2$): 40.1 MJ/kg.

The kinematic viscosity, cetane number and higher heating value of the FAMEs in FWM-CV show good agreement with the findings of Ramírez-Verduzco, Rodríguez-Rodríguez and Jaramillo-Jacob (2011) that the kinematic viscosity, cetane number and higher heating values increase when the number of double bonds decrease.

Table 3.4 Some physical properties of common FAMEs

	Cetane number	Density (g/cm^3)	Kinematic viscosity (40 °C mm^2/s)	Heat of combustion (MJ/kg)
Myristic acid	66.2[a,b,c]	0.867[d]	3.3[e]	38.9[d]
Palmitic acid	74.5[a,c]	0.865[d]	4.38[e]	39.45[d,g]
Palmatoleic acid	51.0[a,b]	0.869[d]	3.67[f]	39.30[d,g]
Stearic acid	86.9[a]	0.864[d]	5.85[e]	40.1[d,g]
Linoleic acid	38.2[a,b]	0.886[d]	3.65[e]	39.7[d,g]
α-Linoleic acid	22.[b,c]	0.901[d]	3.14[e]	39.34[d],[g]

[a] (Knothe, 2005), [b] (Tong et al., 2011), [c] (Bamgboye & Hansen, 2008), [d] (Ramírez-Verduzco et al., 2011), [e] (Knothe & Steidley, 2005), [f] (Knothe & Steidley, 2007), [g] (Knothe, 2008).

Table 3.5 presents the calculated physical properties of the biodiesel from FWM-CV. The table shows that the density of the control and ISC samples were higher than the density of diesel, and were in the same range as biodiesel standards. The control sample presented a higher density than the ISC sample because of the higher percentage of α-linoleic acid methyl ester ($C_{19}H_{32}O_2$) (13.29%), which has a viscosity of 0.901g/cm^3 (Bamgboye & Hansen, 2008).

Table 3.5 also indicates that the kinematic viscosity of biodiesel from the ISC samples was insignificantly higher than that for the control sample by 2.88%. This increase was caused by the high percentage of stearic acid methyl ester ($C_{19}H_{38}O_2$) (31.50%) in the ISC sample, which has a viscosity of 5.85 mm^2/s (at 40 °C), as reported in (Ramírez-Verduzco et al., 2011). However, the percentage of palmitic acid methyl ester ($C_{17}H_{34}O_2$) in the ISC sample at 4.52% was lower than the control sample at 23.74%.

The heats of combustion of the control and ISC samples were relatively close. Biodiesel from FWM-CV presented a heat of combustion lower than that of diesel and in the range of biodiesel standards.

Table 3.5 Density, cetane number and kinematic viscosity for *Chlorella vulgaris*, diesel and biodiesel.

	Density (kg/m)	Cetane number	Kinematic viscosity (40 ^{o}C mm^2/s)	Heat of combustion (MJ/kg)
Control sample	875.31	57.499	4.239	39.6
ISC sample	873.03	59.224	4.361	39.7
Diesel	838[c]	46.00[d]	1.9–4.1[a]	45.3–46.7[f]
Biodiesel	860–900[c]	≥47[e]	1.9–6.0[b]	39.3–39.8[f]

[a] Standard ASTM D957 method ASTM D445 (Knothe & Steidley, 2005), [b] Standard ASTM D6751 method ASTM D445 (Knothe & Steidley, 2005), [c] (Miao & Wu, 2006), [d] D613 ASTM method (Robert et al., 2001), [e] (Meher et al., 2006), [f] Higher heating value (Kahraman, 2008).

3.4.5 Growing of FWM-CV for the Emulsified Water Fuel Experiment

Due to the inability to cultivate the microalgae on a large scale to obtain a proper amount of biodiesel, the FWM-CV that was grown was used as fuel for diesel engines in the form of emulsion. The emulsified water containing FWM-CV cells is described in detail in Chapter 5. For this purpose, a fresh culture was grown using sterilised 15 L water bottles (see Figure 3.6). Each bottle was filled with 8 L of medium, and one g/L of glucose was added to enhance growth. Photoautotrophic growing of microalgae requires light. Heterotrophic growth (the availability of a carbon source such as glucose in the medium) enhances the growth and the lipid accumulation of some microalgae species (Wen & Chen, 2003). The cultures were harvested every month and a new culture started. The growth continued for about 12 months.

Figure 3.6 Growing FWM-CV for the emulsified water experiment

3.5 Conclusion

In this work, FWM-CV was grown in MBL medium to monitor the growth curve, biomass productivity, lipid content and FAME components and evaluate the physical properties of microalgae biodiesel fuel. The growth of FWM-CV was monitored using two methods: cell count per millilitre and OD for the culture. Two linear equations were developed: the first was the relationship between the OD (at 515 nm) and cell density (cell/mL) and the second was the relationship between OD at 515 (nm) and microalgae dry weight (g/L). To increase the lipid content, iron was added to the media as stressor treatment. Adding iron to the culture medium was found to have a positive influence on the lipid content; however, the biomass and lipid productivity were still low. Different growing conditions were found to produce different FAME components, which led to different biodiesel properties. The results demonstrate that the physical properties of FWM-CV biodiesel and conventional diesel are close. The ISC sample produced a higher lipid content and varied FAME components in comparison with the control sample. The control and ISC samples

produced relatively low productivities. The ISC sample produced higher kinematic viscosity and higher heat of combustion compared with the control and diesel. There was an insignificant difference in density and heat of combustion between the control and ISC sample. The kinematic viscosity and the density of FAME from FWM-CV were within the range of the ASTM standard for biodiesel. The cetane number was higher than that of conventional diesel.

CHAPTER FOUR

Diesel Engine Performance and Emissions Using Different MCP-Biodiesel Blend Ratios

4.1 Introduction

This chapter focuses on the experimental work of preparing MCP biodiesel in different blend ratios and evaluating their properties. This chapter also focuses on the experimental work of studying single-cylinder diesel engine performance and exhaust gas emissions using MCP-B20, MCP-B50 and MCP-B100 at different engine speeds with maximum fuel supply line at wide open throttle (WOT). This chapter covers the following:

1. background and literature review
2. methodology and experimental set-up
3. results and discussion
4. conclusion.

4.2 Background and Literature Review

In the following sections, the engine performance and emission parameters from a variety of sources (including microalgae) are reviewed.

4.2.1 Microalgae Biodiesel for Diesel Engine

Microalgae biodiesel has been reported to have fuel properties similar to those of PD and the potential to fuel diesel engines with less modification. Haik et al. (2011) tested microalgae fuels in a Ricardo diesel engine and investigated the factors affecting the in-cylinder pressure wave and maximum in-cylinder pressure rise. They used PD, crude microalgae oil and biodiesel. In their study, the engine emission parameters were not investigated. In a more recent study, Wahlen et al. (2012) investigated engine performance and emission using PD and biodiesel from soybean, microalgae (*Chaetoceros gracilis*), bacteria and yeast. In their study, the exhaust gas emissions were tested only under no-load conditions at 3500 rpm.

Chen et al. (2012) studied MCP-B100 properties prepared from MCP-O obtained from the Soley Institute. Their results showed that MCP-B100 properties are in the acceptable range of fuel properties to run the current diesel engines. Research on the physical and chemical properties of microalgae oil and biodiesel and their behaviour in diesel engines is lacking, according to (Haik et al., 2011). They compared engine performance using crude microalgae oil, microalgae biodiesel prepared using 10% methanol, microalgae biodiesel prepared using 20% methanol, microalgae biodiesel B50 and PD. Their results showed that the crude oil presented better engine performance than the microalgae prepared with 20% methanol and had longer ignition delay. The biodiesel prepared using 10% methanol produced performance characteristics of torque higher than the biodiesel prepared using 20% methanol, and both fuels produced lower torque than the crude microalgae oil. The microalgae biodiesel produced higher heat release than PD at all engine loads in this study.

4.2.2 Engine Performance

Combustion Characteristics

In-cylinder pressure, heat release and ignition delay are parameters that affect the combustion process. Indicated power can be calculated from the in-cylinder pressure. The rapid combustion of fuel produces in-cylinder pressure wave that results in diesel engine clatter (knock).

The well-recognised equation developed by Krieger and Borman in Equation 4.1 has been used widely to calculate heat release (An et al., 2012; Buyukkaya, 2010; Canakci et al., 2009; Fahd et al., 2012; Ozsezen et al., 2009; Prasath et al., 2010; Qi et al., 2010). The heat release rate is calculated according to the first law of thermodynamics while neglecting the effect of certain factors such as temperature gradients, in-cylinder pressure waves and non-equilibrium conditions of fuel vaporisation (Ozsezen et al., 2008).

$$\frac{dQ_n}{d\theta} = \frac{\gamma}{\gamma - 1} p \frac{dv}{d\theta} + \frac{1}{\gamma - 1} v \frac{dp}{d\theta} \qquad \text{Equation 4.1}$$

Where

Q_n is the heat release rate per crank angle (J/ºCA)

γ = the ratio of the heat release, where γ is assumed to be 1.37 for the compression and 1.35 for combustion (An et al., 2012; Buyukkaya, 2010; Ozsezen et al., 2009; Qi et al., 2010; Zheng et al., 2008)

p = in-cylinder pressure (bar)

v = cylinder volume (cm^3).

Ozsezen et al. (2008) revealed that there were insignificant differences between biodiesel and PD in maximum in-cylinder pressure. The peak in-cylinder pressure for

all tested fuels triggered between 2.5º and 6º crank angle after top dead centre (ATDC). Supporting this finding, Canakci et al. (2009) concluded that preheated sunflower oil produced almost the same in-cylinder pressure and fuel line pressure as that of PD. In another study, conducted by Ozsezen et al. (2009), in-cylinder pressure of 0.45 MP at 1500 rpm at full load was found to be higher than that obtained from PD and 0.25 º advance. The reasons for this pressure rise were the higher BSFC, cetane number and oxygen (O_2) content and the advance in the ignition. A slight decrease (less than 1º) was found in ignition delay with biodiesel compared with PD because the cetane number is higher for biodiesel, which leads to easier autoignition (Gumus, 2010; Ozsezen et al., 2009).

Fuel properties affect heat release (Gumus, 2010) and in-cylinder pressure results. Biodiesel fuel spray, evaporation and atomisation are dramatically affected by the higher viscosity of biodiesel, resulting in longer combustion duration (An et al., 2013; Özener et al., 2012). However, this is countered by the fact that biodiesel has a higher cetane number. The higher cetane number generally results in a shorter ignition delay (Özener et al., 2012). An et al. (2013) reported that the combustion of biodiesel from waste cooking oil (B100) started slightly earlier than that of PD and had a shorter ignition delay. They also reported that increasing the biodiesel blend ratio reduced the combustion duration.

Maximum in-cylinder pressure and maximum pressure rise for microalgae fuels studied by Haik et al. (2011) showed a slight increase in the heat release rate from microalgae biodiesel than that from PD.

Engine Power and Torque

The engine brake torque and power is measured at the crankshaft via an engine dynamometer, with no other parasitic losses on the engine. Supplying a diesel engine with different fuels will affect the engine torque and power. According to the reviewed studies, the main fuel characteristic that affects the torque and power is lower heating value. In most studies, the engine power and torque were lower when biodiesel and its blends were used. In support of this, Ozsezen et al. (2008) demonstrated that the overall power and torque decreased when the engine was fuelled with biodiesel from frying palm oil and its blends. This test was conducted at full load conditions at different speeds. The reason for the power reduction was the lower heating value of biodiesel fuel. In the same study, the maximum power was produced at the maximum engine speed for PD and biodiesel blends.

Ozsezen et al. (2009) found that the brake power produced by biodiesel from palm oil and canola was insignificantly lower than that of PD by 1.3 % and 2.8 % respectively because of their lower heating value. The power decreased in spite of the increased volume of fuel injected by the engine to maintain the same speed and power. In this study, the maximum brake torques obtained from biodiesel and PD fuel were relatively close. An et al. (2013) reported that increasing the biodiesel blend ratio in PD dropped the brake power at all engine speeds. A reduction of 5.6% and 9.7% were found with B50 and B100, respectively, at the engine speed of 3600 rpm when waste cooking oil biodiesel was used because of its lower heating value. Similarly, Chokri et al. (2012) reported a reduction in engine power and torque by about 5% when biodiesel from a waste vegetable oil blend was compared with PD. A reduction of 1–4% in engine torque was reported when biodiesel from soybean was

used in a diesel engine (Özener et al., 2012). This was linked to the lower heating value, which dropped by 12% compared with PD. The reason the reduction from biodiesel was only 1–4% compared with PD while the heating value was lower by 12% was that the volume of fuel injected into the engine was increased to overcome the power reduction.

In a study performed by Haik et al. (2011) using microalgae biodiesel, the engine torque produced from microalgae biodiesel prepared using 20% methanol was lower than that from PD.

Brake Specific Fuel Consumption (BSFC) and Engine Thermal Efficiency

BSFC is obtained by dividing the fuel mass flow rate by the engine brake power. It gives an indication of the conversion of the energy in the fuel to mechanical energy. In most biodiesel studies, BSFC has been reported to be higher with biodiesel than with PD because of the lower heating value of biodiesel (Lin & Lin, 2006; Özener et al., 2012; Usta et al., 2005). In a study by Ozsezen et al. (2008), the BSFC was increased by increasing the biodiesel from frying palm oil biodiesel blend ratio because of the lower heating value. In another study, the BSFC was found to have increased when biodiesel fuel was used for the same output power because of the extra fuel injected to compensate for the reduction in the heating value of biodiesel (Ozsezen et al., 2009). The BSFC in this study increased by 7.48% and 6.18% compared with PD when the engine was fuelled with waste palm oil and canola biodiesel. The same finding was reported by Gumus (2010) when hazelnut biodiesel was used in a single-cylinder diesel engine because of the lower heating value and higher viscosity. The increase in BSFC reported by Özener et al. (2012) was approximately 2–9% from soybean biodiesel compared with PD.

Thermal efficiency is the efficiency of converting chemical energy in fuel to mechanical energy. It is the inverse of BSFC (Dorado et al., 2003b) applied a statistical test that revealed that the differences in the engine thermal efficiency and increase in BSFC were statistically insignificant between biodiesel from waste cooking olive oil and PD. In another study, conducted by Ozsezen et al. (2009), the thermal efficiency dropped by 1.4% when waste palm oil biodiesel was used and by 0.12% when canola biodiesel was used in place of PD. Similarly, Canakci et al. (2009) reported that BSFC increased by 5% and thermal efficiency also increased by 1.02% compared with PD. The thermal efficiency was higher than PD at a 100% load with waste cooking biodiesel but it was lower with a 25% load. This was linked to the higher load, which increased the injection pressure that neglects the effect of the high viscosity and the O_2 in the B100, consequently enhancing the combustion (An et al., 2013).

Exhaust Gas Temperature (EG Temp.)

Exhaust gas temperature affects the formation of gas emissions. Usta et al. (2005) reported a higher exhaust gas temperature from biodiesel fuel at high load because of the higher ignition delay, resulting in a late burn. However, Ozsezen et al. (2008) reported generally insignificant differences in the exhaust gas temperature between biodiesel from frying palm oil, its blends ratios and PD. When biodiesel fuel was used, the exhaust gas temperature was found to be lower than that from PD (Lin & Lin, 2006). Similarly, Wahlen et al. (2012) found that microalgae (*Chaetoceros gracilis*) biodiesel gave lower exhaust gas temperatures than PD.

Engine Noise

The sound levels from agriculture machinery and engines are known to be a health-affecting factor. Unwanted sound or sound over a certain limit can be called noise. A sound level between 65 and 85 dB might cause problems in the nervous system or hypertension, and a level above 85 dB can lead to temporary or permanent hearing loss (Celen & Arın, 2003; Durgut & Celen, 2004). Engine noise is considered noise pollution, and it gives an indication of the combustion smoothness. The noise level is a function of the combustion process that is affected by the fuel properties such as cetane number. A high cetane number enhances an easy cold start and reduces engine noise (Prakash, 1998). According to (Ozsezen et al., 2008; Ozsezen et al., 2009), in-cylinder pressure waves lead to engine noise. In these studies, the in-cylinder pressure was smoother in biodiesel fuel than in PD at full load testing, which indicates that biodiesel produces lower engine noise than PD. According to Haik et al. (2011), the engine noise from an engine fuelled with microalgae biodiesel prepared using 20% methanol was found to be higher than that from PD at all studied engine loads. This finding contradicts the findings in the literature and the finding of this work. The cetane number is higher with biodiesel, so a lower pressure wave is expected, which would lead to smoother combustion and reduced noise level.

4.2.3 Exhaust Gas Emissions Using Biodiesel

Each biodiesel has its own FAMEs that affect the biodiesel properties; consequently, the emissions produced from the combustion process will change (Wahlen et al., 2012). However, the emissions from MCP-B100 in any blend ratio have not yet been studied. Following are some extracts from the literature on emissions from various biodiesel fuels.

Carbon Monoxide (CO), Carbon Dioxide (CO_2) and Oxygen (O_2)

The CO level in emission gases can be an indicator of incomplete combustion. The reviewed studies showed a contradiction in the CO and CO_2 produced from biodiesel fuel in comparison with PD. Most researchers that tested biodiesel fuels reported that CO and CO_2 levels reduced when biodiesel fuels were used compared with PD (An et al., 2013; Lin & Lin, 2006). For example, Ozsezen et al. (2009) indicated a reduction of 86.89% in the CO level with biodiesel from waste palm oil and a reduction of 72.68% with biodiesel from canola oil compared with diesel fuel. The CO_2 percentage in the exhaust showed a minor decrease and increase of 1.7% with biodiesel from waste palm oil and canola oil, respectively. These results were linked to various factors, such as the air–fuel ratio and the carbon–hydrogen ratio in the fuel, because a higher carbon content in fuel increases the production of CO_2 emission compared with H_2O.

Valente et al. (2010) detected an increase in the CO_2 emission from biodiesel fuel blends at low engine loads and a decrease at high loads. In the same study, at all the loads studied, the CO emission from biodiesel blends was higher than that from diesel fuel. In a study by Özener et al. (2012), biodiesel from soybean emitted significantly lower CO emissions of about 28–46% with a slight increase of 1.46–5.03% in CO_2 emissions compared with PD. Wahlen et al. (2012) reported that, in comparison with PD, microalgae (*Chaetoceros gracilis*) biodiesel produced about 17.4% lower CO and about 2.6% higher CO_2 during no-load testing at 3500 rpm.

The extra O_2 in the biodiesel chemical composition affects the combustion process and exhaust gas emission. The O_2 percentage in exhaust gases using biodiesel has been found to vary according to the type of biodiesel, engine type and operation

conditions. For example, (Dorado et al., 2003b) found that the O_2 increased up to 17.6% with olive oil biodiesel compared with PD, which contributed extra O_2 to the combustion process.

Nitrogen Oxides (NO_x)

The NO_x formation percentage in the exhaust gas emissions produced by biodiesel fuel compared with PD is still unclear (McCormick et al., 2001). Some studies have reported an increase in NO_x with biodiesel fuel whereas others have reported a reduction. Ozsezen et al. (2009) reported an increase of 22.13% and 6.48% with biodiesel from waste palm oil and canola oil, respectively, compared with PD. This was caused by various factors, such as the air–fuel ratio and O_2 content of the fuel, which increased the flame temperature. Another reason presented was the shorter ignition delay, which increased the combustion temperature, consequently increasing the NO_x. Later, Özener et al. (2012) demonstrated that the NO_x emission from soybean biodiesel was 6.95–17.62% higher than that from PD.

Varatharajan and Cheralathan (2012) reported that the biodiesel market could be limited by the NO_x emission. They also concluded from a review of the causes of the high NO_x produced from biodiesel that fuel properties and characteristics influenced the NO_x emission. An et al. (2013) reported that the NO_x emission from waste cooking biodiesel was lower than that from PD at most engine conditions because it is very sensitive to the exhaust gas temperature. Similarly, Wahlen et al. (2012) found a reduction of about 14% in NO_x with microalgae (*Chaetoceros gracilis*) biodiesel compared with PD. According to Prakash (1998), some researchers have found an inverse correlation between NO_x emissions and the cetane number.

4.2.4 Summary of the Literature

According to the literature reviewed, the engine performance and emissions from biodiesel fuel are dependent on the biodiesel's physical and chemical properties, the engine type and the operating conditions. Engine performance and emissions using biodiesel from different feedstock have been widely studied. The general findings with biodiesel are that biodiesel produces lower in-cylinder pressure, brake power, torque, CO and exhaust temperature, and it provides longer ignition delay. However, there is some contradiction regarding the thermal efficiency, CO_2 and NO_x emissions from biodiesel fuel. Engine performance and emissions using microalgae still have not been fully researched.

4.3 Methodology and Experimental Apparatus

4.3.1 Diesel Engine

In this work, a single-cylinder air-cooled diesel engine Yanmar L48N6 was used. The engine specifications are presented in Table 4.1. To measure the engine performance and exhaust gas emission parameters, minor modifications were made to the engine to mount and install the dynamometer, in-cylinder pressure transducer, wideband lambda sensor, vibration sensor, incremental rotary encoder, air and fuel flow meters, exhaust gas temperature and exhaust gas port sampling point to the gas analyser.

Table 4.1 Engine specifications

Engine type	4-stroke, vertical cylinder diesel engine
Bore × stroke	70 × 57 (mm)
Displacement	0.219 (litres)
Maximum rated output	3.5 (kW) @ 3600 (rpm)
Connecting rod length	91 (mm)
Continuous rating output	3.09 (kW) @ 3600 (rpm)
Crankshaft offset	28.5 (mm)
Dry engine weight	27 (kg)
Lubrication system	Forced lubrication with Trochoid Pump
Length	332 (mm)
Width	384 (mm)
Height (mm)	417
Injection timing	16.5 BTDC

4.3.2 Dynamometer

A Land and Sea water-brake dynamometer was used to load the engine and measure the brake torque, engine speed and brake power (see Figure 4.1). The dynamometer consisted of the dynamometer absorber and a torque arm with load cell attached. The dynamometer was mounted directly to the engine outlet shaft and aligned with the cell key. An adapter was made to hold the dynamometer and to mount the encoder with the engine shaft (see Figure 4.2). The dynamometer absorber had three water ports:

1. absorber inlet line, which was connected to the load valve
2. absorber discharge line to drain the water by gravity to the drainage sump
3. ventilation.

The supplied water flow was checked prior to the test and it was found that the maximum water flow provided by the water pump met the dynamometer water flow and pressure requirement of 4.5 L/min and 6 psi, respectively.

A dynamometer torque arm holder was designed to prevent the dynamometer from rotating with the engine shaft. The torque was measured by the load cell located on

the arm. The connecting part between the arm and the holder was made from polyethylene to absorb the extreme knock associated with single-cylinder diesel engines (see Figure A.6a). The load valve was fixed on the main frame and an indicator holder was fabricated to lock the load valve at a certain position (see Figure A.6b).

The dynamometer had its own Land and Sea data acquisition system (DAQ), which was connected to the wiring harness and connected to the computer via USB cable. The console set-up was configured to fit the experiment's requirement parameters and units. All parameter units of measure were presented in SI units and the frequency of the data fixed on 10 Hz. Prior to the test, the dynamometer and its software were carefully calibrated by applying known torques until the differences between the reading from the software and the real torque applied was less than 0.1 N.m (see details in Appendix A).

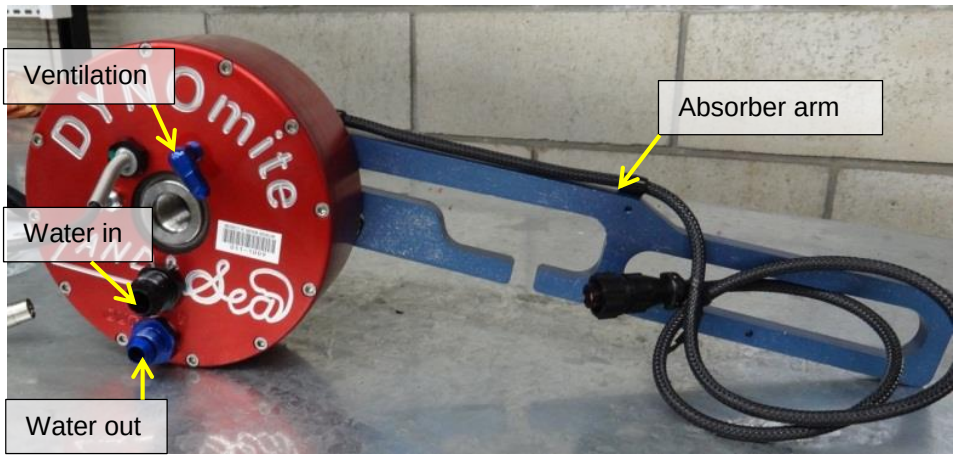

Figure 4.1 Water-brake dynamometer

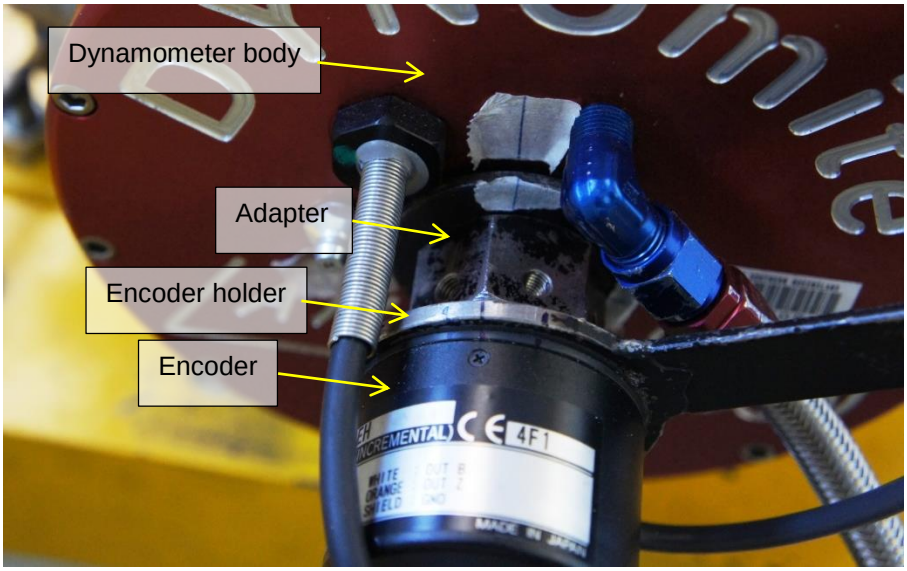

Figure 4.2 Attaching the encoder to the dynamometer body

4.3.3 Instrumentation of the Set-up

Pressure Transducer

It was important to measure the in-cylinder pressure to evaluate the indicated power, torque and power. For that purpose, a Kistler 6125C piezoelectric pressure sensor was installed in the engine cylinder head. This pressure sensor was selected because of its accuracy, fast response and small size that enables installation in a small cylinder head. The sensor was installed into the cylinder head using an adapter to support the sensor in the cylinder head, as shown in Figure 4.3. The sensor was connected to a Kistler SCP slim 2852A11 charge amplifier. This amplifier was connected to the DAQ. The sampling rate of the pressure was synchronised to the crankshaft rotary angle by triggering analogue-to-digital conversion by the encoder pulses of 720 pulses per revolution. LabVIEW software was developed and used to monitor and save the in-cylinder pressure (in bar) versus the engine crank angle. The in-cylinder pressure was calibrated as described in Appendix A. The Kistler SCP

slim 2852A11 charge amplifier was set on drift compensation to offset the problem of charge leakage. The data of the in-cylinder pressure at each point of the engine speed was recorded and the average of 12 continuous cycles was drawn against the crank angle degree.

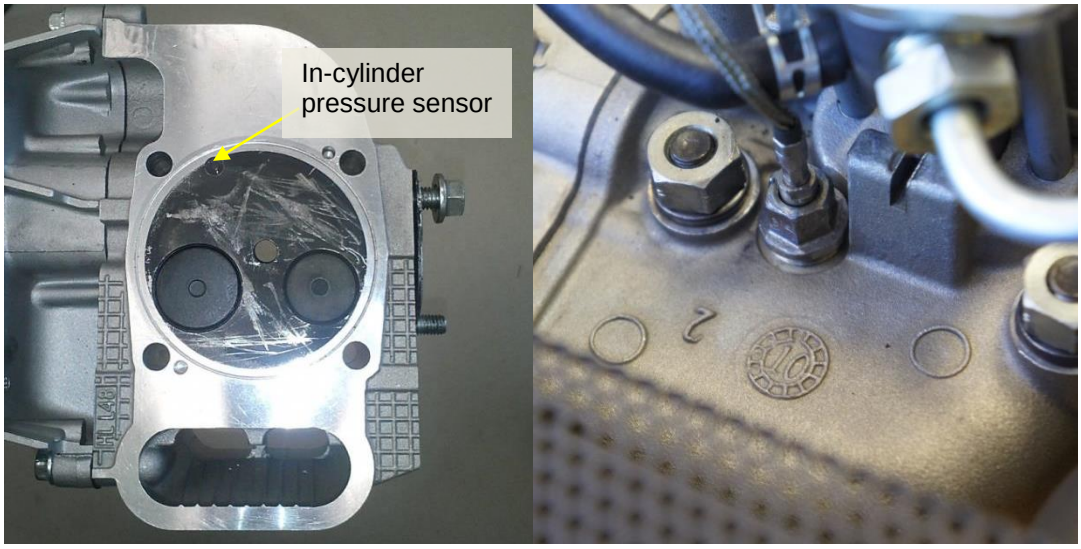

Figure 4.3 Location of the pressure transducer

The heat release was determined based on Equation 4.1. To convert the crank angle measured by the encoder to cylinder volume, Equation 4.2 (Pulkrabek, 2004) was used.

$$V = V_c + (\pi B^2/4)(r + a - s) \qquad \text{Equation 4.2}$$

Where

V_c = clearance volume (mm^3)

B = bore (m)

r = connecting rod length (mm)

a = crank offset (mm)

s = the distance between the crank axis and wrist pin axis (mm) which has been calculated based on Equation 4.3 (Pulkrabek, 2004).

$$s = a\cos\theta + \sqrt{r^2 - a^2\sin^2\theta} \qquad \text{Equation 4.3}$$

Where

a = crankshaft offset

θ = crank angle (zero when the piston is at top dead centre).

Data Acquisition System

A computer was dedicated to obtaining, processing, displaying and saving the data from the test facility. The DAQ was used to record the signals of the measured parameters of the in-cylinder pressure, engine speed, top dead centre (TDC) position, lambda and vibration with a sampling rate of 51,200 samples per second. The signals from the sensors detected by the DAQ were recorded and saved using LabVIEW software designed at USQ.

Encoder

An Omron E6C3-CWZ3EH rotary encoder was fastened to the engine shaft via an adapter. The adapter allowed the encoder shaft to rotate with the engine shaft while the body of the encoder was fixed to the engine body. This encoder provided two voltage signals: A pulse and Z pulse. The A signal gave 720 pulses per revolution, which equalled a 0.5^{o} crank angle interval, and the Z signal gave one pulse per revolution. The A signal was used to identify the crank angle position and as a sampling rate of the in-cylinder pressure, engine speed, lambda and vibration. The Z signal was synchronised to give a pulse when the piston reached the TDC. Synchronising the Z pulse of the encoder and the TDC of the engine is described in Appendix A.

Lambda Values

The lambda value is the result of the actual air–fuel ratio divided by the stoichiometric air–fuel ratio. The stoichiometric air–fuel ratio is the exact air required to produce complete combustion of the fuel with the chemically correct amount of air. Lambda values were measured using a Professional Lambda Meter (PLM) made by MoTeC. This sensor measures the actual lambda regardless of the type of fuel being used. The lambda value measured by the sensor was sent as an analogue voltage signal to the data logger and then recorded using LabVIEW software. The actual air–fuel ratio was calculated from the airflow value divided by the fuel flow rate for each point in the test. The calculated lambda value and the result from the MoTec sensor were found to be in close agreement. Therefore, only the lambda values from the MoTec sensor are considered.

Airflow Meter and Weather Station

A Land and Sea 7.6-cm turbine flow meter was mounted on the intake air system to determine the airflow into the engine (see Figure 4.4). The air cleaner was modified to force the engine intake air to pass through the airflow meter. To achieve this, an adapter was made and mounted on the air cleaner cover. The original air intake hole was closed. The volumetric and the mass flow rate of the inlet air were measured based on the results from the Land and Sea weather station. The weather station was located about 50 cm from the airflow meter. This weather station meter provided the ambient temperature, relative humidity and barometric pressure.

Figure 4.4 Airflow meter

Fuel Flow Meter

Different fuel flow meters were adopted to measure the fuel flow to the engine. However, the output signal from the fuel flow meters fluctuated. The fluctuation in the signal was caused by the intermittent flow from the fuel injection at one pulse per cycle (two revolutions). The FC rate for the engine was measured based on the weight reduction in the fuel container measured over a given time interval. The fuel measurement system was made to siphon the fuel from the top of the beaker. The differences in the weight were measured using a Wedderburn scale with sensitivity of 0.1 g (see Figure 4.5). When the engine was run at a certain speed, the flow was measured by taring the scale. When the scale read zero, the time was measured using a stopwatch. After three minutes, the weight was measured. This was repeated three times at each engine speed and the average taken. After each test, the fuel system was flushed with diesel fuel and the engine was run for 10 minutes with diesel.

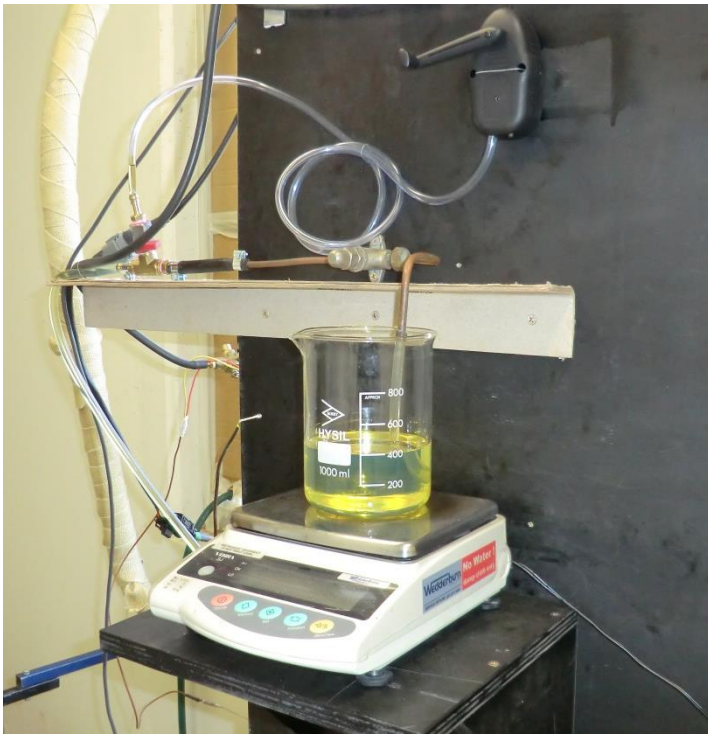

Figure 4.5 Fuel consumption measurement system

Exhaust Gas Temperature

To measure the exhaust gas temperature, a type K thermocouple of 1.5 mm was installed in the exhaust manifold facing the exhaust gas stream close to the exhaust valve, as shown in Figure 4.6. The thermocouple was connected to the DAQ of the dynamometer and all the results of the exhaust temperature were recorded and saved in the dynamometer software.

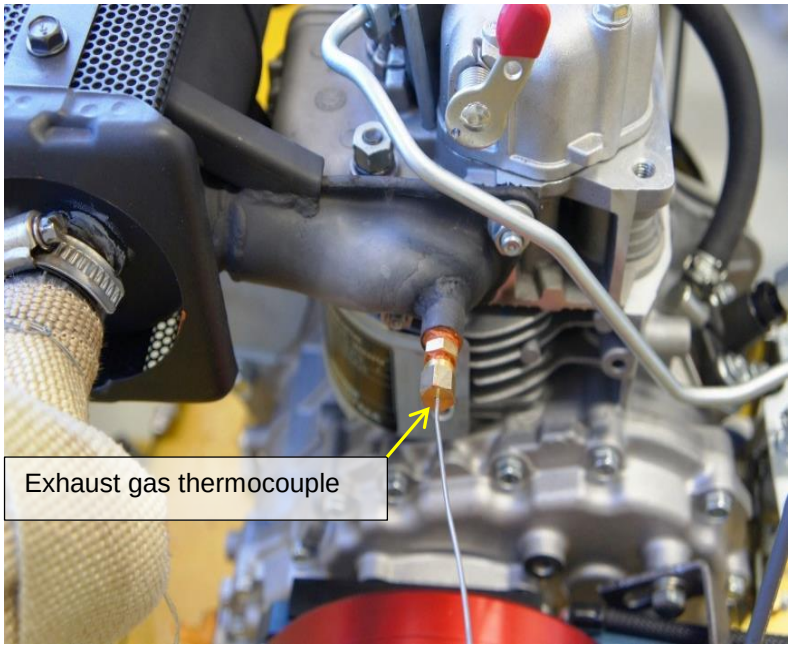

Figure 4.6 Exhaust gas temperature measurement

Noise Level Meter

To compare the noise level produced from the different fuels used in the engine, a Larson Davis SoundTrack LxT Sound Level Meter was placed one meter from the engine. The noise recorded by this device mainly came from the engine. However, the exhaust fan and the water pump produced significant noise. The average noise from the exhaust fan and the water pump was measured when the engine was not running and found to be 67 dB.

4.3.4 Gas Analyser

To evaluate the exhaust gas emissions, a Coda gas analyser was used. The gases that can be detected by this gas analyser are n-Hexane or propane, CO, CO_2, O_2 and NO_x. This gas analyser was new and calibrated by the manufacturer prior to the test. A daily calibration was conducted on the gas analyser and the filters were cleaned. The specifications and accuracy are presented in Table 4.2.

Table 4.2 CODA gas analyser measurement accuracy

Measurement	Range	Accuracy	Accuracy
n-Hexane	0.00–2000 ppm 2001–15,000 ppm 15,000–30,000 ppm	± 4ppm abs.	± 3% ± 5% ± 8%
CO	0.00–10% 10.001–15.00%	± 0.02% abs.	± 3% ± 5%
CO_2	0.00–16% 16.01–20%	± 0.3% abs.	± 3% ± 5%
O_2	0.00–25%	± 0.1% abs.	± 5%
NO	0.00–4 ppm 4.001–5000 ppm	± 20 ppm abs.	± 4% ± 5%

4.3.5 Fuel Preparation

MCP oil (100%) (MCP-O) was obtained from our industrial partner (Soley Institute Turkey). The MCP-O was converted to biodiesel through transesterification.

The transesterification procedure followed in this work included was as follows:

1. The total amount of MCP-O was mixed together to avoid any differences in the oil components and properties.
2. The oil was divided into batches of 500 ml to avoid the risk of losing the entire batch if saponification occurred.
3. A solution of methanol and NaOH was prepared. An amount of 40 g of NaOH was added to each litre of methanol and stirred for 10 minutes using a magnetic stirrer.
4. The 500 ml of MCP-O was heated to 60 ^{o}C with mixing using another magnetic stirrer. A thermometer was inserted into the oil to monitor the temperature (see Figure 4.7).

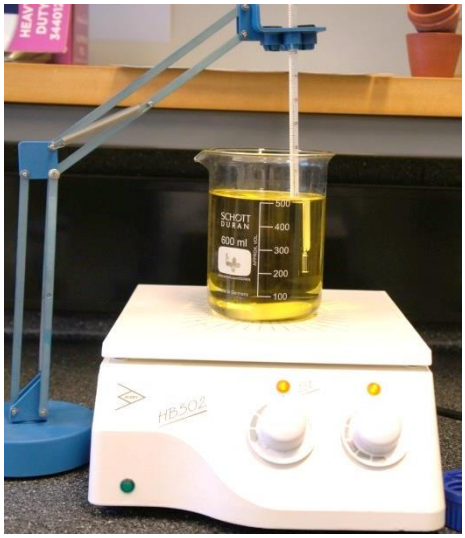

Figure 4.7 Sample of MCP-O under heating, stirring and temperature measurement

5. When the oil temperature reached 60 ºC (Lin & Lin, 2006), 110 ml of the methoxide solution was carefully added to each 500 ml of MCP-O with mixing. The mixture was stirred for 40 minutes.
6. The mixture was left for 24 hours. The top layer (FAMEs) was separated from the lower layer (glycerine). The biodiesel samples were centrifuged for 10 minutes at 3000 rpm to remove any remaining glycerine.
7. The biodiesel was washed by spraying 250 ml of distilled water on the biodiesel (see Figure 4.8). After one hour, another 250 ml of distilled water was sprayed to wash the biodiesel.

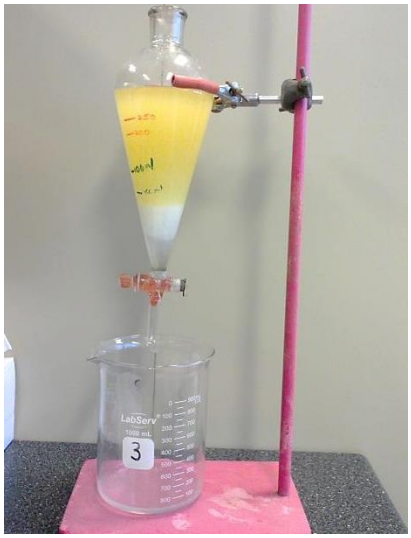

Figure 4.8 Washing the MCP-B100 with water

8. The next day, the lower layer of water was removed. The biodiesel was centrifuged again for 10 minutes at 3000 rpm to extract any remaining water.
9. The different batches of MCP-B100 were mixed together to obtain a homogeneous mixture.
10. The biodiesel was heated to 80 ºC for four hours to evaporate the water and any remaining methanol.
11. The total amount of MCP-B100 was filtered using a microfilter and then kept in plastic containers with labels.

To prepare the blends of MCP-B50 and MCP-B20, PD from British Petroleum (BP) petrol station and MCP-B100 were used. A volumetric cylinder of 500 ml was used to measure the amount of PD and MCP-B100 required for the blend. For example, to prepare one litre of MCP-B20, 800 ml of PD was mixed with 200 ml of MCP-B100. To prepare MCP-B50, 500 ml of PD was mixed with 500 ml of MCP-B100 and so on.

The chemical formula of MCP-B100 was calculated from its FAMEs, as presented in (Allwayzy et al., 2010), to be $C_{18.151}H_{34.376}O_{1.942}$. The specifications of the blends were calculated from the PD and MCP-B100 depending on their volume in the blend.

4.3.6 Fuel Properties

The properties of the FAs in biodiesel indicate the overall properties of the biodiesel fuel. Biodiesel fuel consists of five to seven FAMEs. The properties of the FAMEs vary in the literature. This makes the measurement of the biodiesel's physical properties more accurate than averaging the properties for the FAMEs in the biodiesel.

Chemical Properties

The chemical profile for the MCP-B100 that was obtained from the supplier is presented in Table 4.3. The FAME profile was measured at the USQ chemical lab for comparison. A Shimadzu GCMS-QP2010 Plus gas chromatograph mass spectrometer was used to measure the FAME compositions of the MCP-B100 using the available standards. The results of the measured FAMEs, presented in

Table 4.4, showed good agreement with the FAME profile provided by the supplier with a small degree of error. This difference may have been caused by the technical issues of transesterification and the measuring method. This is also the reason why any oil can vary in its components depending on the growing conditions.

Table 4.3 FAMEs of MCP-B100 (*Soley Biotechnology Institute*)

Formula	FAME name	Relative content (%)
$C_{15}H_{30}O_2$	Methyl tetradecanoate	1.3
$C_{17}H_{34}O_2$	Hexadecanoic acid methyl ester	12.8
$C_{18}H_{36}O_2$	Heptadecanoic acid methyl ester	0.9
$C_{19}H_{34}O_2$	9,12-Octadecadienoic acid methyl ester	17.4
$C_{19}H_{36}O_2$	9-Octadecenoic acid methyl ester	60.8
$C_{19}H_{38}O_2$	Octadecanoic acid methyl ester	2.8
$C_{20}H_{38}O_2$	10-Nonadecenoic acid methyl ester	0.3
$C_{21}H_{40}O_2$	11-Eicosenioc acid methyl ester	0.4
$C_{21}H_{42}O_2$	Eicosanoic acid methyl esteracid ester	0.4

Table 4.4 Measured FAMEs of MCP-B100

Formula	FAME name	Relative content (%)
- N/A		3.10
$C_{17}H_{34}O_2$	Hexadecanoic acid methyl ester	13.64
$C_{19}H_{34}O_2$	9,12-Octadecadienoic acid methyl ester	4.45
$C_{19}H_{36}O_2$	9-Octadecenoic acid methyl ester	70.48
$C_{19}H_{38}O_2$	Octadecanoic acid methyl ester	0.0
$C_{21}H_{42}O_2$	Eicosanoic acid methyl esteracid ester	0.0
- N/A		2.14
- N/A		2.23
- N/A		3.96

The physical properties of the PD and MCP-B100 were also obtained from the suppliers. Some of these properties were measured based on the available equipment. Table 4.5 depicts the physical properties of PD, MCP-B100, MCP-B50 and MCP-B20. The properties of MCP-B50 and MCP-B20 were calculated based on the PD and the MCP-B100 percentage in the fuel. In this table, it can be observed that the MCP-B100 and its blends had a higher density, cetane number, viscosity and flashpoint than the PD. Conversely, they had lower heating value than PD.

Table 4.5 Fuel properties

Fuel Property	PD	MCP-B100	MCP-B50	MCP-B20
Density at 15 ºC (kg/L)*	0.86	0.90	0.88	0.87
Cetane number	51.00	52.00	51.50	51.20
Energy content (MJ/kg)	46.20	40.04*	43.12	44.97
Lower hating value (MJ/kg)	43.25	37.50	40.38	42.10
Viscosity at 40 ºC (cp)*	2.53	4.22	3.20	2.80
Flashpoint (ºC)	66.00	124.00	95.00	77.60
Carbon residue (on 10% distillation residue) % (m/m)	0.01	0.20	0.11	0.05
Total contamination (mg/kg)	–	2		
Oxidation stability, 110 ºC Hours	5.0	12.0	8.5	6.4
Acid value (mg KOH/g)		0.3	0.3	
Iodine value		47		
Sulfated ash content (%)		0.01		
Water content (mg/kg)	<100	80		
Methanol content (%)	–	0.04		
Sulfuret content (mg/kg)	8.0	2.0	5.0	6.8
Phosphorus content (mg/kg)	–	3		
Linolenic acid methyl ester (%)		2		
Monoglyceride content (%)		0.2		
Diglyceride content (%)		0.04		
Triglyceride content (%)		0.02		
Free glycerol (%)		0.008		
Total glycerol (%)		0.02		

PD properties obtained from British Petrolum. MCP-B100 obtained from Soley Institutes.
* Measured.

Viscosity

Viscosity is the measurement of the internal flow resistance of a liquid, which has an important role in the atomisation process of the fuel (Conceição et al., 2005). Biodiesel viscosity has been reported by many researchers to be higher than that of PD, which can cause problems in the engine, especially at a low temperature, such as high injection pressure, and high viscosity can reduce the fuel flow rate, which makes the engine starving for fuel under certain operating conditions (Tat & Van Gerpen, 1999). In contrast, some researchers have commented that the increase in the

power and torque with biodiesel fuels comes from the high viscosity that reduces the internal leakage in the fuel pump (Usta et al., 2005).

The viscosity of PD, MCP-B100, MCP-B80, MCP-B50 and MCP-B20 was measured in the fuel laboratory at USQ. The viscosity was measured using a Brookfield Viscometer DV-II+Pro Extra, which was connected to a Brookfield temperature controller (see Figure 4.9).

Figure 4.9 Viscometer

Injector Nozzle Test

Desantes et al. (2009) reported that the injection characteristics of biodiesel in a diesel engine had not yet been fully studied. Therefore, they studied the characteristics of the injection process using different biodiesel blends.

To study the injection spray properties, an injection system was constructed to simulate the engine injection system. The nozzle tester that was used in this study was fabricated in the engine lab at USQ. The nozzle tester consisted of a fuel pump that was located on a metal frame to hold the fuel pump and a lever to push the piston manually instead of the engine cam. A Kistler pressure transducer was

installed in the fuel pipe between the fuel pump and the injector to measure the instantaneous pressure upstream of the nozzle. This pressure transducer was connected to a Kistler amplifier and then to a computer. Due to an unknown error and the time restrictions, the data for the fuel pressure were removed. A nozzle injector for the Yanmar L45n was fitted on a black box (30 × 30 × 15 cm) to prevent the injected fuel spraying into the environment. A fuel container was fixed close to the fuel pump to reduce the amount of fuel required for the test. The fuel spray was videoed using a Photron high-speed camera using 1000 frames per second.

4.3.7 Test Procedure

Selecting the Test Speeds

A constant engine speed that could be reached through applying load on the engine was selected based on the preliminary test. This test was performed to select the engine speed that was most closely representative of those in the manufacturer's performance curves. The dynamometer and its software captured up to 200 Hz of the data that can cover all engine speeds under a certain load. Running the engine at a fixed speed for a specific time was required to measure the fuel flow rate and to give time for the gas analyser to receive the sample and the readings to be stable. The most representative points that had been initially selected from the manufacturer's performance curves were:

1. maximum engine speed (without load) at 3800 rpm
2. maximum output power at 3600 rpm
3. BSFC at 3000 rpm
4. maximum torque at 2600 rpm
5. smoke line threshold at 1800 rpm.

The primary tests with PD and biodiesel showed an unstable engine speed during the applying of the load at most speeds. The closest engine speeds to those speeds were 3800, 3670, 2900, 2350 and 1770 rpm, respectively. At these engine speeds, the engine was very stable with a variety of fuels with ±5–7 rpm (maximum speed variation is 0.39%).

Engine Tests

The Yanmar single-cylinder engine consumes considerably less fuel than a tractor engine, which allowed testing of different fuel blends with more replications with the limited amount of MCP-B available. The engine test was connected at the maximum fuel line WOT. In this test, the engine speed controller lever (throttle) was fixed on maximum position during all the tests. At the WOT, the engine speed was 3800 rpm with no load. This point was considered the first testing speed (maximum speed with no load). The engine was kept at this condition for 10 minutes. At that time, all the readings were taken and saved in two computers. The first computer was used to monitor and record the data from the dynamometer and the LabVIEW software. The second computer was used to record the data from the gas analyser. The reading of the FC rate and the noise level were recoded manually. The load was then adjusted to achieve the second engine speed of 3670 rpm (the maximum continuous power) and the load valve was carefully adjusted to apply load on the engine until the engine speed dropped to 3670 rpm. It is practically to notice sharp increase in most of the results at this second measurement point than the first measurement point. The dynamometer load valve was fixed at that position using the lever lock. The load valve was then carefully adjusted again to load the engine until the engine speed dropped to 2900 rpm (maximum continuous torque). The same technique was

followed for reading of the data. The fourth point of lower BSFC was found to be close to 2350 rpm and the last speed of the smoke line of 1770 rpm was achieved following the same method.

The engine set-up was carefully calibrated and tested using diesel fuel. The baseline (PD) was repeated four times and averaged. For the MCP-B blends, the tests were repeated three times for each blend and then the final data were averaged. However, the tests were conducted and repeated in comparable environmental conditions, and the power and torque were corrected directly from the dynamometer based on the data obtained from the weather station. The power correction factor selected in this study was the SAE method.

Prior to each test, the instruments were carefully calibrated to reduce experimental error. The engine was run for 10 minutes with PD at the start of each test to warm up the engine at partial load. The type of fuel to be tested was randomly selected. At each run, the gas analyser was calibrated by performing auto zero and reset. Sufficient time of about five minutes was given to the gas analyser to receive the sample from the engine exhaust and to be analysed before recording. The exhaust gas emission data of continuous five minutes were recorded and saved for each run of engine speed after it became relatively constant. The test condition was monitored to perform the entire test at relatively similar ambient conditions to avoid effects of the ambient condition on the results. The ambient conditions were measured and averaged: the ambient temperature was 23 ± 3 ºC, the relative humidity was 44 ± 8%.

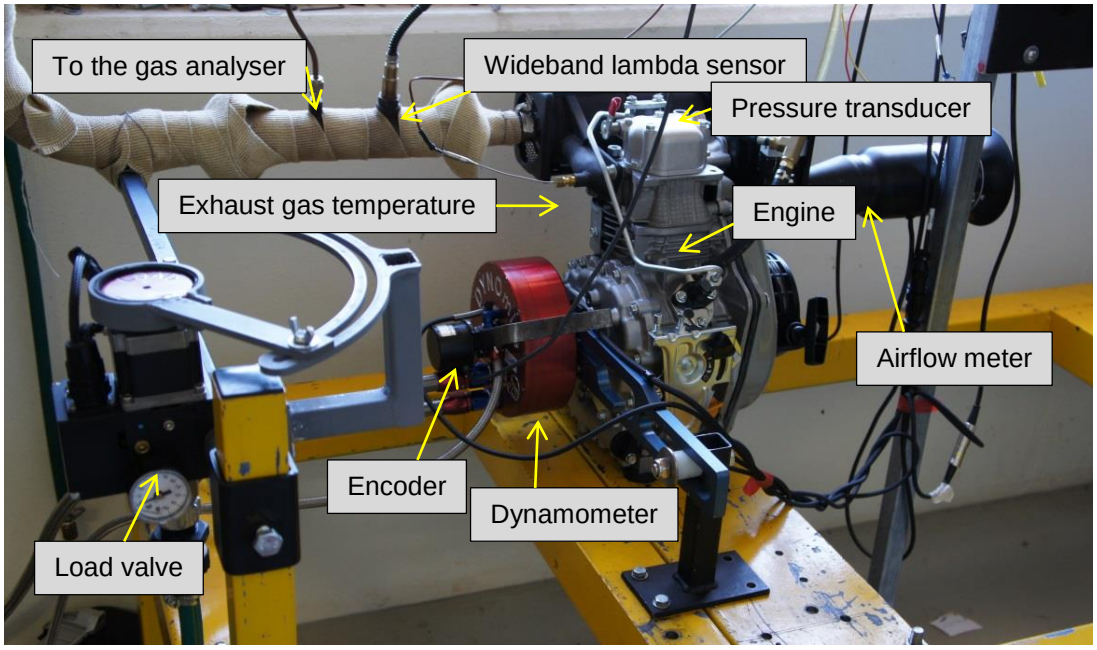

Figure 4.10 Engine set-up

4.4 Results and Discussion

In this section, the results of the tests on the fuel properties, engine performance and exhaust gas emissions are discussed and statistically analysed using SPSS and Microsoft Excel.

4.4.1 Fuel Properties

The relationship between the fuels' viscosity and their temperature is presented in Figure 4.11. This figure indicates that the viscosity curve trends for all the fuels were comparable, which indicates an inverse relationship between the fuels' viscosity and their temperature. MCP-B100 presented the highest viscosity values at the studied temperatures, starting from 10.1 cP at 5 ºC and ending with 2.48 cP at 70 ºC. It can also be observed from this figure that the increase in the proportion of MCP-B100 increased the viscosity. Figure 4.12 presents the relationship between the measured viscosity and the calculated viscosity based on the percentage of PD and MCP-B100

in the fuels. It shows that the measured viscosity values were in high agreement with the calculated ones for all blends. This is consistent with Tat and Van Gerpen (1999) comments that biodiesel viscosity can be calculated as a function of the biodiesel fraction.

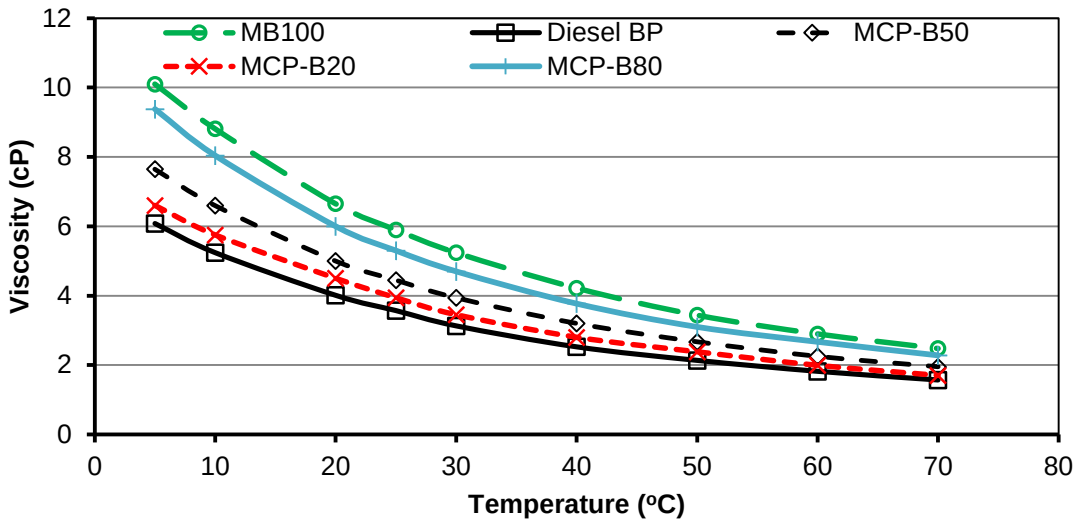

Figure 4.11 The relationship between the viscosity in (cP) and temperature (°C) for PD, MCP-B20, MCP-B50 and MCP-B100

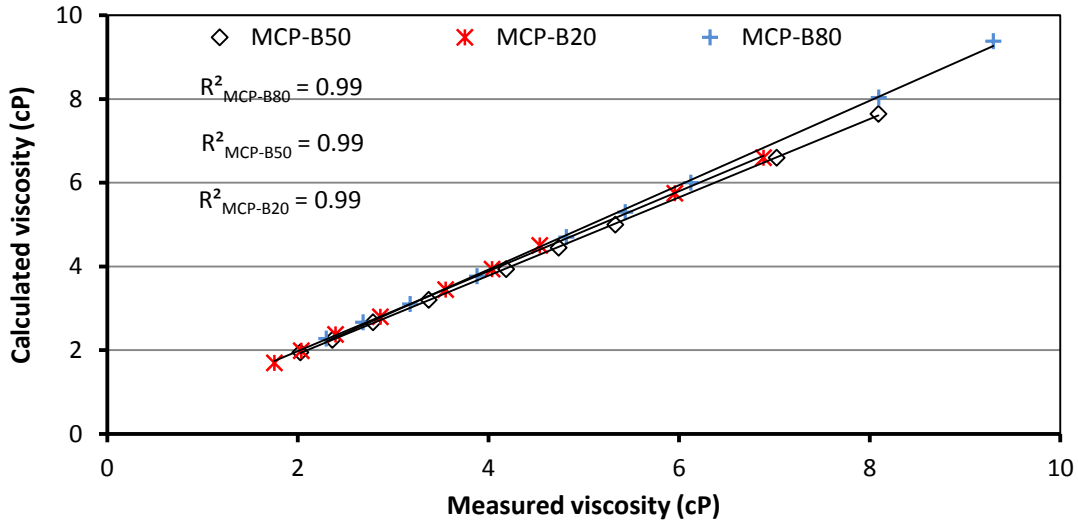

Figure 4.12 The relationship between measured and calculated viscosity

Based on the data shown in Figure 4.11, Equation 4.4, Equation 4.5, Equation 4.6,Equation 4.7 and Equation 4.8 are the equations to calculate the viscosity based on the temperature for PD, MCP-B20, MCP-B50, MCP-B80 and MCP-B100,

respectively. The third-order fit trends show very high representation of the measured viscosities for the fuels with very high R^2 as given below.

$$\mu_{PD} = -1E\text{-}05\ T^3 + 0.0027T^2 - 0.1955\ T + 6.9722 \quad \text{Equation 4.4}$$
$R^2 = 0.9999$

$$\mu_{MCP\text{-}B20} = -1E\text{-}05\ T^3 + 0.0026\ T^2 - 0.2011\ T + 7.5373 \quad \text{Equation 4.5}$$
$R^2 = 0.9997$

$$\mu_{MCP\text{-}B50} = -2E\text{-}05\ T^3 + 0.0035\ T^2 - 0.2499\ T + 8.7907 \quad \text{Equation 4.6}$$
$R^2 = 0.9998$

$$\mu_{MCP\text{-}B80} = -3E\text{-}05\ T^3 + 0.0046\ T^2 - 0.3218\ T + 10.848 \quad \text{Equation 4.7}$$
$R^2 = 0.9998$

$$\mu_{MCP\text{-}B100} = -2E\text{-}05\ T^3 + 0.0043\ T^2 - 0.3204\ T + 11.594 \quad \text{Equation 4.8}$$
$R^2 = 0.9999$

Where

μ is the dynamic viscosity in cP

T is the fuel temperature in ºC.

The percentage differences in the physical properties of MCP-B100 and its blends compared with those of PD are demonstrated in Figure 4.13. In the literature, there is a contradiction regarding the effect of biodiesel viscosity on engine performance between positive and negative. The results in this thesis show that the higher viscosity of the MCP-B100 (66.8%) compared with diesel is in the acceptable limit of biodiesel. The increase in the viscosity of MCP-B100 produces a small improvement in engine performance, as will be discussed later. This is thought to be caused by a reduction in internal leakage in the fuel pump (Usta et al., 2005). Supporting this suggestion, good nozzle spray pattern results were obtained, with a wider spray angle of about 3º recorded for MCP-B100 compared with that of PD, as

presented in Figure 4.14. This would indicate that the higher viscosity, which leads to larger fuel droplet size, had a minimal effect on performance. Another positive factor, as demonstrated in Figure 4.13, is the 2% higher cetane number of MCP-B100 compared with that of PD, which indicates better combustion quality with biodiesel than PD because of the chemical structure. Among the fuel properties, the lower heating value and the cetane number appear to be the main affective factors in the engine performance and emissions, as will be discussed later. The heating values per unit mass for MCP-B100, MCP-B50 and MCP-B20 were lower than those of the PD by 13.3%, 6.7% and 2.7%, respectively, as shown in Figure 4.13. According to the heating value of microalgae (*Chaetoceros gracilis*), biodiesel was reported to be lower than PD by 7% per unit volume if the density of the microalgae biodiesel was taken into account (Wahlen et al., 2012).

Figure 4.13 also shows that the density of MCP-B100 was 4.5% higher than that of PD. If the same volume of fuel was injected into the combustion chamber, the higher density would reduce the negative effect of the lower heating value of MCP-B100 and its blends. This is because the heating value of the fuels is given in mass units.

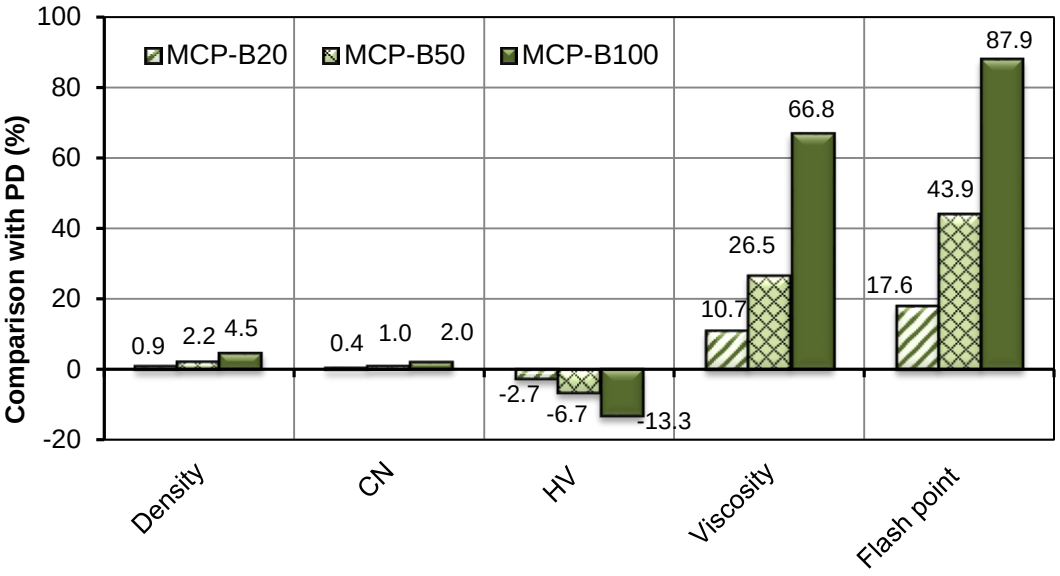

Figure 4.13 The variation percentage in the fuels' physical properties compared with PD

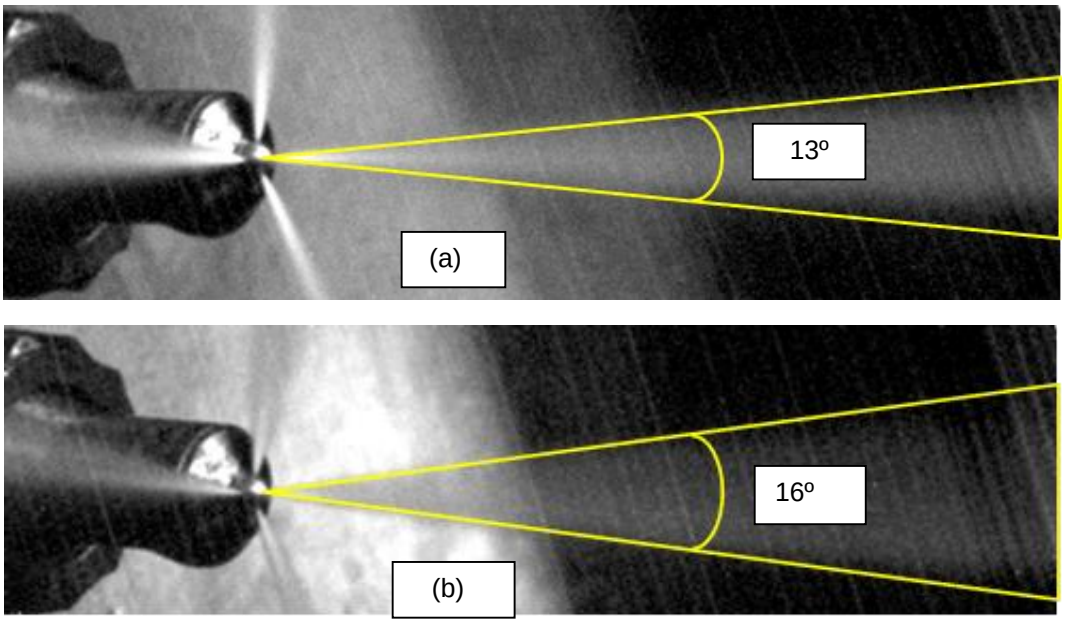

Figure 4.14 Nozzle test (a) PD (b) MCP-B100

4.4.2 Combustion Characteristics

In-Cylinder Pressure

This section discusses the experimental data of the in-cylinder pressure and heat release for the engine speeds of 3600, 2900 and 2350 rpm. Figure 4.15 presents the typical in-cylinder pressure for seven cycles at 3800 rpm (no load) using PD. This figure shows the smoothness of the combustion run and the variation between the cycles at the same speed. The variation between the cycles was minor and acceptable taking into the account that 3800 was the maximum engine speed with no load applied on the engine, which caused some variation. To avoid any variation between the cycles, the average of the 12 cycles was calculated and presented for the in-cylinder pressure and the heat release.

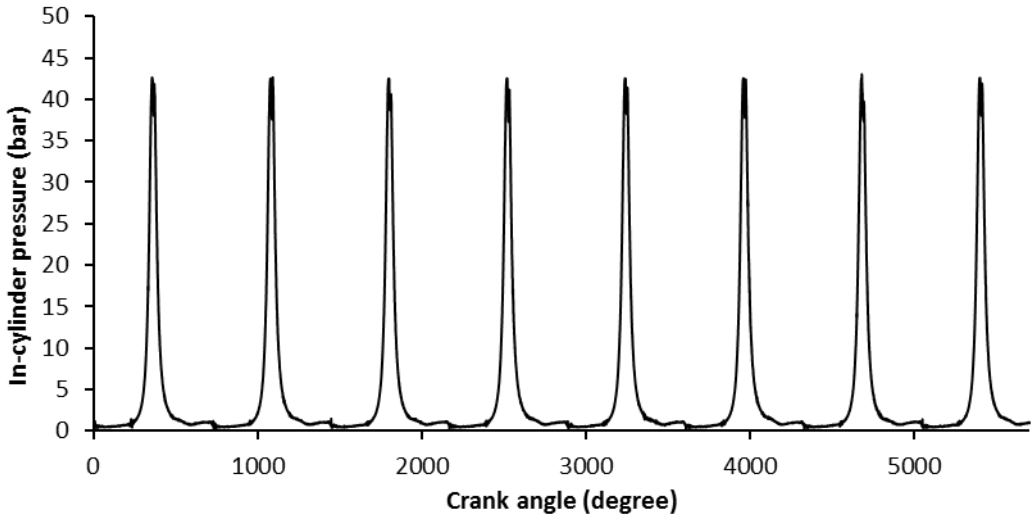

Figure 4.15 Typical in-cylinder pressure for the PD at 3800 rpm (no load)

Figure 4.16, Figure 4.17 and Figure 4.18 present the relationship between the in-cylinder pressure in bar and the crank angle at the engine speeds of 3670, 2900 and 2350 rpm, respectively. These figures show that increasing the load on the engine increased the maximum in-cylinder pressure to about 70 bar at 2900 and 2350 rpm.

The in-cylinder pressure results in Figure 4.16, Figure 4.17 and Figure 4.18 indicate that there was an inverse relationship between the in-cylinder pressure and the percentage of MCP-B100 in the fuel. The maximum in-cylinder pressure was found with PD and the lowest values were found with MCP-B100 at the engine speeds of 3670, 2900 and 2350 rpm. This is consistent with the findings of (An et al., 2013). At the engine speed of 3670 rpm, the maximum drop in the in-cylinder pressure, 5.8%, was found between the PD and MCP-B100. This finding is very close to the reduction in the in-cylinder pressure reported by An et al. (2013), who found a 5.8% reduction with biodiesel fuel compared with PD at 50% load. At the engine speeds of 2900 and 2350 rpm, the in-cylinder pressure showed very comparable results. The maximum drops in the in-cylinder pressure of 1.05%, 5.81% and 9.04% compared with PD were found at 2900 rpm with MCP-B20, MCP-B50 and MCP-B100, respectively. This was caused by the lower heating value. The reduction in the heating value of MCP-B100, as shown in Figure 4.13, was 13.3%, which was higher than the reduction in the in-cylinder pressure because of the higher cetane number and the extra O_2 in the MCP-B100 and its blends. The peak in-cylinder pressure occurred at ATDC for all fuels, which agrees with Gumus (2010), who found that the peak pressure occurred at 2.9–5.89º crank angle.

Ignition delay was found to be lower with MCP-B100 than with PD because of the higher cetane number.

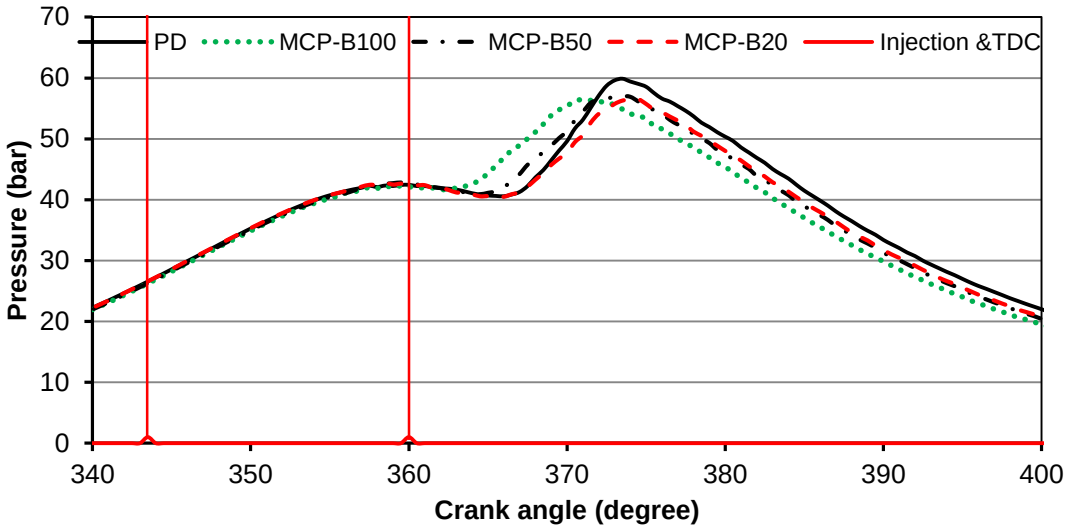

Figure 4.16 In-cylinder pressure at engine speed 3670 rpm

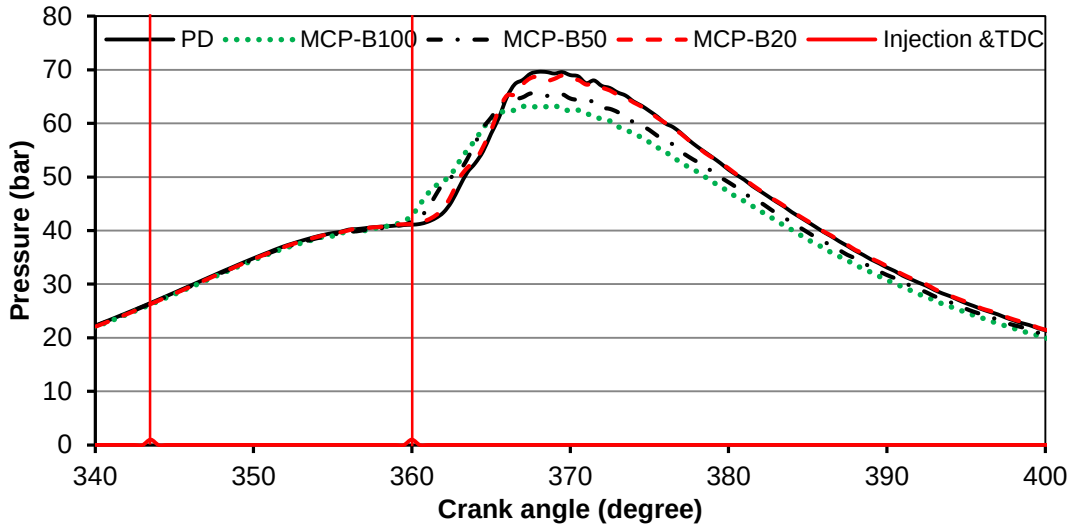

Figure 4.17 In-cylinder pressure at engine speed 2900 rpm

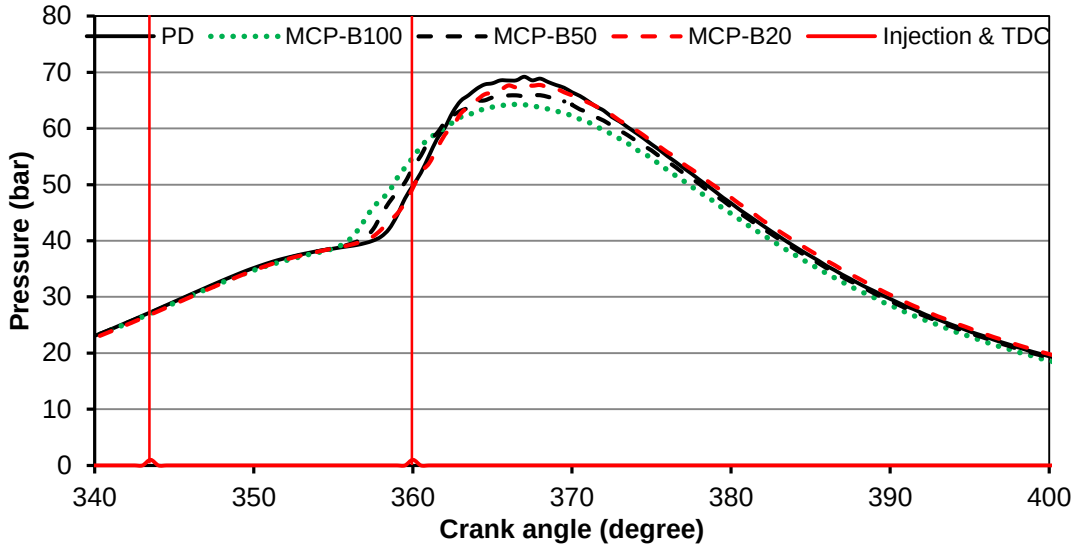

Figure 4.18 In-cylinder pressure at engine speed 2350 rpm

Heat Release Rate

Heat release rate is used to provide a better understanding about the combustion process in an engine (Ozsezen et al., 2008). It gives an indication of the ignition delay and the combustion duration (An et al., 2013). The heat release rate results for MCP-B100 and PD are presented in Figure 4.19, Figure 4.20 and Figure 4.21 at the engine speeds of 3670, 2900 and 2350 rpm, respectively. The results of the heat release of MCP-B50 and MCP-B20 are not presented because of the very close result obtained and to avoid overlap in the results, which makes comparison difficult. It also valuable to see the differences between the MCP-B100 and PD rather than the blends.

The maximum heat release rate was found to vary at different engine speeds. Figure 4.19 shows that the maximum heat release rate of MCP-B100 was lower than that of PD by about 4.2% at the engine speed of 3670 rpm. Since the engine FC rate and the engine thermal efficiency at this speed were relatively the same between these fuels, the reason for this reduction was the lower heating value of the MCP-B100. It has

been reported that the maximum in-cylinder pressure and heat release with biodiesel is lower than that of PD because of the higher energy of evaporation required with biodiesel (Kegl, 2011). The maximum heat release rate was found to be the same for MCP-B100 and PD at the engine speed 2900 rpm, as shown in Figure 4.20. This is because of the higher thermal efficiency (Figure 4.28) due to the MCP-B100 properties and the extra O_2 in its structure (Tesfa et al., 2013), which overcame the negative effect of the lower FC rate at this speed, as shown in Figure 4.26. Further evidence for this was found when the maximum heat release rate of MCP-B100 became higher by about 3.8% compared with PD, as shown in Figure 4.21. This was due to the effect of the higher FC rate at this speed associated with higher thermal efficiency from the fuel properties and the extra O_2 in the biodiesel structure, which was more effective at a higher engine load and lower air–fuel ratio.

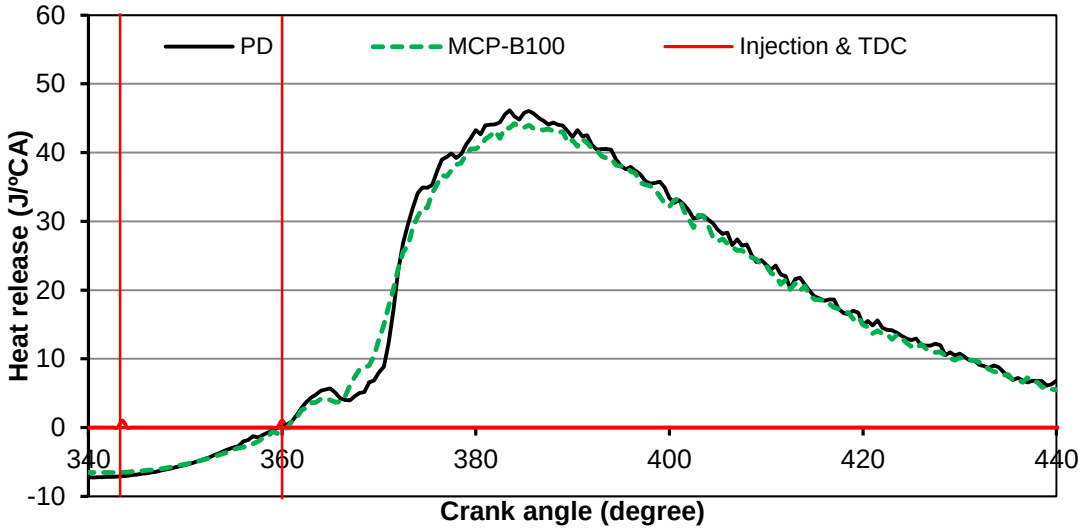

Figure 4.19 Heat release (J/ºCA) at engine speed 3670 rpm

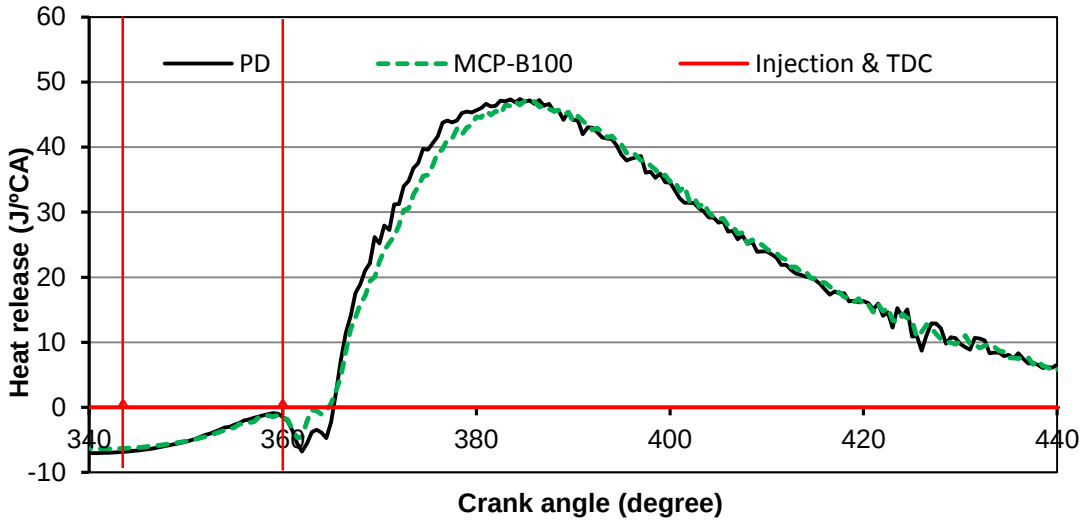

Figure 4.20 Heat release (J/ºCA) at engine speed 2900 rpm

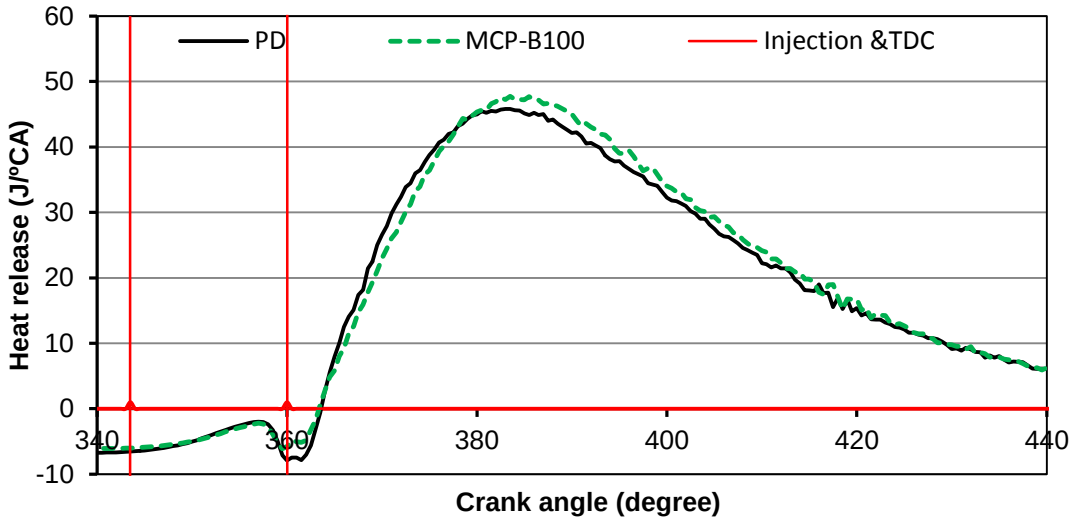

Figure 4.21 Heat release (J/ºCA) at engine speed 2350 rpm

4.4.3 Engine Performance Characteristics

This section presents the engine performance results when MCP-B100, MCP-B50, and MCP-B20 were used as fuel. These results are compared to the results of PD and are presented and discussed individually. The engine performance parameters presented in the following sections are gross input power (GIP), torque, brake power, BSFC, thermal efficiency, exhaust gas temperature and noise level.

Error and Statistical Analysis

The main purpose of the statistical analyse is to consider the total experimental error. This error can be from the instrument, test conditions, calibrations, observations, reading, experimental design etc. (Savariraj et al., 2011). The statistical analysis of the results using SPSS calculates the total combined error for the tests for each parameter and conceder it to indicate the significant differences between the means. The measurement error for the experiment has been considered in this work, and base on it, the readings and the tests have been repeated more than three times to minimise the measurement errors. Sample demonstration of the combined error calculation of the fuel consumption rate (FC) is given below as an example.

The FC is measured using electronic scale and stopwatch. The scale has an accuracy of 0.1g. During each test (at certain speed and load) the FC was measured three times. In each measurement, the time was three minutes.

The maximum error will occur at the lowest amount of fuel consumption. The minimum FC was around 400 g/hour at the engine speed of 3800 rpm.

$$FC = \frac{400}{60} = 6.67\ g/min$$

Each reading takes 3 min, so the minimum amount of fuel per reading is;

$$F_{mass} = 6.67 * 3 = 20\ \text{g}$$

The maximum error percentage in the fuel mass per reading is;

$$Max\ F_{\ Error} = \frac{0.1}{20} = \pm 0.005\%$$

The error in the FC reading is also comes from the time recording. The error assumed to be 0.5 sec at the start of the reading and 0.5 sec at the end of the reading.

$$Time_{Error} = 0.5 + 0.5 = \pm 1\ sec$$

Each reading takes 120 sec, so the time error is

$$Max\ time\ _{Error} = \frac{1}{120} = \pm 0.008\%$$

The FC error, which is the combination of the mass of fuel error and the time error, is;

$$FC_{Error} = 0.005 + 0.008 = \pm 0.013\%$$

The error in FC rate of ±0.013 % is the maximum error. For the higher FC, it can be lower than this value. This value of the error is further reduced by repeating the fuel consumption reading for three times and the whole test for another tree time at least.

The data of the engine performance and exhaust gas emissions were analysed using IBM SPSS Statistics 19 software. Two-way ANOVA was performed to study the effect effect of the different fuels on engine performance and exhaust gas emissions at different engine speeds. The analysis was performed to study the significance of the effect of the independent variables of fuel type and the engine speed on the dependent variables of the engine performance and exhaust gas emissions at p ≤ 0.05. The summary of the ANOVA results have been split into two tables: Table 4.6 presents the engine performance parameters and Table 4.8 (see Section 4.4.4) presents the engine exhaust gas emission parameters. An LSD post hoc test was performed to study the differences between the independent variables. The results of the descriptive statistics and the LSD test are presented in two tables:

Table 4.7 presents the engine performance parameters and Table 4.9 (see Section 4.4) presents the engine exhaust gas emissions parameters. The analysis gives the following results:

1. The effect of the fuel type as an independent factor in four levels (PD, MCP-B20, MCP-B50 and MCP-B100) on the engine performance and exhaust gas emission parameters at the averaged results obtained from all the tested engine speeds.
2. The effect of engine speed as an independent factor in five levels (3800, 3670, 2900, 2350 and 1770 rpm) on the engine performance and exhaust gas emission parameters. The descriptive statistics and LSD post hoc test summary data for the differences between the engine speeds are not presented because the effect of the engine speeds (at the average results of the different studied fuels) on the engine performance and exhaust gas emissions is not the main purpose of this study. The second reason is that the ANOVA test showed, as expected, a very significant difference between different engine speeds on the engine performance and exhaust gas emissions.
3. The significance of the interaction between the independent factors (the fuel type and the engine speed). The descriptive statistics and LSD post hoc test summary data of the interaction are not presented because the interaction between the fuel type and the engine speed is not statistically different. In addition, averaging the results of the studied fuels is not within the scope of this study.

The ANOVA and the descriptive statistics and LSD results are discussed separately in detail for each parameter of the engine performance and exhaust gas emissions in the following subsections. In each case, the discussion first refers to the ANOVA

results (Table 4.6 and/or Table 4.8) and then the descriptive and the LSD test results (

Table 4.7 and/or Table 4.9) as the averaged results of the studied fuels and the averaged results of all the studied engine speeds. The overall effect of each fuel on the parameters is presented as an average of the results obtained from the five studied points of speed. Then, the curves for the behaviour of each studied parameter for the different studied fuels at different engine speeds are presented and discussed.

Table 4.6 Summary of two-way ANOVA of the effect on the type of fuel, engine speed and the interaction between them on the engine performance parameters

Source	Dependent variable	Degrees of freedom	Mean square	F	Sig.*
Fuel	GIP	3.0	5.92	9.40	0.00
	Power	3.0	0.106	3.86	0.02
	Torque	3.0	0.711	2.75	0.05
	Efficiency	3.0	5.69	1.66	0.19
	Fuel cons.	3.0	241.53	0.07	0.98
	BSFC	3.0	4783.1	6.74	0.00
	EG Temp.	3.0	2517.9	2.74	0.05
	Noise level	3.0	18.357	10.2	0.00
Engine speed	GIP	4.0	110.04	174.62	0.00
	Power	4.0	17.605	643.67	0.00
	Torque	4.0	228.772	883.56	0.00
	Efficiency	4.0	920652.18	259.97	0.00
	Fuel cons.	4.0	920652.2	259.97	0.00
	BSFC	4.0	232661.7	327.61	0.00
	EG Temp.	4.0	212737.1	231.72	0.00
	Noise level	4.0	134.693	74.81	0.00
Fuel * Engine speed	GIP	12.0	2.30	3.64	0.00
	Power	12.0	0.035	1.30	0.25
	Torque	12.0	0.370	1.43	0.19
	Efficiency	12.0	4.03	1.18	0.33
	Fuel cons.	12.0	2680.7	0.76	0.69
	BSFC	12.0	1406.6	1.98	0.05
	EG Temp.	12.0	705.5	0.77	0.68
	Noise level	12.0	3.825	2.12	0.03

* The mean difference is significant if $p < 0.05$.

Table 4.7 Descriptive statistics and LSD post hoc test summary for the engine performance at the averaged results obtained from the tested engine speeds

Performance variable	PD		MCP-B20		MCP-B50		MCP-B100	
	M	SD	M	SD	M	SD	M	SD
GIP (kW)	10.05a	3.03	9.64a	3.00	9.44ab	2.88	8.80b	2.55
Brake power (kW)	2.58a	1.11	2.55ab	1.14	2.49ab	1.11	2.40b	1.02
Torque (N.m)	9.04a	4.01	9.06a	3.96	8.93ab	4.00	8.60b	3.78
BSFC (g/kW.h)	365.1a	108	378ab	125	394.6bc	144.2	402.3c	131
Fuel cons. (g/h)	836.6	252	843.9	269	842.3	248.0	844.7	245
Efficiency (%)	24.50	6.35	24.97	6.89	25.22	7.01	25.89	6.91
EG Temp. (^{o}C)	450.6a	119	445ab	121	448.6a	125.1	423.2b	125
Noise level (dB)	98.6a	3.37	97.8a	3.19	96.7b	3.03	96.4b	3.53

Means in the same row that do not share the same letter are significantly different at $p < 0.05$.

The Averaged Engine Performance Percentage Differences Compared with PD

The percentage of the differences of the engine performance and exhaust gas emissions compared with PD when MCP-B20, MCP-B50 and MCP-B100 fuels were used are given in Figure 4.22 and Figure 4.31. The figures present the percentage difference of the fuels as averaged results obtained from all the tested engine speeds. The results of each parameter in Figure 4.22 and Figure 4.31 are discussed separately in detail in the following subsections.

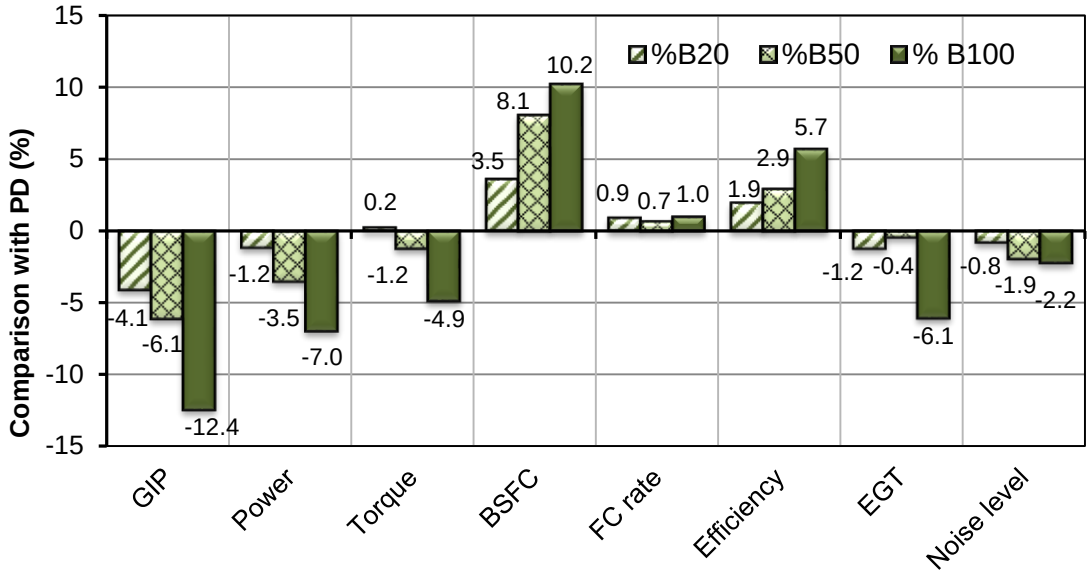

Figure 4.22 The averaged engine performance percentage differences compared with PD when MCP-B100, MCP-B50 and MCP-B20 were used

Gross Input Power (GIP)

The GIP is the function of the FC rate and the lower heating value of the fuel. The ANOVA results in Table 4.6 depict statistically significant differences in the GIP when PD, MCP-B100, MCP-B50 and MCP-B20 were used for the averaged results of all tested engine speeds. They also show that different engine speeds had a significant effect on the engine GIP at the average results of the studied fuels. The interaction between the tested fuels and the engine speed shown in Table 4.6 was significant.

Table 4.7 presents the descriptive statistics and LSD post hoc test summary for the engine performance parameters at the averaged results obtained from the tested engine speeds. This shows that PD, MCP-B20 and MCP-B50 share the same letter (a), which means they statistically had the same GIP, whereas MCP-B50 is statistically give same GIP results of all the fuels. The lowest significant GIP was found with MCP-B100, which dropped by 12.4% compared with PD, as shown in Figure 4.22. This reduction was caused by the lower heating value, which was found to be lower than PD by 13.3% for the MCP-B100. The FC rate was another factor

that affected the GIP. The FC rate was found to affect the GIP insignificantly, as shown in Table 4.6 for the averaged results obtained from the all tested speeds.

Figure 4.23 presents the GIP when PD, MCP-B20, MCP-B50 and MCP-B100 were used at different engine speeds. It can be observed from this figure that MCP-B100 and its blends presented lower GIP at all the tested speeds. It can also be observed that increasing the blend ratio of the MCP-B100 in the fuel reduced the GIP because of the lower heating value of the biodiesel (Ozsezen et al., 2008). The maximum difference (about 17.8%) between PD and MCP-B100 was found at 2900 rpm. This difference was higher than that expected from the lower heating value (13.3%) because, at this speed, the FC rate was found to be lower with MCP-B100 by about 5.3% compared with PD, as will be discussed later.

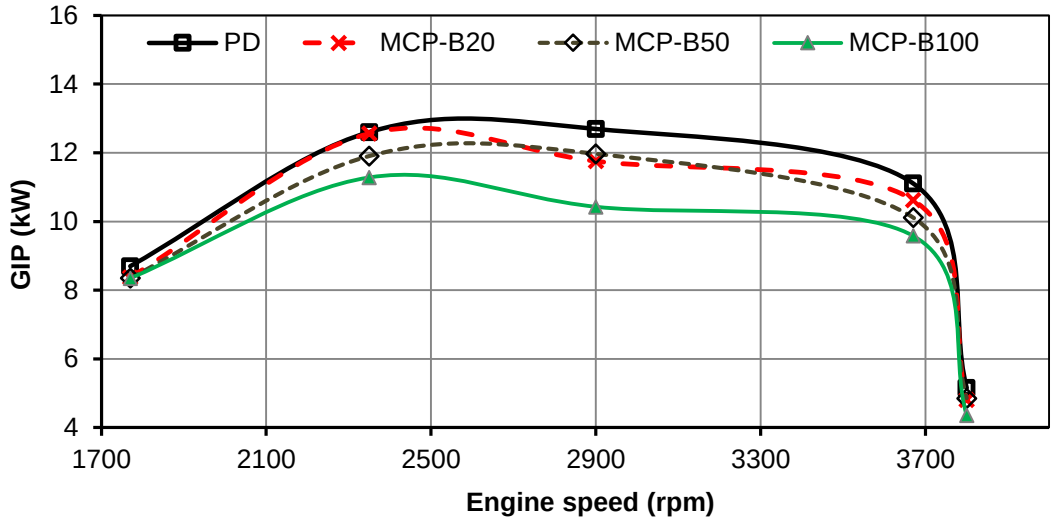

Figure 4.23 The relationship between engine speed (rpm) and engine GIP (kW) for PD, MCP-B20, MCP-B50 and MCP-B100

Brake Power

The engine brake power indicates the engine performance because it represents the engine's useful power that can be used by other devices. As shown in the ANOVA results (see Table 4.6), the engine brake power was significantly affected by the type

of fuel used in this test at the averaged engine speed. Similarly, the engine speed was found to have a highly significant effect on the engine brake power regardless of the fuel type, whereas the interaction between the type of fuel and the engine speed was statistically insignificant. This means that the trends of the brake power were statistically the same when the fuel and the speed changed.

Table 4.7 presents the post hoc LSD test showing the differences between the total brake power results produced when the engine was run with MCP-B100, MCP-B50, MCP-B20 and PD. It can be observed from

Table 4.7 that MCP-B100 produced significantly less averaged brake power than PD and MCP-B20, whereas MCP-B20 produced averaged engine brake power statistically the same as PD because of the lower percentage of microalgae fuel blend. MCP-B50 produced average brake power statistically similar to all the other fuels. This is because it consisted of 50% PD and 50% MCP-B100.

The behaviour of the engine brake power at different engine speeds using PD, MCP-B20, MCP-B50 and MCP-B100 is plotted in Figure 4.24. This figure shows that the brake power trends for all fuels increased as the engine speed increased, reaching its maximum at engine speeds between 2900 and 3670 rpm and then sharply declining. The low brake power at the engine speed of 3800 rpm was caused by the engine running at maximum speed and no load being applied from the dynamometer. When load was applied on the engine associated with high speed (3670 rpm), maximum brake power occurred. The maximum brake power values that occurred at 3670 rpm for PD and MCP-B20 were insignificantly different from the brake power values found at 2900 rpm for the same fuels, whereas the maximum power values for the MCP-B50 and MCP-B100 occurred at 2900 rpm also with insignificant difference from the brake power values produced at 3670 rpm. The variation between fuels was

clear at the engine speed of 3670 rpm. The maximum brake power values were found to be in the following order: PD (3.71 kW), MCP-B20 (3.51 kW), MCP-B50 (3.39 kW) and MCP-B100 (3.14 kW), with a reduction percentage of 5.39%, 8.63% and 15.36%, respectively. The reason for the reduction was the lower heating value of the biodiesel fuel (Ozsezen et al., 2008).

As shown in Figure 4.13, the lower heating value of MCP-B20, MCP-B50 and MCP-B100 was reduced by 2.7%, 6.7% and 13.3%, respectively. The reduction in the averaged brake power, as presented in Figure 4.22, was only by 1.2%, 3.5% and 7.0%, respectively. This reduction was considerably less than expected because of the negative effect of the lower heating value of the biodiesel fuel. This may have been caused by various parameters, such as the higher density and cetane number of the MCP-B100 and its blends compared with PD, which reduced the negative effect of the lower heating value. The higher viscosity can contribute to reducing the fuel leakage in the fuel pump, which enhances engine power (Usta et al., 2005). The brake power was reduced by 7% when the engine was fuelled with MCP-B100 compared with PD, and the heating value was lower by 13.3%, which is in good agreement with the findings of (Wahlen et al., 2012). They found that microalgae biodiesel produced 6.3% less power than PD and stated that this reduction in the power was close to the expected reduction due to the lower heating value (if the higher density was taken into account). Özener et al. (2012) stated that the reduction in power was lower than the reduction in the heating value due to the extra fuel injected and the higher density.

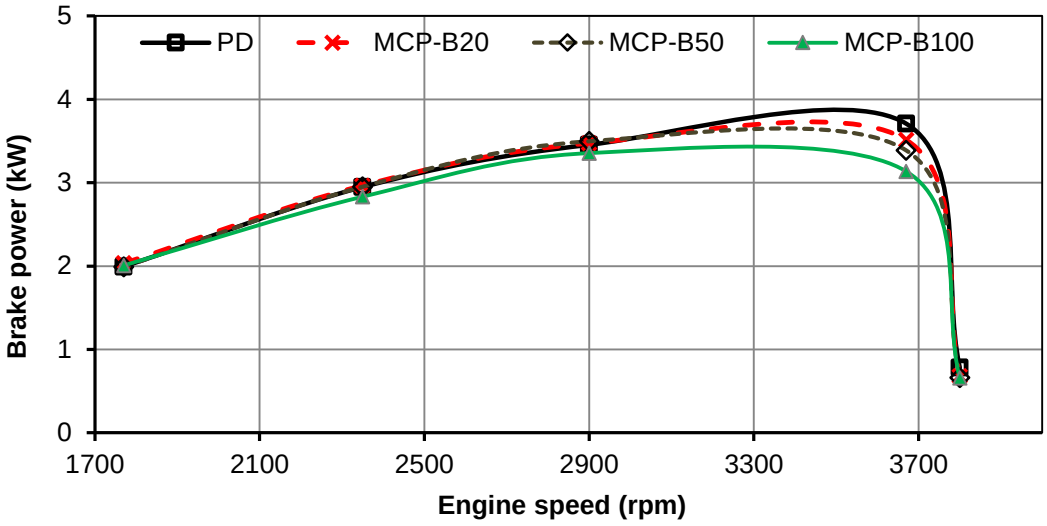

Figure 4.24 The relationship between engine speed (rpm) and engine BP (kW) for PD, MCP-B20, MCP-B50 and MCP-B100

The positive effect of the O_2 in the biodiesel structure is another factor that reduced the negative effect of the lower heating value. The O_2 content in the biodiesel chemical composition was more affective at the full load condition (at rich combustion and low lambda value). Consequently, the results of the brake power were comparable at low engine speeds (high load) for all the fuels. Another possible reason for this is the higher cetane number, which indicates better ignition quality. At engine speeds of 2350 and 1770 rpm, there was also a higher FC rate, which raised the power. At the speed of 2900 rpm, the FC rate for MCP-B100 was lower than that for PD. This is supposed to drop the brake power associated with lower heating value, but the reduction was less than expected for the reasons stated above. This results maximum increase in the combustion efficacy as presented in Figure 4.28.

Torque

Table 4.6 shows that the engine torque was significantly affected by the type of fuel tested and was very significantly affected by the engine speed, whereas the interaction between the fuel type and the engine speed was insignificant.

Table 4.7 indicates that the torque produced by MCP-B100 was significantly lower than the torque from PD and MCP-B20. The reduction in the torque of about 4.9% with MCP-B100, as illustrated in Figure 4.22, is in high agreement with Chokri et al. (2012), who reported a reduction in the engine torque of about 5% with biodiesel from a waste vegetable oil biodiesel blend, and is consistent with Haik et al. (2011). However, the MCP-B50 shares the same letters with all the fuels, which means it produced torque statistically the same as all fuels.

Table 4.7 also shows that the average engine torque was reduced when the biodiesel percentage in the fuel increased. This is in high agreement with (An et al., 2013) and was caused by the lower heating value.

The engine torque measured by the dynamometer for PD, MCP-B20, MCP-B50 and MCP-B100 at different engine speeds is presented in Figure 4.25. It can be observed from Figure 4.25 that the general trends in engine torque for all the fuels were the same, and this is confirmed by Table 4.6 (showing that the interaction between fuel and the engine speed was insignificant). Figure 4.25 shows that the engine torque for all fuels was increased as the engine speed increased, reaching the peak of about 12.02 kW at 2350 rpm and then decreasing slightly until reaching the engine speed of 3670 rpm. The torque dropped sharply as the no-load condition was reached at the maximum engine speed of 3800 rpm.

For all engine speeds except 3670 rpm, all fuels gave comparable torque results. This is because the reduction in the heating value was offset by the higher density and cetane number. The engine speed of 3670 rpm presented the maximum difference between PD and MCP-B100 of 19.12%.

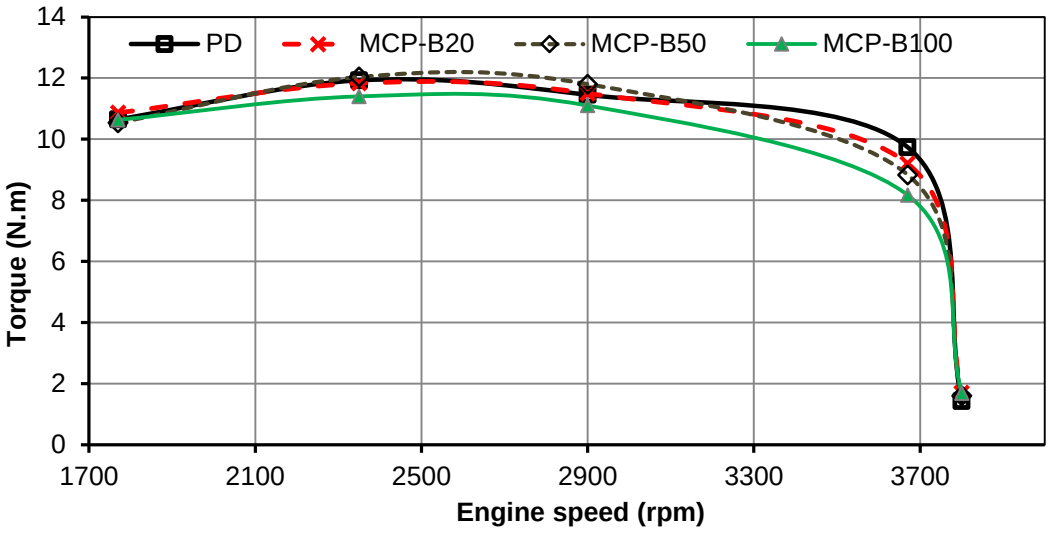

Figure 4.25 The relationship between engine speed (rpm) and engine torque (N.m) for PD, MCP-B20, MCP-B50 and MCP-B100

Fuel Consumption (FC) Rate

The summary of the ANOVA results in Table 4.6 shows insignificant differences between the fuels tested for the FC rate. Therefore, the extra fuel injected to compensate for the reduction in the engine power was insignificant. This indicates that the reduction in engine power was caused by the fuel properties because the fuel injected to the combustion chamber was statistically the same. Figure 4.26 shows the FC rate of the engine fuelled with PD, MCP-B20, MCP-B50 and MCP-B100 at different engine speeds. It can be seen that the FC rate reached the maximum at the engine speed of 2350 rpm for MCP-B100 and MCP-B20, whereas for PD and MCP-B50, the maximum was found at the range of 2350 to 2900 rpm. The reason for this high FC rate was the high load applied on the engine at those speeds. As indicated in Figure 4.25, the maximum torque was found at those engine speeds that justifies the need for extra fuel.

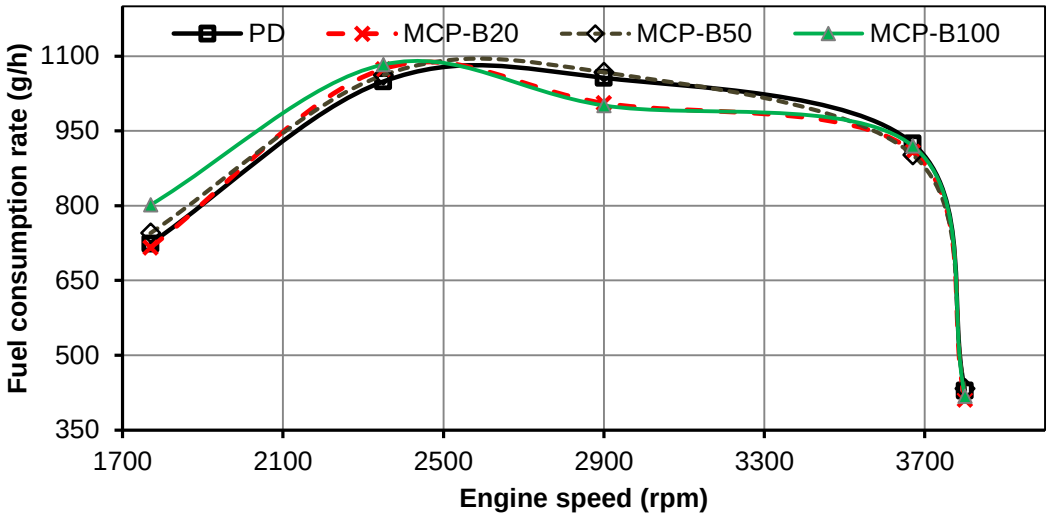

Figure 4.26 The relationship between engine speed (rpm) and fuel consumption rate (g/h) for PD, MCP-B20, MCP-B50 and MCP-B100

Brake Specific Fuel Consumption (BSFC)

Table 4.6 provides a summary of the ANOVA results indicating the difference between the fuels, engine speeds and the interaction between them. It shows that the average BSFC recorded when the engine was fuelled with PD, MCP-B20, MCP-B50 and MCP-B100 were statistically different. More details are presented in

Table 4.7, which shows that the average BSFC was directly proportionate to the MCP-B100 percentage in the fuel. It is clear from

Table 4.7 that the PD presented the lowest value of average BSFC (365g/kW.h), which was statistically the same as the average BSFC from MCP-B20, whereas the MCP-B100 gave the highest value of 401 g/kW.h), which was also statistically insignificant with MCP-B50. Figure 4.22 presents the differences in the average BSFC using MCP-B20, MCP-B50 and MCP-B100 compared with PD: 3.5%, 8.1% and 10.2%, respectively. These differences resulted from the fuels' chemical and physical properties, such as lower heating value, which means the engine was required to burn extra biodiesel fuel to reach the same brake power produced using PD (Canakci, 2009; Özener et al., 2012; Ozsezen et al., 2008; Usta et al., 2005; Wahlen et al., 2012). The increase in BSFC with biodiesel from soybean ranged from

2% to 9% in a study by Özener et al. (2012) and was less than 8.5% with biodiesel from waste cooking olive oil compared with PD in a study by Dorado et al. (2003b) .

The BSFC at each engine speed using different fuels is presented in Figure 4.27. For the engine under load conditions, the maximum BSFC occurred at the lowest speed of 1770 rpm for MCP-B100. This agrees with Ozsezen et al. (2008) that B100 gave a higher BSFC at the lowest engine speed of 1000 rpm. At the engine speed 3670 rpm, when the maximum power was achieved, the lowest BSFC was recorded for all fuels. At the same speed, the variation between PD and MCP-B100 blends was clear, with an increase of 4.5%, 7.4% and 18.0% for MCP-B20, MCP-B50 and MCP-100, respectively. The FC rate was statistically insignificant, especially at this speed, as shown in Figure 4.26; therefore, the higher BSFC was mainly caused by the lower brake power obtained from MCP-B100 and its blends. The BSFC increased as the load increased (lower engine speed). This is consistent with the findings of Usta et al. (2005). The BSFC from microalgae biodiesel was found to be higher than PD (Wahlen et al., 2012).

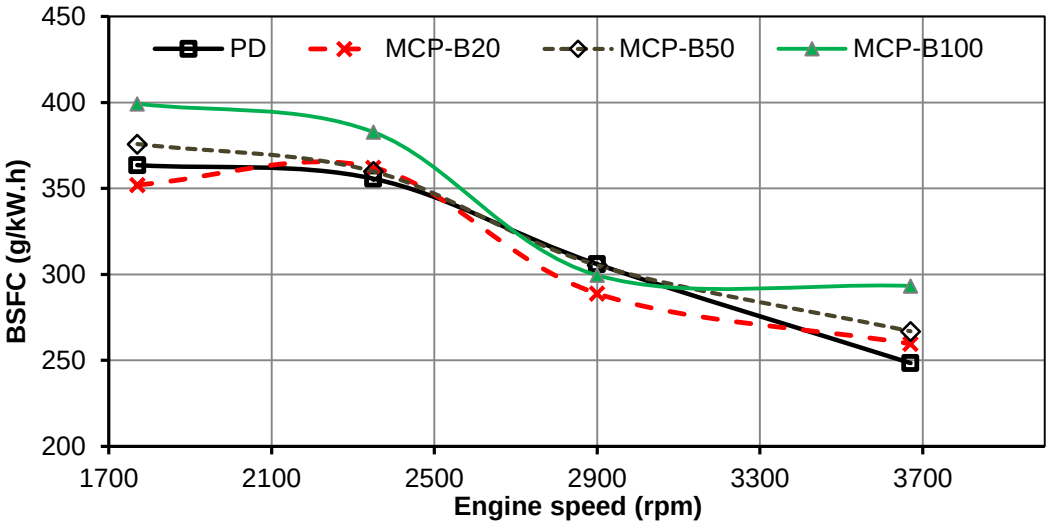

Figure 4.27 The relationship between engine speed (rpm) and BSFC (g/kW.h) for PD, MCP-B20, MCP-B50 and MCP-B100

Thermal Efficiency

The ANOVA summary in Table 4.6 indicates that the type of fuels used in this study insignificantly affected the average thermal efficiency. This agrees with Dorado et al. (2003a), Dorado et al. (2003b) and Usta et al. (2005) that the difference in the thermal efficiency of PD and B17.5 was insignificantly higher because of the lower heating value. In contrast, the engine speed showed a very significant effect on the average thermal efficiency. The interaction between the fuel type and the engine speed was also insignificant. However, the effect of the fuel type on thermal efficiency was insignificant because of the higher standard deviation. As presented in

Table 4.7, PD produced the lower average thermal efficiency of 24.5%. MCP-B100 produced the highest average thermal efficiency of 25.9%. This was caused by the chemical and physical properties of MCP-B100, such as the higher cetane number, density and O_2 content in the biodiesel structure.

Figure 4.28 displays the relationship between the thermal efficiency and engine speed for PD, MCP-B20, MCP-B50 and MCP-B100. At engine speeds of 2900 rpm and below, the thermal efficiency of MCP-B100 and its blends was higher than the thermal efficiency of PD. The maximum difference of 18.6% between MCP-B100 and PD was evident at the engine speed of 2900 rpm. This speed was selected as the lower BSFC speed located by the manufacturer. A lower BSFC is the inverse of thermal efficiency, which means the thermal efficiency was sensitive to the fuel type at this speed.

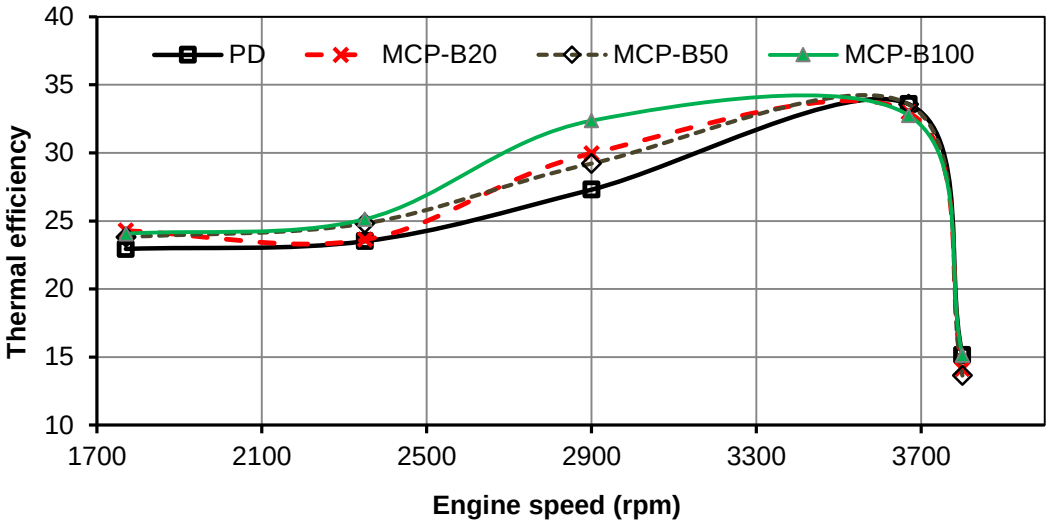

Figure 4.28 The relationship between engine speed (rpm) and engine thermal efficiency (%) for PD, MCP-B20, MCP-B50 and MCP-B100

Exhaust Gas Temperature

The exhaust gas temperature generated from PD, MCP-B20, MCP-B50 and MCP-B100 were analysed using ANOVA, as shown in Table 4.6. This table indicates that the effect of the fuel type and the effect of the engine speed on the exhaust gas temperature were statistically significant. Conversely, the interaction between the fuel type and the engine speed was statistically insignificant.

Table 4.7indicates that the exhaust temperature generated from MCP-B100 was significantly lower from PD and MCP-B50 and insignificantly lower than MCP-B20. This is thought to be due to the lower heating value of the biodiesel and the overall chemical and physical properties. According to Figure 4.22, the exhaust gas temperature of MCP-B100 was 6.1% lower than that of PD.

The exhaust gas temperature of PD, MCP-B20, MCP-B50 and MCP-B100 at every engine speed is shown in Figure 4.29. The exhaust gas temperature curves for all fuels can be described as follows: the exhaust gas temperatures increased with an increase in the engine speed, reaching their respective peaks at engine speeds

between 2350 and 2900 rpm and then reducing gradually until reaching 3670 rpm. Beyond this speed, the exhaust gas temperatures dramatically dropped because of the no load applied on the engine at this speed. At the engine speed of 3670 rpm, the maximum reduction of about 61 ºC (12.4%) of the exhaust gas temperature for MCP-B100 below that for PD occurred, which is very close to what was expected because of the lower heating value of the MCP-B100, which dropped by 13.3%. At the speed of 3670 rpm, the differences in the thermal efficiency between PD and MCP-B100 were comparable, which indicates that the reduction in the exhaust gas temperature was caused by the lower heating value. Overall, the averaged exhaust gas temperature declined by only about 6.1%. This due to the combustion enhanced that clear by higher thermal efficiency with MCP-B100 because of the same factors explained previously. It can be concluded that the exhaust temperature was strongly related to the lower heating value of the fuels and the thermal efficiency. The increase in thermal efficiency with MCP-B100 and its blends reduced the reduction in the exhaust gas temperature because of the lower heating value.

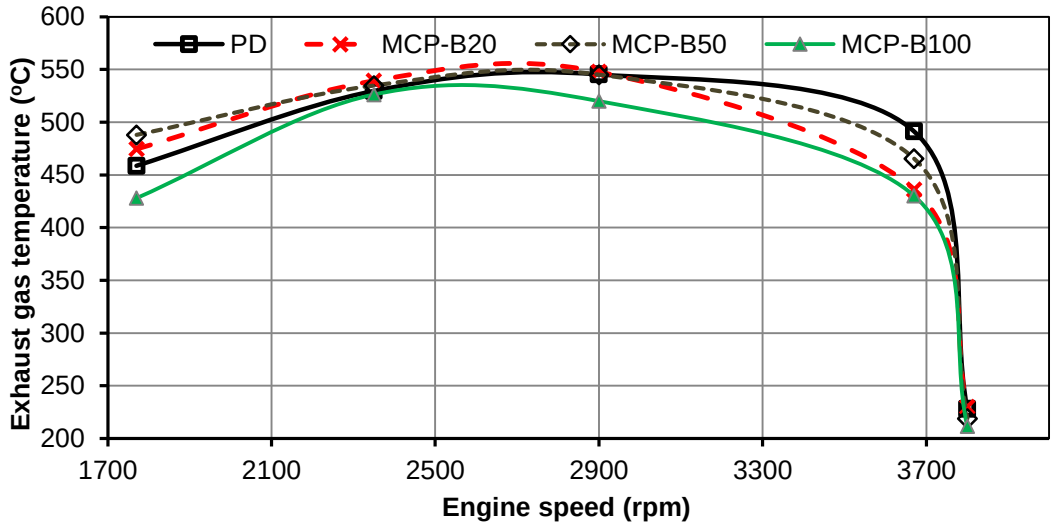

Figure 4.29 The relationship between engine speed (rpm) and exhaust gas temperature (ºC) for PD, MCP-B20, MCP-B50 and MCP-B100

Noise Level

The noise level is a function of the in-cylinder pressure waves during the combustion process. The ANOVA results in Table 4.6 show that the noise level from MCP-B100 and its blends was significantly lower than from PD. From

Table 4.7, which presents the means of the noise level from PD, MCP-B20, MCP-B50 and MCP-B100, and the LSD comparison between them, it can be seen that the noise level from PD and MCP-B20 were statistically insignificant. This was caused by the lower blend ratio and the standard deviation, whereas the MCP-B50 and MCP-B100 generated significantly lower noise levels than PD and MCP-B20. This agrees with Ozsezen et al. (2008) and Ozsezen et al. (2009) due to the higher cetane number of biodiesel fuel (Prakash, 1998). However, this finding is in contrast with that of Haik et al. (2011), who found an increase in the engine noise with biodiesel from microalgae.

The percentage of this reduction is presented in Figure 4.22. This figure shows that MCP-B20, MCP-B50 and MCP-B100 generated 0.8%, 2.0% and 2.3% reductions in the noise level, respectively, compared with PD. It also illustrates that the noise level generated from the engine was inversely related with the MCP-B100 blend ratio in the fuel. Figure 4.30 depicts the results of the noise level generated by PD, MCP-B20, MCP-B50 and MCP-B100 at each engine speed. It can be observed that when the engine speed increased, starting from 1770 rpm, the noise level increased, reaching the maximum at 3670 rpm and then sharply declining. The maximum noise level recorded was 102.4 dB, 101.4 dB, 100.3 dB and 100.4 dB from PD, MCP-B20, MCP-B50 and MCP-B100, respectively. Similar findings reported by Ozsezen et al. (2008) and Usta et al. (2005) showed that addition of biodiesel to PD fuel reduced

engine noise level. However, these researchers reported the variation between biodiesel B17.5 and PD to be about 1 dB.

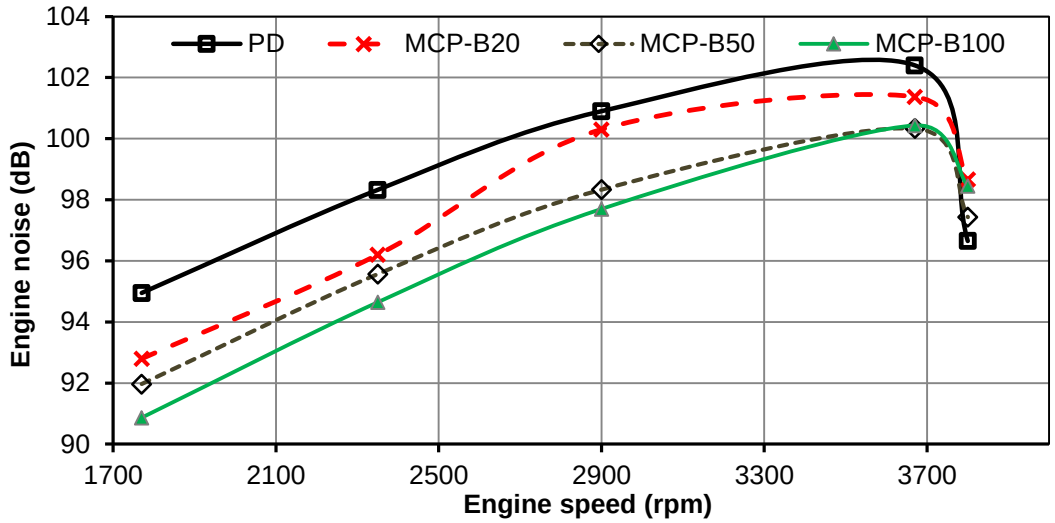

Figure 4.30 The relationship between engine speed (rpm) and engine noise level (dB) for PD, MCP-B20, MCP-B50 and MCP-B100

4.4.4 Emission Characteristics

The averaged exhaust gas emissions from the engine fuelled with PD, MCP-B20, MCP-B50 and MCP-B100 were statistically analysed and are presented in Table 4.8 and Table 4.9. The percentage of the differences of the average exhaust gas emissions compared with PD when MCP-B20, MCP-B50 and MCP-B100 were used are given in Figure 4.31.

Table 4.8 Summary of two-way ANOVA of the effect of the type of fuel, engine speed and the interaction between them on the engine emission parameters

Source	Dependent variable	Degrees of freedom	Mean square	F	Sig.*
Fuel	CO	3.0	1.340	8.08	0.00
	CO_2	3.0	0.323	1.49	0.23
	O_2	3.0	4.40	9.45	0.00
	LDA	3.0	0.177	17.37	0.00
	NO_x	3.0	3200	3.11	0.04
Engine speed	CO	4.0	49.767	300.13	0.00
	CO_2	4.0	80.024	369.23	0.00
	O_2	4.0	305.02	654.32	0.00

	LDA	4.0	15.374	1511.93	0.00
	NO_x	4.0	432460.5	420.08	0.00
Fuel * Engine speed	CO	12.0	0.373	2.25	0.03
	CO_2	12.0	0.193	0.89	0.56
	O_2	12.0	0.52	1.11	0.37
	LDA	12.0	0.036	3.57	0.00
	NO_x	12.0	1413.2	1.373	0.214

* The mean difference is significant if $p < 0.05$.

Table 4.9 Descriptive statistics and LSD post hoc test summary for the engine emissions at the average tested engine speeds

Emissions variable	PD		MCP-B20		MCP-B50		MCP-B100	
	M	SD	M	SD	M	SD	M	SD
CO (%)	2.36a	2.00	2.07b	1.96	1.95bc	1.76	1.70c	1.75
CO_2 (%)	7.56	2.33	7.51	2.34	7.50	2.40	7.24	2.34
O_2 (%)	7.73a	4.68	8.05ab	4.64	8.26b	4.55	8.95c	4.37
Lambda	1.57a	0.90	1.66b	1.04	1.67b	1.00	1.82c	1.13
NO_x (ppm)	396.7a	185	387.0b	175	371.5b	179.6	367.4b	160

Means in the same row that do not share the same letter are significantly difference at $p < 0.05$.

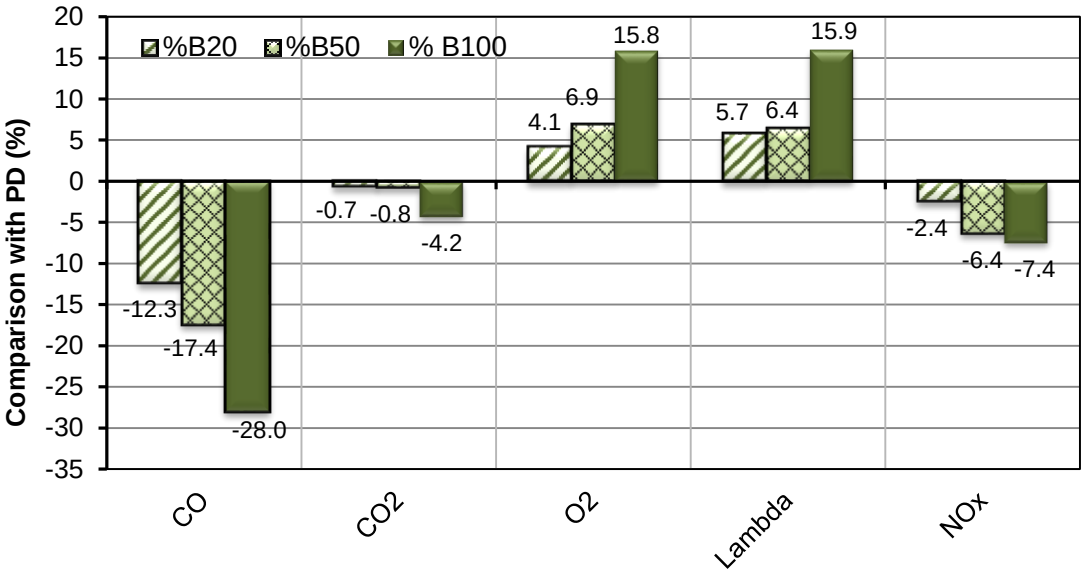

Figure 4.31 The average exhaust emission differences percentage compared with PD when MCP-B20, MCP-B50 and MCP-B100 were used

Carbon Monoxide (CO)

The ANOVA results in Table 4.6 demonstrate that the average CO level emitted using the studied fuels was very significant at the average results of the tested engine speeds. The engine speed also affected the average CO emission very significantly. In In a study by Dorado et al. (2003b) , a statistical test using the unpaired t-test showed that CO emission from olive oil biodiesel and PD were statistically significant. There was a significant interaction between the type of the fuel and the engine speed on the CO percentage. From

Table 4.7, it can be observed that increasing the proportion of MCP-B100 in the fuel decreased the CO emissions. It also shows that PD gave the highest value of CO emission of 2.4% at different engine speeds, and MCP-B100 presented the lowest value of 1.7%. The LSD test results in

Table 4.7 demonstrate that the MCP-B50 produced significantly lower CO percentage than PD and an insignificant difference compared with both MCP-B20 and MCP-B100. As presented in Figure 4.31, the average CO percentage emission was reduced compared with PD by 12.3%, 17.4% and 28.0% for the MCP-B20, MCP-B50 and MCP-B100, respectively. This agrees with Özener et al. (2012) finding that soybean biodiesel B20, B50 and B100 produced 31%, 38% and 46% lower CO than PD, respectively, due to the O_2 in the biodiesel, which indicated more efficient combustion.

The results of the tests on CO emission at different engine speeds for PD, MCP-B20, MCP-B50 and MCP-B100 are presented in Figure 4.32. The figure indicates that the CO percentage curves for all the fuels were relatively steady for engine speeds below 2320 rpm and then the CO emission declined with increases in the engine speed. The maximum variation of 69.4% between the fuels was found at 2900 rpm between PD and MCP-B100. This was because, at this speed, the maximum increase in the

thermal efficiency with MCP-B100 was recorded and the engine was running lean, as shown in Figure 4.35, which is associated with relatively lower BSFC. This indicates better combustion with biodiesel because of the extra O_2 in the biodiesel and the higher cetane number, which was higher in MCP-B100 by 2%, as shown in Figure 4.13. The reduction in the CO level at high engine speeds can be linked to the higher lambda values (see Figure 4.35), which increased the air–fuel ratio and thus helped convert the CO to CO_2 (Özener et al., 2012).

It can be concluded that the CO level was inversely related to the engine speed and inversely related with the MCP-B percentage in the fuel because of the higher O_2 in the biodiesel, which enhanced the combustion process.

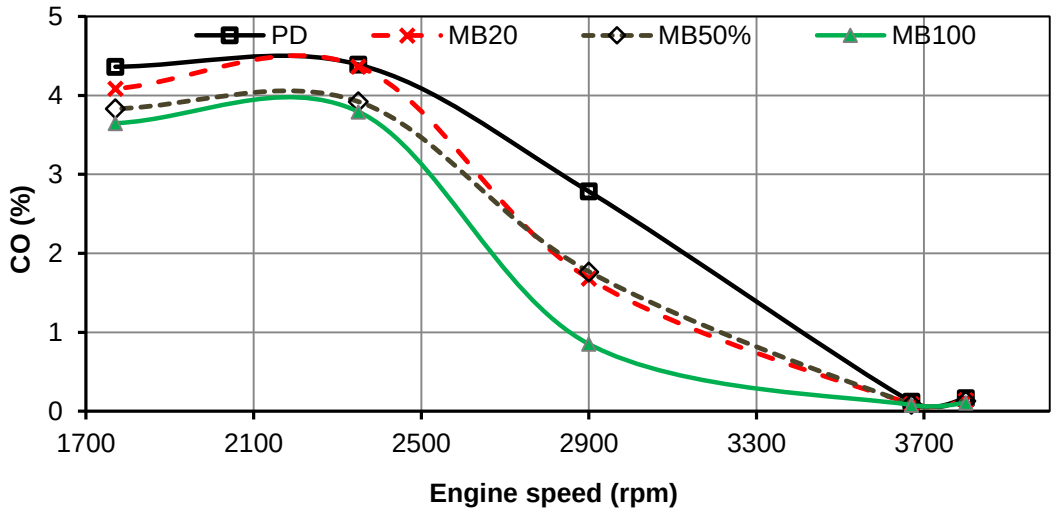

Figure 4.32 The relationship between engine speed (rpm) and CO (%) for PD, MCP-B20, MCP-B50 and MCP-B100

Carbon Dioxide (CO_2)

The ANOVA results in Table 4.6 show that the average CO_2 emissions produced from using PD, MCP-B20, MCP-B50 and MCP-B100 were statistically insignificant and considered statistically the same because of the higher standard deviation. Table shows that increasing the percentage of MCP-B100 in the fuel slightly reduced

the CO_2 emission. The average CO_2 level when the engine was fuelled with MCP-B100 compared with that of PD was found to be 4.2% lower, as shown in Figure 4.31.

Figure 4.33 presents the relationship between the CO_2 percentage and the engine speed for PD, MCP-B20, MCP-B50 and MCP-B100. The maximum CO_2 emissions were found at 2900 rpm in all fuels, and the maximum variation between the fuels was found at 3670 rpm. A possible reason is that the engine was tuned by the manufacturer to give maximum power with PD at 3670 rpm. Meanwhile, there was a strong correlation between the FC rate and CO emissions from all the tested fuels, indicating a strong correlation between CO_2 and combustion efficiency. PD produced an insignificantly higher thermal efficiency at 3670 rpm, which resulted in better combustion with PD and more CO converted to CO_2 than with MCP-B100 and its blends at this speed. It can be also observed that, at low engine speed below 2350 rpm, when the load increased, MCP-B100 and its blends produced insignificantly higher CO_2 compared with PD. The reasons for this were the high load, that the air–fuel ratio was close to the stoichiometric or even a rich mixture, and the availability of the O_2 in MCP-B100 and its blends, associated with an increase in the time for reaction (due to the low engine speed), slightly enhancing the combustion and allowing more CO to be converted to CO_2. This is supported by the results of the thermal efficiency test presented in Figure 4.28. A similar finding and justification was found by Özener et al. (2012).

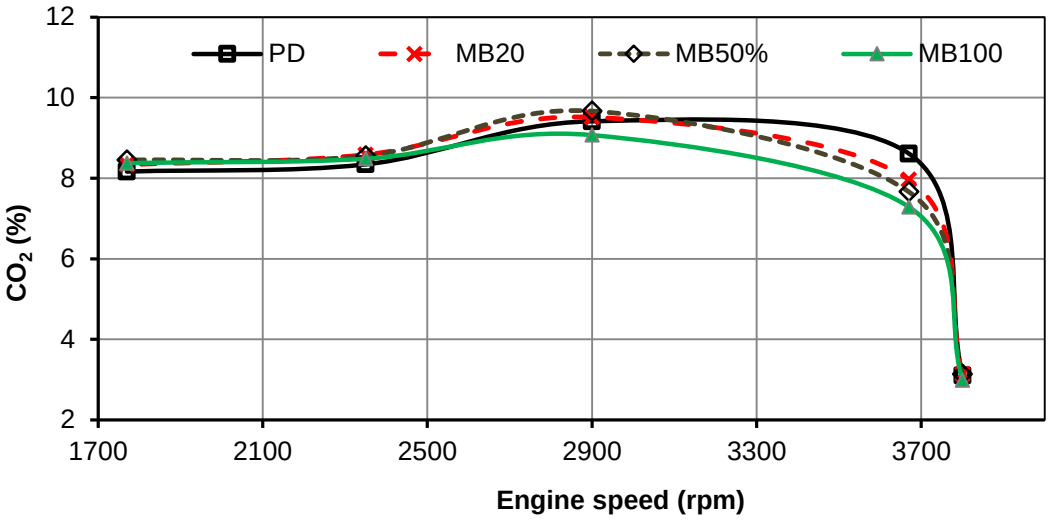

Figure 4.33 The relationship between engine speed (rpm) and CO_2 (%) for PD, MCP-B20, MCP-B50 and MCP-B100

Oxygen (O_2)

As presented in the ANOVA summary in Table 4.6, the O_2 levels from all the fuels at the average of the overall tests were statistically the same because of the high variation between the runs using the same fuel that clear by the high standard deviations presented in

Table 4.7. Nevertheless,

Table 4.7 demonstrates an inverse relationship between the MCP-B100 percentage in the fuels and the O_2 level in the exhaust, because the diesel engine normally runs lean and extra O_2 was already available. The extra O_2 in the MCP-B100 chemical structure contributed to increasing the O_2 level in the exhaust. Figure 4.31 displays an increase in the O_2 level in the exhaust gas emissions by 4.1%, 6.9% and 15.8% when MCP-B20, MCP-B50 and MCP-B100 were used, respectively, compared with PD. This is in strong agreement with the findings of Dorado et al. (2003b) that biodiesel fuel from olive oil produced 17.6% higher O_2 than PD.

Figure 4.34 shows the O_2 percentage in the exhaust gas emissions versus the engine speed using PD, MCP-B20, MCP-B50 and MCP-B100 fuels. It is clear that increasing the engine speed (by reducing the load on the engine) raised the O_2 level in the exhaust due to a rise in lambda. Increasing the load on the engine required extra O_2 to form complete combustion.

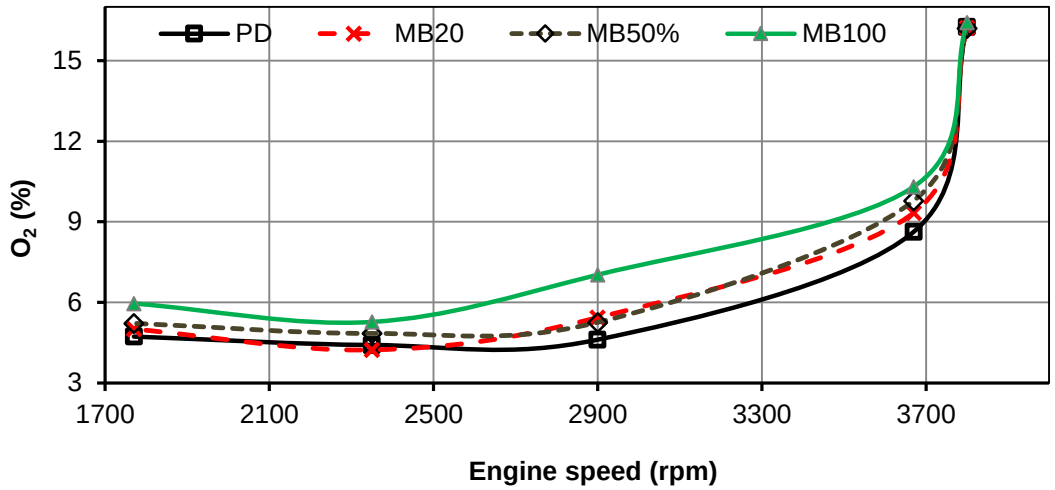

Figure 4.34 The relationship between engine speed (rpm) and O_2 (%) for PD, MCP-B20, MCP-B50 and MCP-B100

Lambda

The results of the lambda percentage can be found in Table 4.6,

Table 4.7 and Figure 4.33 as follows. Table 4.6 explains that the difference between the averaged lambda results were statistically different when the fuel was changed or when the speed was changed. It also shows that the interaction between the fuel type and the engine speed statistically affected the lambda value. Further details can be observed in

Table 4.7, which shows the comparison between fuels. The comparison shows that MCP-B100 produced the highest average lambda value (1.82) compared with all other fuels. The statistically lowest lambda value of 1.57 was recorded with PD, and MCP-B20 and MCP-B50 recorded the same results statistically. This is consistent with the fact that diesel engines generally run lean. It is clear that the extra O_2 in the

biodiesel structure contributed to a higher lambda reading because the lambda sensor measured the level of O_2 in the exhaust to determine lambda.

As shown in Figure 4.31, the increase in lambda values was calculated to be 5.7, 6.4 and 15.9 when MCP-B20, MCP-B50 and MCP-B100 were compared with PD. The relationship between engine speed (rpm) and lambda for PD, MCP-B20, MCP-B50 and MCP-B100 is given in Figure 4.35. Lambda values in this figure are shown to be around 1.0 at lower engine speeds below 2350 rpm because of the higher fuel flow rate required for the high load applied on the engine at those speeds. The engine speed of 2350 rpm is the speed at which the engine ran rich with all fuels. This was because of the higher load associated with higher fuel flow rate consumption recorded at this speed while the airflow rate remained constant. At the engine speeds of 2900 rpm and above, the engine ran lean and the lambda values increased.

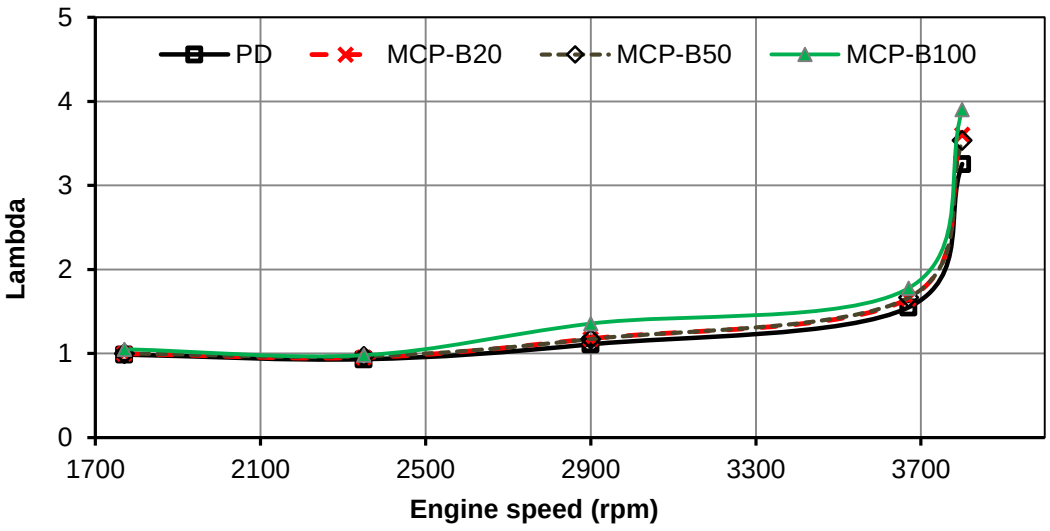

Figure 4.35 The relationship between engine speed (rpm) and lambda for PD, MCP-B20, MCP-B50 and MCP-B100

Nitrogen Oxides (NO_x)

The ANOVA results in Table 4.6 indicate that the NO_x emissions statistically varied when the fuel was changed in the average of the overall test. This finding is consistent with an unpaired t-test performed by Dorado et al. (2003b) that showed

that the difference in NO emission from olive oil biodiesel and PD was very significant. The NO_x results were also significantly different between the tested speeds. The interaction between the fuel type and the engine speed, as shown in Table 4.6, was insignificant.

Table 4.7 presents a comparison of the means of the fuels tested and depicts the NO_x emission decreasing with an increasing percentage of MCP-B100 in the fuel. This table indicates that MCP-B20, MCP-B50 and MCP-B100 statistically produced similar results and all statistically produced lower emission than PD. PD in the overall test emitted an average NO_x of 396.7 ppm, which was about 7.4% higher than MCP-B100. This was caused by the higher cetane number for the biodiesel that decreased the NO_x emissions (Prakash, 1998). This reduction was also caused by the lower exhaust temperature (An et al., 2013) that was recorded with MCP-B100 and its blends, as previously mentioned.

Figure 4.36 presents the results of NO_x emission produced from PD, MCP-B20, MCP-B50 and MCP-B100 for verses engine speeds. This figure shows that the curve trends of all fuels in this test were relatively similar, which is confirmed by the insignificance of the interaction between the fuel type and engine speed shown in Table 4.6. The maximum results of the NO_x were found around the speeds of 2900 and 3670 rpm. At the maximum output power (3670 rpm), the maximum difference between PD and MCP-B100 was recorded to be about 16.4. This reduction and the reduction in the averaged NO_x emission of 7.4% are lower than the reduction reported by Wahlen et al. (2012), who found that the NO_x emission with biodiesel from microalgae (*Chaetoceros gracilis*) was reduced by 24% compared with PD under no load conditions. The reduction is also lower than that reported by Chokri et al. (2012), who found that for every 10% increase in the biodiesel percentage in the fuel, a reduction of 2% in the NO_x was found. The main factors affecting the NO_x

were the exhaust temperature and the O_2 content in the biodiesel structure. Given that the average reduction in the exhaust gas temperature with MCP-B100 was 6.1% compared with PD, the reduction of the averaged NO_x by 7.4% was expected.

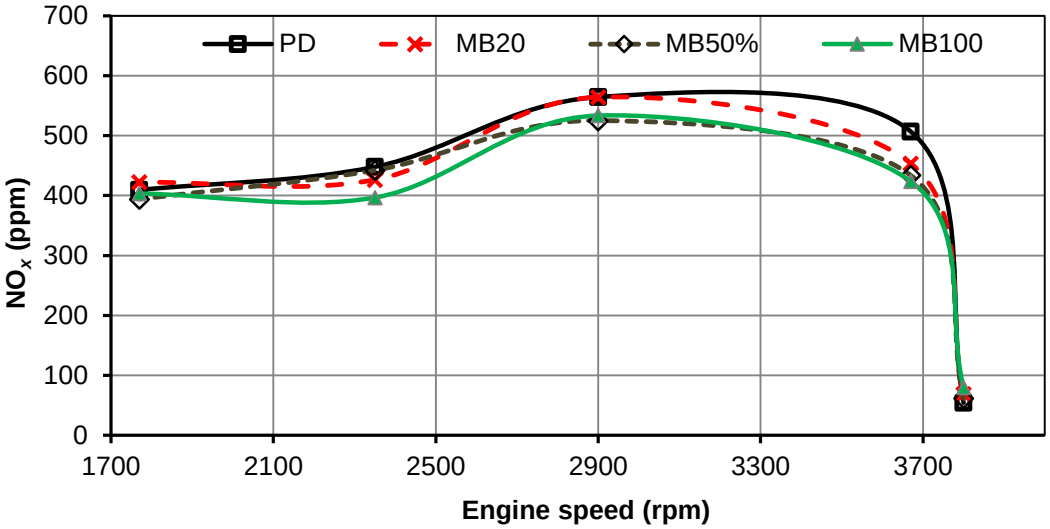

Figure 4.36 The relationship between engine speed (rpm) and NO_x (ppm) for PD, MCP-B20, MCP-B50 and MCP-B100

4.5 Conclusion

This chapter presented the process of preparing and studying the physical properties of MCP-B100 and its blends with PD. The fuels' density, viscosity, heating value and nozzle pattern were measured. An engine set-up was established to study the engine performance and the exhaust gas emission using PD, MCP-B20, MCP-B50 and MCP-B100 under different operating conditions. The results discussed in this chapter can be summarised as follows:

1. MCP-B100 and its blends are a potential alternative and its fuel properties are comparable with PD. MCP-B100 and its blends with PD can be used in diesel engines without any modification.

2. The heating value of MCP-B100 was found to be lower than the heating value of PD by 13.3%. However, the overall reduction in the engine torque and power with MCP-B100 was only 4.9% and 7.0%, respectively. This result indicates better combustion with MCP-B100 and its blends. MCP-B100 viscosity, which increased by 66.8% compared with PD, had a positive effect on the engine's performance characteristics associated with a higher cetane number, which increased by 2% compared with PD. The density of MCP-B100, which was higher than PD by 4.5%, was another factor that contributed to the expected reduction in engine performance as a result of the lower heating value. Chemical properties such as the extra O_2 in MCP-B100 contributed to an increase in engine efficiency compared with PD.
3. The statistical analyses showed that the effect of the fuel type was statistically significant at $p \leq 0.05$ with GIP, brake power, torque, BSFC, exhaust gas temperature, engine noise, CO, O_2, lambda and NO_x. However, other parameters were insignificantly affected by the type of fuel used in the test.
4. MCP-B100 showed a reduction of 12.4%, 7.0%, 4.9%, 6.1%, 2.2%, 28%, 4.2% and 7.4% of the parameters of GIP, brake power, torque, exhaust gas temperature, noise level, CO, CO_2 and NO_x, respectively.
5. MCP-B100 showed an increase by 10.2%, 1.0%, 5.7%, 15.8% and 15.9% of the parameters of BSFC, FC rate, thermal efficiency, O_2 and lambda, respectively.

CHAPTER FIVE

Single-Cylinder Diesel Engine Performance and Emissions Using Emulsified Water with FWM-CV

5.1 Introduction

This chapter focuses on the experimental work performed to test emulsified water fuels in cottonseed biodiesel and the effect of adding FWM-CV cells to water emulsified fuel on the fuel properties, engine performance and exhaust gas emissions. This chapter consists of the following:

- background and literature review of emulsified water fuels
- fuel preparation and fuel properties
- results and discussion
- conclusion.

5.2 Background and Literature Review

Emulsion fuel is a term usually used to describe mixtures of diesel and/or biodiesel with water (Lif & Holmberg, 2006). Owing to the differences in the physical and chemical properties of the mixture components (i.e. water, diesel or biodiesel), emulsifiers are normally used to facilitate the interaction between the mixture components and prolong the stability of the emulsion. According to Fayyad et al. (2010), emulsion fuels were first brought to attention in 1931 by Joseph Vance, and

they are still not very well known or accepted by consumers. Emulsified water in diesel or biodiesel is regarded as a potential fuel in terms of its renewability, emission reduction, economy and adaptability with the current technology.

The use of emulsified water in diesel or biodiesel fuels has been widely investigated by many researchers (Abu-Zaid, 2004; Davis et al., 2012; Davis, 2011; Fahd et al., 2012; Nadeem et al., 2006). Nadeem et al. (2006) identified and evaluated the factors affecting the preparation of emulsified water in diesel and its effect on engine performance and emission. Fahd et al. (2012) performed an experimental test using a four-cylinder 2.5 L direct injection turbocharged diesel engine to study the effect of using 10% emulsified water (DE10) on engine performance and emission at different engine loads. They noticed a reduction in engine power when it was fuelled with DE10 with a concurrent increase in BSFC. An engine test was carried out by JS Basha and Anand (2011) on a diesel engine fuelled with jatropha biodiesel—an emulsion fuel of 83% jatropha biodiesel with alumina nanoparticles, 15% water and 2% emulsifier. The emulsion fuels produced a considerable improvement in the engine's performance and emissions compared with those of biodiesel fuel.

The use of biodiesel fuel in diesel engines has been found to produce a reduction in exhaust gas emissions by many researchers (Lif & Holmberg, 2006; Lin & Lin, 2006; Maiboom & Tauzia, 2011). However, in most cases, as described in Chapter 3 and Chapter 4, the NO_x emission was reported to be higher than PD when the engine was fuelled with biodiesel because of the high O_2 content in biodiesel. Adding water to the biodiesel fuel proved an effective method of reducing the NO_x associated with biodiesel in studies by (Lin & Lin, 2007; Yoshimoto & Tamaki, 2001). In a different study, Grimes et al. (2011) eliminated the increase in NO_x emitted from a B20 biodiesel blend using 6.5% emulsified water in B20. In another study, conducted by

Dantas Neto et al. (2011), a significant reduction of NO_x (1100 to 400 ppm) was observed when using emulsified biodiesel with 30% water, and the BSFC was close to that achieved with PD (Yoshimoto et al., 2001). However, the outcomes and the conclusions of the aforementioned studies differ widely. This could be attributed to many factors, such as the procedure followed in preparing the emulsions, differences in the chemical and physical properties of emulsion constituents, variation in blend ratios, differences in specification and age of the engines used in the tests, and environmental conditions in the laboratories.

Recently, Koc and Abdullah (2013) studied both diesel engine performance and emissions when fuelled with biodiesel blends with and without emulsified water. They prepared the mixture using 1000 W ultrasound. They concluded that the BSFC and CO level were higher with emulsion fuel than with biodiesel blends. They also reported that the rise in the CO level was lower than the reduction in the NO_x.

It is noteworthy that the results of the literature showed diverse findings in the engine power, CO emission and NO_x emission. The majority of the researchers reported reduction in brake power produced by the engine utilising emulsion fuel compared with diesel. Abu-Zaid (2004) and Fayyad et al. (2010) reported an increase in power achieved by using emulsified water fuel. The justification of their finding is summarised in 5.2.3.

A summary of the advantages and disadvantages of emulsified water in diesel or biodiesel reported in the literature is presented in the following sections.

5.2.1 Advantages and Disadvantages of Using Emulsified Water in Diesel Engines

The reported advantages of fuelling diesel engines with emulsified water fuels are listed below:

1. The availability of water in nature has motivated many researchers to explore its usability in combination with fuels in engines. The addition of water to the available fuels provides the key solution to the problem of increasing fuel demand and high fuel prices (Basha & Anand, 2011; Lif & Holmberg, 2006; Lin & Lin, 2006; Nadeem et al., 2006).
2. Diesel engines can be fuelled with a water diesel or biodiesel emulsion with minor or no modification (Fahd et al., 2012; Lif & Holmberg, 2006; Lin & Lin, 2006; Nadeem et al., 2006).
3. Emulsified water in diesel or biodiesel increases the combustion efficiency (Abu-Zaid, 2004; Lif & Holmberg, 2006; Scragg et al., 2003).
4. Emulsified water in diesel improves the injection behaviour, which enhances the fuel and air mixing (Fahd et al., 2012; Nadeem et al., 2006).
5. Micro-explosion may occur due to the presence of tiny water particles, which enhances the atomisation and mixing process (Abu-Zaid, 2004; Armas et al., 2005; Fahd et al., 2012; Kadota & Yamasaki, 2002; Lif & Holmberg, 2006; Nadeem et al., 2006).
6. Emulsified water in diesel has been reported to reduce diesel engine emissions (NO_x, SO_x, CO and PM) with insignificant effect on engine performance (Lif & Holmberg, 2006; Nadeem et al., 2006). Emulsified water in oil has been shown to produce a slight increase in brake efficiency and a

significant decline in NO_x formation, soot, hydrocarbons and PM (Armas et al., 2005).

Problems are associated with emulsified water and microalgae cells combustion. To present a balanced view, it is also important to highlight the shortcomings reported in tests conducted with alternative fuels in diesel engines. This section presents the reported disadvantages of water and microalgae emulsions as an alternative fuel in diesel engines:

1. Lower power and higher BSFC due to a reduction of the heating value of the fuel have been reported (Kumar et al., 2012).
2. High viscosity has been reported (Dantas Neto et al., 2011). However, some researchers found that the extremely high viscosity of water and microalgae slurry emulsion in biodiesel fuel had no negative effect on the injector when the fuel was recirculated to reduce the viscosity (Scragg et al., 2003).
3. The emission of HC and CO was reported to be higher than that of PD (Lif & Holmberg, 2006).

5.2.2 Microalgae Addition to Fuel

Microalgae *Chlorella vulgaris* have the potential to be combusted in the engine and to pass through the injector because they are unicellular with a size range of 5–10 μm (Scragg et al., 2003). Scragg et al. (2003) performed an engine test using emulsion fuel of 20% microalgae *Chlorella vulgaris* slurry in rapeseed methyl ester. This fuel contained 0.2 g of dry algal biomass per 100 ml of emulsion.

Microalgae can be admitted as a powder into the diesel engine. However, the powder injection and powder flow control can be challenging. For this reason, Scragg et al. (2003) used microalgae slurry in emulsion form with biodiesel. The problems

associated with the direct use of microalgae cells in water emulsified in fuel in diesel engines are:

1. The large size of microalgae aggregates causes injection blockage or damage.
2. High viscosity increases the resistance flow through the fuel.
3. The low stability of the emulsified water in diesel or biodiesel fuel results in the settlement of the heavy phase of the emulsion in fuel passages.

5.2.3 Diesel Engine Performance Using Emulsified Water Fuel

In-Cylinder Pressure and Heat Release Analysis

The in-cylinder pressure that occurs at the power stroke is important to identify the indicated engine performance. Fahd et al. (2012) analysed the in-cylinder pressure traces for diesel and ED10 fuels at different engine loads. The comparison of the in-cylinder pressure for the maximum load between diesel and ED10 fuels is shown in Figure 5.1. It is clear from the figure that there was very little difference in the in-cylinder pressure pattern between ED10 and diesel. More importantly, Figure 2.1 shows that the drop in the in-cylinder pressure for ED10 was slightly lower than that of the diesel, and this reduction was justified by the lower heating value of the ED10. Another factor for this reduction was the presence of water in diesel, which absorbs heat and consequently reduces the combustion temperature (Fahd et al., 2012). Fahd et al. (2012) reported that the maximum pressure was relatively close between the two fuels because of the enhancement in the air–fuel mixing and better combustion. Abu-Zaid (2004) explained the increase in the torque when using emulsified water fuel by the extra pressure produced by the steam. Moreover, the longer ignition delay associated with emulsion fuel leads to higher maximum pressure ATDC at expansion stroke, consequently enhancing the combustion process.

The results of the comparison of the heat release between diesel and ED10 found by Fahd et al. (2012) are presented in Figure 5.2. This figure shows that the ED10 generally gave higher heat release or close to that of diesel. Fahd et al. (2012) attributed the higher heat release at low speed with high load to the possible enhancement in the atomisation due to the increase in the injection pressure; to some extent, this offset the negative effect of the higher viscosity of emulsion fuel. In a similar study, Nadeem et al. (2006) concluded that an insignificant reduction was found in the brake mean effective pressure of the diesel engine using emulsion fuel containing 15% water when compared with PD.

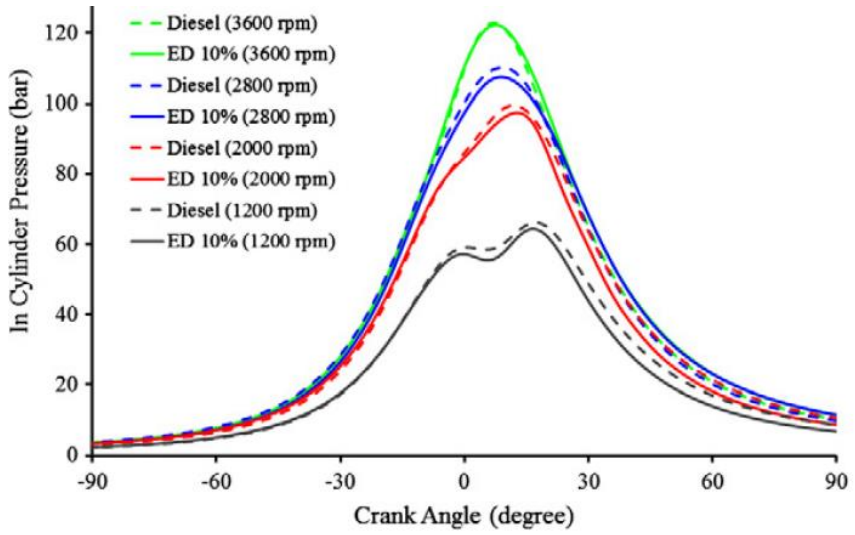

Figure 5.1 In-cylinder pressure traces for diesel and ED10 at 100% load and various engine speeds (Fahd et al., 2012)

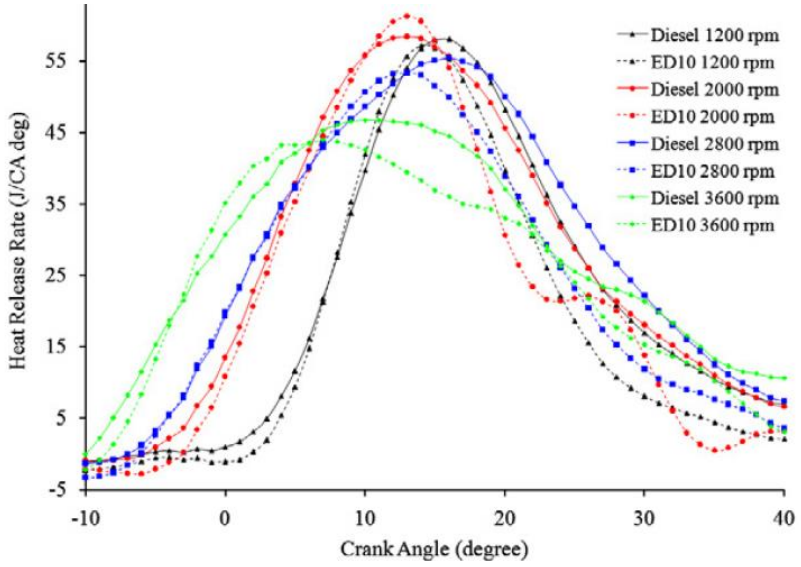

Figure 5.2 Heat release rate for diesel fuel and ED10 at 100% engine load and various engine speeds (Fahd et al., 2012)

Powers and Torque

The use of emulsified water fuel has been reported to reduce the engine power because of its low heating value. Fahd et al. (2012) commented that the maximum reduction in power, when the engine is fuelled with 10% emulsified water, is less than 10% compared with PD. It seems that the emulsifier added some extra energy to the fuel because it contained FAs. Koc and Abdullah (2013) demonstrated a statistically significant reduction in the engine power with emulsion fuels containing 10% and 15% water. This reduction was due to the lower heating value of the emulsion fuels. Other researchers reported an increase in the engine power when feeding it with emulsion fuels (Abu-Zaid, 2004; Alahmer et al., 2010), as will be described later. The contradiction in the researches regarding the increase or decrease in the power has been reported by Davis et al. (2012).

Fuel Consumption (FC) and Thermal Efficiency

Fahd et al. (2012) stated that the maximum thermal efficiency and lower BSFC were found to be in the middle range of engine speed because of the higher heat losses to the cylinder wall at low speed and higher friction losses at high speed. However, they found that ED10 produced lower thermal efficiency and higher BSFC due to the lower heating value; the results were comparable with PD. A similar finding was reported by Nadeem et al. (2006) and Dantas Neto et al. (2011); their results showed an increase in the BSFC associated with emulsion fuel as compared with PD. The reduction in the heating value of the 10% emulsified water in biodiesel resulted in higher FC and BSFC than biodiesel in order to attain the same power (Lin & Lin, 2007). A reduction of 6 kJ/g in the heating value was noted with microalgae slurry in biodiesel fuel compared with neat biodiesel. This reduction was mainly attributed to the water addition (Scragg et al., 2003). However, the calculation of the heating value based on the components percentage in the fuel showed that the microalgae increased the heating value by about 1.5 kJ/g.

Exhaust Gas Temperature

In a study by Scragg et al. (2003), the use of emulsified water containing microalgae fuel reduced the exhaust gas temperature by 47 ºC compared with biodiesel fuel. This finding was later supported by Fahd et al. (2012), whose results showed that the use of emulsified water in diesel at different loads and speeds resulted in lower exhaust gas temperature. This could be attributed to the presence of water, which is thought to reduce the combustion temperature.

5.2.4 Diesel Engine Emissions with Emulsified Water Fuels

Carbone Monoxide (CO) and Carbone Dioxide (CO_2)

The CO emission can be an indicator of combustion efficiency. The generation of CO is governed by a number of factors such as the in-cylinder pressure, air–fuel ratio, temperature and ignition delay. The CO emission from 10% emulsified water fuel at low load conditions was found to be higher than the base fuel (Fahd et al., 2012). Nadeem et al. (2006) found that the CO emission from an engine fuelled with emulsified water was lower than that of PD because of better air–fuel mixing as a result of larger micro-explosions in the case of emulsion.

CO_2 is identified as one of the greenhouse gases causing global warming. According to Koc and Abdullah (2013), the extra O_2 from water is a possible cause of the higher percentage of CO_2% emitted from nano-emulsion B5 and B20 fuels when compared with PD. Scragg et al. (2003) found no difference in the CO_2 level between PD and biodiesel from rapeseed oil, whereas the CO_2 decreased slightly from 5.7% to 5.3% for biodiesel and emulsion fuel containing microalgae. In contrast, the results of Scragg et al. (2003) study showed that CO PPM dramatically increased from 915 PPM for diesel fuel to 1506 PPM emitted from biodiesel fuel and 1904 PPM for the emulsion fuel containing microalgae.

Oxygen (O_2) and Lambda

In a study by Koc and Abdullah (2013), the O_2 level produced from nano-emulsion fuels increased with decreasing load at the lowest load in a WOT test. This reduction occurred as a result of the air–fuel ratio drop as the load increased. Koc and Abdullah

(2013) found that increasing water percentage in the fuel decreased the O_2 emissions because of the micro-explosion phenomenon that occurred during combustion.

Nitrogen Oxides (NO_x)

Many researchers have found that using emulsion fuel reduced the NO_x emission. For example, a reduction in NO_x emission was detected by Koc and Abdullah (2013) when increasing the water content in the emulsion. Similarly, the NO_x fell from 332 ppm when an engine was fuelled with rapeseed biodiesel to 239 ppm when the engine was fuelled with emulsion fuel containing microalgae (Scragg et al., 2003). As a consequence of finely sprinkled water droplets that resulted in lower combustion temperature, a reduction in the NO_x formation was noticed by Fahd et al. (2012) and Nadeem et al. (2006). The NO_x reduction associated with water emulsion fuel was a result of the lower combustion flame temperature and the increases in the OH formation (Davis et al., 2012).

5.2.5 The Objectives of the Chapter

The use of FWM-CV cells in water as additives to biodiesel fuel has been proposed to overcome some of the issues mentioned in Chapter 3 and Chapter 4. The main issue that derived the project to investigate the feasibility of emulsion fuel was the low productivity of FWM-CV on a laboratory scale, which did not allow a sufficient amount of FWM-CV biomass to be gathered for biodiesel fuel production within the time frame of the project. Microalgae cells can be combusted; however, liquid fuel is essential for the current diesel engine (Scragg et al., 2003). Biodiesel fuels can be further enhanced by adding a proportion of microalgae cells in water to reduce the NO_x emission. The objectives covered in this chapter can be summarised as follows:

1. Study the effect of using emulsion water in cottonseed biodiesel fuel on the engine performance and exhaust gas emissions as a proposed solution for the higher NO_x associated with biodiesel fuel.
2. Investigate the effect of adding FWM-CV cells to emulsified water fuel to overcome the power reduction caused by the water content.
3. Measure some of the properties of the emulsified water fuels with and without microalgae cells.
4. Examine the use of ultrasound as a two-stage treatment for preparing emulsified water fuel containing microalgae cells. The first stage includes the breakdown of cells and colonies to overcome the problem of nozzle blockage. The second stage involves the use of ultrasound as a mixing method that improves the quality of the produced emulsion.
5. Finally, test the engine performance and emissions using CS-B100 in comparison with emulsion fuels (with and without microalgae cells).

5.3 Fuel Preparation and Experimental Set-up

This section outlines the methods and the experimental set-up used for the fuel preparation, measurements of some of the physical properties of the fuels and the engine test procedure.

5.3.1 Fuel Preparation

Emulsion fuel is produced by deforming the interface between two immiscible fuels with the aid of mechanical energy (Fahd et al., 2012). Fahd et al. (2012) prepared 10% water emulsified fuel containing 10% surfactant (emulsifier) by volume in diesel fuel using a high-speed rotary blender. The high percentage of the emulsifier

plays an enormous role in the emulsion stability of the fuel. Nadeem et al. (2006) found that a lower percentage of emulsifier formed oil droplets leading to an incomplete emulsification process. Excessive emulsifier made a rapid coalescence. Abu-Zaid (2004) prepared water emulsified fuel using 2% emulsifier to achieve stable emulsion. In another study, Scragg et al. (2003) prepared an emulsion fuel of 20% water and algae slurry in rapeseed biodiesel with 0.5 emulsifier. To emulsify water in diesel or biodiesel, most researchers have used a mechanical mixer. However, Basha and Anand (2011) used an ultrasonicator to mix alumina nanoparticles with emulsion fuel of 83% jatropha biodiesel, 15% water and 2% surfactants.

The fuels used in this work were cottonseed biodiesel 100% (CS-B100), emulsified water 20% in cottonseed biodiesel (CS-E20) and emulsified water 20% containing FWM-CV in cottonseed biodiesel (CS-ME20). The fuel preparation procedure and some properties of the fuels are described in the following subsections.

Pure Cottonseed Biodiesel (CS-B100)

A pure cottonseed biodiesel, CS-B100, was obtained from the Queensland University of Technology (QUT). The cottonseed methyl ester fuel was prepared from cottonseed oil via transesterification. This fuel was used as the baseline in this test.

Emulsified Water in Cottonseed Biodiesel (CS-E20)

The CS-E20 and CS-ME20 fuels were prepared at the engine lab of USQ. An ultrasonic horn reactor (Dr Hielscher, Model UIP 500) with variable input power and fixed frequency of 55 kHz was used for the CS-E20 and CS-ME20 fuel preparation (see Figure 5.3). The emulsion fuels were prepared following the same procedure for

both CS-E20 and CS-ME20 except that the water in CS-ME20 was supplemented with FWM-CV. The fuel was prepared based on a volumetric ratio of 79.2% of CS-B100 and 19.8% water and 1% emulsifier. A more detailed description is given in the next section.

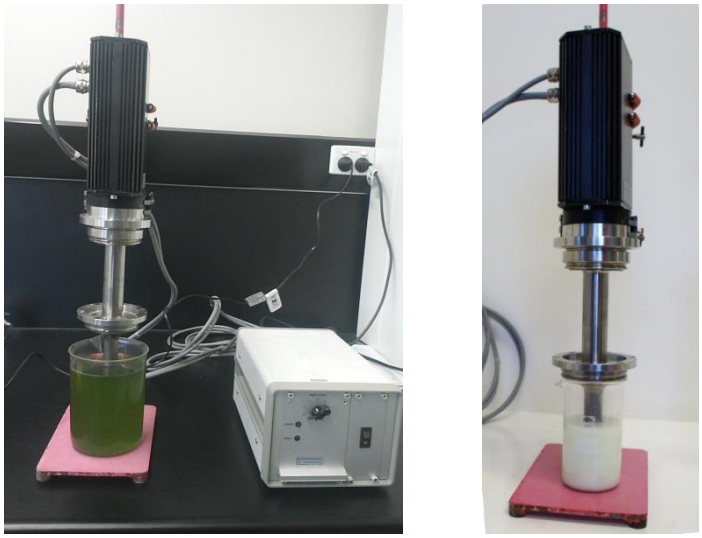

Figure 5.3 Ultrasound device with emulsion fuel batch

Emulsified Water with FWM-CV in Cottonseed Biodiesel (CS-ME20)

The CS-ME20 consisted of CS-B100, water containing FWM-CV and emulsifier. Based on observations of the FWM-CV during the growing process and pre-testing of the fuel preparation, an issue of microalgae colony size was detected. It can be observed in Figure 5.4 that the injector orifice diameter expressed by equivalent circle diameter was 193.698 µm and the average sample of FWM-CV colonies' diameter averaged 2011 µm, as presented in Figure 5.5. The size of the aggregates was much higher than the injector orifice size, which would have led to orifice blockage and possibly injector damage. To overcome this, the emulsion preparation was performed in two stages: breaking down the aggregates of FWM-CV and mixing the pre-sonicated microalgae in water with CS-B100 and surfactant using ultrasound.

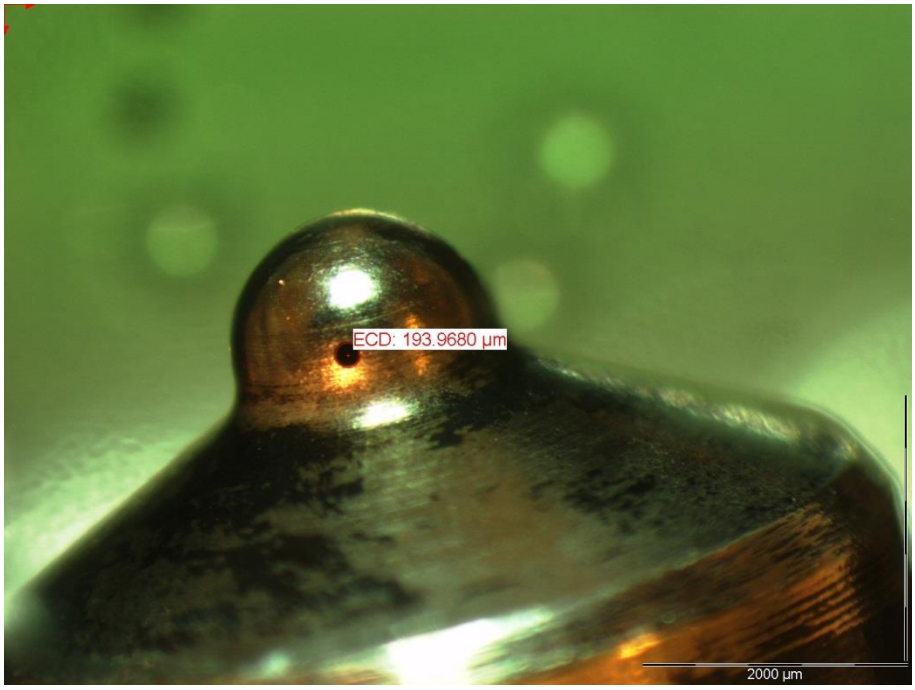

Figure 5.4 The injector orifice equivalent circle diameter (ECD)

A. Disintegration of FWM-CV aggregates by sonication

Ultrasound is an effective method for deagglomeration of microalgae clusters (Halim et al., 2012). Therefore, it was adopted in this study to break down the aggregates of FWM-CV prior to mixing the slurry with biodiesel and surfactant. A sample of 200 mL of FWM-CV slurry was treated with ultrasound for five minutes. The ultrasonic power intensity applied in this experiment was 21.52 W/cm^2.

To achieve the maximum benefit of the ultrasound energy, no temperature control measure was applied in this experiment. The temperature rise that usually accompanies ultrasound treatment was utilised to help the rupture of individual microalgae cells in the treated slurry because the increase in temperature makes cells more susceptible to ultrasound treatment (Al-juboori, 2012). The temperature of the microalgae slurry during the sonication treatment was monitored using a Digi-Sense Type K thermocouple. The maximum temperature reached in this experiment was 62 °C. Such a high temperature, together with the ultrasound effect, formed a

valuable tool for rupturing some of the FWM-CV cells and releasing the lipid content of the FWM-CV into the slurry. The release of the lipids into the slurry may make the final emulsion more combustible.

The efficiency of ultrasound in breaking down FWM-CV aggregates was evaluated by comparing the microscopic photos of the untreated (see Figure 5.5) and treated slurries (see Figure 5.6). Microalgae aggregates and cells in the untreated and treated slurries were visualised using a Motic Stereo microscope. Photos of the microalgae cells and aggregates were captured using a CC12 camera, which was attached to the microscope, and the images were analysed using AnalySIS software, as is shown in Figure 5.5 and Figure 5.6. It can be clearly observed in Figures 3.3 and 3.4 that ultrasound treatment successfully disintegrated the microalgae aggregates into dispersed cells in the slurry. This in turn reduced the chances of nozzle blockage caused by the entrapment of large microalgae aggregating in the nozzle orifice. It can also be observed in Figure 5.6 that the maximum aggregate size was 47.281 µm. The small cell size enhanced the emulsion stability because the larger aggregates tend to precipitate faster.

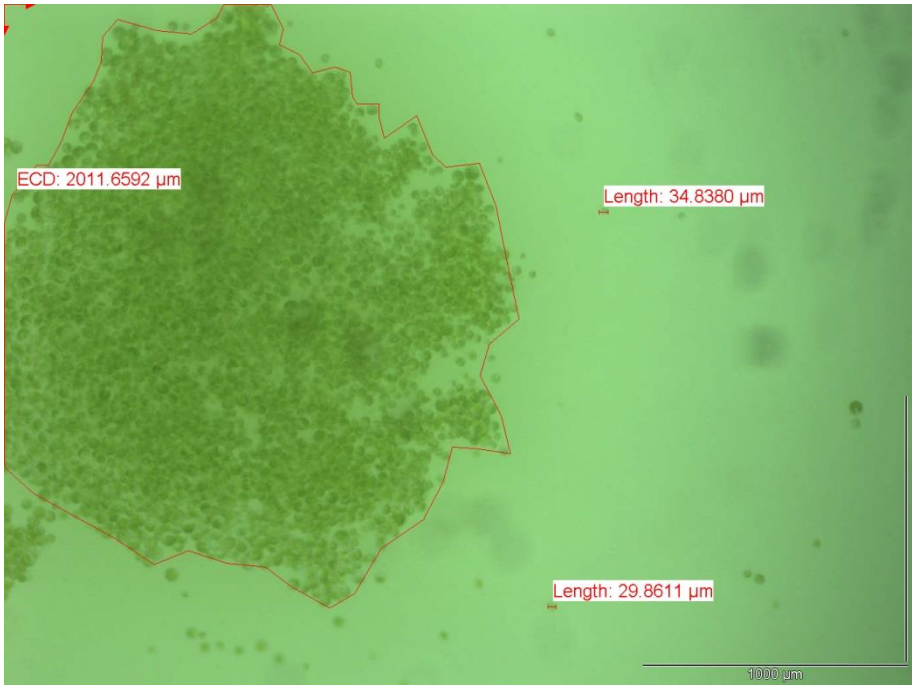

Figure 5.5 Microscopic photos for FWM-CV colonies before ultrasound treatment

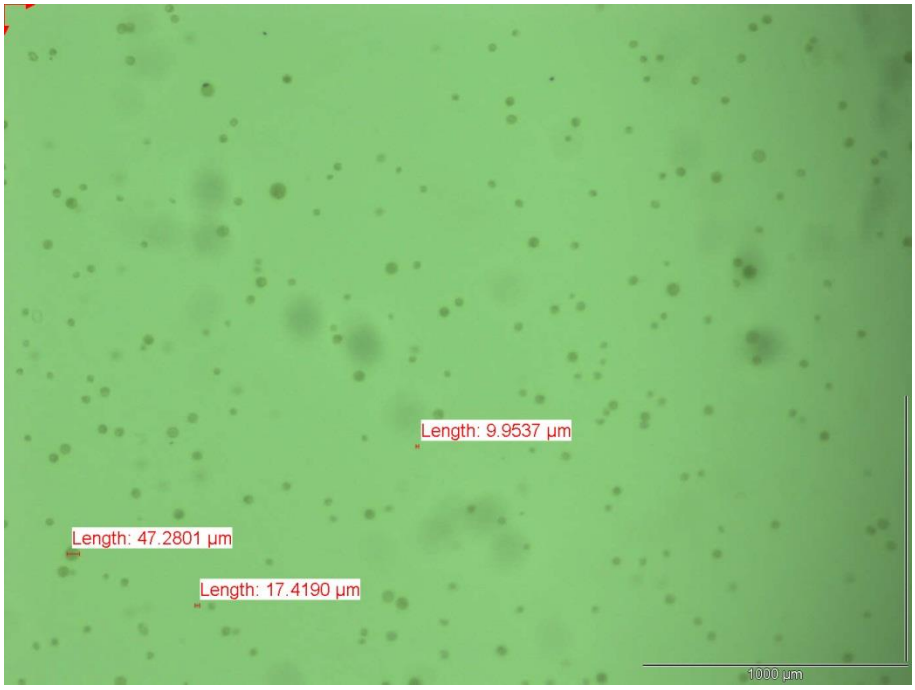

Figure 5.6 Microscopic photos for FWM-CV after ultrasound treatment

Figure 5.7 Treating FWM-CV in water with ultrasound

B. Mixing pre-sonicated microalgae slurry with biodiesel

In this stage of the emulsion preparation, the pre-sonicated microalgae slurry was mixed with cottonseed biodiesel and surfactant in a 300 mL Pyrex beaker. The total volume of the emulsion was 250 mL made up of 19.8% volumetric percentage of microalgae slurry (49.5 mL), 79.2% volumetric percentage of cottonseed biodiesel (198 mL) and 1% surfactant (2.5 mL). The dry weight percentage of microalgae biomass in the slurry was 2 g/L. Surfactants are normally added to the emulsion to prevent the separation between the emulsion constituents and maintain stable emulsion for a certain period of time (Benter et al., 1997). Triton X-100 was used as a surfactant in this study, as recommended by Scragg et al. (2003). The mixture of microalgae slurry, biodiesel and surfactant was treated in batches with ultrasound. The batch volume was 250 mL. Each batch was treated with ultrasonic power intensity of 24.17 W/cm^2 for 10 minutes. No temperature control measure was applied during ultrasound mixing.

The produced emulsion using ultrasound emulsification in this study showed clear separation between two distinct layers: a milk-like layer consisting mostly of water and an oil-like layer consisting mostly of biodiesel (see Figure 5.8). The occurrence of two layers in the produced emulsion can most likely be attributed to the adverse effect of temperature rise during sonication (maximum of 82 °C in the emulsion preparation step) on the degree of mixing between the emulsion constituents.

(a) (b)

Figure 5.8 The separation between two layers in the produced emulsion of (a) CS-biodiesel, water and Triton X-100 and (b) CS-biodiesel, FWM-CV slurry and Triton X-100 without cooling

Several studies such as those of Floury et al. (2003) and Marie et al. (2002) have highlighted the negative effect of temperature rise on the quality of the emulsion. Increasing the temperature of the mixture during the emulsification process can increase the collision between droplets, which in turn leads to coalescence of the disrupted droplets (Tesch & Schubert, 2002). Jafari et al. (2007) found that applying cooling to the emulsification process using micro-fluidisation resulted in a decrease in the volume mean diameter of the oil droplets in water-oil emulsion from 846 nm (without cooling) to 685 nm (with cooling). Therefore, the produced emulsion from

the ultrasound treatment was left at room temperature to cool down for 30 minutes. It was found that cooling the emulsion after ultrasound treatment (post cooling) combined with the stirring process (using magnetic stirrer model HB502) could bring the emulsion to an acceptable homogeneity, as shown in Figure 5.9. Applying post cooling has the advantage of being a simple process compared with the cooling procedure during ultrasound emulsification.

Figure 5.9 Homogenous emulsions of (a) CS-E20 and (b) CS-ME after cooling at room temperature and continuous stirring for 30 minutes

5.3.2 Fuel Properties

Density and Viscosity

The physical properties of the fuel significantly affect the fluid dynamics in the injection and combustion process. Fuel prices and FC are normally based on volume and the heating value of the fuels is usually normalised by mass unit such as MJ/kg; therefore, determining the fuel density was essential. The density of the CS-B100, CS-E20 and CS-ME20 are presented in Table 5.1. The density was measured for all fuels using volumetric and weighing measurements (LabCo pipette and Ohaus Explorer E12140 balance). The density of each fuel was taken as the average of 10

readings at 20 ºC. It can be observed in Table 5.1 that the variations in the density values were insignificant and the differences were in the error range. Emulsion fuels contain some degree of fine air bubbles as a result of the mixing process. The fine air bubbles reduced the density, which was expected to be higher because of the presence of water in the emulsion. This in turn resulted in close density values for all the fuels.

Table 5.1 also presents the dynamic viscosity values for CS-B100, CS-E20 and CS-ME20 measured at 25 °C and 40 °C. The viscosity was measured using a Brookfield Viscometer DV-II+Pro EXTRA, supplied by Thermo Fisher Scientific Australia, as described in Chapter 4. The viscosity of the emulsion fuels was extremely higher than that of the CS-B100.

The surface tension and heat of combustion were measured at QUT. The surface tension of CS-ME20, 31.675 mN/m was slightly lower than that of the CS-E20, which was 32.105 mN/m. The difference in the surface tension between CS-ME20 and CS-E20 can be ascribed to the additional FWM-CV cells and fragments of cells that lowered the surface tension of the fuel.

Table 3.1 shows that, in general, emulsion fuels with and without microalgae have a lower heat of combustion compared with cottonseed biodiesel. A lower value of heat of combustion for the emulsion fuels was expected because of the water content in the emulsion fuels. However, the heat of combustion of the emulsion was slightly enhanced (increased from 30.18 to 31.07 MJ/kg) by adding FWM-CV to it.

Table 5.1 Fuel properties

Fuel	Density (kg/L)	Dynamic viscosity (cP)	Surface tension mN/m	Heat of combustion MJ/kg
CS-B100	0.898 ± 0.015*	8.2 **	28.54 @28.8 ºC	39.3
CS-E20	0.908 ± 0.015*	205.1**	32.105@26.8 ºC	30.18
CS-ME20	0.912 ± 0.015*	210.3**	31.675@26.8 ºC	31.07

* Measured at 20 ºC. ** Measured at 25 ºC.

Fuel Stability

One of the most important characteristics of emulsion fuel is the stability. The separation of the layers causes many problems, such as abnormal combustion or even engine stoppage, due to the injection of a high percentage of water. The stability of the CS-E20 and the CS-ME fuel was monitored after four hours and two days as illustrated in Figure 5.10 (a) and (b) respectively. It is clear from the figures that both fuels were very stable for more than two days. The enhancement of the emulsion fuel homogeneity was mainly a result of the presence of the emulsifier and the effective mixing method using ultrasound.

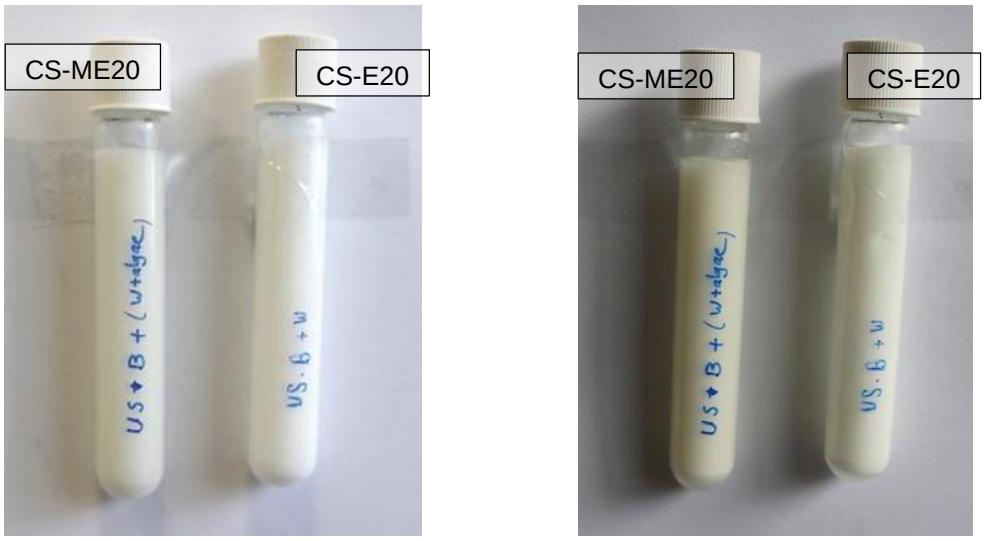

(a) (b)

Figure 5.10 The emulsion fuel samples (a) after four hours (b) after two days

Injector Nozzle Test

The nozzle test is an important experimental evaluation to determine the feasibility of emulsion as an alternative fuel in diesel engines. As mentioned in the fuel preparation section, the pre-sonication treatment was performed to break down the aggregates of the FWM-CV into cells that could easily pass through the injector orifice. The injector nozzle tester is described in the previous chapter. Prior to the test, samples of the emulsion fuels were tested in the nozzle tester and a 1000 frames per second video was recorded using a high-speed camera (Photron model SA3). Samples of the injection process of the CS-B100 and CS-ME20 are presented in Figure 5.11. It can be observed in Figure 3.9 that the spray pattern of both CS-B100 and CS-ME20 is relatively consistent and no problem with the fuel pattern was recognised. The CS-ME20 produced a spray angel of 18º, which was slightly wider than that of the CS-B100 (16º). This difference may be explained by the presence of water and microalgae cells that formed fine droplets in the CS-ME20.

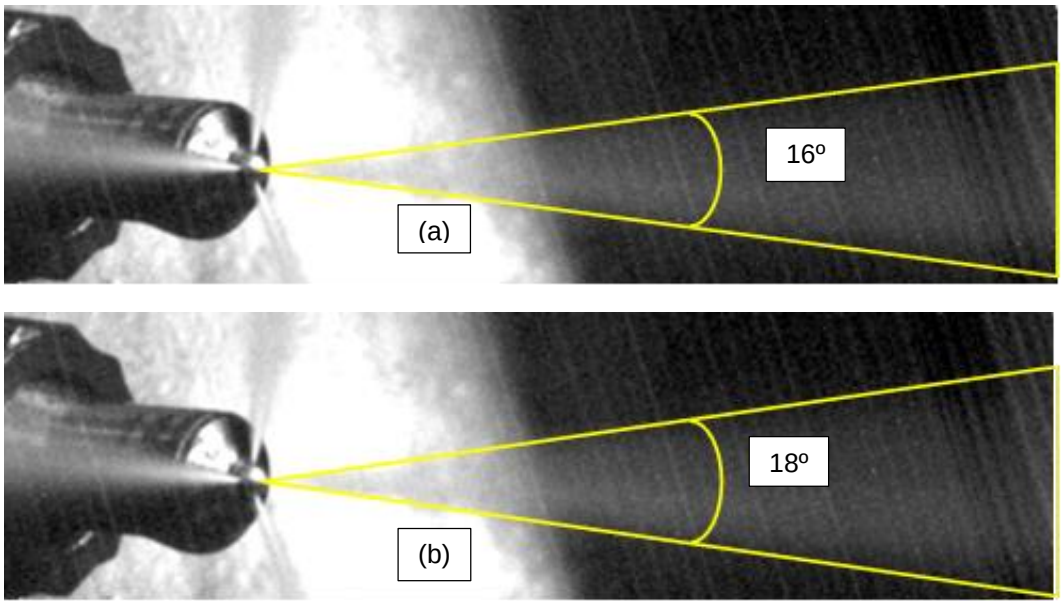

Figure 5.11 Nozzle test (a) CS-B100 (b) CS-ME

5.3.3 Engine Test Procedure

The engine test procedure adopted in this work is the same as the procedure described in Chapter 4. During the preliminary test with CSB-E20, the engine could not reach the maximum speed of 3800 rpm, which was achieved with the baseline (CS-B100) in the experimental work of this chapter, because of the high viscosity of the fuel. According to Tat and Van Gerpen (1999), the engine can be starved of fuel because of high viscosity, which reduces the fuel flow through the filters and fuel lines.

The engine showed instability at the speeds of 2350 and 1770 rpm, which were achieved by the baseline CS-B100. The stable speed closest to 2350 rpm was found to be in the range of 2320 to 2312 rpm with maximum variation of 38 rpm (1.6% variation). However, the variation was not very significant at this speed; the data of the performance and emissions are presented at the actual speed recorded by the instruments for the CSB-E20 and CSB-ME20.

5.4 Results and Discussions

5.4.1 In-Cylinder Pressure and Heat Release Analysis

To present a valid comparison of the in-cylinder pressure and heat release data between the various fuels tested in this chapter, only the data recorded at the exact engine speed that was achieved with all fuels are presented. As explained before, consistent engine performance that allowed constant reading for the in-cylinder pressure was only obtained at speeds of 3870 rpm and 2900 rpm for all fuels. Based on the engine manufacturer's data, fuel injection starts at 16.5° before top dead

centre (BTDC) (360°) as marked in Figure 5.12, Figure 4.2, Figure 4.3 and Figure 4.4.

The in-cylinder pressure at the engine speed of 3670 rpm is presented in Figure 5.12. At the crank angle 343.5º (the injection point), the pressure produced from the emulsion fuels was about 13.06% lower than that of the CS-B100 (28.62 bar). This may have been due to the lower engine temperature when operated with emulsion fuels. It is known that, before 343.5º, the charge in the cylinder is mainly air. The air temperature depends on the engine temperature. The engine temperature is lower when run with emulsion fuels; therefore, the pressure for the charge before the injection was expected to be lower than that of the base fuel. Figure 5.12 shows that the ignition delay increased with emulsion fuels. It can also be observed that the ignition duration was less for both emulsion fuels. The maximum pressure occurred at about 10º ATDC for the CS-B100, whereas a reduction in the maximum pressures of 28.6% and 16.4% were recorded for the CS-E20 and CS-ME20, respectively. The main reason for the drops in pressure was the higher viscosity and lower heating value of the emulsion fuels, which were 30.18 and 31.07 Mj/kg for CS-E20 and CS-ME20, respectively.

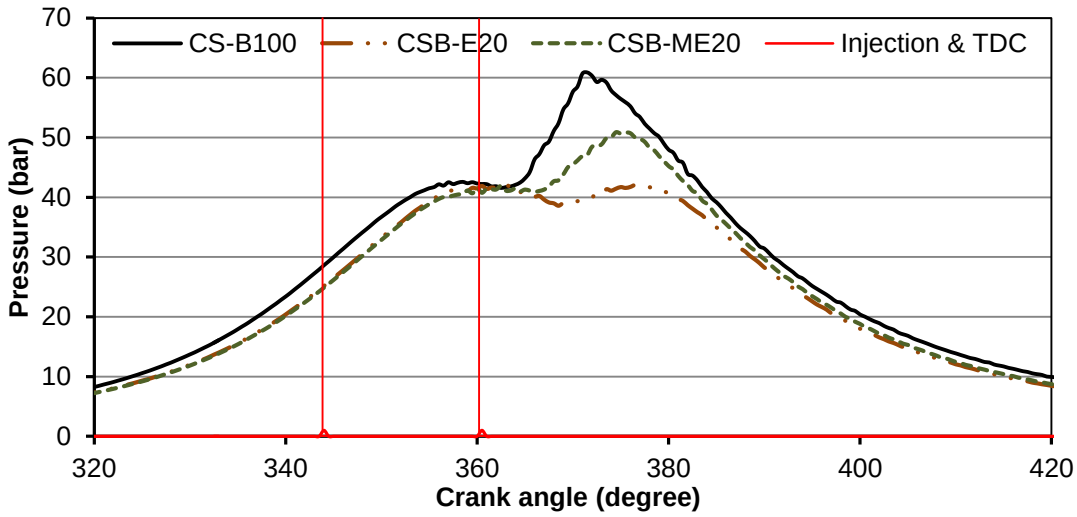

Figure 5.12 In-cylinder pressure at engine speed 3670 rpm

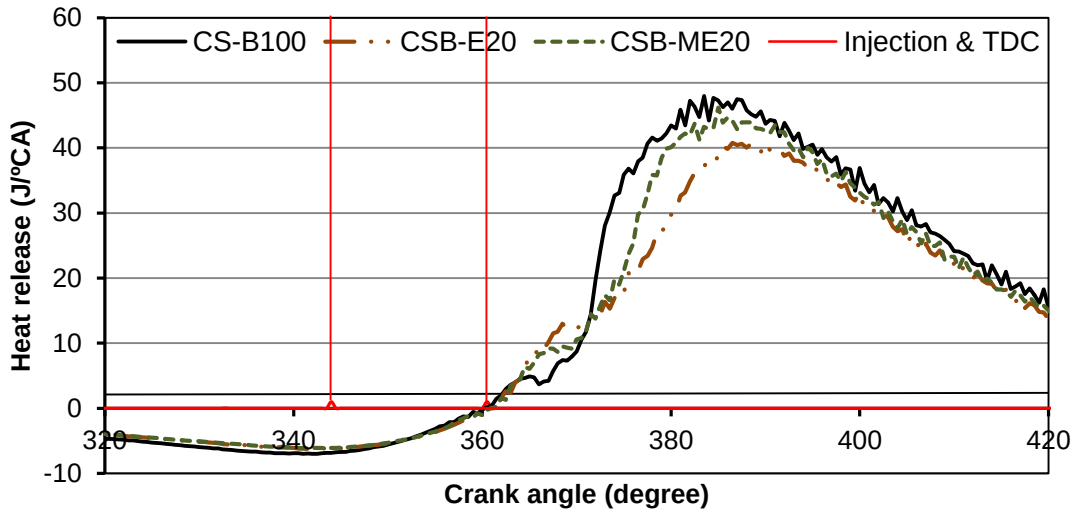

Figure 5.13 Heat release (J/ºCA) at engine speed 3670 rpm

At the engine speed of 2900 rpm, which is shown in Figure 5.14, the same finding was observed with a slight reduction percentage of 12.1% and 11.31% for the CS-E20 and CS-ME20, respectively. The results shown in Figure 5.14 are in agreement with those of Fahd et al. (2012), which indicated that the reduction percentage in the in-cylinder pressure with emulsion fuel was less than the percentage of water in the emulsion fuel because of the better combustion.

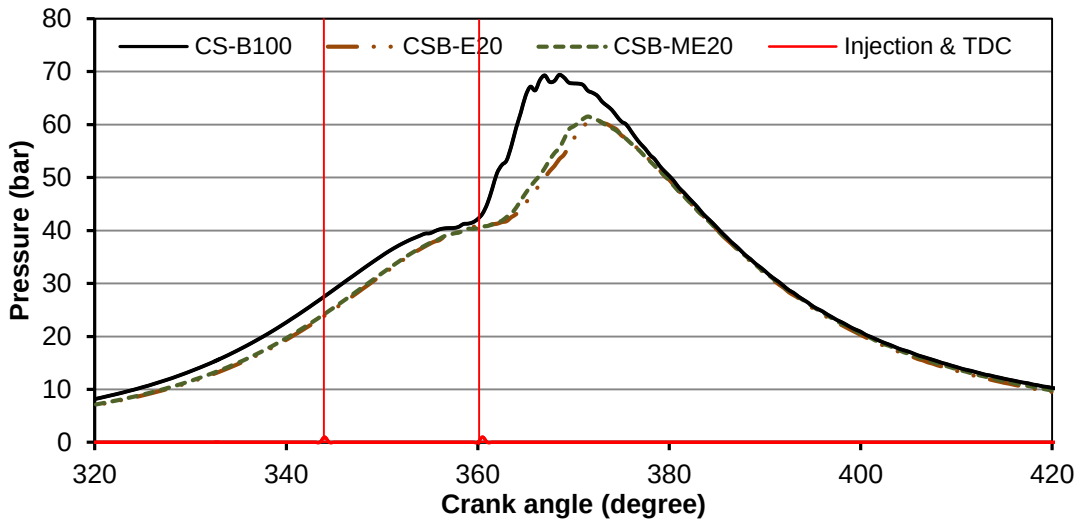

Figure 5.14 In-cylinder pressure at engine speed 2900 rpm

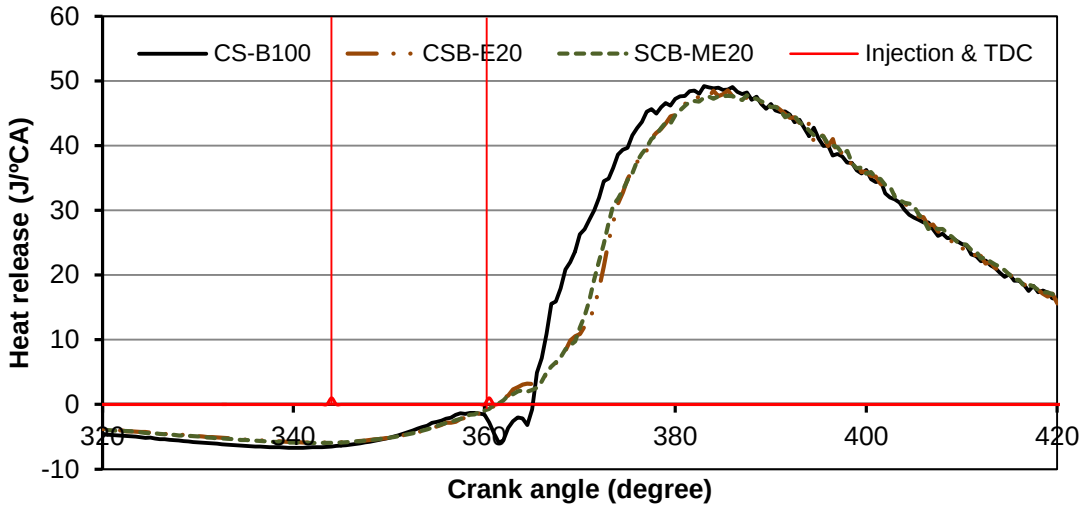

Figure 5.15 Heat release (J/ºCA) at engine speed 2900 rpm

5.4.2 Engine Performance

In this section, the effect of running the engine with CS-B100, CSB-E20 and CSB-ME20 on engine performance parameters is presented and discussed. The performance parameters discussed in this chapter are engine GIP, break power, break torque, FC rate, BSFC, exhaust temperature and break thermal efficiency.

Gross Input Power (GIP)

The relationship between engine speed and the GIP of the engine operated with CSB100, CS-BE20 and CSB-ME20 is depicted in Figure 5.16. The general trends of GIP for all fuels can be described as follows: when the speed increased (when on the engine load is reduced), the GIP increased, reaching the maximum at 2320–2350 rpm (the adjusted maximum torque point). After this speed, the GIP power started to decrease gradually as the engine speed reached 3670 rpm. A sharp reduction was observed for the speed after 3670 rpm to the maximum speed when there was no load on the engine. The gross power is a function of the fuel flow rate and the lower heating value of the fuel. CS-BE20 produced lower GIP than CS-BME20 and both were found to be lower than CS-B100. This reduction was mainly caused by the fuel properties such as the lower heating value and higher viscosity.

At higher emulsion fuels flow rate at certain speed, heating value and viscosity are the main factors affecting GIP. Adding FWM-CV to the emulsion fuel significantly increased the GIP at most engine speeds in comparison with CS-E20. The minimum difference in GIP between the base fuel and CS-ME20 fuel was 0.028 kW at the speed of 2900 rpm. This is a significant finding: although fuel loses 20% of it is energy by adding water, the minimum GIP loss was only 2.8%, and it is likely this was because FWM-CV was added to the fuel. This may be due to a number of factors, such as the energy content in the FWM-CV cells, the extra fuel flow rate added by the governor to maintain the same speed and torque, and better mixing and atomisation caused by microalgae cells. As reported by (Lif & Holmberg, 2006), the interface of oil in the presence of water leads to finer droplets. The FWM-CV cells may have helped to form even finer droplets because of the difference in the

interface layers. The different mass and volume of the CS-ME20 broke down the agglomeration of the large drops during the process of high pressure and speed.

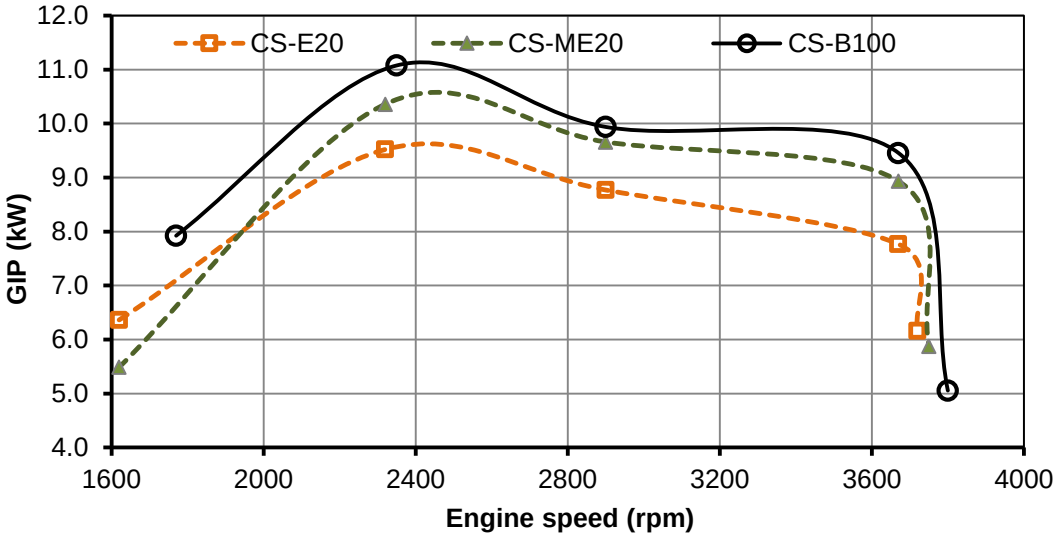

Figure 5.16 The relationship between engine speeds (rpm) and GIP (kW) for CS-B100, CS-E20 and CS-ME20

Brake Power

Figure 5.17 shows the test results for the break power curves produced using CS-B100, CS-E20 and CS-ME20 at different engine speeds. The maximum break power for the emulsion fuels was found to be predictably lower than for CS-B100. For all fuels, the break power increased as the engine speed increased, reaching the maximum at around 2320 rpm for the emulsion fuels and 2900 rpm for the base fuel. At a low engine speed of around 1800 rpm, all fuels presented relatively consistent brake power. In general, the emulsion fuels at speeds higher than 2350 rpm produced lower brake power than the base fuel. This can be attributed to the factors discussed in the previous subsection about GIP. It can be observed that the differences in brake power between CS-E20 and CS-ME20 in comparison with CS-B100 were very significant, except at the speeds around 2320 and 2350 rpm. The maximum differences of 0.79 kW occurred at 2900 rpm between the CS-B100 and CS-E20.

This finding shows some degree of agreement with Fahd et al. (2012) and Koc and Abdullah (2013) in terms of the reduction in power due to the emulsified water. The reason for the reduction was justified by the lower heating value. However, in terms of the reduction of 24.8%, this was higher than the reduction below 10% with diesel emulsion DE 10%. This can be attributed to the high mechanical losses resulting from the high speed and the extra power required to inject the more viscous fuel. Another factor affecting this reduction was the surface tension of the emulsion without microalgae (32.105 mN/m). This high value could have generated a higher droplet size of the CS-E20 in the injection process in comparison with the base fuel. The larger the droplet size, the lower the contact surface area between the droplets and air, which results in more energy being taken to evaporate and a longer time taken for reaction, whereas the time for reaction is short, especially at high engine speeds.

With regard to the comparison in the engine brake power of emulsions, Figure 5.17 shows that supplementing the emulsion fuel with FWM-CV significantly enhanced the break power. The maximum difference of 19.4% between the emulsion fuels of CS-E20 and CS-ME20 occurred at 2320 rpm. The reason behind this difference could be the energy content in the FWM-CV and the presence of segregated FWM-CV cells that resulted from ultrasound treatment, which reduced the size of the droplet during the injection process. When the fuel that contained biodiesel, water, surfactant and microalgae cells and cell fragments was injected, the fuel droplets consisting of those components were released from the injector at different speeds based on their size and mass. This difference may have broken down the larger droplets.

The general outcomes presented in Figure 5.17 are inconsistent with the results of Davis et al. (2012) and Abu-Zaid (2004). Davis et al. (2012) found that emulsion fuel produced more power than net biodiesel fuel at all engine speeds in spite of the 11.1% lower heating value of the emulsion fuel.

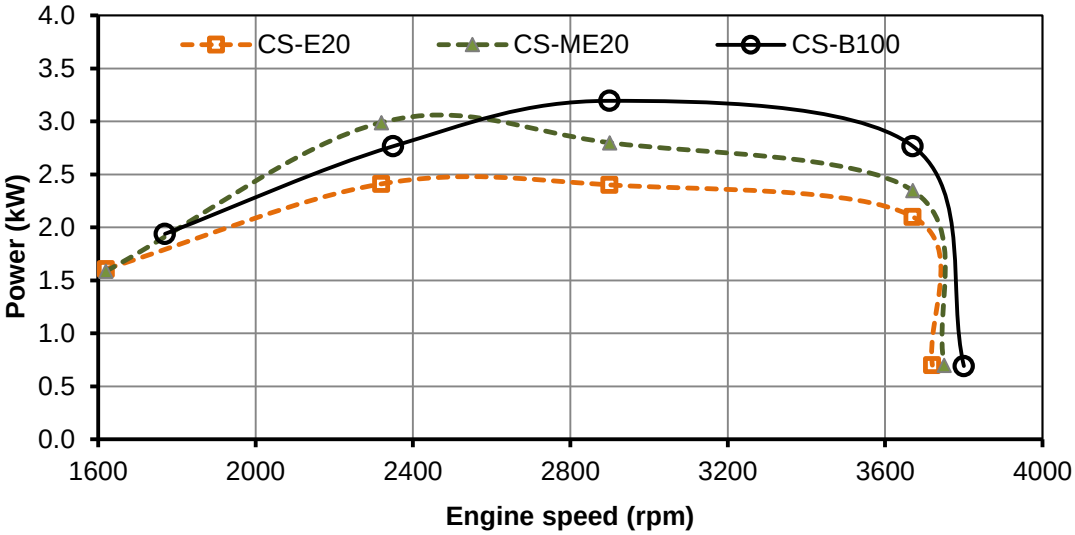

Figure 5.17 The relationship between engine speeds (rpm) and engine brake power (kW) for CS-B100, CS-E20 and CS-ME20

Brake Torque

The relationship between engine torque and engine speed for CS-B100, CS-E20 and CS-ME20 fuels is displayed in Figure 5.18. Power is a function of torque; therefore, the trends in Figure 5.17 are similar to those presented in Figure 5.18. It can be seen that the maximum torque produced by the engine occurred at the speeds around 2320 rpm to 2350 rpm for all fuel types. The values of the torque below and above these speeds dropped.

The torque curves were in general agreement with the engine performance curve provided by the manufacturer, in which the maximum power occurred at around 2400 rpm to 2600 rpm. The variation in the curves trend was a result of a number of

factors. Mainly, the engine had not been designed for these types of fuel. This engine is mass produced and a certain degree of variance was expected.

To produce the maximum torque from the fuels that had less heating value, the governor tried to supply extra fuel to compensate. The governor failed to achieve that goal at the high speed and, as a result, the engine speed became unsteady. This can be justified by the high viscosity that lowered the fuel flow supplied to the combustion chamber as well as increased the mechanical losses and the parasitic losses (higher viscosity requires extra power to inject the fuel). The maximum torque at stable speed shifted to 2320 rpm for the emulsion fuels and 2350 for the CS-B100. The maximum torque of 12.26 N.m was achieved when the engine was fuelled with CS-ME20.

For engine speeds up to 2350 rpm, CS-ME20 produced higher torque but produced below the base fuel as the speed increased. However, it still outperformed CS-E20 for the same reason presented in the previous subsection. These results are supported by the results shown in Figure 5.12 and Figure 5.14 that the in-cylinder pressure for the emulsion fuel was lower than the base fuel. A similar finding was presented by Nadeem et al. (2006) and Koc and Abdullah (2013) in their studies, the emulsion fuels produced less torque than diesel fuel because of the lower heating value of the emulsion fuels.

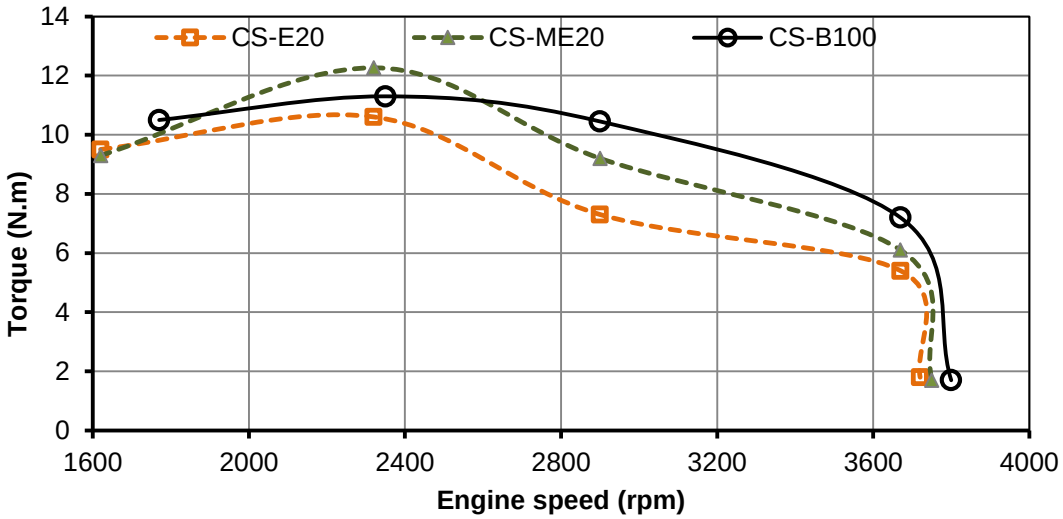

Figure 5.18 The relationship between engine speeds (rpm) and engine torque (N.m) flow for CS-B100, CS-E20 and CS-ME20

Engine Brake Specific Fuel Consumption (BSFC)

The relationship between the BSFC expressed in g/kW.h and the engine speed for CS-B100, CS-E20 and CS-ME20 is plotted in Figure 5.19. It can be observed that the BSFC was nearly constant for the engine speeds below 2350 rpm for all the fuels. BSFC is a function of the brake power and the FC rate; therefore, the lower BSFC was found to be around 2900 rpm in which the maximum power was recorded. As the engine speed continue increased, the BSFC increased because of the proportional increase in the friction power (Fahd et al., 2012). The engine appeared to reach its 'sweet spot' at 2900 rpm, with the lowest BSFC (around 284.2 g/kW.h) produced when CS-B100 was used, which was significantly lower than 399.9 g/kW.h and 437.5 g/kW.h for CS-E20 and CS-ME20, respectively. These results match the results of Fahd et al. (2012) and Koc and Abdullah (2013) who recorded a reduction in the brake power with emulsion fuels, and are not consistent with Abu-Zaid (2004) and Davis et al. (2012), who found higher brake power with emulsion fuels. In order to produce a required brake power output from lower heating value fuel, it is

necessary for extra fuel to be injected that raise the BSFC values, as is the case with emulsion fuels (Koc & Abdullah, 2013). The CS-ME20 presented significant enhancement in BSFC of about 37.5 g/kW.h (8.6%) in comparison with CS-E20 fuel. This may have been caused the existence of FWM-CV, which increased the thermal efficiency and enriched the heating value.

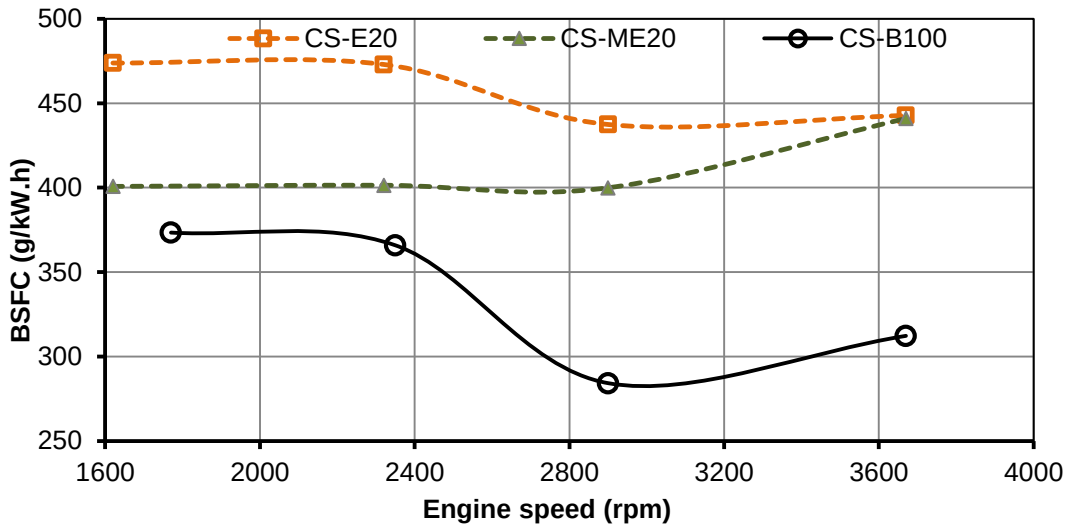

Figure 5.19 The relationship between engine speeds (rpm) and BSFC (g/kW.h) for CS-B100, CS-E20 and CS-ME20

Thermal Efficiency

Figure 5.20 presents the thermal efficiency of CS-B100, CS-E20 and CS-ME20 at various engine speeds. Thermal efficiency of the base fuel and CS-E20 increased with the increase of the engine speed, reaching the maximum value at the speeds between 2900 rpm and 3670 rpm. The lower thermal efficiency at a low speed mainly comes from the heat losses transferred through the cylinder wall (Fahd et al., 2012). In contrast, the thermal efficiency of CS-ME20 showed an almost constant value within the speed range of 1600 to 2800 rpm. This finding agrees with the results presented in Chapter 6 of this thesis, Al-lwayzy and Yusaf (2013), Allwayzy et al. (2010) Raheman and Phadatare (2004). At engine speeds above 2900 rpm,

emulsion fuels produced noticeably lower thermal efficiency compared with the base fuel and CS-E20 converged with CS-ME20. At low engine speeds from 1600 to 2350 rpm, CS-E20 and CS-ME20 surpassed the efficiency of the base fuel, which is consistent with the work of Davis et al. (2012), Abu-Zaid (2004) and Scragg et al. (2003).

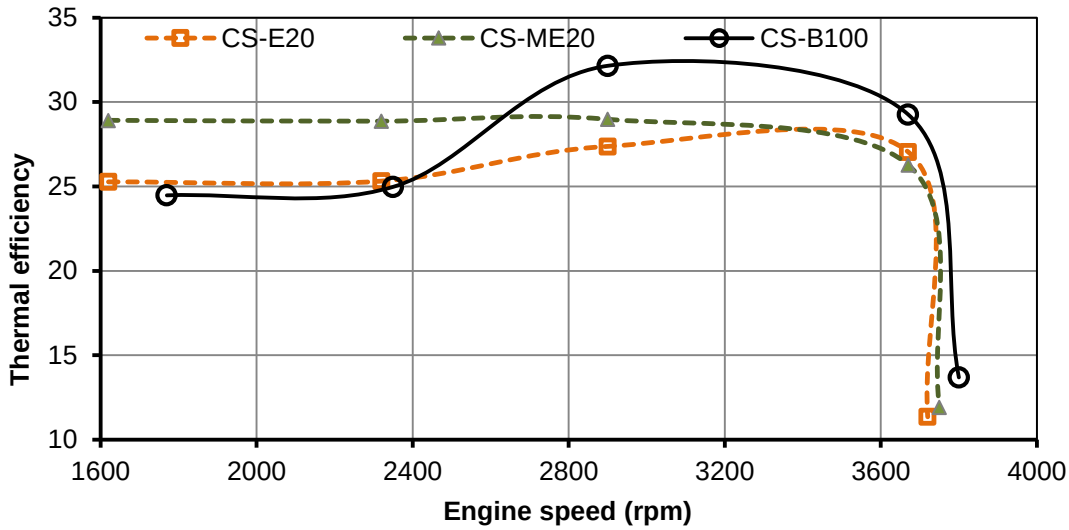

Figure 5.20 The relationship between engine speeds (rpm) and thermal efficiency (%) for CS-B100, CS-E20 and CS-ME20

Exhaust Gas Temperature

The trends and the comparison between the engine exhaust temperatures for CS-B100, CS-E20 and CS-ME20 are depicted in Figure 5.21. For all fuels, the exhaust gas temperature increased with increases in the engine speed until a peak temperature was reached, after which it decreased to the lowest value at maximum speed (engine at no load). The peak temperatures varied depending on the fuel type used. The trend of exhaust gas temperatures showed agreement with Koc and Abdullah (2013) and the engine manufacturer's performance curve. The maximum temperature of 507 °C was reached at 2350 rpm for the base fuel. The maximum exhaust gas temperature in the standard performance curve (see Appendix B) was about 560 °C, which is higher

than the maximum exhaust temperature obtained with the current fuels (around 507 ºC). This was because the heating values of the fuels in this experiment were lower than that of PD, the standard fuel for the engine. The reason for the maximum exhaust gas temperature occurring at about 2350 rpm was that the maximum fuel flow rate consumption was found at this speed (the maximum torque). The maximum fuel flow rate associated with lower speed offers extra time for the reaction and temperature rise (Koc & Abdullah, 2013).

At most engine speeds, the CS-E20 and CS-ME20 demonstrated a reduction in the exhaust gas temperature compared with the base fuel. This is consistent with the results shown in Figure 5.12, Figure 5.13, Figure 5.14 and Figure 5.15 for the in-cylinder pressure and heat release in which the emulsion fuels produced lower heat because of the lower heating value. This phenomenon was also caused by the water content, which absorbed some heat in the combustion process (Fahd et al., 2012; Koc & Abdullah, 2013).

Insignificant differences in the exhaust temperature were found between B100 and 10% emulsified water in B100 fuels at all engine speeds (Davis et al., 2012). This disagrees with the main findings shown in Figure 5.21. It may have been caused by the lower percentage of water in the emulsion of 10%, which was half of the water content in this study.

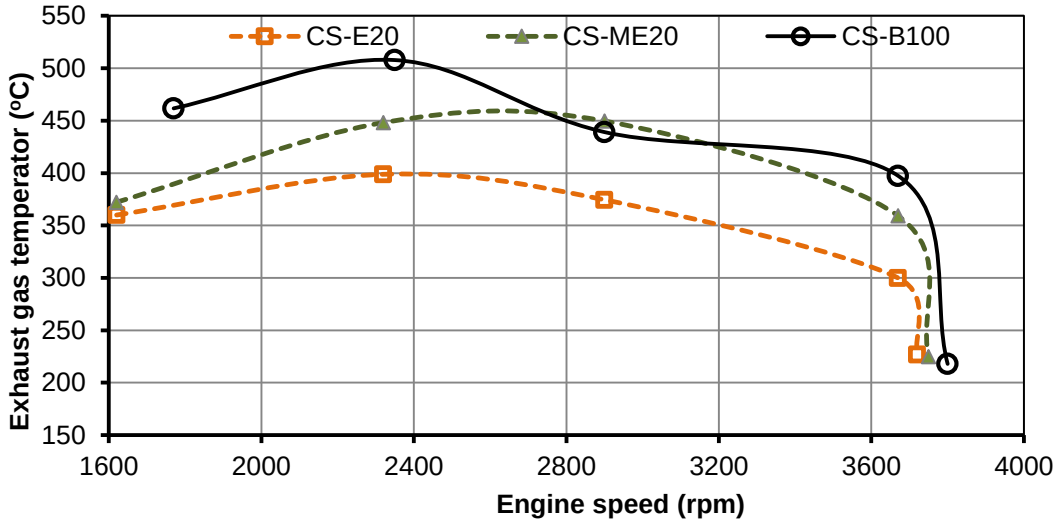

Figure 5.21 The relationship between engine speeds (rpm) and exhaust gas temperature (ºC) for CS-B100, CS-E20 and CS-ME20

5.4.3 Exhaust Gas Emissions

Carbone Monoxide (CO)

The percentage of CO emission at different engine speeds for CS-B100, CS-E20 and CS-ME20 is presented in Figure 5.22. The trend shows that the CO percentage considerably decreased when the engine speed increased for all fuels. The maximum CO percentage occurred with CS-B100 fuel up to 2350 rpm. For the low speeds and high loads, the level of CO of 3.55% for CS-B100 compared with 2.0% for CS-E20 and to 1.93% with CS-ME20. The lower CO levels for the emulsified fuels at low speed was caused by the increase in the thermal efficiency due to the available time for complete combustion and converting CO to CO_2. All fuels showed a reduction in CO percentage at high engine speeds. This sharp transition, which occurred at around 2350 rpm may have been caused by the improved combustion resulting from increased in-cylinder pressure (note the lambda graph in Figure 5.25).

According to Koc and Abdullah (2013), the water content in fuel contributes to reducing the CO level because of the increased percentage of OH, which enhances the chance to form CO_2. Similarly, Nadeem et al. (2006) reported that the water in biodiesel facilitates extra micro-explosions that enhance the mixing process. This reduction agrees with Fahd et al. (2012) results for low load. However, the results disagree with Fahd et al. (2012) conclusion in that the CO level at high engine load was insignificant in their study. As Figure 5.22 shows, higher CO level at high load (low speed). The reduction of CO percentage is confirmed by the test result on thermal efficiency, which decreased at high engine load. This may also be linked to the fact that the emulsion fuels contained 20% water with less carbon to O_2 ratio, which allowed the CO to form CO_2 at low speed. At 2900 rpm, the CS-E20 and CS-ME20 produced almost the same CO level that was produced by CS-B100 due to the shortage in time of reaction. The CO plateaued at a very low level because of the excess O_2 and turbulent mixing combustion as the speed increased.

The results show agreement with the findings of (Scragg et al., 2003) when they ran an engine with emulsified fuel containing microalgae at low load for speeds below 2900 rpm. The variation in their results between the emulsified fuel and the base fuel was found to be higher than that presented in Figure 5.22. The most likely reason for that difference is the different engine design and the operating conditions.

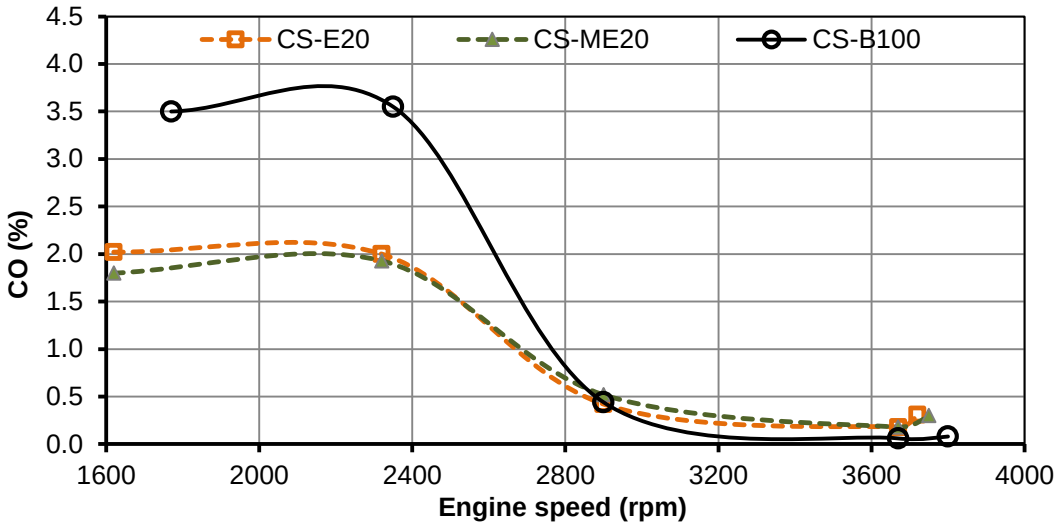

Figure 5.22 The relationship between engine speeds (rpm) and CO (%) for CS-B100, CS-E20 and CS-ME20

Carbone Dioxide (CO_2)

The CO_2 percentage emitted from CS-B100, CS-E20 and CS-ME20 is plotted against the engine speed in Figure 5.23. From this figure, it can be observed that the CS-E20 and CS-ME20 produced lower CO_2 at all engine speeds. Similarly, Scragg et al. (2003) detected a slight decline in the CO_2 percentage in the exhaust produced from emulsion fuel containing microalgae compared with biodiesel fuel. The opposite finding was reported by Koc and Abdullah (2013), who reported that emulsion fuel emitted higher CO_2 possibly because of the higher O_2 in the emulsified water fuels.

The results also confirm that adding FWM-CV to the emulsion fuel increased the CO_2 when comparing CS-ME20 with CS-E20. This was mainly because of the higher fuel injected with CS-ME20 associated with better combustion that allowed CO to be converted to CO_2.

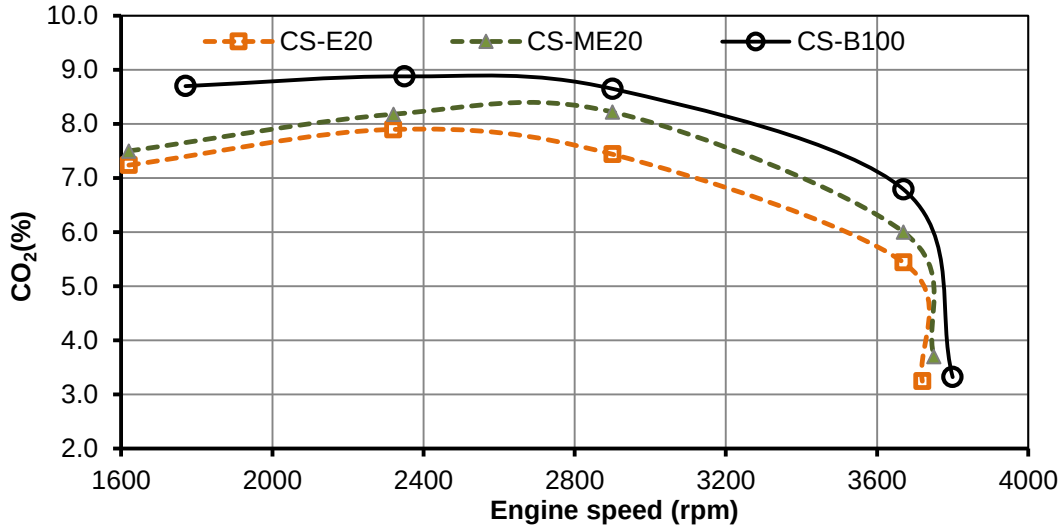

Figure 5.23 The relationship between engine speeds (rpm) and CO_2 (%) for CS-B100, CS-E20 and CS-ME20

Oxygen (O_2) and Lambda

Figure 5.24 and Figure 5.25 show the effect of the engine speed on the O_2 percentage and lambda for the engine fuelled by CS-B100, CS-E20 and CS-ME20 fuels. As the diesel engine in most cases runs lean, this means, a higher air–fuel ratio than stoichiometric. However, the air–fuel ratio, in-cylinder pressure turbulence, time of reaction, droplet size and spray pattern were all important factors affecting the chemical kinetic reaction of carbon with the available O_2. It can be seen that the higher the engine speed was, the higher the excess O_2 % and lambda values were. Reducing the engine speed (applying extra load) increased the reaction time. The shorter time reduced the in-cylinder turbulence, which reduced the combustion efficiency and increased the fuel usage resulting in an increase in a lower air–fuel ratio. A similar finding and justifications were reported by Koc and Abdullah (2013). The lower heating value in the emulsion fuels required less O_2 for the combustion process, which contributed to the higher excess O_2 from CS-E20 and CS-ME20 fuels than from CS-B100 fuel. As a result of the presence of the extra HC provided by

FWM-CV in CS-ME20 compared with CS-E20 fuel, the O_2 level was slightly lower. The O_2 level shown in Figure 5.24, especially at 3670 rpm, agrees with Scragg et al. (2003) outcome, in which the O_2 increased from 13.3% with neat biodiesel to 13.9% when the emulsion fuel was implemented.

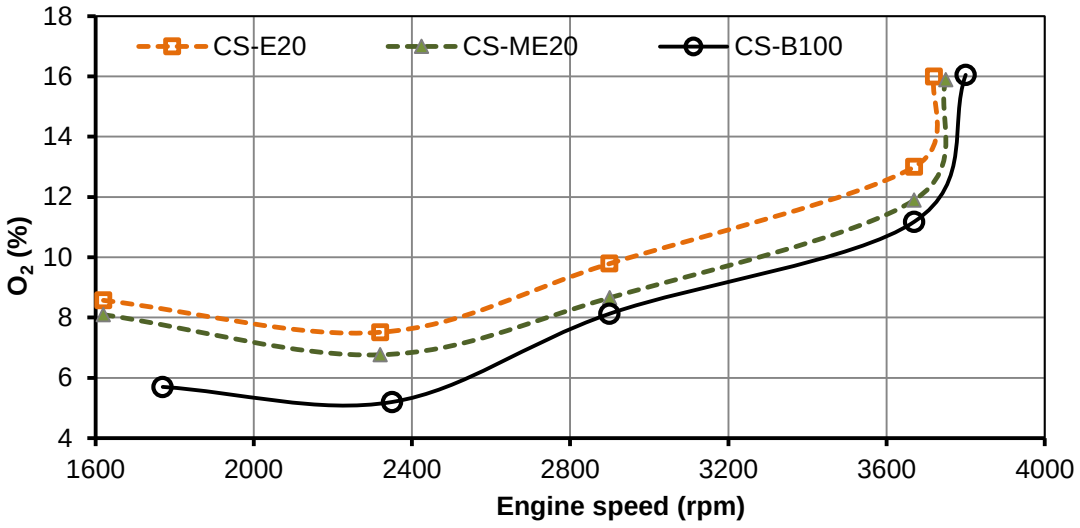

Figure 5.24 The relationship between engine speeds (rpm) and O_2 (%) for CS-B100, CS-E20 and CS-ME20

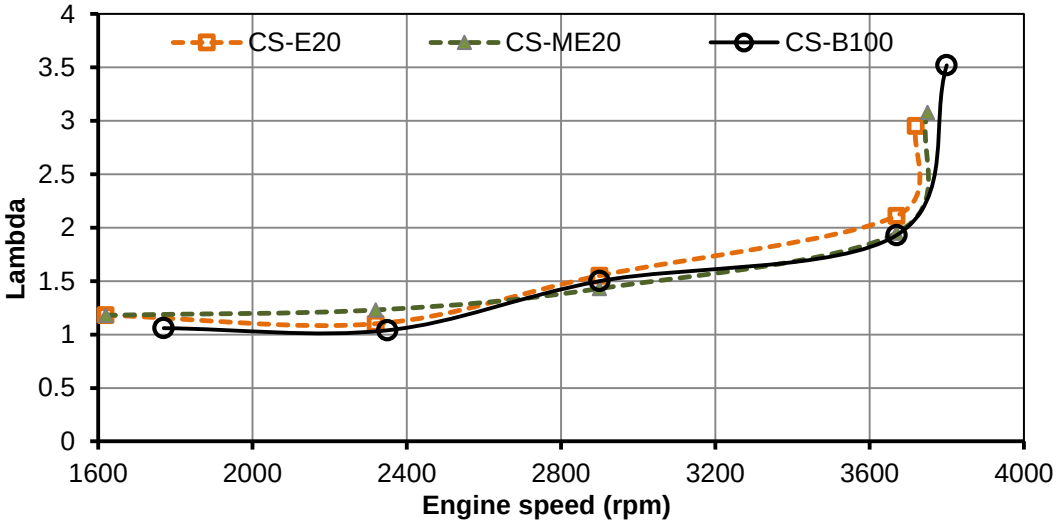

Figure 5.25 The relationship between engine speeds (rpm) and lambda for CS-B100, CS-E20 and CS-ME20

Nitrogen Oxides (NO_x)

The NO_x emission produced by the engine utilising CS-B100, CS-E20 and CS-ME20 fuel as a function of engine speed is represented in Figure 5.26. The significant differences between the test fuels can be clearly noticed at all engine speeds. The maximum reduction occurred at 2900 rpm. The NO_x level fell from 505 PPM with CS-B100 to 378 PPM and 339 PPM for the CS-E20 and CS-ME20 with a reduction of 25.14% and 32.87%, respectively. Maiboom and Tauzia (2011) reported a similar reduction of up to 50% of NO_x when using emulsified water and exhaust gas recycling. The water content in the emulsion fuels generate heat sinking, which lowers the combustion temperature and retards the NO_x formation (Fahd et al., 2012; Maiboom & Tauzia, 2011). Supporting results were found by Koc and Abdullah (2013). The NO_x reduction was caused by the presence of the water droplets, which reduced the combustion temperature (Davis et al., 2012). The statistical analysis of specific NO_x emissions performed by Davis et al. (2012) for B100 and emulsion of 10% water in B100 proved an interesting finding. They reported that the NO_x emission from the emulsion fuel was significantly lower than that emitted by B100 in spite of the insignificant difference in the exhaust gas temperature. They linked that reduction to the increase in the percentage of OH radicals in the emulsion fuel, which is in agreement with the findings of this work.

At the engine speed of 3670 rpm and 2350–2320 rpm, the reduction in the NO_x level showed very strong agreement with the reduction found by (Scragg et al., 2003) when compared with biodiesel fuel from rapeseed with emulsion fuel containing microalgae slurry.

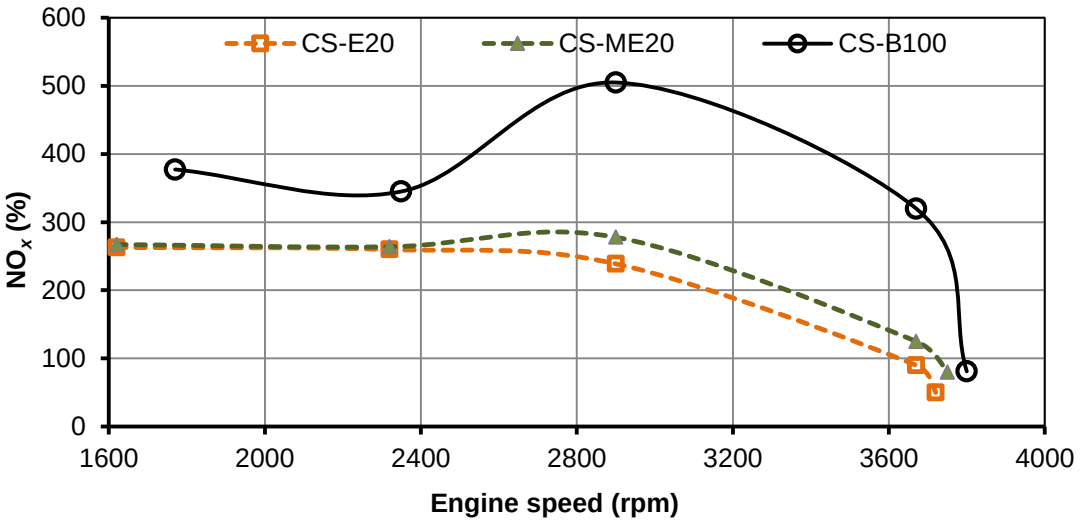

Figure 5.26 The relationship between engine speeds (rpm) and NO_x (PPM) for CS-B100, CS-E20 and CS-ME20

5.5 Conclusion

This chapter discussed the preparation and testing of three types of fuels in a single-cylinder diesel engine tuned for petroleum-based diesel fuel. The fuels were pure cottonseed biodiesel (CS-B100), emulsified water fuel containing 20% water in CS-B100 (CS-E20) and emulsified fuel containing 20% water with FWM-CV added (CS-ME20). One of the main objectives of the test in this chapter was to overcome the problems faced in obtaining an amount of FWM-CV biodiesel from small-scale production, such as the low productivity and lengthy process that consumes time and money. The use of direct biomass of FWM-CV in liquid form was a proposed solution. The preparation of the emulsion fuels was conducted using ultrasound for the mixing purpose. To prepare water containing FWM-CV, ultrasound was also used to break down the microalgae colonies because they were found to be larger than the injector orifice size. The results of the engine performance and emission tests can be concluded as follows:

1. The in-cylinder pressure and the heat release for the emulsion fuels produced higher ignition delay and shorter ignition duration. The emulsion fuels indicated lower in-cylinder pressure than the 100% biodiesel. At the engine speed of 3670 rpm, the CS-ME20 gave higher in-cylinder pressure than the CS-E20.
2. In general, CS-E20 resulted in lower values than CS-ME20 and both were lower than CS-B100 in the GIP, brake power, torque, CO_2 and NO_x. In contrast, the CS-E20 resulted in higher values than CS-ME20 and both were higher than CS-B100 in the BSFC and O_2. The emulsion fuels gave higher and lower values than the base fuel in CO and the thermal efficiency depending on the engine load and speed.

CHAPTER SIX

Microalgae *Chlorella Protothecoides* (MCP) as an Alternative Fuel for Tractor Diesel Engines

6.1 Introduction

The use of MCP biodiesel in the blends of MCP-B100, MCP-B50 and MCP-B20 in a single-cylinder diesel engine was discussed in Chapter 4. This chapter presents the investigation of a tractor PTO performance test using the MCP-B20 blend. As detailed in Chapter 4, this blend showed insignificant changes in the averages of the overall engine performance and insignificant reduction in the CO and NO_x levels. With this blend, a smaller amount of MCP-B100 was required to perform the PTO test at different operating conditions. The effect of the biodiesel fuel on the tractor engine parts (if any) would be minor with this blend. This chapter covers the following topics with reference to MCP biodiesel:

- introduction
- background and literature review
- methods
- results and discussion
- conclusion.

6.2 Background and Literature Review

Testing of vegetable-based oil or biodiesel fuel in a tractor diesel engine has been reported by several researchers. Most studies have reported comparable tractor performance and promising emissions reduction. For example, sunflower oil fuel was used in a wide range of agricultural tractors by Fuls et al. (1984). This study found that the tractors' performance was very comparable with that of tractors fuelled with PD. However, some problems were noticed, such as carbon accumulating on injector nozzles and sticking piston rings. Converting this oil to biodiesel fuel through transesterification was proposed to remarkably overcome these problems. A reduction in the brake power was expected if the same volume of biodiesel fuel was injected into the engine because of its lower heating value. In a study by Zanche *et al.* (1997), a tractor was tested in both bench and field testing using biodiesel fuel. They commented that, in comparison with PD, the biodiesel fuel showed a reduction of 7% in average test power and an increase of about 18% in BSFC. In addition, they reported no major changes in the engine performance and an insignificant effect was found on the lubricant, cylinders and engine valves. However, the crankshaft bearings showed slightly higher wear with biodiesel, and higher carbon and sludge was found on different engine parts.

Dorado et al. (2003a) tested biodiesel from waste cooking oil (extracted from olives) in a direct injection Perkins diesel engine. A satisfactory performance and statistically insignificant differences were achieved throughout the test using biodiesel and diesel fuel. However, an increase of up to 26% in BSFC and less than 8% of the power loss in comparison with PD were noted. Li *et al.* (2006) tested a farm tractor fuelled with soybean biodiesel in different blends (B100, B50, B20 and

PD) in a 12-hectare field when undertaking spring tillage and soybean planting. The B20 results showed very comparable tractor performance for power, fuel efficiency and NO_x compared with PD. In another study, Jablonický et al. (2009) reported that the rated power of the tractor diesel engine dropped by 15% with biodiesel fuel and BSFC increased by15%. The use of B100 biodiesel in a tractor under hard operating conditions was tested by Celik et al. (2009) in a three-month study to determine the effect of biodiesel on the engine components. The study found that biodiesel did not have any effect on the pistons, engine intake or exhaust valves or the fuel pump. In addition, the injector did not show any drop in the fuel pressure and no problems were encountered with the injector spray after 1000 litres of biodiesel had been used.

Kim et al. (2010) tested different blends of biodiesel (B20, B50 and PD) in a tractor, both in the field and in a PTO test. They commented that the tractor PTO power was insignificantly affected, and reduction in CO_2 and increase in the NO_x were found when biodiesel fuel was compared with PD. Biodiesel B20 was recommended as the optimal biodiesel blend by Kulkarni et al. (2011) because the performance was similar to that of diesel.

Power can be utilised from a tractor in several ways, with the drawbar power and the PTO power being the most important from a tillage perspective. Drawbar and field tests results are dependent on many factors, such as soil and tyre type and conditions, the former crop planted, and the type of equipment used with the tractor. PTO testing requires less time and can be performed under controlled conditions, which gives more accurate results that reflect the engine performance and emissions.

6.2.1 Tractor PTO Test

PTO power is the power that is taken from the PTO shaft, located in the rear of the tractor, to power the agricultural machinery. This shaft is connected to the tractor engine through the gear train. The approximate relationships between the tractor axle power, PTO power and engine power are given in Equation 6.1 and Equation 6.2 (Zoz and Grisso (2003).

$$Axle_{Power} = 0.96\ (PTO_{power}) \quad \text{Equation 6.1}$$

$$PTO_{Power} = 0.85\ (Engine_{brake\ power}\ ) \quad \text{Equation 6.2}$$

Matthew et al. (2007) used a John Deere 3203 tractor to test the performance and emissions when using PD, B20 and B100. The test focused on the variation in BSFC, PTO torque, PTO power, thermal efficiency and NO_x emissions between these different fuels. The results showed that there were no statistically significant differences between PD and B20. Shrivastava et al. (2007) concluded that the Sonalika tractor performance in a PTO test using B20 karanja biodiesel and PD gave very comparable PTO power, resulting in the recommendation that the B20 blend could replace diesel fuel. Neel et al. (2008) also used a John Deere 3203 23.9 kW compact utility tractor to compare PTO power performance, fuel efficiency and NO_x using PD, a biodiesel blend of B20 and B100 at rated PTO speed (540 rpm) and at peak torque load conditions. The results showed that when the tractor was fuelled by PD or B20, similar performance was found at peak torque. Sahoo et al. (2009) used a water-cooled three-cylinder tractor engine fuelled with 10 fuels at full and partially open throttle. The fuels used in their study were from non-edible oil derived from jatropha, karanja and polanga methyl esters. These biodiesels were blended with

diesel as B20, B50 and B100. The results of the WOT test showed that the engine power was slightly reduced at all the speeds with biodiesel blends of KB20, KB100, JB100, PB20 and PB100. Sahoo et al. (2009) found an insignificant difference for all the biodiesel blends, at lower speeds of 1200 and 1400 rpm. Meanwhile, Godeša et al. (2010) studied the effect of using a cold-pressed rapeseed oil mixture with PD on the tractor engine power, torque and FC. In their study, they applied the load using a PTO dynamometer. They stated that using biodiesel from soybean at a blend of up to 20% can run a diesel engine without any concern for the engine's durability.

PTO testing gives an indication of the tractor engine performance. The best known tractor PTO test is the Nebraska test. The main limitation of the Nebraska test, and of the test adopted in Europe, is that the tractors to be tested are selected by the manufacturer. The test only presents the tractor performance at the full fuel line WOT setting. No consideration is given to tractors that run under a wide range of loads, and hence throttle settings. The Australian Tractor Testing Committee follows a modified procedure in which the tractors for the test are randomly selected. However, none of these tests reports the emissions from the engine during the PTO test.

The increase in the output power of modern tractors has increased the side effect of tractor noise. According to Ned and Steinbruegge (1972), requests by farmers to include the noise level of new tractors encouraged the Nebraska Board of Tractor Test Engineers to include sound measurements in Nebraska tractor test reports. Engine noise is an important factor that indicates the degree of combustion smoothness and can affect human health. Tractors in most developing countries do not have operator cabs or sound isolation. Farmers in developing counties generally

do not wear hearing protection that reduces the high risk of hearing loss. Therefore, an alternative fuel that produces less noise would be valuable.

Tractor manufacturers and farmers have concerns about using B100 fuel in the long term because it may cause problems in the engine parts. Using low blends of biodiesel of about B20 has been reported as safe for running engines. Biodiesel from non-edible microalgae has not yet been tested in a tractor diesel engine. In this work, tractor PTO tests were conducted to evaluate tractor engine performance and emissions using PD and microalgae biodiesel (MCP-B20) under different tractor operating conditions. A performance and exhaust gas emissions map was drawn for WOT) and half open throttle (HOT). Further analyses were conducted using SPSS analytics software for the PTO rated speed and peak power during the WOT test. ANOVA testing was used to identify the significant differences between the means values of the two fuels at the selected speeds.

6.3 Methodology

6.3.1 Experimental Apparatus

Stationary PTO tests were conducted at the Agricultural Equipment Laboratory at USQ. The test aimed to study the performance and emissions of a farm tractor fuelled with MCP-B20.

Tractor

The tractor used in the experiment was a John Deere 4410 eHydro, as shown in Figure 6.1. The engine in the John Deere 4410 tractor is a Yanmar 3TNE88 three-cylinder water-cooling diesel engine with a compression ratio of 18.8:1. The engine

power is 25.8 kW and the manufacturer's estimated PTO power is 21.3 kW. The engine torque at rated speed is 87.9 N.m.

Figure 6.1 The experiment set-up (a) the tractor (b) fuel system (c) gas analyser (d) dynamometer (e) PTO connecting rod

Dynamometer

In order to apply load on the tractor engine, an AW Dynamometer Inc., Colfax, Illinois, PTO dynamometer (the Nebraska model was used; see Figure 6.1[d] and [e]). The dynamometer had been previously modified by Rimik Toowoomba, by adding a load cell and digital monitor to measure PTO speed (rpm) and torque (N.m), and then to calculate the power (kW). The load cell, and hence the dynamometer, was calibrated prior to each test. The calibration was started by setting the display in the calibration mode. Then, the zero torque was set. Standard weights of 100 kg were suspended on a one-meter arm to apply load/torque on the load cell, resulting in a torque of 981 N.m being set on the display. An optical tachometer was used to check

the PTO speed. The ratio of the engine to the PTO speeds was found to be 4.815. The specification of the load cell indicated an accuracy of ±2.5%.

Gas Analyser

A Bosch BEA 460 gas analyser was used to monitor the tractor exhaust gases of O_2, CO, CO_2, NO and lambda. The gas analyser was connected to a laptop to record and save the data (see Figure 6.1[c]). The operating ranges (sensitivity) and resolutions are shown in Table 6.1. Prior to the test, the device was subjected to maintenance and calibration by the manufacturer and daily standard calibrations were undertaken.

Table 6.1 The gas analyser ranges, accuracy and resolution

Component	Min.	Max.	Resolution
CO (%) vol	0	10.00	0.001
CO_2 (%) vol	0	18.00	0.01
Lambda	0.5	22.00	0.001
NO (ppm)	0	5000	1

Noise Level Meter

The tractor noise and vibration are important factors influencing the driver's productivity and health, and should be considered in modern tractor development (Jurić et al., 2001). To compare the noise level produced by the tractor engine using the different fuels, a Larson DavisSoundTrack LxT Sound Level Meter was placed in a position equivalent to the operator's head.

6.3.2 Fuel Preparation

MCP-B20 was prepared as described in Chapter 4. However, to prepare the MCP-B20 blend, 20% by volume of MCP-B100 was mixed with 80% by volume of PD; the PD was a commercial product obtained from the local Shell petrol station. The

specification of MCP-B20 was calculated from the PD (obtained from Shell Australia) and MCP-B100 depending on their volume in the blend.

Table 6.2 Fuel properties

Fuel property	Petroleum diesel (PD)	MCP-B20
Cetane number	49.0	49.6
Calorific value (MJ/kg)	46.0	44.8
Density at 15 ºC (kg/L)	0.83	0.84
Viscosity at 40 ºC (cp)	2.53	4.22
Flashpoint (ºC)	79	88
Acid value (mg KOH/g)	<0.10	0.14
Sulfuret content (mg/kg)	8.0	6.8

6.3.3 Fuel Consumption (FC) Measurement

The FC rate was measured using the measuring cylinder shown in Figure 6.2. Initially, a digital flow meter was used to measure the mass flow rate of diesel; however, the data fluctuated due to the pulsing of the injectors. Thus, a volumetric cylinder was successfully and accurately used (Al-lwayzy et al., 2012; Godeša et al., 2010). The measuring cylinder was fitted with two-way valves at both the top and bottom. The top two-way valve allowed the fuel returning from the injectors to either enter the cylinder or return to the tank. The bottom two-way valve allowed the fuel either to be drawn from the cylinder or to be supplied from the tank. In order to obtain an FC reading, the top and bottom valves were opened simultaneously allowing return fuel to enter the cylinder while fuel was being drawn from the bottom. The time was recorded using a stopwatch for the fixed volume of fuel consumed. The FC was repeated three times at each speed to reduce the error.

A separate tank was connected while MCP-B20 fuel was being used to prevent cross-contamination. The fuel lines were completely drained when changing fuel sources.

At the end of the test using PD, the system was cleaned and the fuel filter was changed to prevent any contamination from the previous test.

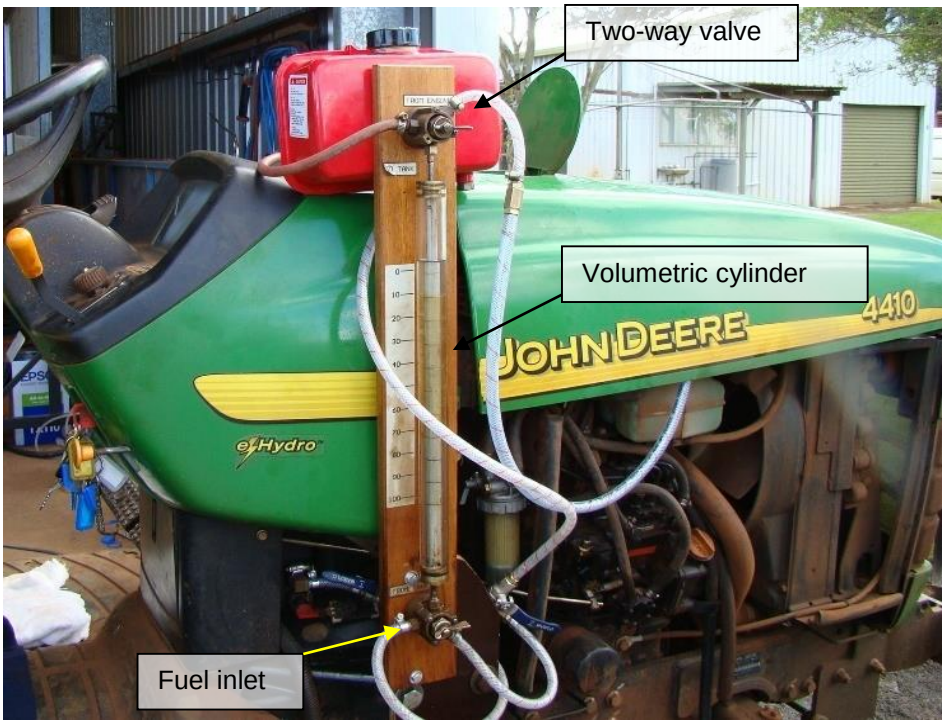

Figure 6.2 Fuel consumption measurement system

6.3.4 Engine Test Procedure

This section details the tractor PTO test results for the comparison between PD and MCP-B20 using the WOT and HOT tests. At WOT, the engine speed was fixed at 2700 rpm (PTO speed 550 rpm) at no load using a fuel controller lever (throttle). The load was then applied by the dynamometer until a fixed reduction in speed was achieved. During the test, PTO and engine speed, torque and power, FC, exhaust gas temperature, noise level and exhaust gas emissions were monitored and recorded.

The same procedure was followed for the HOT test, with the engine speed without load being set at 2000 rpm (PTO speed about 415 rpm). In each test, the tractor engine was warmed up for 30 minutes using PD fuel. The tests were conducted at the

same atmospheric conditions at which humidity, atmospheric pressure and temperature were constant (the variation was about 4 ºC in temperature and 6% humidity). The dynamometer was carefully calibrated prior to the tests. Each test was repeated three times and the average data were used and reported in this work.

6.4 Results and Discussion

6.4.1 Statistical Analysis

ANOVA and LSD tests were performed in a recent studies on tractor PTO performance by Mohebbi et al. (2012), Hunt et al. (2013) and Tomić et al. (2013). As discussed in Chapter 4, in the current study, MCP-B20 revealed insignificant differences in the average of the overall test compared with PD in most of the engine performance and the emission characteristics. The average results of the PTO test using MCP-B20 compared with PD for engine performance and exhaust gas emissions are presented in Figure 6.3 and Figure 6.4. Figure 6.3 shows that the maximum difference in the averaged total test result of the performance parameters of MCP-B20 compared with PD is 6.9% for the BSFC. In the WOT test, the GIP, brake power and torque were insignificantly reduced by 2.2%, 0.8% and 0.3% when MCP-20 was used. Such a reduction was expected because of the decrease of 2.7% in the heating value. The brake power and torque were insignificantly lower than those from PD. This result is in agreement with that of Shrivastava et al. (2007), whose PTO test with biodiesel from karanja produced a slight decline (1.82%) in power in comparison with PD. It is also consistent with the results of Godeša et al. (2010), who reported that blends of rapeseed oil in PD produced an insignificant

difference in the PTO torque compared with PD, whereas the differences at the engine speeds above 2600 rpm were higher than at low engine speed.

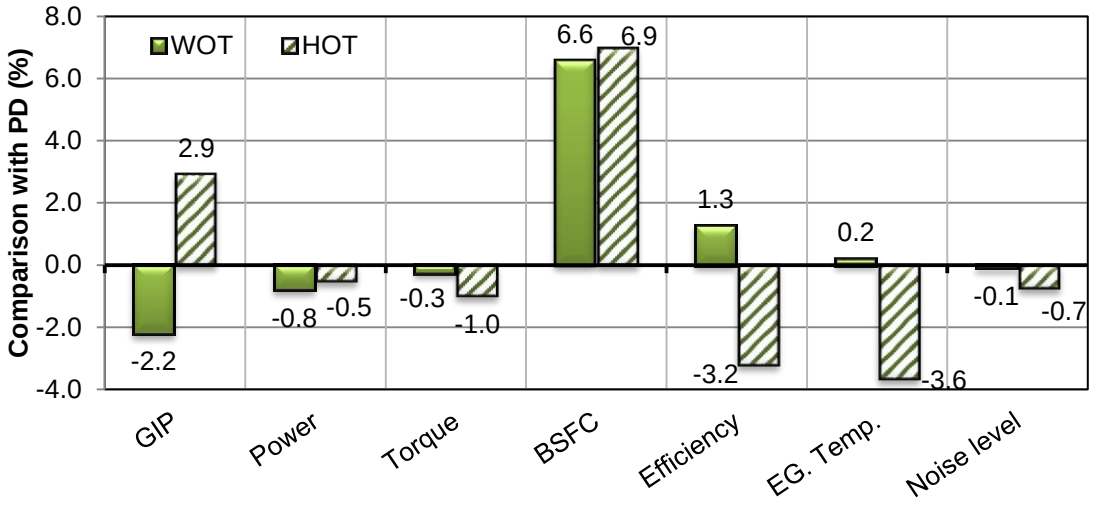

Figure 6.3 The average tractor performance parameter differences percentage compared with PD when MCP-B20 was used at WOT and HOT

The maximum differences between the fuel parameters were recorded with BSFC, which was higher in MCP-B20 than PD by 6.6 and 6.9 at WOT and HOT, respectively. In the WOT test, the thermal efficiency and the exhaust gas temperature insignificantly increased by 1.3% and 0.2%. In contrast, in the HOT test, the thermal efficiency and the exhaust gas temperature decreased. The engine noise level insignificantly dropped by less than 1%. The overall insignificant differences between MCP-B20 and PD were caused by the same factors discussed in Chapter 4. Taghizadeh-Alisaraei et al. (2012) reported that an engine fuelled with biodiesel fuel of B20 and B40 produced significantly less engine vibration than PD, which indicates smother combustion and less noise.

The differences percentage of average tractor exhaust gas emissions compared with PD when MCP-B20 was used at WOT, rated PTO and peak PTO torque are given in Figure 6.4. This figure shows that the CO level was significantly reduced with MCP-

B20 compared with PD, by 12.7% and 23.1%. In the WOT and HOT tests, the CO_2, O_2, lambda and NO insignificantly varied with MCP-B20 compared with PD. This occurred for the same reasons provided in Chapter 4, such as the low percentage of MCP-B100 in the fuel and the relatively close exhaust gas temperatures.

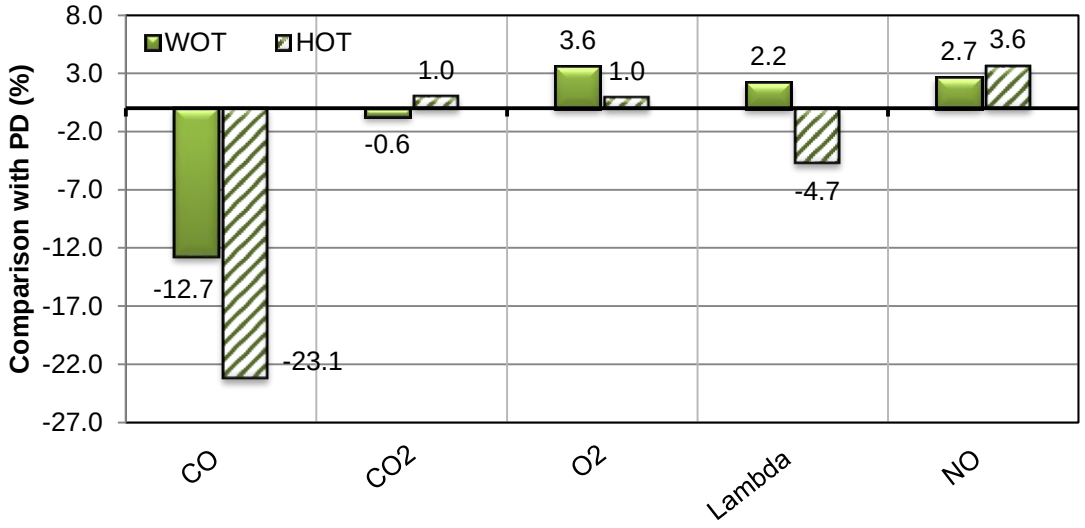

Figure 6.4 The average tractor exhaust gas emissions differences percentage when MCP-B20 was used at WOT and HOT compared with PD

Many researchers, such as Kulkarni et al. (2011), Davis et al. (2012) and Hunt et al. (2013) have performed a one-way ANOVA to analyse the differences between tested fuels under varying operating conditions of speed and load. Similarly to the work of this thesis, one-way ANOVA was performed on data of the PTO rated speed and peak PTO torque of a tractor by Hunt et al. (2013) and Neel et al. (2008). Table 6.3 and Table 6.4 depict summaries from the performance experiment of the descriptive statistical and one-way ANOVA test for the tractor at WOT for two selected speeds. The first speed was rated PTO speed 540 rpm (engine speed 2600 rpm). The second speed was at peak PTO torque (engine speed 1500 rpm). In these tables, the F value shows the significant difference (statistically) between PD and MCP-B20 fuel for all the parameters in this study.

Table 6.3 Descriptive statistics and ANOVA summary for tractor engine performance and emissions at WOT, rated PTO speed 540 rpm (engine speed 2600 rpm)

Variable	PD		MCP-B20		ANOVA F
	Mean	SD	Mean	SD	
Engine torque (N.m)	38.21	1.25	35.37	0.65	16.25***
PTO torque (N.m)	220.25	7.18	203.90	3.75	16.29***
GIP (kW)	55.35	2.34	50.30	1.95	10.95**
Engine power (kW)	10.40	0.34	9.63	0.18	16.21***
PTO power (kW)	12.23	0.40	11.33	0.21	16.13***
BSFC (kg/kW.h)	451.65	31.64	453.74	25.47	0.01
Efficiency (%)	18.83	1.37	19.16	1.08	0.15
Noise level (dB)	90.9	0.408	90.375	0.33	4.00
EG temp. (°C)	356.00	4.08	350.00	4.32	4.08
CO_2 (%)	7.97	0.05	7.38	0.15	56.72***
CO (%)	0.036	0.006	0.030	0.005	7.188***
O_2 (%)	9.58	0.26	10.53	0.30	23.54***
NO (ppm)	541.50	20.68	493.50	22.22	10.01**
Lambda	1.84	0.04	2.02	0.033	59.11***

** The difference is significant at $p < 0.01$. *** The difference is significant at $p < 0.001$.

Table 6.4 Descriptive statistics and ANOVA summary for tractor engine performance and emissions at WOT, peak PTO torque (1500 rpm)

Variable	PD		MCP-B20		ANOVA F
	Mean	SD	Mean	SD	
Engine torque (N.m)	79.11	0.58	78.24	0.59	4.38
PTO torque (N.m)	456.00	3.37	451.00	3.35	4.42
GIP (kW)	50.94	3.12	50.88	2.58	0.001
Engine power (kW)	12.42	0.09	12.28	0.09	4.292
PTO power (kW)	14.60	0.11	14.45	0.11	4.30
BSFC (kg/kW.h)	347.55	23.80	359.35	17.56	0.64
Efficiency (%)	24.45	1.59	24.18	1.16	0.08
Noise level (dB)	86.30	0.62	85.90	0.65	0.79
EG temp. (°C)	470.00	5.77	480.00	5.79	5.99*
CO_2 (%)	12.11	0.09	12.03	0.88	1.59
CO (%)	0.90	0.02	0.85	0.01	37.80***
O_2 (%)	2.98	0.08	3.12	0.07	5.25
NO (ppm)	970.0	5.7	994.0	3.65	50.09***
Lambda	1.13	0.09	1.14	0.02	1.20

* The difference is significant at $p < 0.05$. *** The difference is significant at $p < 0.001$

6.4.2 Tractor Engine Performance

This section discusses the results of the tractor PTO tests that were conducted to evaluate and compare the tractor engine performance using PD and MCP-B20 at WOT and HOT. The GIP, brake power, brake torque, BSFC, noise level and exhaust gas temperature are presented in the following sections.

Tractor Engine Gross Input Power and Tractor Engine Brake Power

Figure 6.5 and Figure 6.6 show the relationship between the tractor engine speeds and the engine GIP, and engine brake power using PD and MCP-B20 for the WOT and HOT tests. GIP power is the result of the lower heating value of the fuel multiplied by the fuel flow rate. Figure 6.5 and Figure 6.6 shows that the maximum GIP occurs at the engine speed of around 2500 rpm for both fuels at WOT. The maximum GIP are 75.9 and 73.1 kW for PD and MCP-B20, respectively, and the maximum brake power is 15.8 kW for both fuels. Table 6.3 and Figure 6.5 and Figure 6.6 show that at the rated PTO speed (2600 rpm engine speed) there were significant reductions in GIP of 5.05 kW (9.12%) and brake power 0.71 kW (6.86%) compared with PD when the tractor was fuelled by MCP-B20. This finding agrees with that of Neel et al. (2008), who found a significant difference in the PTO power between PD and B20 biodiesel at rated PTO speed. There was insignificant difference, as shown in Table 6.4, at the speed of maximum PTO torque between PD and MCP-B20. This result agrees with the insignificant difference between PD and B20 biodiesel at typical pumping PTO speed and peak PTO torque found by Kulkarni et al. (2011) and Neel et al. (2008) respectively. A similar trend was found for the HOT and WOT tests; however, MCP-B20 produced higher GIP and brake power at 1800 rpm. These findings associated with the results presented in Table 6.4, Figure 6.5 and Figure 6.6

show that the differences between PD and MCP-B20 for the general case were insignificant. The close results between PD and MCP-B20, as explained in Chapter 4, were caused by the higher density and cetane number for MCP-B20, which reduced the effect of the reduction in the lower calorific value for MCP-B20 compared with PD. The results of Godeša et al. (2010), who used 10%, 30% and 50% rapeseed oil blends with PD in a tractor PTO test, showed a comparable PTO power curves trend. It also showed agreement with the finding that the maximum differences in PTO power between the fuels tested occurred at the engine speeds above 2600 rpm and, at low engine speed, the results were close.

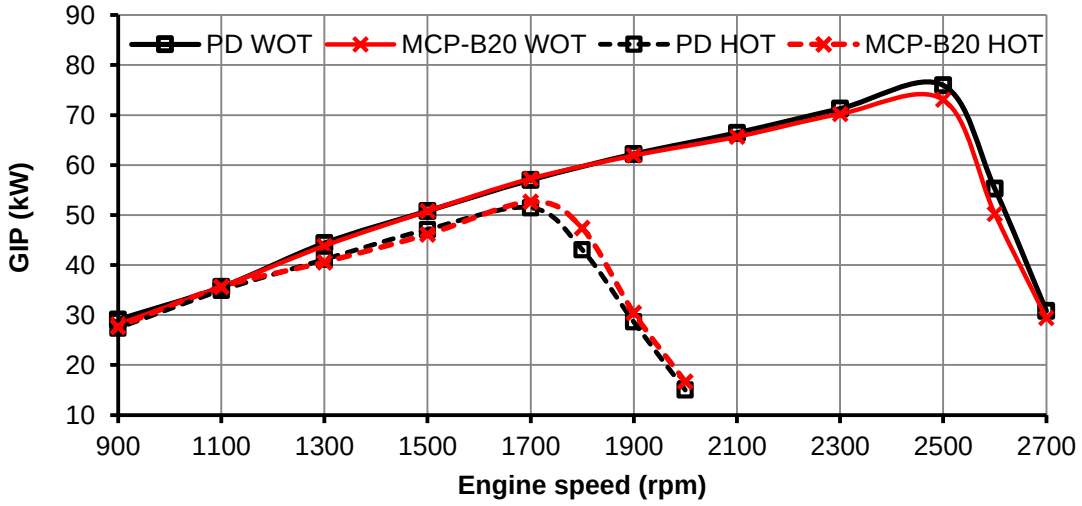

Figure 6.5 The relationship between tractor engine speeds (rpm) and engine GIP (kW) for PD and MCP-B20

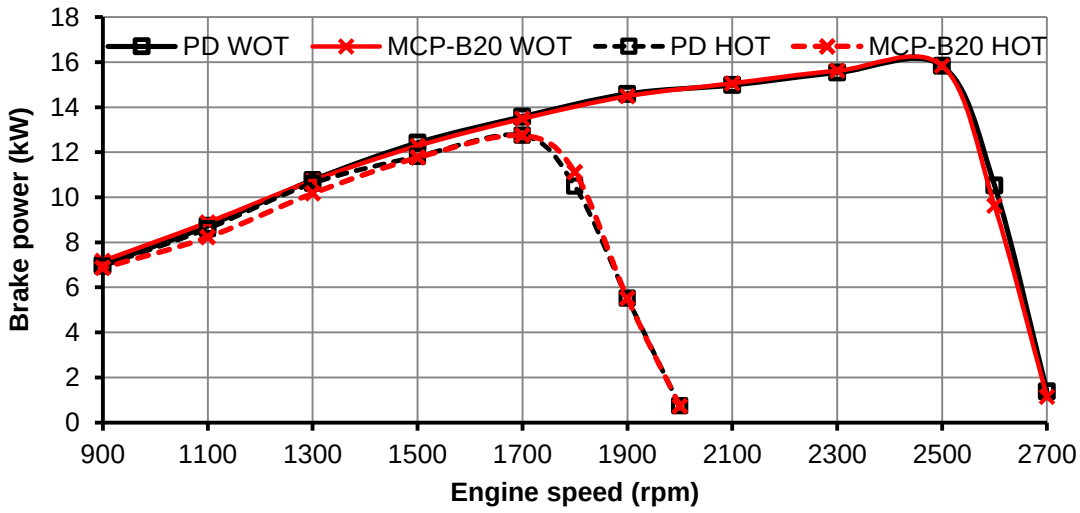

Figure 6.6 The relationship between tractor engine speeds (rpm) and engine power (kW) for PD and MCP-B20

Tractor Engine Torque and Engine Efficiency

Figure 6.7 presents the tractor engine torque for the WOT and HOT for a range of tractor engine speeds. The maximum tractor engine torque was found at engine speeds between 1300 rpm and 1500 rpm for both fuels. The maximum difference between the PD and MCP-B20 for the WOT test of 2.84 N.m (7.4%) occurred at rated PTO speed (2600 rpm engine speed). The ANOVA test for this speed shown in Table 6.3 indicates that there was a significant different in tractor engine torque between the two fuels. This finding agrees with the results of Neel et al. (2008) for PTO torque between PD and B20 fuel. However, Kulkarni et al. (2011) found an insignificant difference in the engine torque between PD and B20 fuel. At the peak torque speed, and all speeds shown in Figure 6.7, the results show comparable outcomes for the WOT test. These results agree with the findings of Kulkarni et al. (2011) and Neel et al. (2008) at 1800 rpm and the peak torque results, respectively. The HOT test indicated that when the tractor was fuelled by MCP-B20, both a reduction and increment occurred when compared with PD.

Figure 6.8 shows that the engine efficiency decreased when the engine speed increased for both fuels. The higher engine efficiency at low engine speeds was caused by the high load applied, which reduced the engine speed. This reduction resulted from low heat losses at high load (Raheman & Phadatare, 2004). The HOT test indicated that MCP-B20 surpassed PD in giving higher engine efficiency for the speeds below 1700 rpm. The higher efficiency for MCP-B20 was caused by the lower GIP in spite of the slightly lower brake power from PD. This result is related to the better combustion caused by the extra O_2 in biodiesel (Xue et al., 2011). Table 6.3 and Table 6.4 illustrate that there were insignificant differences in tractor engine efficiency between PD and MCP-B20 at the rated PTO speed and for the peak torque. This is in agreement with the findings of Kulkarni et al. (2011), Neel et al. (2008) and Shrivastava et al. (2007) because they found insignificant differences in thermal efficiency at rated speed, pumping and peak torque between PD and B20 biodiesel.

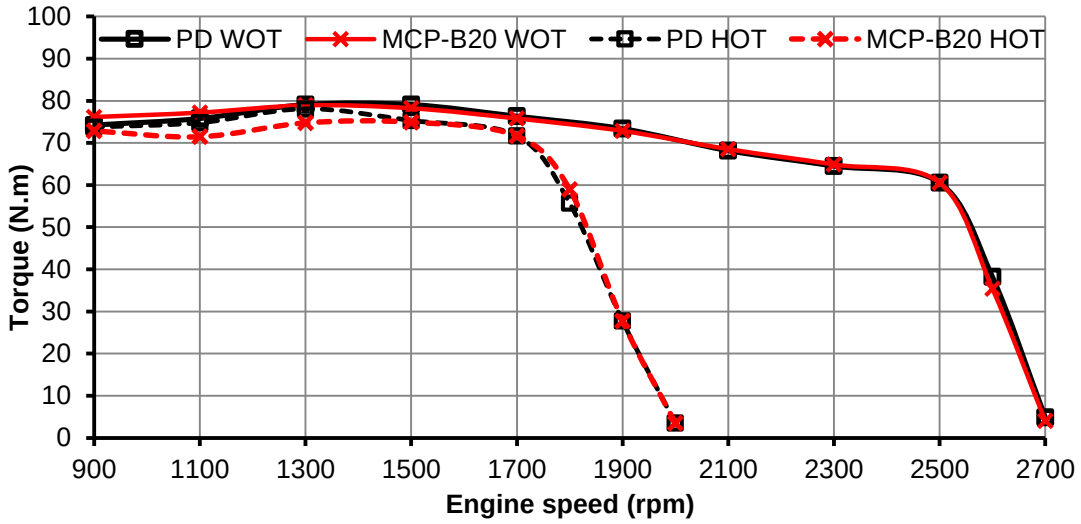

Figure 6.7 The relationship between tractor engine speeds (rpm) and engine torque (N.m) for PD and MCP-B20

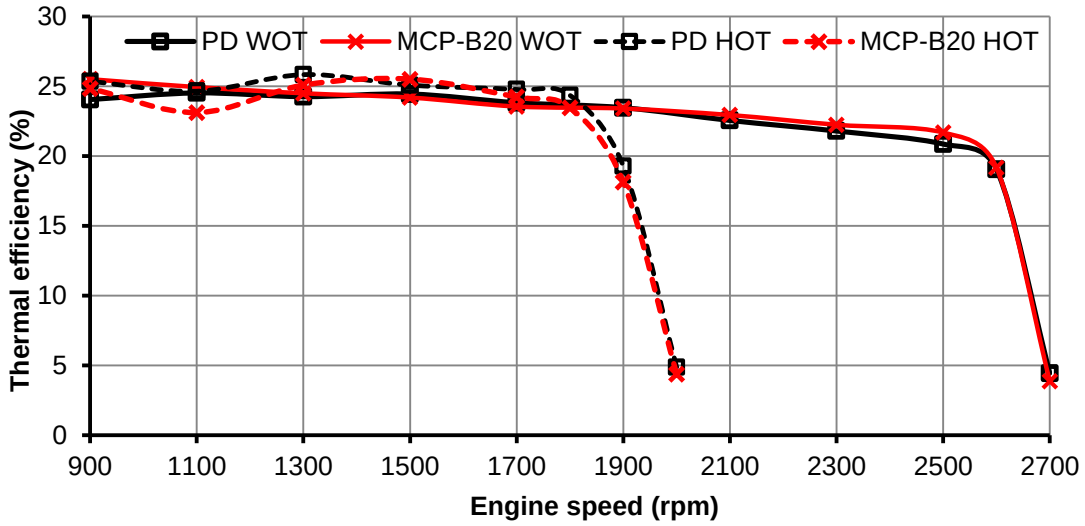

Figure 6.8 The relationship between tractor engine speeds (rpm) and engine thermal efficiency (%) for PD and MCP-B20

Brake Specific Fuel Consumption (BSFC)

The BSFC was calculated by dividing the FC rate by the engine brake power. Figure 6.9 illustrates the relationship between the tractor engine speeds (rpm) and engine BSFC (g/kW h) for PD and MCP-B20. This figure shows an increase in the BSFC when the tractor was fuelled by MCP-B20 in comparison with PD at most engine speeds except 900 and 2500 rpm for the WOT test and 1500 rpm for the HOT test. Table 6.3 and Table 6.4 show that there were statistically insignificant differences in BSFC between the two fuels at rated PTO speed and at the peak torque points. This outcome was caused by the high standard deviation found at this parameter.

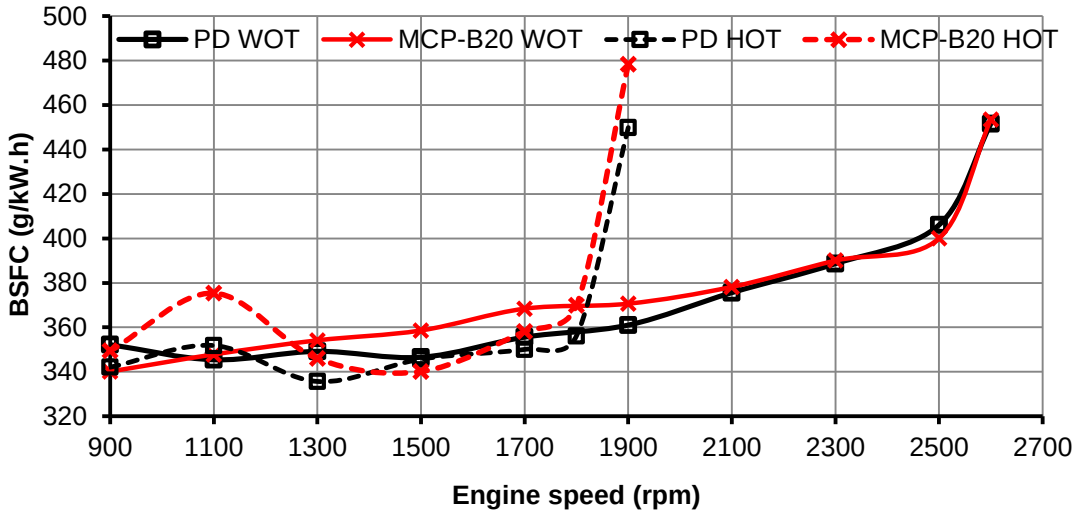

Figure 6.9 The relationship between tractor engine speeds (rpm) and engine BSFC (g/kW.h) for PD and MCP-B2ah

Exhaust Gas Temperature and Tractor Noise Level

Figure 6.10 shows the relationship between exhaust gas temperatures (°C) and engine speed (rpm) for PD and MCP-B20. From the WOT and HOT tests, it can be observed that the exhaust gas temperature increased when the engine speed increased until reaching the maximum, then the temperature declined. The maximum exhaust gas temperature for the WOT test for both fuels was between the engine speeds 1700 rpm and 2500 rpm, and for the HOT test, the maximum exhaust temperatures were found at the engine speeds between 1300 rpm and 1700 rpm. Table 6.3 and Table 6.4 show that there were insignificant differences in the tractor exhaust gas temperature between the two fuels at the rated PTO speed and peak torque speed. This finding is consistent with Shrivastava et al. (2007), who reported an insignificant reduction in the exhaust gas temperature with B20 compared with PD. The maximum difference between the two fuels of 59 °C was found at 1300 rpm for the WOT test.

The relationship between tractor engine speed (rpm) and noise level (dB) measured at the position of the operator's head, for both PD and MCP-B20, are presented in Figure 6.11 for the two throttle settings (WOT and HOT). The noise caused by the tractor vibration, which contributes to tractor noise, was insignificant when fuelled by PD and MCP-B20, as revealed in Table 6.3 and Table 6.4. The peak noise occurred at the engine speed 2500 rpm for both fuels. At this point, there was a considerable load associated with the high engine speed, which resulted in the highest noises of about 92 dB and 92.1 dB for PD and MCP-B20, respectively, for the WOT.

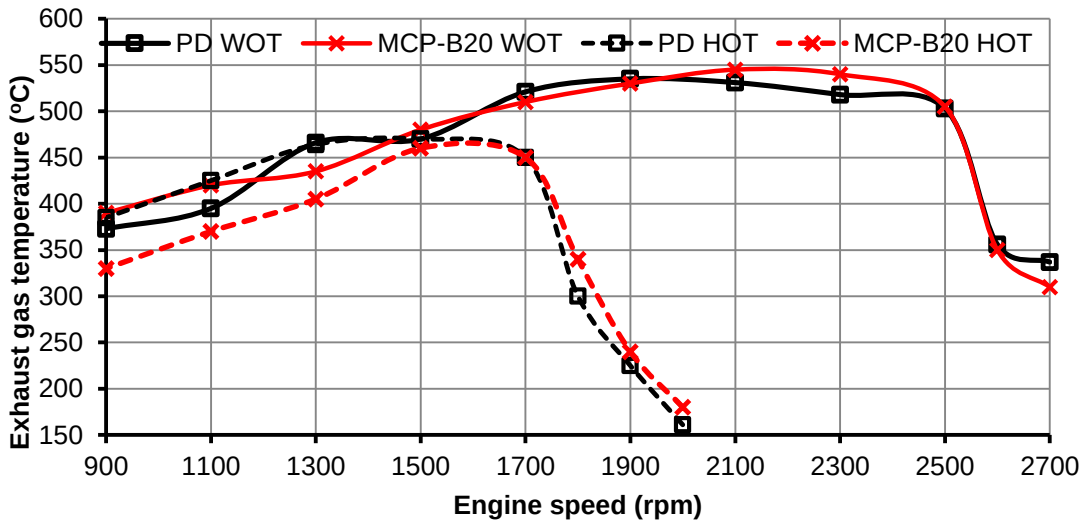

Figure 6.10 The relationship between tractor engine speeds (rpm) and exhaust temperature (ºC) for PD and MCP-B20

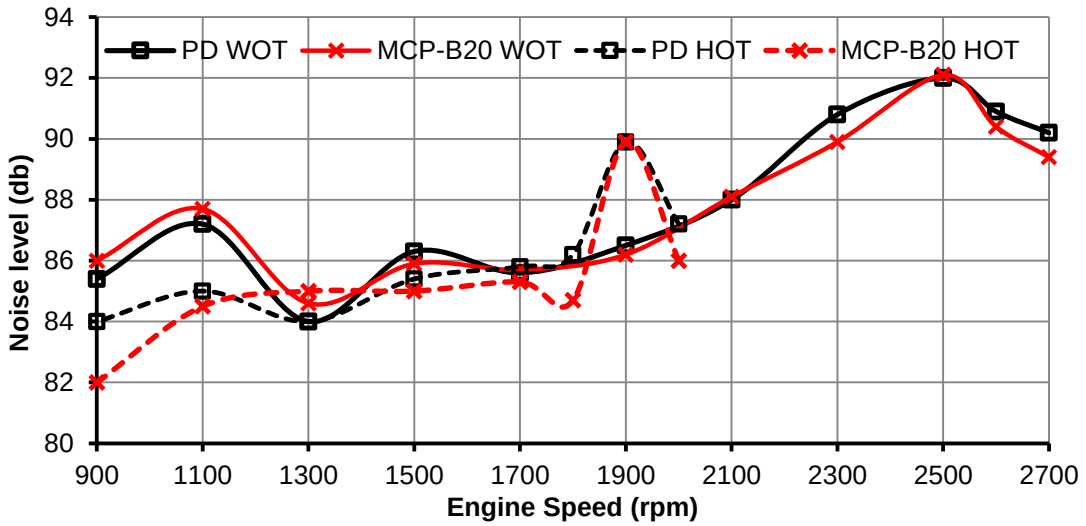

Figure 6.11 The relationship between tractor engine speeds (rpm) and noise level (dB) for PD and MCP-B20

6.4.3 Tractor Engine Emissions

The exhaust gases emissions from the tractor fuelled with MCP-B20 and PD are discussed in the following subsections.

Carbon Monoxide (CO) and Carbon Dioxide (CO_2)

The comparison of CO emission from PD and MCP-B20 presented in Figure 6.12 shows that MCP-B20 produced significantly less CO percentage than PD at most engine speeds in the WOT test and at most engine speeds in the HOT test except 1800 rpm in which MCP-B20 produced a slightly higher CO percentage. This result agrees with the conclusion of Nabi et al. (2009) that biodiesel from cottonseed oil produces less CO than PD. Less CO is an indication of the better combustion in MCP-B20 compared with PD, which is caused by the extra O_2 in the biodiesel form. This significant reduction in CO percentage was confirmed by ANOVA, as presented in Table 6.3 and Table 6.4 , which indicated a significantly high reduction in CO percentage produced by the tractor engine when fuelled with MCP-B20 compared

with PD at the rated PTO speed and peak torque speed. The maximum differences between the concentration of CO were clearly noticable at low engine speeds ranging between 1300 rpm and 1100 rpm for both the WOT and HOT tests. These results agree with those of Yusaf et al. (2011); however, there is disagreement with the higher result they found in CO ppm produced by an engine fuelled with B25 of crude palm oil biodiesel when compared with diesel fuel.

Figure 6.13 depicts the effect of tractor engine speed (rpm) on CO_2 (%) for PD and MCP-B20. The CO_2 percentage was relatively steady for the engine speeds below 2500 rpm for the WOT test and below 1700 rpm for the HOT test. The percentages of CO_2 then declined dramatically during both throttle tests for both fuels. This declination may have been caused by the lower load applied on the engine at the high speeds and the considerably lower FC rate making the engine produce lower CO_2 (%). Table 6.3 and Table 6.4 show that both fuels produces very comparable percentages of CO_2 at most engine speeds. In contrast, Table 6.3 illustrates that MCP-B20 emitted significantly lower CO_2 percentage than PD at rated PTO speed. This may have occurred because, in a complete combustion, the lower carbon to hydrogen ratio in biodiesel results in less CO_2 emissions being produced from biodiesel than diesel (Xue et al., 2011).

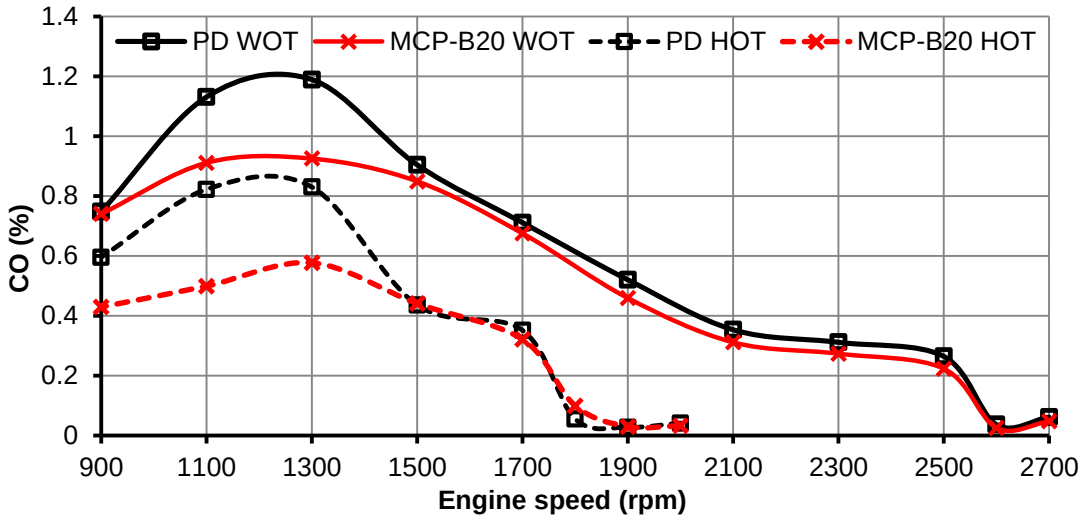

Figure 6.12 The relationship between tractor engine speeds (rpm) and CO (%) for PD and MCP-B20

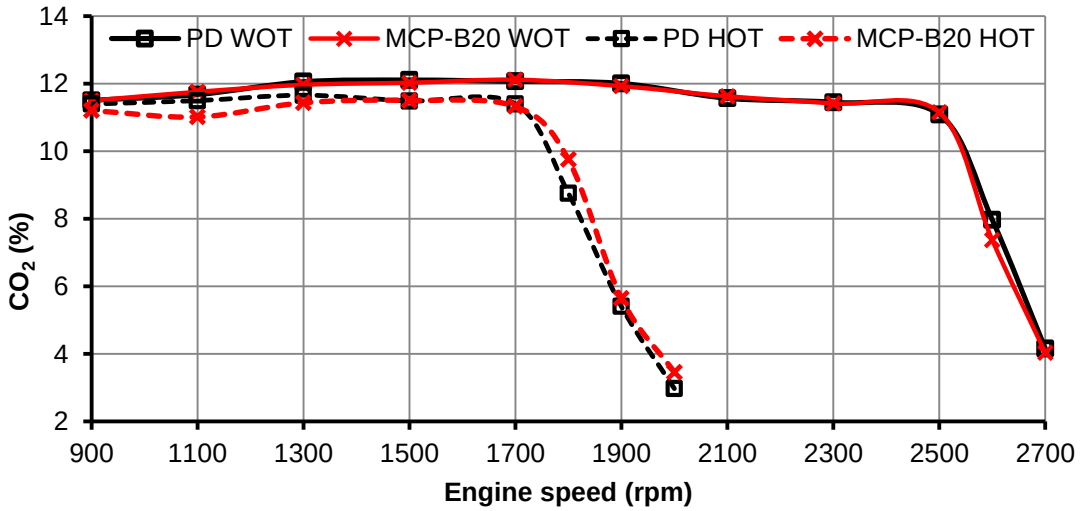

Figure 6.13 The relationship between tractor engine speeds (rpm) and CO_2 (%) for PD and MCP-B20

Oxygen (O_2) and Lambda (λ)

The results of the WOT test and HOT test, which display the O_2 percentage against the tractor engine speeds, are given in Figure 6.14. In stoichiometric air–fuel ratio and complete air–fuel mixing, the presence of O_2 in the exhaust gases provides an indication of the quality of combustion. Figure 6.14 shows that, at high engine speed,

the existence of O_2 in the exhaust gases increased for both fuels in both the WOT and HOT tests. This increase may have been caused by the higher air–fuel ratio at high engine speeds that results from the low load applied on the engine at high speeds. This result was confirmed by the lambda results shown in Figure 6.15, which presented a comparable pattern between O_2 and lambda. Diesel engines normally run with maximum airflow, while the fuel can be controlled. This shows the difference between the WOT and HOT tests; the air was constant but the fuel flow was reduced for the HOT test, which justifies the lower O_2 percentage for the HOT test compared with the WOT test at the same speed. Comparable results of O_2 percentage were found between MCP-B20 and PD, as shown in Table 6.3 and Table 6.4. However, Table 6.3 shows a very high increase in O_2 percentage when the tractor was fuelled by MCP-B20 compared with PD at the rated PTO speed. At the same speed, there was an insignificant difference in the engine thermal efficiency between the two fuels. The higher O_2 percentage may have been caused by the extra O_2 in the biodiesel structure.

Lambda is the actual air–fuel ratio divided by the stoichiometric air–fuel ratio. When lambda is higher than one, the engine runs lean, which is normal in diesel engines (Al-lwayzy et al., 2012; Andersson, 2001). Lambda's values for the tractor engine when running on MCP-B20 and PD in the WOT and HOT tests are graphically presented in Figure 6.15. This figure presents very comparable curve trends and values between the two fuels in the WOT and HOT tests. At all engine speeds, the lambda's value indicated lean combustion. However, Table 6.4 indicates an insignificant difference in the lambda's value in the WOT test at the peak PTO

speed, and Table 6.3 shows that PD produced significantly lower lambda value (by 9.8%). This result was mainly due to the higher O_2 in the MCP-B20 structure.

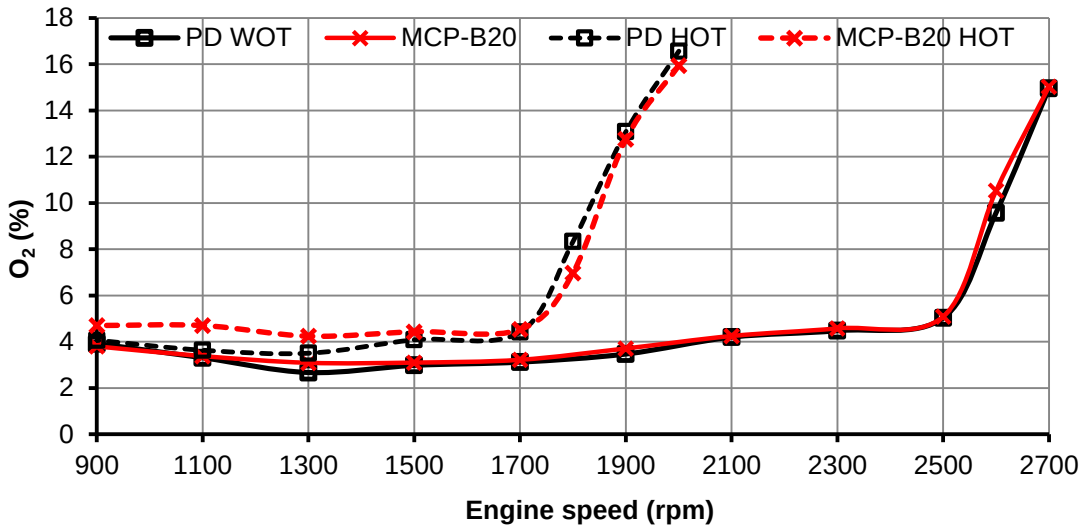

Figure 6.14 The relationship between tractor engine speeds (rpm) and O_2 (%) for PD and MCP-B20

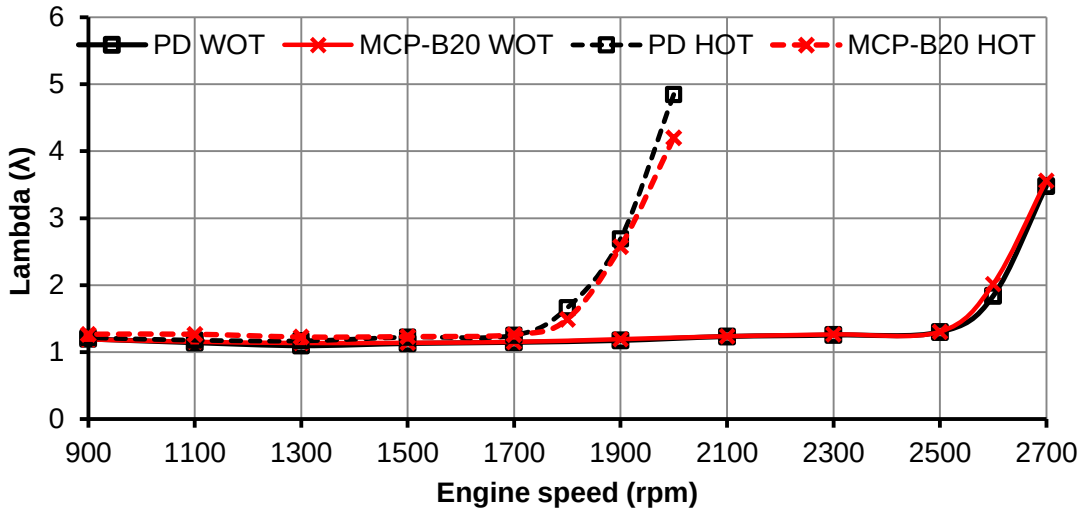

Figure 6.15 The relationship between tractor engine speeds (rpm) and lambda for PD and MCP-B20

Nitrogen Monoxide (NO)

Figure 6.16 shows the effect of the engine speed on the NO emission measured by ppm for the tractor engine fuelled by PD and MCP-B20 for the WOT and HOT tests. A similar curve trend can be observed for both fuels for the WOT and HOT tests in the emission of NO. Figure 6.16 shows that the NO emission decreased when the engine speed increased by reducing the torque applied on the engine. Substantial differences were found between low and high engine speeds for both fuels. The maximum values of 1126 ppm and 1194 ppm at 900 rpm were found to decline to 170 ppm and 161 ppm for PD and MCP-B20, respectively.

Figure 6.4 illustrates that the overall NO results of the total WOT and HOT tests insignificantly increased with MCP-B100 compared with PD. The insignificant result is in agreement with the NO_x results from the single-cylinder engine test because of the low amount of biodiesel in the fuel. It is normal and expected, based on the engine type, to have some variation around the average value. The insignificant difference in the overall WOT test can be justified by the variation in the results and the contradiction in the difference between the fuels at different engine speeds. At 266 rpm, as shown in Table 6.3, the NO was significantly lower than that of PD, whereas at 1500 rpm, as shown in Table 6.4, the NO was significantly higher than that of PD. This increase in the NO with MCP-B20 compared with PD in the WOT test resulted in overall insignificant differences in the NO level between the fuels. The overall findings show some degree of agreement with the findings of Kulkarni et al. (2011) and Neel et al. (2008), who reported an insignificant difference between the NO_x from PD and biodiesel B20.

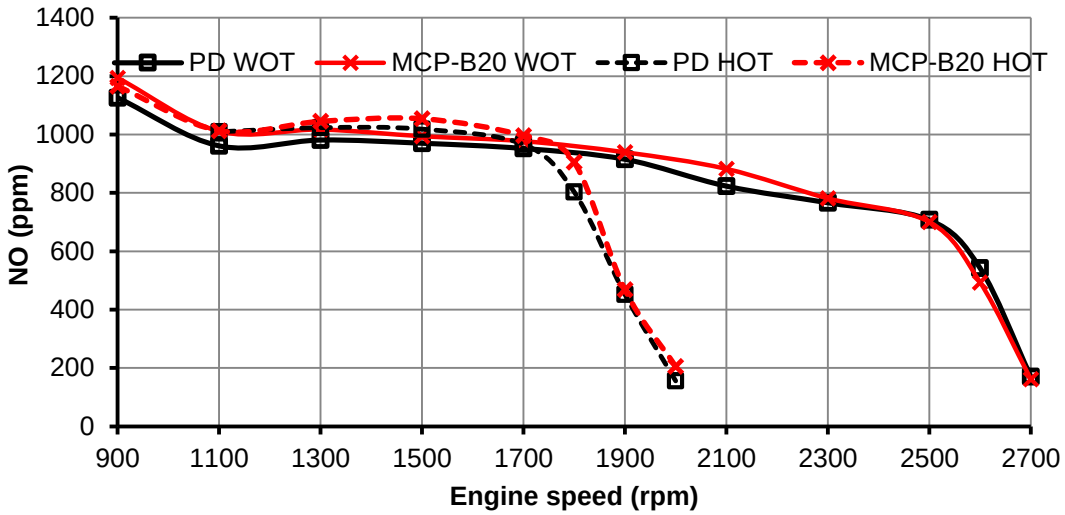

Figure 6.16 The relationship between tractor engine speeds (rpm) and NO (ppm) for PD and MCP-B20

6.5 Conclusion

Microalgae biodiesel is environmentally friendly and can be used as an alternative fuel for diesel engines in agricultural machinery such as tractors. The results of this work demonstrate that MCP-B20 can be commercially used as fuel for tractors with no modification. The overall PTO tests for the tractor engine at WOT and HOT showed that the tractor performance and exhaust gas emissions from MCP-B20 and PD were close and acceptable. The emissions results demonstrated great reduction in CO when MCP-B20 was used. ANOVA analysis at rated PTO speed and maximum PTO torque at WOT was performed to identify the differences between the fuel at $p \leq 0.05$. The ANOVA summary of the WOT test showed that there was a significant reduction in the values of torque, power, CO, CO_2 and NO and significant increase in the O_2 lambda with MCP-B20 compared with PD. The ANOVA summary of comparison between MCP-B20 and PD at peak PTO torque at WOT showed only a

significant increase in the exhaust gas temperature and NO; the only significant reduction was recorded in the CO level.

CHAPTER SEVEN

Conclusion and Future Work

7.1 Conclusion

Microalgae are a potential source of biomass and oil to meet the world's demand for fuels. Microalgae biofuels can be alternative fuels for diesel engines, especially in agricultural tractors. Recent research on microalgae biofuels has focused on the production of microalgae biomass and the fuel properties; however, research on the use of microalgae biofuels in diesel engines is not evident. In this thesis, an effort was made to understand the real effect of using microalgae biodiesel and emulsified water fuel with microalgae cells on diesel engine performance and exhaust gas emissions.

The overall aim of this study is to contribute to filling the gap in the research on the use of microalgae biofuels in diesel engines (in a laboratory-scale engine test and in an agricultural tractor). The biofuels used in this research work were biodiesel and emulsified water with microalgae cells. In Chapter 1 and Chapter 2, it was reported that different biodiesel sources (from different agricultural crops or from different microalgae species) produced different biodiesel properties and different engine performance and emissions. Biodiesels produced relatively less power than PD and higher NO_x emissions. Few data are currently available on the performance and emission of engines fuelled with microalgae biodiesel. Emulsified water fuel has also been reported to produce higher engine power in some studies, and lower engine

power in others. The effect of adding microalgae cells to enhance the energy content of emulsified water fuel has not yet been fully addressed.

Chapter 3 showed that the growing conditions of FWM-CV were not optimum for biodiesel production. The lipid content and biomass productivity were enhanced in an ISC by 114% and 39.3%, respectively; however, the biomass and lipid productivity were lower than that reported in the literature because of the growing conditions. It was also shown that enhancing the lipid content in FWM-CV made a significant change in the FAMEs component and increased the cetane number by 3.0%. The FWM-CV biodiesel properties were within the range of the biodiesel fuel limits.

An extensive study on the use of MCP was provided in Chapter 4. A statistical analysis was performed to evaluate the differences between the independent parameters of fuel type and engine speeds in engine performance and exhaust gas emission parameters. The results showed that:

1. The properties of MCP-B100 and its blends are comparable with PD and it can be used in a diesel engine without modifications. Compared with PD, MCP-B100 has lower heating value by 13.3%, higher cetane number by 2% and higher viscosity by 66.8%.
2. The engine power and torque produced when the engine was fuelled with MCP-B100 and its blends were found to be lower than when fuelled with PD. The maximum reduction in the engine power and torque was 7.0% and 4.9%, respectively, for the overall test. This reduction is lower than the reduction expected from the lower heating value (13.3%) of MCP-B100, which

indicates better combustion with MCP-B100 and the blends because of the fuel properties.

3. The ANOVA test on the effect of the fuel type on engine performance and exhaust gas emissions indicated that, compared with PD, MCP-B100 produced a significant reduction in GIP (12.4%), brake power (7%), torque (4.9%), exhaust gas temperature (6.1%), noise level (2.2%), CO level (28.0%) and NO_x level (7.4%). MCP-B100 produced significantly higher results than PD in the average of the tested speeds of 10.2% for BSFC, 15.8% for O_2 and 15.9% for lambda value.
4. MCP-B20 produced insignificant differences in all of the engine performance parameters compared with PD, whereas a significant reduction in CO and NO_x level was found.

FWM-CV biomass was used as additives to emulsified water fuel in CS-B100 and tested in a single-cylinder diesel engine. Three fuels were studied: cottonseed biodiesel (CS-B100), emulsified water fuel (CS-E20) consisting of 19.8% water in 79.2% CS-B100 and 1.0% emulsifier, and emulsified water fuel (CS-ME20) but with FWM-CV cells added to the water. The results showed that:

1. Using ultrasound in two steps was an effective method to overcome the problems of FWM-CV colonies that are larger than the injector orifice, and to form homogeneous suspension of cells. Ultrasound was also an effective method for mixing water with CS-B100 to form homogenous and stable emulsified water fuel (with and without FWM-CV).
2. The engine test results showed that the engine run without any modifications and the emulsion fuels produced lower in-cylinder pressure than CS-B100

because of its lower heating value. Adding FWM-CV to the water emulsion fuel enhanced the engine performance, and both emulsion fuels resulted in lower GIP, brake power, torque, CO_2 and NO_x than those produced by CS-B100.

3. The CS-E20 presented higher values of BSFC and O_2 than CS-ME20, and both produced higher values than CS-B100.

MCP-B20 was found to have properties and engine performance very close to those of PD and lower exhaust gas emissions compared with PD. It is proposed that it would have less effect on the engine life because of the lower percentage of biodiesel. This fuel was used for testing in a tractor engine and to perform a PTO test at WOT and HOT. The results were as follows:

1. The tractor performance and exhaust gas emission results were found to be comparable when the MCP-B20 and PD were used.
2. Compared with PD, a significant reduction in the values of torque, power, CO, CO_2 and NO, and a significant increase in the O_2 lambda was found at rated PTO speed when the tractor was fuelled with MCP-B20. The comparison between MCP-B20 and PD at peak PTO torque at WOT indicated significant increases only in the exhaust gas temperature and NO. The only significant reduction was recorded in the CO level.

7.2 Future Work

For a full understanding of the relationship investigated as part of this study, the fuel preparation and performance need to be investigated further. Based on the limitations

identified in the progression of this research, the following investigations are suggestions for valuable future work:

- the effect of microalgae biodiesel and emulsified water fuel on engine life and durability in a long running test
- an extended study of the effect of viscosity on nozzle pattern and droplet size with consideration of the injection pressure
- adjusting some engine parameters such as the compression ratio, injection timing and injection duration to increase the engine thermal efficiency
- testing of the PM and soot formation and total unburned hydrocarbon
- the effect of using a higher percentage of microalgae cells on emulsified water fuel properties and engine performance and emission
- optimisation of the ultrasound power, time and energy consumption required to form the optimum emulsion with deferent water content and surfactant
- further study of emulsified water fuel properties, including using microscopic photographs of the droplet size and reducing the viscosity of emulsified water fuels through methods that will not affect the stability of the emulsion fuel.

References

Abdullah, H 2010, 'High Energy Density Fuels Derived from Mallee Biomass: Fuel Properties and Implications', Ph.D. thesis, Curtin University.

Abdullah, H, Mourant, D, Li, C-Z and Wu, H 2010, 'Bioslurry as a Fuel. 3. Fuel and Rheological Properties of Bioslurry Prepared from the Bio-oil and Biochar of Mallee Biomass Fast Pyrolysis', *Energy & Fuels*, vol. 24, no. 10, pp. 5669-76.

Abu-Zaid, M 2004, 'Performance of single cylinder, direct injection diesel engine using water fuel emulsions', *Energy Conversion and Management*, vol. 45, no. 5, pp. 697-705.

Ahmad, A L, Yasin, N H M, Derek, C J C and Lim, J K 2011, 'Microalgae as a sustainable energy source for biodiesel production: A review', *Renewable and Sustainable Energy Reviews*, vol. 15, no. 1, pp. 584-93.

Al-juboori, R A 2012, 'Ultrasound technology as a pre-treatment for biofouling control in reverse osmosis (RO) system', University of Southern Queensland.

Al-lwayzy, S and Yusaf, T 2013, 'Chlorella protothecoides Microalgae as an Alternative Fuel for Tractor Diesel Engines', *Energies*, vol. 6, no. 2, pp. 766-83.

Al-lwayzy, S H, Yusaf, T and Jensen, T 2012, 'Evaluating tractor performance and exhaust gas emissions using biodiesel from cotton seed oil', paper presented to IOP Conference Series: Materials Science and Engineering.

Al-Widyan, M I, Tashtoush, G and Abu-Qudais, M d 2002, 'Utilization of ethyl ester of waste vegetable oils as fuel in diesel engines', *Fuel Processing Technology*, vol. 76, no. 2, pp. 91-103.

Alahmer, A, Yamin, J, Sakhrieh, A and Hamdan, M 2010, 'Engine performance using emulsified diesel fuel', *Energy Conversion and Management*, vol. 51, no. 8, pp. 1708-13.

Allwayzy, S, Yusaf, T, McCabe, B K, Pittaway, P and Aravinthan, V 2010, 'Microalgae as alternative fuel for compression ignition (CI) Engines'.

Amin, S 2009, 'Review on biofuel oil and gas production processes from microalgae', *Energy Conversion and Management*, vol. 50, no. 7, pp. 1834-40.

An, H, Yang, W M, Chou, S K and Chua, K J 2012, 'Combustion and emissions characteristics of diesel engine fueled by biodiesel at partial load conditions', *Applied Energy*, vol. 99, no. 0, pp. 363-71.

An, H, Yang, W M, Maghbouli, A, Li, J, Chou, S K and Chua, K J 2013, 'Performance, combustion and emission characteristics of biodiesel derived from waste cooking oils', *Applied Energy*, no. 0.

Anderson, J and Sorek, B 2009, 'Microalgae: The Fuel of Tomorrow '.

Andersson, C 2001, 'Observations on Electric Hybrid Bus Design', Licenatiate thesis, Lund Institute of Technology.

Armas, O, Ballesteros, R, Martos, F and Agudelo, J 2005, 'Characterization of light duty diesel engine pollutant emissions using water-emulsified fuel', *Fuel*, vol. 84, no. 7, pp. 1011-8.

Atadashi, I M, Aroua, M K and Aziz, A A 2010, 'High quality biodiesel and its diesel engine application: A review', *Renewable and Sustainable Energy Reviews*, vol. 14, no. 7, pp. 1999-2008.

Balat, M and Balat, H 2010, 'Progress in biodiesel processing', *Applied Energy*, vol. 87, no. 6, pp. 1815-35.

Bamgboye, A I and Hansen, A C 2008, 'Prediction of cetane number of biodiesel fuel from the fatty acid methyl ester (FAME) composition', *International Agrophysics*, vol. 22,, pp. 21-9.

Basha, S A and Anand, R 2011, 'Role of nanoadditive blended biodiesel emulsion fuel on the working characteristics of a diesel engine', *Journal of Renewable and Sustainable Energy*, vol. 3, p. 023106.

Basha, S A, Raja Gopal, K and Jebaraj, S 2009, 'A review on biodiesel production, combustion, emissions and performance', *Renewable and Sustainable Energy Reviews*, vol. 13, no. 6-7, pp. 1628-34.

Benter, M M, Gilmour, I A and Arnoux, L 1997, 'Biomass-oil slurry fuels: an investigation into their preparation and formulation', *Biomass and Bioenergy*, vol. 12, no. 4, pp. 253-61.

Bettis, B L, Peterson, C L, Auld, D L, Driscoll, D J and Peterson, E D 1982, 'Fuel Characteristics of Vegetable Oil from Oilseed Crops in the Pacific Northwest1', *Agron. J.*, vol. 74, no. 2, pp. 335-9.

Bowman, M, Hilligoss, D, Rasmussen, S and Thomas, R 2006, 'Biodiesel: a renewable and biodegradable fuel', *Hydrocarbon Processing*, vol. 85, no. 2, p. 103.

Boylu, F, Dinçer, H and Ateşok, G 2004, 'Effect of coal particle size distribution, volume fraction and rank on the rheology of coal–water slurries', *Fuel Processing Technology*, vol. 85, no. 4, pp. 241-50.

Buyukkaya, E 2010, 'Effects of biodiesel on a DI diesel engine performance, emission and combustion characteristics', *Fuel*, vol. 89, no. 10, pp. 3099-105.

Campbell, M N 2008, 'Biodiesel: algae as a renewable source for liquid fuel', *Guelph Eng J*, vol. 1, pp. 2-7.

Canakci, M 2009, 'NO_x emissions of biodiesel as an alternative diesel fuel', *International Journal of Vehicle Design*, vol. 50, no. 1-4, pp. 213-28.

Canakci, M, Ozsezen, A N and Turkcan, A 2009, 'Combustion analysis of preheated crude sunflower oil in an IDI diesel engine', *Biomass and Bioenergy*, vol. 33, no. 5, pp. 760-7.

Celen, I and Arın, S 2003, 'Noise levels of agricultural tractors', *Pakistan Journal of Biological Sciences*, vol. 6, no. 19, p. 1706.

Celik, I, Sensogut, C and Aydin, O 2009, 'Usage of Biodiesel as Fuel and Examining Its Effects on an Engine', *Energy Sources, Part A: Recovery, Utilization, and Environmental Effects*, vol. 31, no. 20, pp. 1857-65.

Cheirsilp, B and Torpee, S 2012, 'Enhanced growth and lipid production of microalgae under mixotrophic culture condition: Effect of light intensity, glucose concentration and fed-batch cultivation', *Bioresource Technology*, vol. 110, no. 0, pp. 510-6.

Chen, Y-H, Huang, B-Y, Chiang, T-H and Tang, T-C 2012, 'Fuel properties of microalgae (Chlorella protothecoides) oil biodiesel and its blends with petroleum diesel', *Fuel*, vol. 94, no. 0, pp. 270-3.

Chisti, Y 2007, 'Biodiesel from microalgae', *Biotechnology Advances*, vol. 25, no. 3, pp. 294-306.

Chisti, Y 2008, 'Biodiesel from microalgae beats bioethanol', *Trends in Biotechnology*, vol. 26, no. 3, pp. 126 -31.

Choix, F J, de-Bashan, L E and Bashan, Y 2012, 'Enhanced accumulation of starch and total carbohydrates in alginate-immobilized Chlorella spp. induced by Azospirillum brasilense: II. Heterotrophic conditions', *Enzyme and microbial technology*, vol. 51, no. 5, pp. 300-9.

Chokri, B, Ridha, E, Rachid, S and Jamel, B 2012, 'Experimental Study of a Diesel Engine Performance Running on Waste Vegetable Oil Biodiesel Blend', *Journal of energy resources technology*, vol. 134, no. 3.

Conceição, M M, Candeia, R A, Dantas, H J, Soledade, L E B, Fernandes, V J and Souza, A G 2005, 'Rheological Behavior of Castor Oil Biodiesel', *Energy & Fuels*, vol. 19, no. 5, pp. 2185-8.

Converti, A, Casazza, A A, Ortiz, E Y, Perego, P and Del Borghi, M 2009, 'Effect of temperature and nitrogen concentration on the growth and lipid content of Nannochloropsis oculata and Chlorella vulgaris for biodiesel production', *Chemical Engineering and Processing: Process Intensification*, vol. 48, no. 6, pp. 1146-51.

Crookes, R J, Kiannejad, F and Nazha, M A A 1997, 'Systematic assessment of combustion characteristics of biofuels and emulsions with water for use as diesel engine fuels', *Energy Conversion and Management*, vol. 38, no. 15, pp. 1785-95.

Dantas Neto, A, Fernandes, M, Barros Neto, E, Castro Dantas, T and Moura, M 2011, 'Alternative fuels composed by blends of nonionic surfactant with diesel and water: engine performance and emissions', *Brazilian Journal of Chemical Engineering*, vol. 28, no. 3, pp. 521-31.

Davis, J, Johnson, D, Edgar, D, Wardlow, G and Sadaka, S 2012, 'NO_x emissions and performance of a single-cylinder diesel engine with emulsified and non-emulsified fuels', *Applied Engineering in Agriculture*, vol. 28, no. 2, pp. 179-86.

Davis, J A 2011, 'NOx Emissions and Performance of a Single-cylinder Diesel Engine Fueled with Emulsified Biodiesel Blends', University of Arkansas, Fayetteville.

Demirbas, A 2007, 'Importance of biodiesel as transportation fuel', *Energy Policy*, vol. 35, no. 9, pp. 4661-70.

Demirbas, A 2010, 'Use of algae as biofuel sources', *Energy Conversion and Management*, vol. 51, no. 12, pp. 2738-49.

Demirbas, A and Demirbas, M F 2010, *Algae energy: algae as a new source of biodiesel*, Springer.

Demirbas, A and Demirbas, M F 2011, 'Importance of algae oil as a source of biodiesel', *Energy Conversion and Management*, vol. 52, no. 1, pp. 163-70.

Demirbas, M F 2010, 'Microalgae as a feedstock for biodiesel', *Energy Education Science and Technology Part a-Energy Science and Research*, vol. 25, no. 1-2, pp. 31-43.

Desantes, J M, Payri, R, García, A and Manin, J 2009, 'Experimental study of biodiesel blends' effects on diesel injection processes', *Energy & Fuels*, vol. 23, no. 6, pp. 3227-35.

Diya'uddeen, B H, Abdul Aziz, A R, Daud, W M A W and Chakrabarti, M H 2012, 'Performance evaluation of biodiesel from used domestic waste oils: A review', *Process Safety and Environmental Protection*, vol. 90, no. 3, pp. 164-79.

Dorado, M P, Ballesteros, E, Arnal, J M, Gómez, J and López, F J 2003a, 'Testing Waste Olive Oil Methyl Ester as a Fuel in a Diesel Engine', *Energy & Fuels*, vol. 17, no. 6, pp. 1560-5.

Dorado, M P, Ballesteros, E, Arnal, J M, Gómez, J and López, F J 2003b, 'Exhaust emissions from a Diesel engine fueled with transesterified waste olive oil', *Fuel*, vol. 82, no. 11, pp. 1311-5.

Durgut, M R and Celen, I H 2004, 'Noise levels of various agricultural machineries', *Pakistan Journal of Biological Sciences*, vol. 7, no. 6, pp. 895-901.

Fahd, M, Wenming, Y, Lee, P, Chou, S and Yap, C R 2012, 'Experimental investigation of the performance and emission characteristics of direct injection diesel engine by water emulsion diesel under varying engine load condition', *Applied Energy*.

Fayyad, S M, Abu-Ein, S, Al-Marahleh, G, Al-Momani, W, Al-Momani, M, Abulghanam, Z, Badran, O and Abu-Rahmah, T 2010, 'Experimental Emulsified Diesel and Benzen Investigation', *Research Journal of Applied Sciences, Engineering*, vol. 2, no. 3, pp. 268-73.

Floury, J, Desrumaux, A, Axelos, M A V and Legrand, J 2003, 'Effect of high pressure homogenisation on methylcellulose as food emulsifier', *Journal of Food Engineering*, vol. 58, no. 3, pp. 227-38.

Folch, J, Lees, M & Sloane Stanley, GH 1957, ' A simple method for the isolation and purification of total lipides from animal tissues', *Journal of Biological Chemistry* vol. 226, pp. 497-509.

Fuls, J, Hawkins, C S and Hugo, F J C 1984, 'Tractor engine performance on sunflower oil fuel', *Journal of Agricultural Engineering Research*, vol. 30, no. 0, pp. 29-35.

Ghobadian, B, Rahimi, H, Nikbakht, A M, Najafi, G and Yusaf, T F 2009, 'Diesel engine performance and exhaust emission analysis using waste cooking biodiesel fuel with an artificial neural network', *Renewable Energy*, vol. 34, no. 4, pp. 976-82.

Godeša, T, Jejčič, V and Poje, T 2010, 'Characteristics of a tractor engine using mineral and biodiesel fuels blended with rapeseed oil', *Scientia Agricola*, vol. 67, no. 5, pp. 510-6.

Grimes, P, Hagstrand, W, Psaila, A, Seth, J and Waldron, J 2011, 'Emulsified Biodiesel Fuel Effects on Regulated Emissions'.

Gumus, M 2010, 'A comprehensive experimental investigation of combustion and heat release characteristics of a biodiesel (hazelnut kernel oil methyl ester) fueled direct injection compression ignition engine', *Fuel*, vol. 89, no. 10, pp. 2802-14.

Haik, Y, Selim, M Y E and Abdulrehman, T 2011, 'Combustion of algae oil methyl ester in an indirect injection diesel engine', *Energy*, vol. 36, no. 3, pp. 1827-35.

Halim, R, Harun, R, Danquah, M K and Webley, P A 2012, 'Microalgal cell disruption for biofuel development', *Applied Energy*, vol. 91, no. 1, pp. 116-21.

Hansen, A C, Zhang, Q and Lyne, P W L 2005, 'Ethanol–diesel fuel blends — a review', *Bioresource Technology*, vol. 96, no. 3, pp. 277-85.

Harwood, J 2004, 'Membrane lipids in algae', *Lipids in Photosynthesis: Structure, Function and Genetics*, pp. 53-64.

Harwood, J L and Guschina, I A 2009, 'The versatility of algae and their lipid metabolism', *Biochimie*, vol. 91, no. 6, pp. 679-84.

Hossain, Salleh A, Nasrulhaq A, Chowdhury P and Naqiudden M 2008, 'Biodiesel fuel production from algae as renewable energy', *American Journal of Biochemistry and Biotechnology*, pp. 250-45.

Hossain, A S, Salleh, A, Boyce, A N and Naqiuddin, M 2008, 'Biodiesel fuel production from algae as renewable energy', *American Journal of Biochemistry and Biotechnology*, vol. 4, no. 3, p. 250.

Huang, G, Chen, F, Wei, D, Zhang, X and Chen, G 2010, 'Biodiesel production by microalgal biotechnology', *Applied Energy*, vol. 87, no. 1, pp. 38-46.

Hunt, C L, Johnson, D M and Edgar, D W 2013, 'NO_x Emissions and Performance of a Compact Diesel Tractor Fueled with Emulsified and Non-Emulsified Biodiesel', *Journal of Agricultural Systems, Technology, and Management*, vol. 24, pp. 12-22.

Illman, A M, Scragg, A H and Shales, S W 2000, 'Increase in Chlorella strains calorific values when grown in low nitrogen medium', *Enzyme and microbial technology*, vol. 27, no. 8, pp. 631-5.

Jablonický, J, Műllerová, D, Bohát, M and Žikla, A 2009, 'Operation properties of tractor diesel engine with diesel fuel and new sample of biodiesel', *Traktori i pogonske mašine*, vol. 14, no. 1, pp. 7-14.

Jafari, S M, He, Y and Bhandari, B 2007, 'Production of sub-micron emulsions by ultrasound and microfluidization techniques', *Journal of Food Engineering*, vol. 82, no. 4, pp. 478-88.

Jindal, S, Nandwana, B P, Rathore, N S and Vashistha, V 2010, 'Experimental investigation of the effect of compression ratio and injection pressure in a direct injection diesel engine running on Jatropha methyl ester', *Applied Thermal Engineering*, vol. 30, no. 5, pp. 442-8.

Jurić, T, Emert, R, Kraljević, D and Šumanovac, L 2001, 'The importance of agricultural tractors maintenance for ergonomics and the ecological agricultural production', *Prospects*.

Kadota, T and Yamasaki, H 2002, 'Recent advances in the combustion of water fuel emulsion', *Progress in energy and combustion science*, vol. 28, no. 5, pp. 385-404.

Kahraman, B 2008, 'Biodiesel as an alternative motor fuel: Production and policies in the European Union', *Renewable and Sustainable Energy Reviews*, vol. 12, no. 2, pp. 542-52.

Kass, M D, Lewis, S, Swartz, M, Huff, S P, Lee, D W, Wagner, R and Storey, J 2009, 'Utilizing Water Emulsification to Reduce NO_x and Particulate Emissions Associated with Biodiesel', *Transactions of the ASABE*, vol. 52, no. 1, pp. 5-13.

Kegl, B 2011, 'Influence of biodiesel on engine combustion and emission characteristics', *Applied Energy*, vol. 88, no. 5, pp. 1803-12.

Kim, Y, Park, S, Kim, C, Im, D, Kim, H, Chung, S and Kim, S 2010, 'Characteristics of paddy operations with biodiesel fuelled tractor', paper presented to XVIIth World Congress of the International Commission of Agricultural Engineering (CIGR).

Knothe, G 2005, 'Dependence of biodiesel fuel properties on the structure of fatty acid alkyl esters', *Fuel Processing Technology*, vol. 86, no. 10, pp. 1059-70.

Knothe, G 2008, '"Designer" Biodiesel: Optimizing Fatty Ester Composition to Improve Fuel Properties' ', *Energy & Fuels*, vol. 22, no. 2, pp. 1358-64.

Knothe, G and Steidley, K R 2005, 'Kinematic viscosity of biodiesel fuel components and related compounds. Influence of compound structure and comparison to petrodiesel fuel components', *Fuel*, vol. 84, no. 9, pp. 1059-65.

Knothe, G and Steidley, K R 2007, 'Kinematic viscosity of biodiesel components (fatty acid alkyl esters) and related compounds at low temperatures', *Fuel*, vol. 86, no. 16, pp. 2560-7.

Knothe, G, Krahl, J and Van Gerpen, J 2005, *The Biodiesel Handbook*.

Koc, A B and Abdullah, M 2013, 'Performance and NO_x emissions of a diesel engine fueled with biodiesel-diesel-water nanoemulsions', *Fuel Processing Technology*, vol. 109, no. 0, pp. 70–7.

Kulkarni, S, Johnson, D, Davis, J and Kennon, D 2011, 'Irrigation power unit performance, efficiency, and NO_x emissions with petroleum diesel, biodiesel, and biodiesel blends', *Appl. Eng. Agric*, vol. 27, no. 2, pp. 217-22.

Kumar, S, Chaube, A and Jain, S K 2012, 'Experimental evaluation of CI engine performance using diesel blended with Jatropha biodiesel', *Intl J Energ Environ*, vol. 3, pp. 471-84.

Lam, M K and Lee, K T 2012, 'Potential of using organic fertilizer to cultivate *Chlorella vulgaris* for biodiesel production', *Applied Energy*, vol. 94, pp. 303-8.

Lardon, L, Helias, A, Sialve, B, Stayer, J P and Bernard, O 2009, 'Life-Cycle Assessment of Biodiesel Production from Microalgae', *Environmental Science & Technology*, vol. 43, no. 17, pp. 6475-81.

Lee, J Y, Yoo, C, Jun, S Y, Ahn, C Y and Oh, H M 2010, 'Comparison of several methods for effective lipid extraction from microalgae', *Bioresource Technology*, vol. 101, pp. S75-S7.

Lif, A and Holmberg, K 2006, 'Water-in-diesel emulsions and related systems', *Advances in Colloid and Interface Science*, vol. 123–126, no. 0, pp. 231-9.

Lin, C-Y and Lin, H-A 2006, 'Diesel engine performance and emission characteristics of biodiesel produced by the peroxidation process', *Fuel*, vol. 85, no. 3, pp. 298-305.

Lin, C-Y and Lin, H-A 2007, 'Engine performance and emission characteristics of a three-phase emulsion of biodiesel produced by peroxidation', *Fuel Processing Technology*, vol. 88, no. 1, pp. 35-41.

Liu, Z-Y, Wang, G-C and Zhou, B-C 2008, 'Effect of iron on growth and lipid accumulation in Chlorella vulgaris', *Bioresource Technology*, vol. 99, no. 11, pp. 4717-22.

Lv, J-M, Cheng, L-H, Xu, X-H, Zhang, L and Chen, H-L 2010, 'Enhanced lipid production of Chlorella vulgaris by adjustment of cultivation conditions', *Bioresource Technology*, vol. 101, no. 17, pp. 6797-804.

Magara-Gomez, K T, Olson, M R, Okuda, T, Walz, K A and Schauer, J J 2012, 'Sensitivity of hazardous air pollutant emissions to the combustion of blends of petroleum diesel and biodiesel fuel', *Atmospheric Environment*, vol. 50, pp. 307-13.

Maiboom, A and Tauzia, X 2011, 'NO_x and PM emissions reduction on an automotive HSDI Diesel engine with water-in-diesel emulsion and EGR: An experimental study', *Fuel*, vol. 90, no. 11, pp. 3179-92.

Makareviciene, V, Skorupskaite, V and Andruleviciute, V 2013, 'Biodiesel fuel from microalgae-promising alternative fuel for the future: a review', *Reviews in Environmental Science and Bio/Technology*, vol. 12, no. 2, pp. 119-30.

Mariasiu, F and Varga, B 2010, 'Possibilities to improve the cold start process of tractor engines fuelled with biodiesel', *Journal of Food, Agriculture & Environment*, vol. 8, no. 3&4, p. 1121.

Marie, P, Perrier-Cornet, J M and Gervais, P 2002, 'Influence of major parameters in emulsification mechanisms using a high-pressure jet', *Journal of Food Engineering*, vol. 53, no. 1, pp. 43-51.

Mata, T M, Martins, A A and Caetano, N S 2010, 'Microalgae for biodiesel production and other applications: A review', *Renewable & Sustainable Energy Reviews*, vol. 14, no. 1, pp. 217-32.

Matthew, K H, Tonya, B, Melanie, R R, Donald, M J and George, W W 2007, *Effects of No.2 diesel, B-20 soy biofuel blend, and B-100 soy biofuel on performance, efficiency, and emissions in a compression ignition tractor*.

McCormick, R L, Graboski, M S, Alleman, T L, Herring, A M and Tyson, K S 2001, 'Impact of biodiesel source material and chemical structure on emissions of criteria pollutants from a heavy-duty engine', *Environmental science & technology*, vol. 35, no. 9, pp. 1742-7.

Meher, L, Vidya Sagar, D and Naik, S 2006, 'Technical aspects of biodiesel production by transesterification--a review', *Renewable and Sustainable Energy Reviews*, vol. 10, no. 3, pp. 248-68.

Mehta, P S and Anand, K 2009, 'Estimation of a Lower Heating Value of Vegetable Oil and Biodiesel Fuel', *Energy & Fuels*, vol. 23, no. 8, pp. 3893-8.

Miao, X and Wu, Q 2006, 'Biodiesel production from heterotrophic microalgal oil', *Bioresource Technology*, vol. 97, no. 6, pp. 841-6.

Mishra, S, Senapati, P and Panda, D 2002, 'Rheological behavior of coal-water slurry', *Energy Sources*, vol. 24, no. 2, pp. 159-67.

Mohebbi, A, Komarizade, M H, Jafarmadar, S and Pashai, J 2012, 'Use of waste cooking oil biodiesel in a tractor DI diesel engine', *Journal of Food, Agriculture & Environment*, vol. 10, no. 2, pp. 1290-7.

Mustafa, B 2011, 'Potential alternatives to edible oils for biodiesel production – A review of current work', *Energy Conversion and Management*, vol. 52, no. 2, pp. 1479-92.

Nabi, M N, Rahman, M M and Akhter, M S 2009, 'Biodiesel from cotton seed oil and its effect on engine performance and exhaust emissions', *Applied Thermal Engineering*, vol. 29, no. 11–12, pp. 2265-70.

Nadeem, M, Rangkuti, C, Anuar, K, Haq, M, Tan, I and Shah, S 2006, 'Diesel engine performance and emission evaluation using emulsified fuels stabilized by conventional and gemini surfactants', *Fuel*, vol. 85, no. 14, pp. 2111-9.

Ned, H M and Steinbruegge, G W 1972, 'Tractor Noise Measurement at University of Nebraska', vol. 15, no. 4.

Neel, C, Johnson, D and Wardlow, G 2008, 'Performance, efficiency, and NO_x emissions of a compact diesel tractor fueled with D2, B20, and B100 under steady-state loads', *Applied Engineering in Agriculture*, vol. 24, no. 6, pp. 717-21.

Özener, O, Yüksek, L, Ergenç, A T and Özkan, M 2012, 'Effects of soybean biodiesel on a DI diesel engine performance, emission and combustion characteristics', *Fuel*, no. 0.

Ozsezen, A N, Canakci, M and Sayin, C 2008, 'Effects of biodiesel from used frying palm oil on the performance, injection, and combustion characteristics of an indirect injection diesel engine', *Energy & Fuels*, vol. 22, no. 2, pp. 1297-305.

Ozsezen, A N, Canakci, M, Turkcan, A and Sayin, C 2009, 'Performance and combustion characteristics of a DI diesel engine fueled with waste palm oil and canola oil methyl esters', *Fuel*, vol. 88, no. 4, pp. 629-36.

Patil, P D and Deng, S 2009, 'Optimization of biodiesel production from edible and non-edible vegetable oils', *Fuel*, vol. 88, no. 7, pp. 1302-6.

Pereira, R G, Oliveira, C D, Oliveira, J L, Oliveira, P C P, Fellows, C E and Piamba, O E 2007, 'Exhaust emissions and electric energy generation in a stationary engine using blends of diesel and soybean biodiesel', *Renewable Energy*, vol. 32, no. 14, pp. 2453-60.

Pragya, N, Pandey, K K and Sahoo, P K 2013, 'A review on harvesting, oil extraction and biofuels production technologies from microalgae', *Renewable and Sustainable Energy Reviews*, vol. 24, no. 0, pp. 159-71.

Prakash, C B 1998, *A critical review of biodiesel as a transportation fuel in Canada*, Transportation Systems Branch Air Pollution Prevention Directorate Environment Canada.

Prasath, B R, Porai, P and Shabir, M F 2010, 'An Experimental Comparison Of Combustion, Performance And Emission In A Single Cylinder Thermal Barrier Coated Diesel Engine Using Diesel And Biodiesel', *Global Journal of Science Frontier Research*, vol. 10, no. 4.

Pulkrabek, W W 2004, *Engineering fundamentals of the internal combustion engine*, 2 edn, Pearson Prentice Hall New Jersey.

Qi, D H, Chen, H, Geng, L M, Bian, Y Z and Ren, X C 2010, 'Performance and combustion characteristics of biodiesel–diesel–methanol blend fuelled engine', *Applied Energy*, vol. 87, no. 5, pp. 1679-86.

Raheman, H and Phadatare, A G 2004, 'Diesel engine emissions and performance from blends of karanja methyl ester and diesel', *Biomass and Bioenergy*, vol. 27, no. 4, pp. 393-7.

Ramadhas, A S, Muraleedharan, C and Jayaraj, S 2005, 'Performance and emission evaluation of a diesel engine fueled with methyl esters of rubber seed oil', *Renewable Energy*, vol. 30, no. 12, pp. 1789-800.

Ramírez-Verduzco, L F, Rodríguez-Rodríguez, J E and Jaramillo-Jacob, A d R 2011, 'Predicting cetane number, kinematic viscosity, density and higher heating value of

biodiesel from its fatty acid methyl ester composition', *Fuel*, vol. In Press, Corrected Proof.

Robert, L, McCormick, R L, Graboski, M S, Alleman, T L, Herring, A M and Tyson, K S 2001, 'Impact of Biodiesel Source Material and Chemical Structure on Emissions of Criteria Pollutants from a Heavy-Duty Engine', *Environmental science & technology*, vol. 35, no. 9, pp. 1742-7.

Sahoo, P K, Das, L M, Babu, M K G and Naik, S N 2007, 'Biodiesel development from high acid value polanga seed oil and performance evaluation in a CI engine', *Fuel*, vol. 86, no. 3, pp. 448-54.

Sahoo, P K, Das, L M, Babu, M K G, Arora, P, Singh, V P, Kumar, N R and Varyani, T S 2009, 'Comparative evaluation of performance and emission characteristics of jatropha, karanja and polanga based biodiesel as fuel in a tractor engine', *Fuel*, vol. 88, no. 9, pp. 1698-707.

Savariraj, S, Ganapathy, T and Saravanan, C G 2011, 'Experimental Investigation of Performance and Emission Characteristics of Mahua Biodiesel in Diesel Engine', *ISRN Renewable Energy*, vol. 2011, p. 6.

Scragg, A H, Morrison, J and Shales, S W 2003, 'The use of a fuel containing Chlorella vulgaris in a diesel engine', *Enzyme and microbial technology*, vol. 33, no. 7, pp. 884-9.

Shen, Y, Yuan, W, Pei, Z J, Wu, Q and Mao, E 2009, 'Microalgae Mass Production Methods', *Transactions of the ASABE*, vol. 52, no. 4, pp. 1275-87.

Shrivastava, A K, Verma, P and Jena, P C 2007, 'Karanja esterified oil (blended biodiesel) for tractor PTO performance evaluation', p. unpaginated.

Singh, S P and Singh, D 2010, 'Biodiesel production through the use of different sources and characterization of oils and their esters as the substitute of diesel: A review', *Renewable and Sustainable Energy Reviews*, vol. 14, no. 1, pp. 200-16.

Soley Biotechnology Institute, Soley Institute, viewed 20/8/2010 2010, <http://www.soleybio.com/>.

Spolaore, P, Joannis-Cassan, C, Duran, E and Isambert, A 2006, 'Commercial applications of microalgae', *Journal of Bioscience and Bioengineering*, vol. 101, no. 2, pp. 87-96.

Stalin, N and Prabhu, H 2007, 'Performance test of IC engine using karanja biodiesel blending with diesel', *ARPN Journal of Engineering and Applied Sciences*, vol. 2, no. 5, pp. 32-4.

Stevens, J P 1999, *Intermediate statistics: A modern approach*, 2nd edn, Mahwah, NJ: Erlbaum.

Taghizadeh-Alisaraei, A, Ghobadian, B, Tavakoli-Hashjin, T and Mohtasebi, S S 2012, 'Vibration analysis of a diesel engine using biodiesel and petrodiesel fuel blends', *Fuel*, vol. 102, no. 0, pp. 414-22.

Tat, M E and Van Gerpen, J H 1999, 'The kinematic viscosity of biodiesel and its blends with diesel fuel', *Journal of the American Oil Chemists' Society*, vol. 76, no. 12, pp. 1511-3.

Tesch, S and Schubert, H 2002, 'Influence of increasing viscosity of the aqueous phase on the short-term stability of protein stabilized emulsions', *Journal of Food Engineering*, vol. 52, no. 3, pp. 305-12.

Tesfa, B, Mishra, R, Zhang, C, Gu, F and Ball, A D 2013, 'Combustion and performance characteristics of CI (compression ignition) engine running with biodiesel', *Energy*, vol. 51, no. 0, pp. 101-15.

Tomić, M D, Savin, L Đ, Mićić, R D, Simikić, M Đ and Furman, T F 2013, 'Effects of fossil diesel and biodiesel blends on the performances and emissions of agricultural tractor engines', *Thermal Science*, no. 00, pp. 263-78.

Tong, D, Hu, C, Jiang, K and Li, Y 2011, 'Cetane Number Prediction of Biodiesel from the Composition of the Fatty Acid Methyl Esters', *Journal of the American Oil Chemists' Society*, vol. 88, no. 3, pp. 415-23.

Ugwu, C U, Aoyagi, H and Uchiyama, H 2008, 'Photobioreactors for mass cultivation of algae', *Bioresource Technology*, vol. 99, no. 10, pp. 4021-8.

Usta, N, Öztürk, E, Can, Ö, Conkur, E, Nas, S, Con, A, Can, A Ç and Topcu, M 2005, 'Combustion of biodiesel fuel produced from hazelnut soapstock/waste sunflower oil mixture in a Diesel engine', *Energy Conversion and Management*, vol. 46, no. 5, pp. 741-55.

Valente, O S, da Silva, M J, Pasa, V M D, Belchior, C R P and Sodré, J R 2010, 'Fuel consumption and emissions from a diesel power generator fuelled with castor oil and soybean biodiesel', *Fuel*, vol. 89, no. 12, pp. 3637-42.

Varatharajan, K and Cheralathan, M 2012, 'Influence of fuel properties and composition on NO_x emissions from biodiesel powered diesel engines: A review', *Renewable and Sustainable Energy Reviews*, vol. 16, no. 6, pp. 3702-10.

Wahlen, B D, Morgan, M R, McCurdy, A T, Willis, R M, Morgan, M D, Dye, D J, Bugbee, B, Wood, B D and Seefeldt, L C 2012, 'Biodiesel from Microalgae, Yeast, and Bacteria: Engine Performance and Exhaust Emissions', *Energy & Fuels*, vol. 27, no. 1, pp. 220-8.

Wen, Z-Y and Chen, F 2003, 'Heterotrophic production of eicosapentaenoic acid by microalgae', *Biotechnology Advances*, vol. 21, no. 4, pp. 273-94.

Widjaja, A, Chien, C-C and Ju, Y-H 2009, 'Study of increasing lipid production from fresh water microalgae Chlorella vulgaris', *Journal of the Taiwan Institute of Chemical Engineers*, vol. 40, no. 1, pp. 13-20.

Wilson, R J and Farag, I H 2012, 'Parametric study of biodiesel quality and yield using a bench-top processor', *International Journal of Oil, Gas and Coal Technology*, vol. 5, no. 1, pp. 92-105.

Woertz, I C 2008, 'Lipid productivity of algae grown on dairy wastewater as a possible feedstock for biodiesel', *Master's Theses and Project Reports*, p. 183.

Xu, H, Miao, X and Wu, Q 2006, 'High quality biodiesel production from a microalga Chlorella protothecoides by heterotrophic growth in fermenters', *Journal of Biotechnology*, vol. 126, no. 4, pp. 499-507.

Xue, J, Grift, T E and Hansen, A C 2011, 'Effect of biodiesel on engine performances and emissions', *Renewable and Sustainable Energy Reviews*, vol. 15, no. 2, pp. 1098-116.

Yoo, C, Jun, S-Y, Lee, J-Y, Ahn, C-Y and Oh, H-M 2009, 'Selection of microalgae for lipid production under high levels carbon dioxide', *Bioresource Technology*, vol. 101, no. 1, Supplement 1, pp. S71-S4.

Yoshimoto, Y and Tamaki, H 2001, 'Reduction of NO_x and smoke emissions in a diesel engine fueled by biodiesel emulsion combined with EGR', *SAE paper*, pp. 01-0649.

Yoshimoto, Y, Onodera, M and Tamaki, H 2001, 'Performance of a Diesel Engine Using Transesterified Fuel from Vegetable Oil (Effects of Water Emulsification)', *Transactions of the Japan Society of Mechanical Engineers, Ser. B*, pp. 67-653.

Yusaf, T, Yousif, B and Elawad, M 2011, 'Crude palm oil fuel for diesel-engines: Experimental and ANN simulation approaches', *Energy*.

Zheng, M, Mulenga, M C, Reader, G T, Wang, M, Ting, D S K and Tjong, J 2008, 'Biodiesel engine performance and emissions in low temperature combustion', *Fuel*, vol. 87, no. 6, pp. 714-22.

Zoz, F M and Grisso, R D 2003, 'Traction and Tractor Performance', paper presented to Agricultural Equipment Technology Conference, Louisville, Kentucky, USA.

Appendix A

A.1 Introduction

This appendix explains the calibration and the error analysis of the devices and the equipment used in this thesis.

A.2 Engine Selection

Selecting the engine for the microalgae biodiesel test started by connecting the available new F72 diesel engine to the dynamometer and inserting the pressure transducer into the cylinder head. The runs with diesel fuel and microalgae emulsion showed that the engine rotational speed was unstable and it was difficult to fix the engine at a specific speed. Another test was conducted with a new Yanmar L48N5 diesel engine. The test result and the standard performance curve from the supplier showed that the engine torque was almost constant at a wide range of speeds. The result of using the Land and Sea dynamometer with this engine showed very limited control on engine speed through applying load. The speed dropped from 3000 rpm to below 2000 rpm suddenly. After discussion with the engine and the dynamometer suppliers to obtain data with different loads at different engine speeds, the L48N6 was selected based on the performance curve and its high quality.

A.3 Pressure Transducer

This section presents the calibration process of the piezoelectric pressure transducer, which was used to record the in-cylinder pressure in this thesis. The calibration

process was performed using a DH Budenberg 580 dead weight tester (Figure A.1) to apply hydraulic pressure on the pressure transducer.

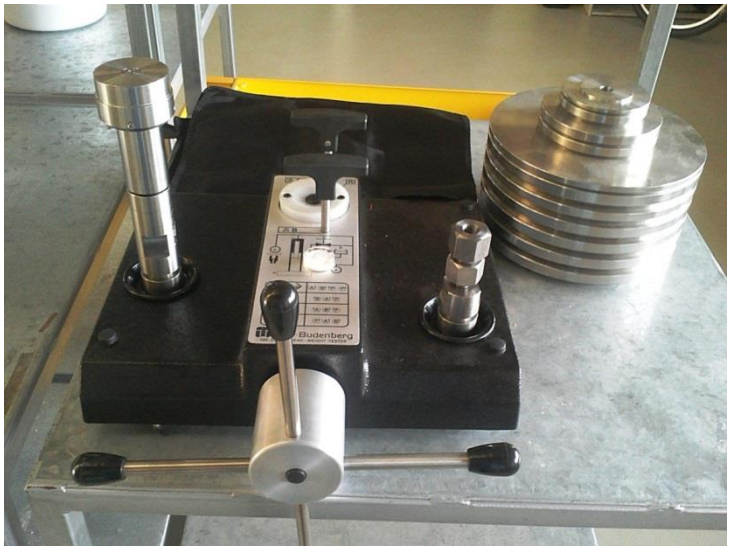

Figure A.1 DH Budenberg 580 dead weight tester

Prior to the calibration, an adapter was fabricated to fit the pressure transducer on the device. The voltage signal from the pressure transducer was recorded using a LabVIEW data acquisition program, which received the signal through a Kistler amplifier. The calibration was performed by applying known weights to the transducer to produce a voltage signal. A correlation between the applied weights and the voltage signal was used to generate Equation A.1, which was used in the LabVIEW scale to measure the in-cylinder pressure in bar units. The correlation between the voltage signal and the pressure is given in Figure A.2.

$$Pressure = 19.783\ voltage\ signal - 0.3994 \qquad \text{Equation A.1}$$

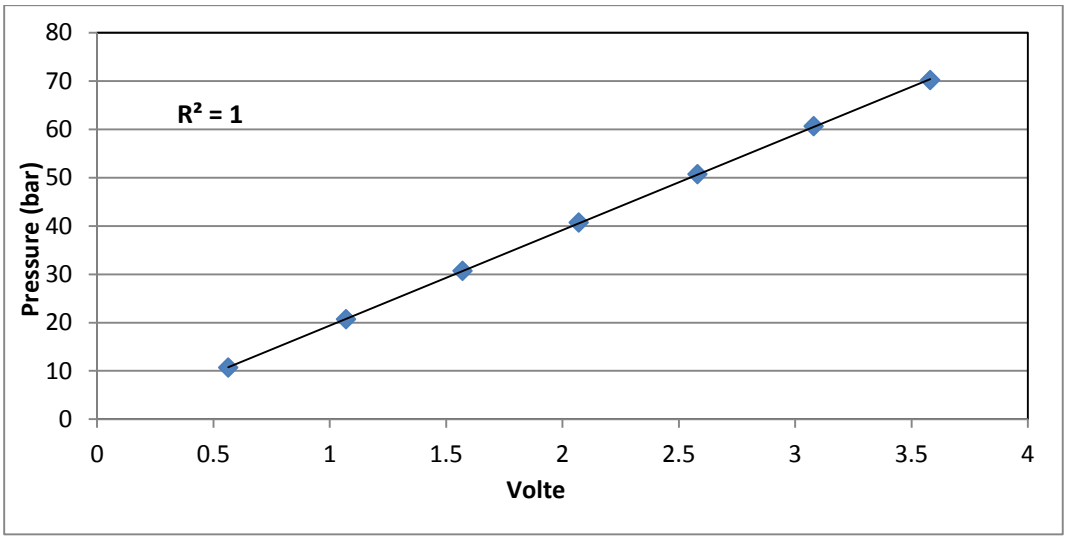

Figure A.2 Voltage to pressure conversion

A.4 Encoder

This section describes the matching of the engine TDC with the encoder's Z pulse. The engine manufacturer had labelled the TDC position on the flywheel. The procedure of finding the TDC was followed as described in the engine catalogue. After setting the engine on the TDC, a mark was put on the encoder's shaft adapter, which was mounted on the engine shaft and aligned with a mark on the dynamometer (non-rotating part). The encoder's rotary shaft was then fixed on the adapter in a position at which the Z pulse signal was occurring. The encoder's body holder was designed to allow adjustment of the encoder's rotational position. When the engine was on the TDC, the encoder was slightly and carefully rotated to detect the Z pulse on the oscilloscope monitor. When the signal was detected, a mark was put on the encoder body and another mark was put on the encoder holder. When the exact position was detected, the encoder was fixed using three screws. At this position, the encoder's Z pulse emitted a signal when the engine piston was on the TDC position.

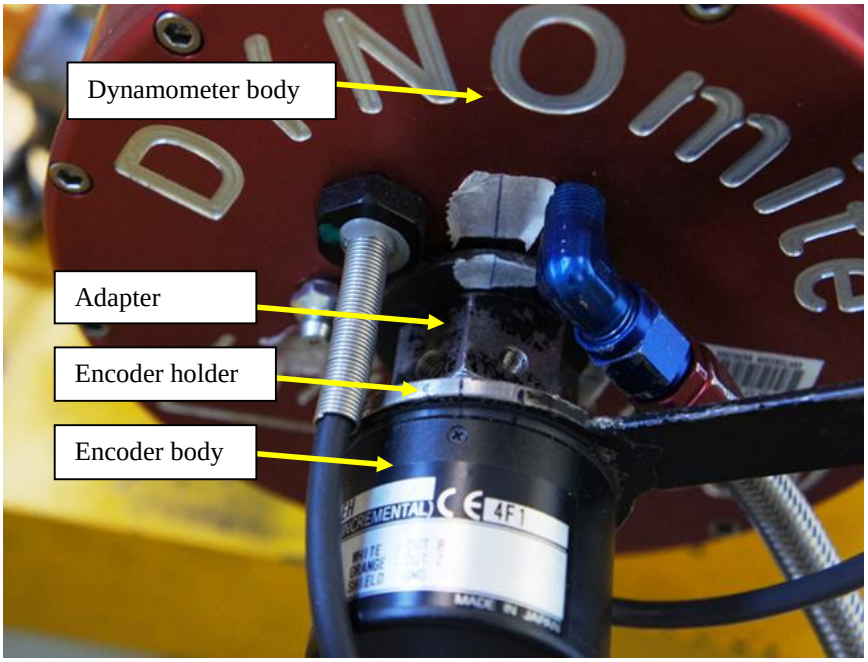

Figure A.3 Allying the TDC of the engine with the Z pulse starting position of the encoder

A.5 Dynamometer

The dynamometer used in this work was made by Land and Sea. Initially, the dynamometer was designed to adapt to a wide range of engine types and test conditions, and different units of measurement. First, the dynamometer and its software was set to fit the test condition of setting the engine specifications and SI units.

To calibrate the torque value in the dynamometer software, a specially made beam was fabricated to hold the dynamo body and apply statistic weights on a 0.5 m arm, as shown in Figure A.4.A.

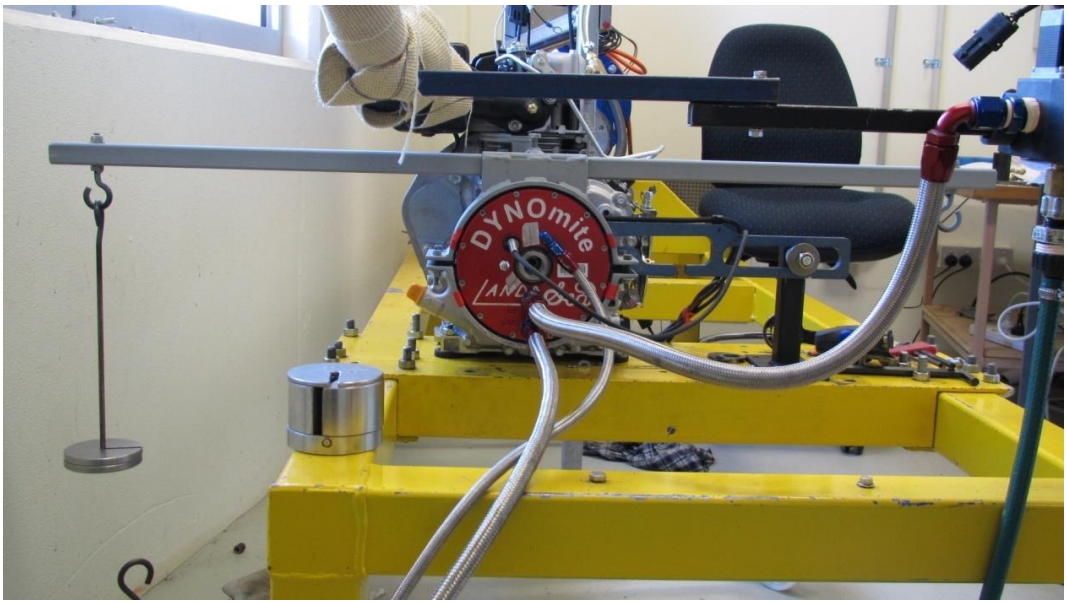

Figure A.4 Dynamometer calibration

A range of weights was applied, from 1.0 N.m to 13.0 N.m, based on the expected range of torque expected from the engine. The readings of the dynamometer software were then adjusted using Equation A.2 with R^2 of 0.9991.

$$Corrected\ reding = 1.431844\ (old\ reding) - 0.137 \qquad \text{Equation A.2}$$

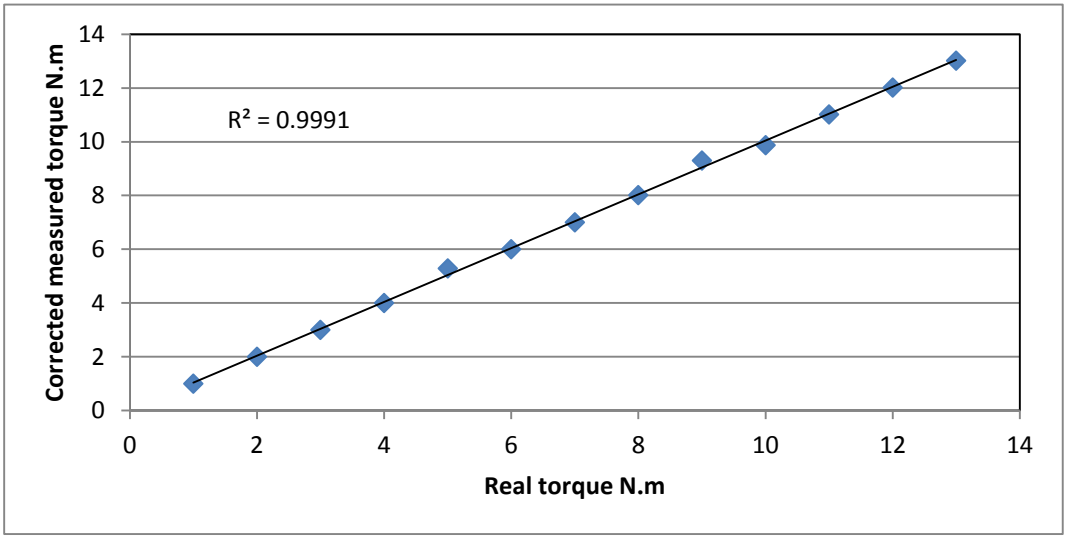

Figure A.5 Calibration curve of the torque

The dynamometer arm holder that was fabricated to prevent the dynamometer body from rotating with the engine shaft and the load control valve holder are presented in the Figure A.6.

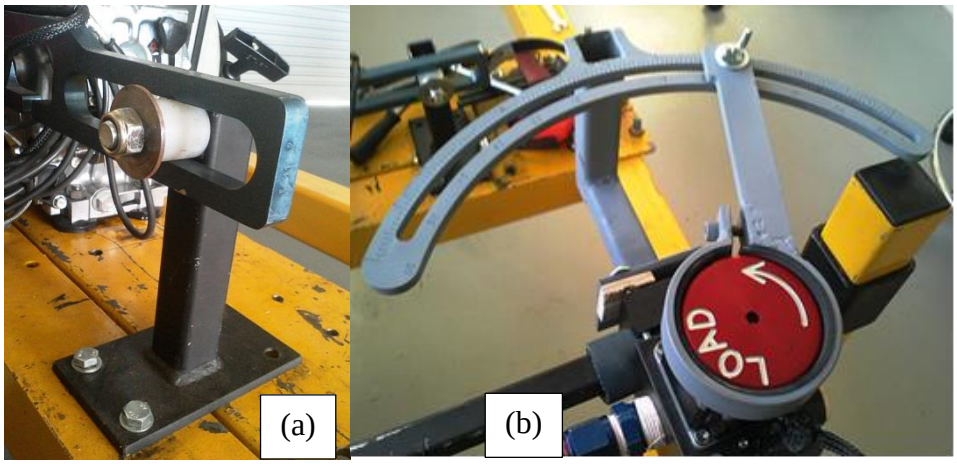

Figure A.6 (a) Dynamometer arm holder (b) load valve controller

Appendix B

BFigure B.1 shows the performance curves that were provided by the manufacturer (Yanmar) for the engine L48N6 that was used in the tests discussed in Chapter 4 and Chapter 5.

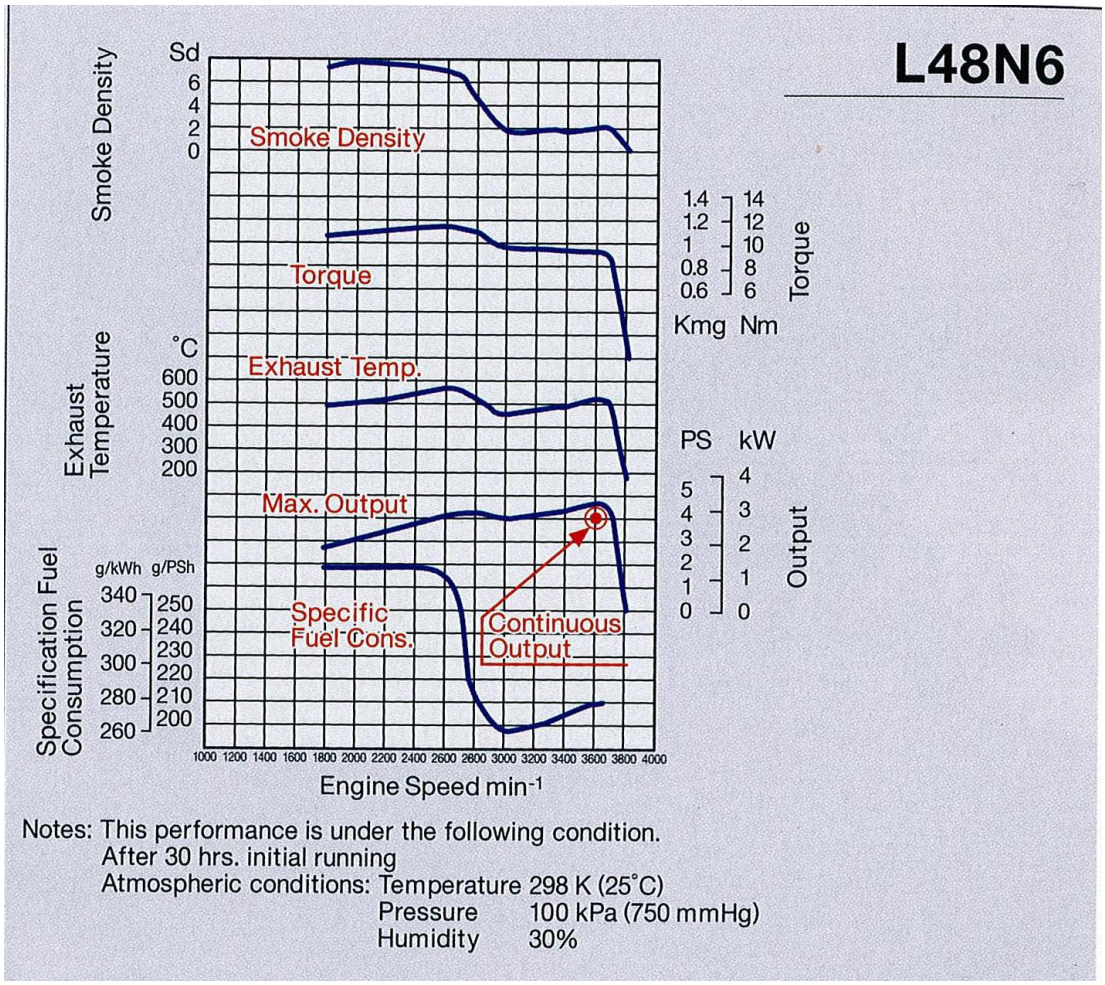

Figure B.1 Yanmar L48N6 performance curve